

# **Bubble behaviour in frother and inorganic salt solutions**

**Jarrett Quinn**

Department of Mining and Materials Engineering,  
McGill University,  
Montreal, Canada

A thesis submitted to McGill University in partial fulfillment of the  
requirements of the degree of Doctor of Philosophy

© Jarrett Quinn  
April 2014

# Abstract

Bubble formation, coalescence and break-up processes coupled with bubble velocity determine gas dispersion properties in a flotation cell. Frothers are typically added to inhibit bubble coalescence (decrease bubble size) and reduce bubble rise velocity. If present at elevated concentration the presence of certain inorganic salts has been shown to have a similar capability to frother.

Much of the literature focuses on the role of bubble coalescence on the production of fine bubbles. Researchers have hinted that the presence of frother may also affect bubble break-up. For the most part, little attention has been paid to the role of frother in bubble break-up. A few researchers have noted that bubble-bubble interactions may play a role in bubble break-up processes.

The first study in the thesis examines bubble formation in water at a capillary using high-speed photography and reviews the processes which lead to bubble break-up. Several authors have noted bi-modal bubble size distributions (BSD) in flotation systems at low frother or inorganic salt concentrations. The origin appears to be related to bubble-bubble interactions. The study provides visual evidence of coalescence-related and wake-related mechanisms creating fine bubbles and bi-modal distributions. Four coalescence mechanisms are identified: coalescence-induced break-up, droplet formation and collision, liquid jet formation and collision, liquid jet disruption to droplets and collision; and two wake-related events: distortion and break-up of trailing bubble, and premature detachment. Comparing the fine/coarse mode ratio in water only systems (ca. 1/10) the possible relevant mechanisms are suggested. Knowing that frothers produce a mono-modal BSD and act to retard coalescence, the origin of the bi-modal BSD is argued to be coalescence-related.

The second study uses a similar technique to quantify the effect of frothers and inorganic salts on bubble regimes at a capillary. High-speed photography was used to determine the transition air flow rate between non-coalescence, coalescence, and coalescence with fine bubble production (break-up). The addition of solute inhibited bubble coalescence and delayed the onset of fine bubble production. The tests allow for frother and salt strength characterization.

The third set of experiments uses passive acoustic emission monitoring to study the role of solid particles on bubble coalescence. The systems being opaque argue against the use of optical techniques. The effect of 1 to 10% w/w talc (hydrophobic) or silica (hydrophilic) on air bubble formation and coalescence at a capillary in the presence of MIBC or sodium chloride was determined. Both solids slightly inhibited bubble coalescence while the silica created a larger region of partial coalescence compared to talc. At 10% w/w the silica appeared to promote coalescence at high MIBC concentration.

Frothers and certain inorganic salts not only inhibit bubble coalescence but also reduce bubble rise velocity. Upon inspection of high-speed records of rising bubbles, it became clear that the presence of solute affected bubble shape and rise velocity in tandem. A study was undertaken to examine the relationship between bubble shape and rise velocity for a single rising bubble. Individual bubbles ca. 2.3 mm in diameter were produced at a capillary in water containing an inorganic salt ( $\text{NaClO}_4$ ,  $\text{KCl}$ ,  $\text{NaCl}$ ,  $\text{Na}_2\text{SO}_4$ , or  $\text{CaCl}_2$ ). Using high-speed photography and image analysis techniques, bubble aspect ratio and rise velocity were measured at 1 ms time intervals over a distance ca. 1.15 to 1.20 m above the capillary. All conditions showed oscillations in bubble aspect ratio and velocity that were related. Increasing concentration, on average, created more spherical bubbles that rose at lower velocities. The same observations were made in the presence of MIBC frother. Results suggest a unique relationship between bubble shape and rise velocity independent of solute type.

# Résumé

Les procédés de formation, coalescence et scission des bulles couplés à la vitesse d'ascension déterminent la dispersion du gaz dans une cellule de flottation. Des agents moussants sont généralement ajoutés à la pulpe afin d'éviter la coalescence et réduire la vitesse des bulles. Avec une concentration élevée, certains composés inorganiques ont le même effet que les agents moussants.

La documentation actuelle focus sur le rôle de l'inhibition de la coalescence dans la production de bulles de tailles fines. Certaines recherches semblent montrer que la présence des agents moussants peut aussi affecter la scission des bulles. Généralement, peu d'attention est accordée au rôle de la scission de bulles. D'autres recherches ont aussi montré des liens entre la coalescence et la scission.

La première étude présentée met l'emphase sur la formation des bulles au bout d'un tube capillaire immergé dans l'eau en utilisant la photographie à haute vitesse afin de réexaminer les procédés à l'origine de la scission. Plusieurs auteurs ont noté la présence d'une distribution de la taille des bulles (DTB) qui est bimodale pour des systèmes de flottation ayant de faibles concentrations d'agent moussant ou de composé inorganique. Cette distribution semble être reliée à des interactions bulles-bulles. L'étude démontre visuellement des mécanismes reliés à la coalescence et à la trainée d'une bulle créant des bulles plus fines et ainsi une distribution bimodale. Quatre mécanismes reliés à la coalescence ont été identifiés : la scission causée par la coalescence, la production de gouttelettes et collision, la formation de jet-liquide et collision ainsi que la formation de liquide-jet suivi d'une fragmentation en gouttelettes et collision. Deux mécanismes reliés à la trainée ont aussi été identifiés : la distorsion et la scission de la bulle de trainée et le détachement prématuré. La comparaison des modes des petites et grosses bulles (d'un rapport 1/10) révèle les mécanismes potentiels. Sachant que les agents moussants produisent une DTB monomodal et que leurs rôles est de prévenir la coalescence, la création de la DTB bimodal semble être relié à la coalescence.

La deuxième étude utilise une technique similaire pour quantifier l'effet des agents moussant et des composés inorganiques sur le type de bulles produites au bout d'un tube capillaire. La photographie à haute vitesse a été utilisée pour déterminer la transition entre la non-coalescence,

la coalescence, et la coalescence avec scission. L'ajout d'un soluté inhibe la coalescence des bulles et retarde le début de la production des petites bulles. Les résultats permettent la caractérisation des agents moussants en termes de puissance.

Le troisième groupe d'expériences utilise l'enregistrement des signaux sonores passifs pour étudier le rôle des particules (hydrophobes et hydrophiles) sur la coalescence des bulles. Plusieurs études utilisent des techniques optiques pour mesurer directement ou indirectement l'effet d'un soluté sur la coalescence des bulles. Les techniques optiques sont typiquement limitées à l'étude de systèmes biphasés (solution-air) puisque les systèmes triphasés (solution-air-particules) sont généralement opaques. L'enregistrement des signaux sonores passifs a été utilisé pour déterminer l'effet des particules (en concentration de 1 à 10 % m/m de talc ou de silice), sur la formation et la coalescence des bulles produites au bout d'un tube capillaire en présence de MIBC ou chlorure de sodium. Les deux types de particules ont inhibé la coalescence de bulles et la silice a créé la plus grande région de coalescence partielle en comparaison au talc. À 10 % m/m de silice, la coalescence est favorisée s'il y a haute concentration de MIBC.

Non seulement les agents moussants et certains composés inorganiques inhibent la coalescence des bulles, mais ils réduisent aussi la vitesse d'ascension. La photographie des bulles ascendantes a clairement montré que la présence de soluté affectait la forme et la vitesse des bulles de façon combinée. Une étude a donc été menée afin d'examiner la relation entre la forme et la vitesse des bulles. Des bulles individuelles d'environ 2.3 mm de diamètre ont été produites au bout d'un tube capillaire immergé dans de l'eau contenant un composé inorganique ( $\text{NaClO}_4$ ,  $\text{KCl}$ ,  $\text{NaCl}$ ,  $\text{Na}_2\text{SO}_4$ , or  $\text{CaCl}_2$ ). À l'aide de la photographie à haute vitesse et de techniques d'analyse d'image, le facteur de forme et la vitesse d'ascension de bulles ont été mesurés à un intervalle de 1 ms à une distance d'environ 1.15 à 1.20 m au-dessus du capillaire. Tous les mélanges ont montré des oscillations du facteur de forme et de la vitesse d'ascension reliées. Généralement en augmentant la concentration, on crée des bulles plus sphériques montant à une vitesse plus faible. Les mêmes observations ont été faites en présence de MIBC. Les résultats suggèrent une corrélation unique entre la forme et la vitesse d'ascension des bulles, indépendamment du type de soluté présent. Les effets des composés inorganiques sur le comportement des bulles et la dispersion du gaz dans un système de flottation sont aussi discutés.

# Acknowledgements

It has been a pleasure to do my graduate studies under the supervision of Professor James A. Finch. His encouragement, enthusiasm and wealth of knowledge have brought about this work. I very much appreciate the many hours spent proof-reading and correcting this thesis and the articles we have written.

Funding for this work was sponsored by Vale, Teck Resources, Xstrata Process Support, Barrick Gold, Shell Canada, SGS Lakefield Research, COREM and Flottec through the Chair in Mineral Processing under the Natural Sciences and Engineering Research Council of Canada (NSERC) Collaborative Research and Development (CRD) program. I would also like to acknowledge the Hydro-Quebec doctoral award and the Vadasz fellowship for financial support under the McGill Engineering Doctoral Award (MEDA) program.

The McGill mineral processing group is ever changing and I would like to thank all my colleagues past and present for their friendship. I would especially like to thank Dr. Miguel Maldonado, Ray Langlois and Prof. Kristian Waters for their help.

I would also like to thank my family for all their encouragement and a very big thank you to Vera for all her love and support.

# Table of contents

<b>Abstract</b> .....	<b>i</b>
<b>Acknowledgements</b> .....	<b>v</b>
<b>Table of contents</b> .....	<b>vi</b>
<b>List of figures</b> .....	<b>x</b>
<b>Chapter 1 – Introduction</b> .....	<b>1</b>
1.1 Introduction .....	1
1.2 Thesis objectives .....	4
1.3 Thesis structure .....	5
1.4 Contribution of authors .....	5
References .....	6
<b>Chapter 2 – Literature review</b> .....	<b>10</b>
2.1 Frothers: Chemistries and classifications .....	10
2.1.1 Hydrophilic-lipophilic balance (HLB) .....	12
2.2 Inorganic salts .....	13
2.3 Bubble formation, coalescence and break-up .....	16
2.4 Frother characterization techniques .....	20
2.4.1 Bubble coalescence tests .....	21
2.4.2 Critical coalescence concentration (CCC) .....	22
2.4.3 Gas holdup vs. frother / salt concentration .....	23
2.5 The behaviour of a single rising bubble .....	24
2.5.1 Surfactants, bubble rigidity and internal circulation .....	25
2.5.2 Bubble terminal velocity .....	25
2.5.3 Forces acting on a rising bubble .....	28

2.5.4 Dimensionless numbers .....	28
2.5.5 Single bubble regimes.....	30
2.5.6 Terminal velocity models .....	33
2.5.7 Bubble shape, rise velocity and the effect of release condition .....	36
2.6 Bubbles and sound .....	40
References.....	42
<b>Chapter 3 – Origin of bi-modal bubble size distributions in the absence of frother.....</b>	<b>58</b>
3.1 Introduction.....	58
3.2 Experimental .....	60
3.3 Results.....	61
3.4 Discussion .....	66
3.5 Conclusions.....	68
References.....	68
<b>Chapter 4 – Effect of frother and inorganic salts on bubble regimes at a capillary .....</b>	<b>71</b>
4.1 Introduction.....	71
4.1.1 Gas dispersion: Frothers and inorganic salts .....	71
4.1.2 Effect of gas rate on bubble formation at a capillary.....	72
4.1.3 Motivation for the present study.....	73
4.2 Experimental .....	75
4.2.1 Setup .....	75
4.2.2 Determining bubble regime transitions.....	75
4.2.3 Bubble sizing and image analysis .....	76
4.3 Results.....	77
4.4 Discussion .....	84

4.5 Conclusions.....	87
References.....	87
<b>Chapter 5 – Passive acoustic emission monitoring to detect bubble coalescence in presence of solid particles .....</b>	<b>93</b>
5.1 Introduction.....	93
5.2 Experimental.....	96
5.3 Results.....	98
5.4 Discussion.....	103
5.5 Conclusions.....	104
References.....	105
<b>Chapter 6 – Experimental study on the shape - velocity relationship of an ellipsoidal bubble in inorganic salt solutions .....</b>	<b>109</b>
6.1 Introduction.....	109
6.2 Experimental.....	111
6.2.1 Setup and image collection.....	111
6.2.2 Image analysis.....	113
6.3 Results.....	114
6.4 Discussion.....	121
6.5 Conclusions.....	123
References.....	124
<b>Chapter 7 – Unifying discussion.....</b>	<b>128</b>
References.....	130
<b>Chapter 8 – Conclusions, contributions, and future work .....</b>	<b>132</b>
8.1 Conclusions.....	132
8.2 Contributions to original knowledge .....	133

8.3 Suggestions for future work .....	134
<b>References.....</b>	<b>135</b>
<b>Appendices .....</b>	<b>154</b>

# List of figures

Figure 2.1 – Sketch of negative (A) and positive (B) adsorption at the air-water interface (modified from Foulk and Miller, 1931) .....	15
Figure 2.2 – A) Superior, B) intermediate and C) successor bubble coalescence which creates a growing bubble which is susceptible to fragmentation (© IOP Publishing Ltd and European Physical Society. Reproduced by permission of IOP Publishing. All rights reserved. (Leighton et al., 1991)) .....	18
Figure 2.3 – Schematic of bubble coalescence-induced break-up (Reprinted with permission from Elsevier. (Tse et al., 2003)) .....	19
Figure 2.4 – Bubble coalescence-induced break-up (modified from Finch et al., 2008) .....	19
Figure 2.5 – Schematic of a rising bubble depicting internal and external flow patterns and a surface concentration gradient (Reprinted with permission from Elsevier. (Dukhin et al., 1998)).....	25
Figure 2.6 – Typical single bubble velocity profiles (Reprinted with permission from Elsevier. (Zhang et al., 2001)) .....	27
Figure 2.7 – Left: Terminal velocity of air bubbles in water at 20°C (Reprinted with permission from Dover Publishing, Inc. (Clift et al., 2005)), Right: bubble shapes and the force dominant regimes (modified from Tomiyama and Hayashi, 2002).....	31
Figure 2.8 – Bubble shape regimes (Reprinted with permission of Dover Publications , Inc. (Clift et al., 2005) and Cambridge University Press (Bhaga and Weber, 1981)).....	33
Figure 2.9 – Bubble terminal velocity models for water .....	35
Figure 2.10 – Rise velocities for fast and slow bubbles in tap water (Reprinted with permission from Elsevier. (Peters and Els, 2012)).....	37
Figure 2.11 – A) Velocity and aspect ratio as a function of time and B) velocity as a function of aspect ratio for various solution chemistries (Reprinted with permission from Elsevier. (Kracht and Finch, 2010)).....	38

Figure 2.12 – Bubble velocity as a function of aspect ratio for three bubble sizes (modified from Gomez et al., 2010).....	38
Figure 2.13 – A) The effect of MIBC concentration on bubble rise velocity and aspect ratio (shape), and B) rise velocity as a function of aspect ratio for various solute types (for all concentrations tested) (Reprinted with permission from Elsevier. (Maldonado et al., 2013)) .....	39
Figure 2.14 – Example hydrophone output showing sound emitted upon bubble formation (modified from Leighton and Walton, 1987).....	41
Figure 3.1 – Left: Bubble size distribution (number frequency) in water and 10 ppm MIBC solution, Right: Example image showing large irregular shaped bubbles and fine bubbles (identified by dashed circle) in the water-only system (modified from Quinn et al., 2007)	58
Figure 3.2 – Experimental setup .....	60
Figure 3.3 – Coalescence-induced bubble break-up (note the reduced time interval - 0.5 ms - for final three frames). Bubble produced at 500 $\mu\text{m}$ capillary at 70 sccm. ....	62
Figure 3.4 – Coalescence-induced droplet formation (4 - 8 ms images) and subsequent bubble expulsion (16 and 18 ms images). Bubble produced at 500 $\mu\text{m}$ capillary at 70 sccm.....	63
Figure 3.5 – Coalescence-induced liquid jet formation and subsequent bubble expulsion. Bubble produced at a 500 $\mu\text{m}$ capillary with air flow rate 250 sccm.....	63
Figure 3.6 – Disruption of liquid jet inside bubble leads to droplet which upon impact with the rear bubble wall expels fine bubbles (13 ms image - indicated with dashed circle). Bubbles produced at 500 $\mu\text{m}$ capillary at 250 sccm. ....	64
Figure 3.7 – Wake-related force causes subsequent bubble deformation and break-up. Bubble produced at 500 $\mu\text{m}$ capillary at 250 sccm. ....	65
Figure 3.8 – Fine bubble formed by premature detachment from the orifice due to the wake of a previous bubble. Bubble produced at 500 $\mu\text{m}$ capillary at 100 sccm. ....	65
Figure 3.9 – Schematics showing: a) coalescence-induced bubble break-up, b) coalescence-induced droplet formation and, c) coalescence-induced droplet formation and subsequent bubble break-up. ....	67

Figure 4.1 – Coalescence plot for 1-pentanol (Reprinted with permission from Elsevier. (Kracht and Finch (2009b)).....	74
Figure 4.2 – Experimental set-up.....	75
Figure 4.3 – Example image sequence showing bubble formation, coalescence and/or fine bubble production at A) 5 sccm, B) 15 sccm, C) 25 sccm .....	78
Figure 4.4 – Bubble regime plot for MIBC showing the three regimes and the two major transitions (i.e., ignoring partial coalescence) (Kracht and Finch (2009b) coalescence data shown as x's) .....	79
Figure 4.5 – Bubble size distributions in water and 0.98 mM MIBC solution at various air flow rates.....	80
Figure 4.6 – Number frequency of bubbles below 1 mm and greater than 2.6 mm in water and 0.98 mM MIBC.....	81
Figure 4.7 – Bubble regime plots for commercial frothers (closed markers identify the transition to coalescence and open markers identify the transition to fine bubble production).....	82
Figure 4.8 – Bubble regime plots for 1-alcohols (closed symbols represent lower transition, open symbols represent upper transition).....	83
Figure 4.9 – Bubble regime plots for inorganic salts.....	84
Figure 4.10 – Bubble regime transitions for inorganic salts as a function of ionic strength .....	85
Figure 4.11 – Example images of bubbles formed in water and in 0.98 mM MIBC .....	87
Figure 5.1 – Coalescence plots for MIBC and sodium chloride (modified from Kracht and Finch, 2009).....	96
Figure 5.2 – Experimental set-up.....	97
Figure 5.3 – Example acoustic signals in 0.01 M NaCl at air flow rates of 8 sccm (non-coalescence), 9 sccm (partial coalescence), and 10 sccm (complete coalescence) .....	98
Figure 5.4 – Coalescence plot (transition flow rate vs. concentration) for MIBC (Kracht and Finch (2009) data shown as closed triangles).....	99

Figure 5.5 – Coalescence plot for NaCl (literature data (Lit.) from Kracht and Finch (2009) shown).....	100
Figure 5.6 – Coalescence plots for 0%, 1% and 10% w/w talc in MIBC solution.....	101
Figure 5.7 – Coalescence plots for 0%, 1% and 10% w/w silica in MIBC solution .....	101
Figure 5.8 – Coalescence plots for 0%, 1%, and 10% w/w talc in sodium chloride solution ....	102
Figure 5.9 – Coalescence plots for 0%, 1%, and 10% w/w silica in sodium chloride solution..	103
Figure 6.1 – Experimental setup.....	112
Figure 6.2 – Image analysis procedure: a) original bubble image, b) image after applying threshold, c) ellipse fitting, and d) determination of major (a) and minor (b) semi-axes...	113
Figure 6.3 – Image sequences (at 20 ms time intervals) of a rising bubble in: A) water, B) 0.02 M NaCl, and C) 1 M NaCl solutions (1 mm reference bar is shown above the uppermost bubble in each sequence) .....	115
Figure 6.4 – Example of oscillations in the length of the major and minor axis and the calculated volume equivalent diameter as a function of time in 0.02 M NaCl.....	116
Figure 6.5 – Examples of bubble aspect ratio (upper) and rise velocity (lower) as a function of time in water, 0.02 M NaCl and 1.0 M NaCl.....	117
Figure 6.6 – Examples of the effect of salt (NaClO <sub>4</sub> and KCl) concentration on bubble rise velocity and aspect ratio .....	118
Figure 6.7 – Average bubble rise velocity and aspect ratio for various concentrations of calcium chloride .....	119
Figure 6.8 – Average bubble rise velocity and aspect ratio for various MIBC solutions.....	120
Figure 6.9 – Average bubble rise velocity and aspect ratio for all conditions tested .....	121
Figure 6.10 – Rise velocity and specific bubble surface area for all conditions tested .....	123

## List of tables

Table 2.1 – Example hydrophilic / lipophilic group values used in the Davies equation.....	13
Table 2.2 – HLB values for 1-alcohols and common industrial frothers.....	13
Table 2.3 – Effect of inorganic salts on surface tension gradient.....	14
Table 2.4 – Examples of flotation operations which utilize(d) saline process water .....	16
Table 2.5 – Transition concentrations for inorganic salts.....	22
Table 2.6 – Critical coalescence concentration of common industrial frothers.....	23
Table 2.7 – Summary of various frother characterization techniques .....	24
Table 2.8 – Example Morton numbers for various liquids.....	29
Table 2.9 – Bubble shapes (abbreviations refer to Figure 2.8).....	32
Table 3.1 – Summary of daughter to parent bubble sizes.....	66
Table 4.1 – Reagent specifications .....	76
Table 5.1 – Reagent specifications .....	97
Table 6.1 – Reagents and concentration range .....	112
Table 6.2 – Bubble size population data for each chemistry tested.....	114
Table 6.3 – Bubble aspect ratio (E) and rise velocity (Vel.) at 0.05 M and 0.5 M.....	118

## Figures reproduced with permission

- Figure 2.2     Reproduced from Leighton, T.G., Fagan K.J., and Field, J.E., 1991. Acoustic and photographic studies of injected bubbles. *European Journal of Physics* 12, 77-85, with permission from IOP Publishing Ltd.
- Figure 2.3     Reprinted from *Chemical Engineering Science*, 58, Tse, K.L., Martin, T., McFarlane, C.M., and Nienow, A.W., Small bubble formation via a coalescence dependent break-up mechanism, 275-286, 2003, with permission from Elsevier.
- Figure 2.5     Reprinted from *Studies in Interfacial Science, Drops and Bubbles in Interfacial Research*, Möbius, D., Miller, R. (Eds.), Elsevier Science, 6, Dukhin, S.S., Miller, R., and Loglio, G., Physico-chemical hydrodynamics of rising bubbles, 367-432, 1998, with permission from Elsevier. Reproduced from, 1998, with permission from Elsevier.
- Figure 2.6     Reprinted from *Chemical Engineering Science*, 56, Zhang, Y., McLaughlin, J.B., and Finch, J.A., Bubble velocity profile and model of surfactant mass transfer to bubble surface, 6605-6616, 2001, with permission from Elsevier.
- Figure 2.7     Reprinted from *Bubble, Drops, and Particles*, Clift, R., Grace, J.R., and Weber, M., 2005, with permission from Dover Publications Inc.
- Figure 2.8     Reprinted from *Bubble, Drops, and Particles*, Clift, R., Grace, J.R., and Weber, M., 2005, with permission from Dover Publications Inc.
- Reprinted from *Journal of Fluid Mechanics*, 82, Bhaga, D., and Weber, M.E., Bubbles in viscous liquids: shapes, wakes and velocities, 61-85, 1981, with permission from Cambridge University Press.

- Figure 2.10 Reprinted from *Chemical Engineering Science*, 82, Peters, F., and Els, C., An experimental study on slow and fast bubbles in tap water. 194-199, 2012, with permission from Elsevier.
- Figure 2.11 Reprinted from *International Journal of Mineral Processing*, 94, Kracht, W., and Finch, J.A., Effect of frother on initial bubble shape and velocity, *International Journal of Mineral Processing*, 115-120, 2010, with permission from Elsevier.
- Figure 2.13 Reprinted from *Chemical Engineering Science*, 98, Maldonado, M., Quinn, J.J., Gomez, C.O., and Finch, J.A., An experimental study examining the relationship between bubble shape and rise velocity, 7-11, 2013, with permission from Elsevier.
- Figure 4.1 Reprinted from Kracht, W., and Finch, J.A., *Journal of Colloid and Interface Science*, 332, Using sound to study bubble coalescence, 237–245, 2009, with permission from Elsevier.

# Chapter 1 – Introduction

## 1.1 Introduction

Froth flotation is a process used to selectively separate particles based on surface hydrophobicity and is widely used in the mining industry to separate minerals. Initially used to process base-metal sulphide minerals, flotation is presently used for a wide variety of minerals (e.g., oxides, silicates, salts) and energy resources such as coal and bitumen.

Frothers (surfactants) are typically added to flotation circuits to reduce bubble size in the dispersion of gas (air) in the pulp phase and to promote frothing. Over the past decades, water availability and quality has become a major issue facing the mining industry. The limited availability of fresh water in many remote mining locales has forced flotation operations to recycle water, or to use sea or hyper-saline bore water (Alexander et al., 2012). Research has shown that the presence of certain soluble inorganic salts can replace the function of frother (Quinn et al., 2007).

The flotation process evolved in the mid-to-late 1800's. Much of the early flotation work involved bulk-oil flotation (patented by William Haynes, 1860). These techniques employed large amounts of oil that formed agglomerates with the desired mineral which rose through the slurry due to buoyancy (due to the oil and most probably air entrained in the agglomerates).

Gebrueder Bessel patented a process in 1877 for the recovery of graphite which closely resembles present-day flotation practice (Lynch et al., 2007). The process involved mixing ground feed slurry with 1-10% non-polar oil and bringing it to a boil. The graphite particles attached to the bubbles and rose to the surface where they were skimmed off.

A widely used bulk-oil process was patented by Francis and Alexander Elmore in 1898 for processing of lead sulphide minerals. Advancements to the process were patented in 1905 and employed a machine which applied vacuum to generate fine bubbles (Fuerstenau, 1999). Techniques at the time employed various methods of bubble generation: boiling, air entrainment during mixing, pressure reduction, or the addition of acid to carbonate bearing ore which would generate carbon dioxide gas (Fuerstenau, 2007).

The modern flotation process is commonly attributed to a patent by Alcid Fromont in 1902 which utilized minute amounts of oil and gas bubbles (Lynch et al., 2007). The patent was later purchased by Mineral Separations Ltd. (1903) who went on to patent several processes that resemble current flotation practice (although pneumatic flotation machines, widely used today, were only developed ca. 1915 (Nesset, 2008)).

The first major commercial flotation operation began in 1905 at Broken Hill, Australia (Broken Hill Proprietary (BHP)) and produced sphalerite concentrate (Lynch et al., 2007). The flotation process replaced traditional gravity circuits. Flotation spread and the Butte and Superior Copper Company operated the first U.S. operation at Basin, Montana starting in 1911 (separating fine sphalerite from galena) (Fuerstenau, 2007). The first use of flotation in Canada occurred at the Britannia Beach Copper mine in 1912 which was the first application for copper minerals (Nesset, 2008). It was noted that the widespread use of the flotation process was somewhat impeded in the early days due to litigation surrounding patent infringement (Lynch et al., 2007).

Growth in the industry and the advent of chemical companies producing reagents specifically for the flotation process greatly improved process performance. One major breakthrough was the decoupling of the action of collectors and frothers. The introduction of water-soluble thiocarbanilid as a collector improved the operability of the flotation circuit (Perkins and Sayre, 1921; Fuerstenau, 2007). One operator described the development: “thiocarbanilid for the first time gave the laboring metallurgist something that he could add which would improve the collection of the sought-for mineral without, at the same time, increasing the frothing to an uncontrollable degree” (Bean, 1971).

Historically, natural oils (e.g., eucalyptus or pine oil) were used as frothers (Wills and Napier-Munn, 2006). These reagents typically contained collecting properties which could interfere with the separation process. The grade of the natural oils was not constant which complicated control. In a similar fashion to the introduction of thiocarbanilid, the introduction of synthetic non-collecting frothers (e.g., methyl isobutyl carbinol (MIBC, 4-methyl-2-pentanol) and the Dowfroth line of frothers (polypropylene glycol (PPG) ether-type)) allowed for the independent control of collecting and gas dispersion and frothing properties. MIBC and PPG ethers are the most commonly used frothers and accounted for 80-90% of all frothers used in metallic ore

flotation (Pugh, 2007). Many types of synthetic frothers are now available and researchers continue to develop new chemistries to better suit industry needs (Cappuccitti and Finch, 2007).

Early investigators noted the importance of bubbles in the flotation process. T.A. Rickard (1916) stated “the key to the flotation process is to be found not in the oil, the acid, or the apparatus, but in the bubbles.” Gaudin (1934) later said “it is not unlikely that control of flotation can be exercised through control of the gas.”

The effect of reagent type on the process was noted: “An effective froth represents a multiplicity of persistent bubbles. The relative stability of the bubbles depends also upon the kind of oil employed. Pine-oil makes a brittle film: creosote yields an elastic envelope” (Rickard, 1916). More recently, the terms ‘selective’, ‘powerful’, ‘weak’ or ‘strong’ have been used to qualitatively characterize frother strength (Cho and Laskowski, 2002a,b; Cappuccitti and Finch, 2007). It was only in the mid-1970s that laboratory characterization techniques were developed specifically to characterize flotation frothers based on gas dispersion (Pomianowski et al., 1973). Since then, research has placed an emphasis on understanding the role gas dispersion plays in the flotation process. The development of industrial gas dispersion sensors (Gomez and Finch, 2002, 2007), analytical techniques to measure frother concentration (Gélinas and Finch, 2005, 2007), and procedures to quantify the effect of surfactants and inorganic salts (Cho and Laskowski, 2002a,b; Azgomi et al., 2007; Quinn et al., 2007) have allowed for improved understanding of the role of gas dispersion. Gorain et al. (1997) systematically studied the role of gas dispersion properties on particle collection and showed that the rate of flotation was directly related to the available surface area of bubbles passing through the cell (bubble surface area flux,  $S_b$ ). It is evident that understanding bubble behaviour is fundamental as bubbles collect and transport hydrophobic particles from the pulp phase to the froth phase (and then to the launder for collection).

The mechanisms resulting in bubble formation at a gas dispersing device and the effect frothers have on bubble formation are not well understood. Much of the research literature has focused on frothers’ ability to hinder bubble coalescence. Few studies have considered the possible effect of frothers on bubble break-up though several researchers (Crozier and Klimpel, 1989; Leighton et al. 1991; Hofmeier et al., 1995; Grau and Laskowski, 2005; Finch et al., 2008; Kracht and Finch, 2009a) have hinted at the importance of break-up in dictating gas dispersion properties. Test

procedures are required that are able to discriminate between an anti-coalescence and a break-up mechanism. This would help explain bubble size reduction in the presence of frother, inorganic salt, or, indeed, solid particles. Researchers have linked break-up to a coalescence-induced mechanism, meaning the two processes are possibly linked to one another (Tse et al., 2002; Quinn et al., 2012). Bubble size and shape also appear to play a role in the break-up process.

Measuring gas dispersion properties in a 3-phase slurry can be difficult. Visual measurements are typically impossible due to the opacity of the slurry. Special techniques have been developed to measure gas dispersion properties using various signals (e.g., pressure or conductivity) or specialized sampling methods (Gomez and Finch, 2002, 2007). Recently, the use of passive acoustic emission monitoring has been implemented in the laboratory (Kracht and Finch, 2009b) and in industry (Vanegas et al., 2010; Spencer et al., 2010) to measure properties related to gas dispersion and particle collection. Bubbles produce sound when they coalesce and break-up and acoustic monitoring enables detection of these events.

An often overlooked role of frother is the reduction in the rate at which bubbles rise through the cell (Klimpel and Isherwood, 1991). For typical bubble sizes present in flotation systems (ca. 0.5 - 3 mm diameter), frothers and inorganic salts have been shown to reduce single bubble rise velocity (Fuerstenau and Wayman, 1958; Detsch, 1991; Nasset et al., 2006). The reduction in velocity has been linked to change in the shape of the rising bubble (Fuerstenau and Wayman, 1958; Jameson, 1984; Tomiyama et al., 2002; Clift et al., 2005). Investigations into how different solute types affect this relationship will further our understanding of single bubble systems and possibly provide clues as to the behaviour of bubbles in a swarm.

## **1.2 Thesis objectives**

The objective of the thesis is to determine the effect of frothers and inorganic salts on bubble coalescence and break-up, and the shape - rise velocity relationship. Specific objectives include:

1. Determination of the processes of bubble coalescence and break-up at a capillary
2. Determine the effect of frother and inorganic salts on bubble coalescence and break-up at a capillary in a two-phase (solution-air) system

3. Determine coalescence behaviour using acoustic emission monitoring in the presence of hydrophobic and hydrophilic particles (three-phase system, solution-air-solids) with frother or inorganic salt present
4. Determine the relationship between bubble shape and rise velocity in frother and inorganic salt solutions

### **1.3 Thesis structure**

The thesis is presented as a ‘manuscript-based’ thesis. The thesis comprises eight chapters. Chapter 1 gives an introduction to froth flotation, a brief history of the process and the role of frothers and inorganic salts. Four of the chapters are manuscripts (chapters 3 - 6). Chapters 3 and 6 have been published in Minerals Engineering:

Quinn, J.J., and Finch, J.A., 2012. On the origin of bi-modal bubble size distributions in the absence of frother. *Minerals Engineering* 36, 237-241.

Quinn, J.J., Maldonado, M., Gomez, C.O., and Finch, J.A., 2014. Experimental study on the shape - velocity relationship of an ellipsoidal bubble in inorganic salt solutions. *Minerals Engineering* 55, 5-10.

Chapters 4 and 5 will be submitted for publication. Chapter 7 presents a unifying discussion which links the individual topics covered in each manuscript. Finally, Chapter 8 presents conclusions, contributions to knowledge and suggestions for future work.

### **1.4 Contribution of authors**

All the manuscripts are co-authored by Prof. James A. Finch in his capacity as research supervisor. The manuscript entitled ‘Experimental study on the shape - velocity relationship of an ellipsoidal bubble in inorganic salt solutions’ (Chapter 6) was also co-authored by Dr. Miguel Maldonado (Post-doctoral fellow), and Dr. Cesar O. Gomez (Senior research associate), both of McGill University. Dr. Maldonado aided in running the experiments (i.e., image acquisition) and Dr. Gomez assisted in proofreading the manuscript. Jarrett Quinn performed the experiments,

image analysis, data tabulation and analysis for all the tests and wrote the first draft of each chapter and considered the comments of the co-authors in preparation of the final manuscripts.

## References

Alexander, S., Quinn, J., van der Spuy, J.E., and Finch, J.A., 2012. Correlation of graphite flotation and gas holdup in saline solutions. In: Drelich, J. (Ed.), *Water in Mineral Processing: Proceedings of the First International Symposium*, SME, 41-50.

Azgoni, F., Gomez, C.O., and Finch, J.A., 2007. Characterizing frothers using gas hold-up. *Canadian Metallurgical Quarterly* 46, 3, 237-242.

Bean, J.J., May 1971. Tale of tails. *Mining World*, 59.

Cappuccitti, F., and Finch, J.A., 2007. Development of new frothers through hydrodynamic characterization. In: Folinsbee, J. (Ed.), *Proceedings 39th Annual Meeting of the Canadian Mineral Processors of CIM*, 399-412.

Cho, Y.S., and Laskowski, J.S., 2002a. Effect of flotation frothers on bubble size and foam stability. *International Journal of Minerals Processing* 64, 69-80.

Cho, Y.S., and Laskowski, J.S., 2002b. Bubble coalescence and its effect on bubble size and foam stability. *Canadian Journal of Chemical Engineering* 80, 299-305.

Crozier, R.D., and Klimpel, R.R., 1989. Frothers: Plant practice. *Mineral Processing and Extractive Metallurgy Review*, 5, 1-4, 257-279.

Detsch, R.M., 1991. Small air bubbles in reagent grade water and seawater: Rise velocities of 20 to 1000- $\mu\text{m}$  diameter bubbles. *Journal of Geophysical Research* 96, C5, 8901-8906.

Elmore, F.E., 1898. British Patent 21,948.

Fuerstenau, D.W., 1999. The froth flotation century. In: Parekh, B.K., and Miller, J.D. (Eds.), *Advances in Flotation Technology*. SME, 3-21.

Fuerstenau, D.W., 2007. A century of developments in the chemistry of flotation processing. In: Fuerstenau, M.C., Jameson, G.J., and Yoon, R.H. (Eds.), *Froth Flotation: A Century of Innovation*. SME, 3-64.

Fuerstenau, D.W., and Wayman, C.H., 1958. Effect of chemical reagents on the motion of single air bubbles in water. *Mining Engineering, Transactions of AIME*, 694-699.

Gaudin, A.M., 1934. Flotation's future beset with difficult problems. *Engineering and Mining Journal* 135, 1, 29.

Gebrueder Bessel, 1877. Verfahren zur Reinigung von Graphit (process for the purification of graphite). German patent 42, Class 22.

Gelinas, S., and Finch, J.A., 2005. Colorimetric determination of common industrial frothers. *Minerals Engineering* 18, 2, 263-266.

Gélinas, S., and Finch, J.A., 2007. Frother analysis: Some plant experience. *Minerals Engineering* 20, 14, 1303-1308.

Gomez, C.O., and Finch, J.A., 2002. Gas dispersion measurements in flotation machines. *CIM Bulletin* 95, 1066, 73-78.

Gomez, C.O., and Finch, J.A., 2007. Gas dispersion measurements in flotation cells. *International Journal of Mineral Processing* 84, 1-4, 51-58.

Gorain, B.K., Franzidis, J.P., and Manlapig, E.V., 1997. Studies on impeller type, impeller speed and air flow rate in an industrial flotation cell. Part 4: Effect of bubble surface area flux on flotation performance. *Minerals Engineering* 10, 4, 367-379.

Haynes, W., 1860. British Patent 488.

Jameson, G.J., 1984. Physics and hydrodynamics of bubbles. In: Ives, K.J. (Ed.), *The Scientific Basis of Flotation. Series E: Applied Sciences – No. 75*. Martinus Nijhoff Publishers, Boston, 53-78.

Klimpel, R.R, and Isherwood, S., 1991. Some industrial implications of changing frother chemical structure. *International Journal of Mineral Processing* 33, 369-381.

Kracht, W., and Finch, J.A., 2009a. Bubble break-up and the role of frother and salt. *International Journal of Mineral Processing* 92, 153–161.

Kracht, W., and Finch, J.A., 2009b. Using sound to study bubble coalescence. *Journal of Colloid and Interface Science* 332, 237–245.

Lynch, A.J., Watt, J.S., Finch, J.A., and Harbort, G.E., 2007. History of flotation technology. In: Fuerstenau, M. C., Jameson, G. J., and Yoon, R. H. (Eds.), Froth Flotation: A Century of Innovation. SME, 65-92.

Nesset, J.E., Hernandez-Aguilar, J.R., Acuna, C., Gomez, C.O., and Finch, J.A., 2006. Some gas dispersion characteristics of mechanical flotation machines. Minerals Engineering 19, 807-815.

Nesset, J.E., 2008. 100 years of blowing bubbles for profit (with an emphasis on the bubbles). CIM Distinguished Lecturer 2008-2009.

Perkins, C.L., and Sayre, R.E., 1921. Flotation of Minerals, United States Patent Office, serial number 284,981. Publication number US1364308 A.

Pomianowski, A., Malysa, K., and Para, G., 1973. Annual Report for the Institute of Nonferrous Metals, 6.

Pugh, R.J., 2007. The physics and chemistry of frothers. In: Fuerstenau, M.C., Jameson, G., and Yoon, R.-H. (Eds.), Froth Flotation: A Century of Innovation, SME, 259-281.

Quinn, J.J., and Finch, J.A., 2012. On the origin of bi-modal bubble size distributions in the absence of frother. Minerals Engineering 36, 237-241.

Quinn, J.J., Kracht, W., Gomez, C.O., Gagnon, C., and Finch, J.A., 2007. Comparing the effects of salts and frother (MIBC) on gas dispersion and froth properties. Minerals Engineering 20, 1296-1302.

Rickard, T.A. (Ed.), 1916. The Flotation Process, Mining and Scientific Press, Dewey Publishing Company, San Francisco.

Spencer, S.J., Bruniges, R., Roberts, G., Sharp, V., Catanzano, A., Bruckard, W.J., Davey, K.J., and Zhang, W., 2012. An acoustic technique for measurement of bubble solids mass loading: (b) Monitoring of Jameson cell flotation performance by passive acoustic emissions. Minerals Engineering 36, 21-30.

Tomiyama, A., Celata, G.P., Hosokawa, S., and Yoshida, S., 2002. Terminal velocity of single bubbles in surface tension force dominant regime. International Journal of Multiphase Flow 28, 1497-1519.

Vanegas, C., and Holtham, P., 2008. On-line froth acoustic emission measurements in industrial sites. *Minerals Engineering* 21, 883–888.

Wills, B.A., and Napier-Munn, T., 2006. *Wills' Mineral Processing Technology: An Introduction to the Practical Aspects of Ore Treatment and Mineral Recovery*. Butterworth-Heinemann, Burlington, MA, USA.

# Chapter 2 – Literature review

## 2.1 Frothers: Chemistries and classifications

Frothers are added to flotation systems to decrease bubble size in the pulp phase and promote frothing. A frother is a surface active agent (surfactant) whose molecular structure is generally hetero-polar. The molecule consists of a polar head group, which readily attracts water molecules, and a non-polar hydrocarbon chain which has little interaction with water. The hetero-polar nature of the molecules promotes adsorption at the air-water interface. Frothers decrease bubble size in the pulp phase by inhibiting bubble coalescence. Coalescence occurs when bubbles interact in such a way as to rupture the intervening water film between the bubbles, thus forming a larger bubble from two (or more) smaller ones. A combination of properties, Gibbs elasticity (which stabilizes a film in response to a mechanical disturbance) and the Marangoni effect (which induces flow in liquid adjacent to the interface) form the basis for understanding how frothers resist coalescence (Harris, 1982; Pugh, 1996; Finch et al., 2008). The concentration of frother at the air-water interface determines the surface tension and thus variations in concentration (e.g., due to mechanical disturbances) produce surface tension gradients, i.e. a force which opposes film drainage.

Klimpel and Isherwood (1991) qualitatively summarized the role of frother in flotation processes:

- 1) Enhanced froth formation
- 2) Increased air dispersion in the flotation cell
- 3) Reduction in the rate at which the bubbles rise to the surface (increased bubble residence time)
- 4) Reduction in the coalescence of individual bubbles within the flotation pulp

The first frother used in mineral flotation was eucalyptus oil, widely available in Australia where the first large-scale flotation process was operated in the early 1900's (Wills and Napier-Munn, 2006). As flotation expanded to North America and Europe, pine oil (which contains aromatic alcohols and whose main component is  $\alpha$ -terpineol) became the most widely used frother primarily due to its low cost and wide availability (Wills and Napier-Munn, 2006; Crozier and

Klimpel, 1989). Cresol (cresylic acid) has also seen wide use (Wills and Napier-Munn, 2006). The use of natural oils diminished over the years due principally to the inability to maintain quality. Some collecting properties of the natural oils also interfered with process selectivity (Crozier and Klimpel, 1989; Wills and Napier-Munn, 2006). The presence of collecting and frothing properties in the same reagent often makes selective flotation difficult (Wills and Napier-Munn, 2006).

Methyl isobutyl carbinol, MIBC, a synthetic non-collecting reasonably soluble alcohol, has been the most widely used frother for decades. Polypropylene glycol (PPG) ethers (e.g., Dowfroth 250) have also seen widespread use in industry since the early 1950's. Pugh (2007) estimated that MIBC and PPG ethers accounted for 80-90% of all frothers used in metallic ore flotation. Many types of synthetic frothers are now available and reagent companies continue to develop new frothers to better suit industry needs (Cappuccitti and Finch, 2007; Aston et al., 2013). Availability and cost are still major drivers but many operations look to new frothers or frother blends which are tailored to the operation (Riggs, 1986; Zhang et al., 2012b).

Alcohols are organic compounds which contain a hydroxyl ( $\text{OH}^-$ ) functional group bound to a carbon atom in a hydrocarbon chain. There are three main categories of alcohols which are used as frothers: aliphatic, cyclic and aromatic. Methyl isobutyl carbinol is a branched structure, with the formal chemical name 4-methyl-2-pentanol. Alcohols are structurally related to water,  $\text{H}_2\text{O}$  ( $\text{HOH}$ ), in that both possess a hydroxyl function (Roberts and Caserio, 1977). The  $\text{OH}^-$  group is polar, meaning molecules associate with one another which decreases volatility, raises melting points and increases solubility in polar liquids (water). Water-solubility of alcohols falls off rapidly with increasing length of the carbon chain. Once the hydrocarbon chain is sufficiently long, typically six or more carbon atoms, the hydrocarbon (hydrophobic) nature becomes dominant and dictates physical properties (Roberts and Caserio, 1977). Alcohols employed as frothers in flotation contain 5 to 8 carbon atoms. Availability, cost, solubility and the fact that alcohols have practically no collecting properties make them practical choices for industry (Wills and Napier-Munn, 2006).

Polyglycols emerged in the early 1950's (Dowfroth (DF) range of products) and usage as frothers quickly grew. The term "glycol" indicates a diol, which is a substance with two alcoholic hydroxyl groups. Polyhydric alcohols in which the hydroxyl groups are situated on

different carbons are relatively stable and have high boiling points and considerable water solubility (Roberts and Caserio, 1977). The polyglycol group presents great flexibility with varying molecular weight and chemical structure allowing for control of the flotation process (Klimpel and Isherwood, 1991). Solubility of this group ranges from totally miscible to partially soluble, depending on the nature of the molecule. Trade names for polyglycols include the Dowfroth line of products, Cytec Oreprep 549 and Cytec Aerofroth 65 (Wills and Napier-Munn, 2006).

### 2.1.1 Hydrophilic-lipophilic balance (HLB)

The concept of hydrophilic-lipophilic balance (HLB) was developed to quantify the molecular structure of surfactants (Griffin, 1949, 1954; Davies, 1957). The term lipophilic refers to an affinity (-philic) for oil (lipo-). In relation to flotation frothers, the term lipophilic is analogous to hydrophobic (water repellent or an affinity for air). The measure quantifies the degree of hydrophobicity of surfactants (frothers) based on the nature of the molecule and the various groups it contains. The most commonly used method of determining HLB is by Davies (1957) developed to characterize surfactants used in the cosmetics industry. The method accounts for the degree of hydrophobicity / hydrophilicity of each constituent group. High HLB values (>7) indicate hydrophilic surfactants and low values (<7) hydrophobic compounds. The HLB calculation is shown in Equation (2.1).

$$HLB = 7 + \sum mH_h + \sum nH_l \quad (2.1)$$

where:

- $m$  = Number of hydrophilic groups in the molecule
- $H_h$  = Value of the hydrophilic group
- $n$  = Number of lipophilic groups in the molecule
- $H_l$  = Value of the lipophilic group

Example hydrophilic ( $H_h$ ) / lipophilic ( $H_l$ ) values for functional groups are given in Table 2.1.

**Table 2.1 – Example hydrophilic / lipophilic group values used in the Davies equation**

<b>Group</b>		<b>H Value</b>
-OH	Hydrophilic	1.9
-O-	Hydrophilic	1.3
-CH-, CH <sub>2</sub> , -CH <sub>3</sub> -, =CH	Lipophilic	-0.475

Table 2.2 outlines HLB values for 1-alcohols and frothers commonly used in industry (Laskowski, 2004; Zhang et al., 2012a). Water solubility decreases with decreasing HLB value due to the hydrophobic nature of the molecule.

**Table 2.2 – HLB values for 1-alcohols and common industrial frothers**

<b>Frother</b>	<b>HLB</b>
1-Pentanol	6.53
1-Hexanol	6.05
1-Heptanol	5.58
1-Octanol	5.1
MIBC	6.1
DF-250	7.83
F150	8.63

## **2.2 Inorganic salts**

It has been well documented that certain inorganic salts inhibit bubble coalescence (Marrucci and Nicodemo, 1967; Lessard and Zieminski, 1971; Craig et al., 1993; Hofmeier et al., 1995; Laskowski et al., 2003). Inorganic ions slow film drainage and hinder coalescence. There is evidence that specific ion hydration effects play a role in determining the magnitude of the anti-coalescence force (Craig, 2004).

Researchers have determined transition concentrations at which salts inhibit bubble coalescence (Lessard and Zieminski, 1971; Craig et al., 1993; Zahradnik et al., 1999; Christenson et al., 2008). The majority of the tests involve contacting bubble pairs and determining the proportion of coalescing bubbles as a function of salt concentration. Zieminski and Whittemore (1971) have shown that many ions of high valence have a greater ability to hinder bubble coalescence

compared to mono-valent ions. Craig et al. (1993) created a combining rule (table) which assesses whether a given cation / anion pair would inhibit bubble coalescence. This table does not predict the magnitude of anti-coalescence. Researchers have shown correlations between ionic strength and bubble size (Zieminski and Whittemore, 1971; Onken and Kietel, 1982) and gas holdup (Quinn et al., 2007).

The gas dispersion properties of certain inorganic salt solutions are similar to those produced by frothers. Quinn et al. (2007) showed that a 0.4 M ionic strength solution behaved similarly to a solution of 8 - 10 ppm MIBC in terms of increase in gas holdup and decrease in bubble size. There are, however, significant differences between inorganic salts and frothers. The first is the need for high salt concentrations (> 0.05 M) for coalescence inhibition (Lessard and Zieminski, 1971; Craig et al., 1993; Zahradnik et al., 1999) compared to a few parts per million (< 1 mM) of frother.

The majority of inorganic ions in water, especially those containing multi-valent ions, have a net attraction towards the bulk solution and away from the air-water interface as they favor being fully hydrated and cause surface tension to increase. Surface tension typically increases linearly with salt concentration, thus one can compare the change in surface tension with change in concentration ( $d(\Delta\gamma)/dC$ ) to compare inorganic salts (Table 2.3).

**Table 2.3 – Effect of inorganic salts on surface tension gradient**

Salt	$d(\Delta\gamma)/dC^*$ mN/m
NaClO <sub>4</sub>	0.73
KCl	1.60
NaCl	1.55
Na <sub>2</sub> SO <sub>4</sub>	2.96
CaCl <sub>2</sub>	3.22
MgSO <sub>4</sub>	2.24

\*Pugh et al. (1997)

Ions are commonly referred to as ‘structure breaking’ or ‘structure making’ depending on their propensity towards the air-water interface or towards the bulk solution, respectively (Bonner and

Jumper, 1973). The ion size, charge, and the presence of strong, specific interactions between ions and water molecules seem to dictate their effect on water structure (Bonner and Jumper, 1973). As depicted in Figure 2.1, Foulk and Miller (1931) noted that both positive and negative adsorption could lead to the formation of stable films. The schematic depicts: A) negative adsorption where the interfacial solute concentration is lower than in the bulk solution, the case for most inorganic salts; and B) positive adsorption where the interfacial concentration is higher than the bulk solution, similar to the case of a frother.

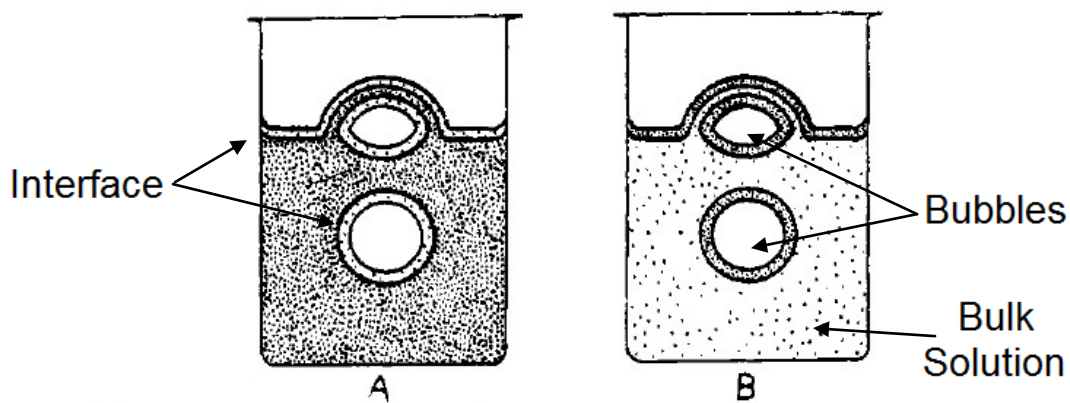


**Figure 2.1 – Sketch of negative (A) and positive (B) adsorption at the air-water interface (modified from Foulk and Miller, 1931)**

Given the large concentration of inorganic salts needed they will not be used in place of frothers. However, several mineral flotation operations around the world use water with high inorganic salt content such as sea or bore water, or as the result of processing soluble minerals. Water recycling can also lead to increased salt content. Sea water contains roughly 35 g/L dissolved salts. A number of operations (mostly in Australia) use hyper-saline bore water (higher salinity than sea water) which can be saturated in dissolved salts. Table 2.4 gives examples of flotation concentrators that utilize(d) highly saline process water and typical compositions (Haig-Smillie, 1972; George, 1996; Nessel et al., 2007; Laskowski et al. 2003b; Quinn et al., 2007; Cole, 2009; Peng and Seaman, 2011; Castro, 2012; Dunne, 2012; Blin and Dion-Ortega, 2013). An extreme case is potash processing where flotation occurs in a saturated brine solution.

An example of a flotation plant with high inorganic salt (Table 2.4) concentration is Xstrata's Raglan operation in northern Quebec. Major sources include the addition of calcium chloride in

the mine to prevent freezing and the use of soda ash for pH control. The mill has a closed-loop recycle water system which causes the build-up of soluble inorganic species in the process water. As an apparent consequence, the flotation circuit operates effectively without the use of frother (Quinn et al., 2007). This observation corresponds to previous evidence suggesting that flotation in salt water results in lower reagent consumption (Haig-Smillie, 1974; Yoon and Sabey, 1989).

**Table 2.4 – Examples of flotation operations which utilize(d) saline process water**

Operation	Location	Water Type	TDS* (ppm)	Major Elements
Texada (Texada Mines) Black Angel (Angel Mining) Las Luces (Grupo Cenizas) PTNNT- Batu Hijau (Newmont) Minera Esperanza (AMSA)	Canada Greenland Chile Indonesia Chile	<b>Sea</b>	~35 000	Na <sup>+</sup> , Cl <sup>-</sup>
Raglan (Glencore Xstrata)	Canada	<b>Recycle</b>	~30 000	Na <sup>+</sup> , Ca <sup>2+</sup> , SO <sub>4</sub> <sup>2-</sup> , S <sub>2</sub> O <sub>3</sub> <sup>2-</sup>
Mt. Keith (BHP-B) Leinster (BHP-B) Kanowna Belle (Barrick) Fimiston (KCGM)	Australia	<b>Bore</b>	60 000 – 120 000	Na <sup>+</sup> , K <sup>+</sup> , Ca <sup>2+</sup> , Mg <sup>2+</sup> , Cl <sup>-</sup> , SO <sub>4</sub> <sup>2-</sup>
Potash	Various	<b>Brine</b>	~ 450 000 saturated	Na <sup>+</sup> , K <sup>+</sup> , Cl <sup>-</sup>

\* Total dissolved solids (TDS)

### 2.3 Bubble formation, coalescence and break-up

Hofmeier et al. (1995) discussed bubble interactions in bubble swarms produced at an orifice as a function of gas flow rate:

- 1) At low gas flow rates bubbles are released individually. Anti-coalescence agents have little effect on bubble generation.
- 2) At intermediate gas flow rate bubbles begin to interact in proximity to the orifice: In pure liquids, bubbles are more likely to coalesce and create larger bubbles. In systems containing anti-coalescence agents, bubbles are more likely to bounce creating a system with finer bubbles.

- 3) At high gas flow rates the system becomes chaotic with large bubbles being formed through coalescence and fine bubbles due to break-up. According to Hofmeier et al. the nature of the solute no longer has significant influence on events at the orifice but does influence the bubbles further away generally retarding coalescence. Fine bubbles are produced by inertia from a preceding bubble causing subsequent bubbles to break away from the tip prematurely (before they have grown to full size) and by the break-up of large unstable bubbles.

At sufficiently low gas rate bubble size is determined by orifice dimensions and solution surface tension, given by the Tate equation (Tate, 1864; Hernandez-Aguilar et al., 2006). At concentrations of industrial interest frothers and salts have little impact on surface tension and thus little impact on the size of a single bubble produced at a capillary as shown by several authors (Hofmeier et al., 1995; Zhang and Shoji, 2001; Cho and Laskowski 2002a). The effect of frothers or salts is only seen once bubbles begin to interact, typically close to the point of bubble generation (Marrucci and Nicodemo, 1967). Bubble interactions at a capillary can be controlled using gas flow rate.

Marrucci and Nicodemo (1967) ascribed increased coalescence at higher gas flow rates to the increase in the number of bubbles produced which increases collision frequency and convection forces which result in more effective coalescence-inducing impacts.

Leighton et al. (1991) discussed coalescence events (occurring at sufficiently high gas flow rates) at a capillary in terms of superior (A), intermediate (B), and successor (C) bubbles which allow the smaller bubbles to be continually 'pumped into' the growing larger bubble (Figure 2.2).

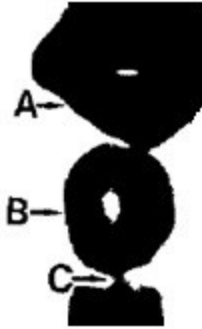


**Figure 2.2 – A) Superior, B) intermediate and C) successor bubble coalescence which creates a growing bubble which is susceptible to fragmentation (© IOP Publishing Ltd and European Physical Society. Reproduced by permission of IOP Publishing. All rights reserved. (Leighton et al., 1991))**

The process is repeatable several times until the growing bubble outpaces the subsequent ones (Hofmeier et al., 1995). Coalescence events have been variously described as the formation of secondary bubbles (Kupferberg and Jameson, 1969), bubble pairing and doubling (Miyahara et al., 1982, 1984; Kyriakides et al., 1997) and a swallowing up process (Osterwegel and de Groot, 1980).

With increasing gas flow rate the surface tension force no longer determines bubble size and bubbles become large, variable in shape (i.e., unstable) and prone to fragmentation (Leighton, 1994). It was noted that the range of bubble size produced at high gas flow rates can be very wide. Ohnishi et al. (1999) discussed a mechanism for secondary bubble creation induced by bubble coalescence. One possible explanation presented was that the rapid deformation process upon coalescence produced one or two lobes at one or both ends of the bubble which could lead break away.

Schäfer et al. (2002) showed visual evidence of bubble break-up at a nozzle. They noted that an increase in pressure led to an increase in break-up and related the effect to inertia of the gas in the fluctuating bubble.

Tse et al. (2003) described a mechanism for small bubble formation based on bubble break-up induced by bubble coalescence. Upon coalescence, they argued, an annular wave is created in the newly formed bubble which travels the length of the bubble resulting in extension and pinching-off of a daughter bubble (Figure 2.3). Tse et al. (2003) contacted bubbles at two facing

capillaries and noted this break-up mechanism. Bubble break-up was also shown to occur in the swarm away from the bubble generation device.

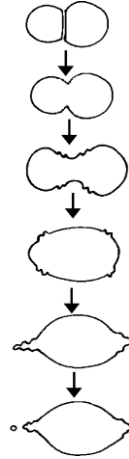


**Figure 2.3 – Schematic of bubble coalescence-induced break-up (Reprinted with permission from Elsevier. (Tse et al., 2003))**

Finch et al. (2008) also demonstrated bubble coalescence-induced break-up close to the point of bubble generation at a single node of a slot sparger (Figure 2.4). An initial bubble is formed and released from the slot with a subsequent bubble drawn into the low pressure region behind the initial bubble resulting in bubble coalescence. They suggested that as the distorted bubble recoils to attain a more spherical shape a ‘daughter’ bubble is expelled.

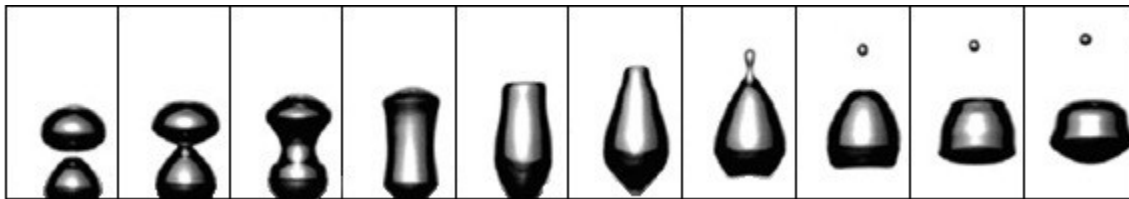


**Figure 2.4 – Bubble coalescence-induced break-up (modified from Finch et al., 2008)**

Zhang and Thoroddsen (2008) studying coalescence-induced break-up showed that for equal sized parent bubbles, the size of the daughter bubble is roughly  $1/10^{\text{th}}$  that of the mother bubble.

The authors, using high-speed video imaging, characterized the capillary waves which converge at the bubble apex and pinch off the daughter bubble.

The break-up of air bubbles in surfactant-free systems has been related to surface instabilities initiated by turbulence. Several authors (Lee et al., 1987; Prince and Blanch, 1990; Miyahara et al., 1991; Stewart, 1995) have attributed both coalescence and break-up events to wake forces (turbulence or bubble wake eddy collisions). Coalescence, detachment and bubble collisions (with or without coalescence) lead to bubble shape oscillations (Leighton et al., 1991; Leighton, 1994). Hofmeier et al. (1995) attributed the oscillations upon coalescence to the sudden release of surface energy which could result in bubble break-up. Leighton (1994) demonstrated that shape oscillations in one bubble could cause a bubble in close proximity to break-up. Martinez-Bazan et al. (2000) and Hesketh et al. (1991) noted that bubble size was an important factor, and that there was a critical size above which bubbles were prone to break-up. Several authors have also attempted to determine a critical Weber number (which is a function of bubble size) above which break-up occurs (Hinze, 1955; Sevik and Park, 1973; Lewis and Davidson, 1982; Wilkinson et al., 1993).

## **2.4 Frother characterization techniques**

In the early days of flotation it became evident that various reagents modified gas dispersion and froth properties in different ways. T.A. Rickard (1916) in the classic monograph ‘The Flotation Process’ noted “an effective froth represents a multiplicity of persistent bubbles. The relative stability of the bubbles depends upon the kind of oil employed. Pine-oil makes a brittle film: creosote yields an elastic envelope”. More recently, the terms selective and powerful were common in the literature to describe frother strength, typically focusing on froth properties (Crozier and Klimpel, 1989; Klimpel and Isherwood, 1991; Cytec, 2002; Laskowski, 2004; Wills and Napier-Munn, 2006). MIBC and alcohol-type frothers are typically considered to be selective while polyglycol-type frothers are considered powerful (Crozier and Klimpel 1989; Cytec, 2002). The terms strong and weak have also been used, in a similar manner, to describe how frother affects gas dispersion properties (Cappuccitti and Nasset, 2009).

The last three decades have seen the development of sensors and techniques to measure gas dispersion properties (Finch and Dobby, 1990; Tucker et al., 1994; Chen et al., 2001; Hernandez-

Aguilar et al., 2002; Gomez and Finch, 2002, 2007;) which have allowed quantitative characterization of frothers. Procedures have been designed to quantify the effect of solute on gas dispersion using the following measurements: bubble coalescence (Fouk and Miller, 1931; Lessard and Zieminski, 1971; Drogaris and Weiland, 1983), bubble size (Keitel and Onken, 1982; Cho and Laskowski, 2002a,b) and gas hold-up (Keitel and Onken, 1982; Azgomi et al., 2007; Quinn et al., 2007).

#### **2.4.1 Bubble coalescence tests**

One of the simplest methods to study bubble interactions is to bring two bubbles together in some manner. Fouk and Miller (1931) contacted bubbles at two vertically opposing capillaries. Drogaris and Weiland (1983) contacted bubble pairs and measured the coalescence time (induction time). Other researchers (Lessard and Zieminski, 1971; Cain and Lee, 1984; Zahradnik et al., 1999; Christenson et al., 2008) have determined the transition concentration at which inorganic salts inhibit bubble coalescence. The concentration at which 50% of the pairs coalesced was termed the transition concentration. Similar experiments have been undertaken in bubble swarms (Craig et al., 1993). For inorganic salts which affected coalescence, salts with multi-valent ions showed lower transition concentrations than mono-valent salts. Table 2.5 shows literature transition concentrations for inorganic salts.

For 1-alcohols, Drogaris and Weiland (1983) showed that transition concentration decreased with increasing chain length. It should be noted that bubble size and gas rate have been shown to affect the transition concentration (Drogaris and Weiland, 1983; Tsang et al., 2004; Nguyen et al., 2012). Kracht and Finch (2009b) developed a method which used acoustics to detect bubble coalescence at a capillary. Frothers and salt were shown to delay the onset of coalescence.

**Table 2.5 – Transition concentrations for inorganic salts**

Salt Type	Transition Concentration, M			
	Bubble Pairs			Bubble Swarm
	Lessard and Zieminski 1971	Zahradnik et al. 1999	Christenson et al. 2008	Craig et al. 1993
<b>KCl</b>	0.23	0.202	-	0.120
<b>NaCl</b>	0.175	0.145	0.208	0.078
<b>Na<sub>2</sub>SO<sub>4</sub></b>	0.061	0.051	-	-
<b>CaCl<sub>2</sub></b>	0.055	-	0.060	0.037
<b>MgSO<sub>4</sub></b>	0.032	0.036	0.036	0.020

#### 2.4.2 Critical coalescence concentration (CCC)

Cho and Laskowski (2002a) developed what is now probably the most widely used parameter to quantify the effect of flotation frothers on bubble size namely the critical coalescence concentration (CCC). From a plot of Sauter mean diameter ( $d_{32}$ ) vs. concentration, CCC represents the concentration above which the  $d_{32}$  is minimum and constant. Laskowski and co-workers used a graphical method to determine CCC by finding the intersection of the horizontal asymptote to the  $d_{32}$  - concentration curve at high concentration with a sloped line approximating the curve at lower concentrations (Grau et al., 2005). Comley et al. (2002) suggested fitting an exponential decay function to model  $d_{32}$  vs. frother concentration. Nasset et al. (2007) similarly applied a three-parameter model fitting to the  $d_{32}$  - concentration curve and estimated CCC using the CCC95, the concentration achieving 95% of bubble size reduction from that of the water-only system to the minimum bubble size.

Cho and Laskowski (2002a) conducted tests using both a 3-hole sparger and an open-top Leeds flotation cell. The University of Cape Town (UCT) bubble size meter was used to measure bubble size distributions and determine the  $d_{32}$  at increasing frother concentration. Sauter mean bubble diameter decreased to a limiting value at a given frother concentration which was attributed to complete coalescence prevention. Large bubbles obtained at frother concentrations below the CCC were ascribed to bubble coalescence. Above the CCC, coalescence is prevented and bubble size is dictated by sparger geometry and hydrodynamic conditions. Table 2.6 shows literature CCC (or CCC95) values for common industrial frothers. Similar techniques have been

used to determine the effect of surfactants and inorganic electrolytes on bubble size in a swarm (Marrucci and Nicodemo, 1967; Zieminski and Lessard, 1969; Zieminski and Whittemore, 1971; Zieminski et al., 1976; Tucker et al., 1994).

**Table 2.6 – Critical coalescence concentration of common industrial frothers**

Frother Type	Critical Coalescence Concentration, ppm (mg/l)							
	Cho and Laskowski 2002a	Cho and Laskowski 2002b	Grau et al. 2005	Nesset et al. 2007	Nesset 2011	Castro et al. 2012	Zhang et al. 2012	Quinn et al. 2014
MIBC	8.5	8.8	11.2	10.4	12.4 - 14.1	9	11	13.4
DF250	-	-	8.7 - 9.1	8.35	10.1 - 16.8	11.1	10	9.1
F150	-	-	-	3.74	4.2 - 6.0	-	6	-

### 2.4.3 Gas holdup vs. frother / salt concentration

Finch and Dobby (1990) and Azgomi et al. (2007) used gas holdup measurements to characterize frother strength. Finch and Dobby (1990) show various methods for measuring gas holdup in the bubbly (pulp) zone. Azgomi et al. (2007) reviewed the effects of various frother types on gas holdup in a 2-phase (solution/air) bubble column. For alcohols, gas hold-up was shown to increase with hydrocarbon chain length and the effect is the same whether the chain is branched or straight. For polyglycol frothers, gas hold-up increased with the number of propoxy groups present on the molecule.

Similar test work has been used to characterize the effect of inorganic salts on gas holdup (Quinn et al., 2007). Salts containing multi-valent ions increased gas holdup at lower concentration than mono-valent salts. The researchers showed a correlation between ionic strength and gas holdup.

Table 2.7 summarizes results of the various frother characterization techniques, namely, bubble coalescence (Kracht and Finch, 2009b), bubble size measurements (CCC determination) (Sweet et al., 1997; Laskowski et al., 2003; Zhang et al., 2012a), gas holdup (Azgomi et al., 2007). The results, in terms of classifying frothers from weak to strong, indicate that all the techniques show a similar ranking.

**Table 2.7 – Summary of various frother characterization techniques**

	<b>Bubble Coalescence</b>	<b>Bubble Size / CCC</b>	<b>Gas Holdup</b>
<b>Weak</b>	1-Butanol	1-Butanol	-
	1-Pentanol	1-Pentanol	1-Pentanol
↓	1-Hexanol	MIBC	MIBC
	MIBC	1-Hexanol	1-Hexanol
<b>Strong</b>	-	DF200	DF200
	1-Heptanol	1-Heptanol	1-Heptanol
	1-Octanol	1-Octanol	1-Octanol
	DF250	DF250	DF250
	F150	-	F150

## 2.5 The behaviour of a single rising bubble

Besides bubble size reduction another role of frother in the pulp phase is to reduce the rate of bubble rise (Klimpel and Isherwood, 1991). In a 2-phase (solution-air) system for a single rising bubble, researchers have noted the effect in frother (Fuerstenau and Wayman, 1958; Sam et al., 1996; Zhang et al., 2001; Krzan and Malysa, 2002; Tan et al., 2013) and inorganic salt solutions (Detsch and Harris 1989; Detsch 1991; Kugou et al., 2003; Wichterle et al., 2009; Rafiei et al., 2010; Maldonado et al., 2013).

The decreases in rise velocity is often ascribed to the stagnant cap model. This model describes how surfactant molecules on the bubble surface are swept to the rear of a rising bubble creating surface tension gradients which increase drag and retard bubble rise (Frumkin and Levich, 1947; Savic, 1953; Levich, 1962; Dukhin et al., 1998). The effect of inorganic salts on bubble rise velocity (as opposed to their effect on bubble coalescence) is not widely addressed. Quinn et al. (2013) hint that surface tension gradients may similarly retard bubble rise in inorganic salt solutions (which, recall, typically slightly increase surface tension).

Several authors have noted that rising bubbles become more spherical upon addition of surfactant (Krzan and Malysa, 2002a, 2002b, 2007; Clift et al., 2005; Finch et al., 2008). The change in shape can also be related to surface tension gradients, the associated force opposing the deformation resulting from the dynamic pressure across the rising bubble (Dukhin et al., 1998).

The following section gives an overview of the behaviour of a single rising bubble in an aqueous system focusing on bubble rise velocity and shape. Emphasis will be placed on bubble sizes typically present in flotation systems, ca. 0.5 - 3 mm in diameter (Nesset et al., 2006).

### 2.5.1 Surfactants, bubble rigidity and internal circulation

When a fluid particle (e.g., organic droplet or bubble) is in motion internal circulation occurs when the surface is mobile. There is no internal circulation in a fluid particle with a rigid (immobile) surface. The presence of surface active agents and the nature of the interface determine internal circulation. Figure 2.5 shows external and internal flow patterns for a rising bubble with surfactant present. For the case of surfactant, the bubble rise velocity may decrease because water molecules interact with polar groups through hydrogen bonding which increases drag on the bubble (Fuerstenau and Wayman, 1958; Leja, 1982; King, 1982; Crozier, 1992; Urry, 1995) by inducing surface tension gradients (Dukhin et al., 1998; Finch et al., 2008) and possibly by increasing surface viscosity (Dukhin et al., 1998; Nguyen and Schulze, 2004).

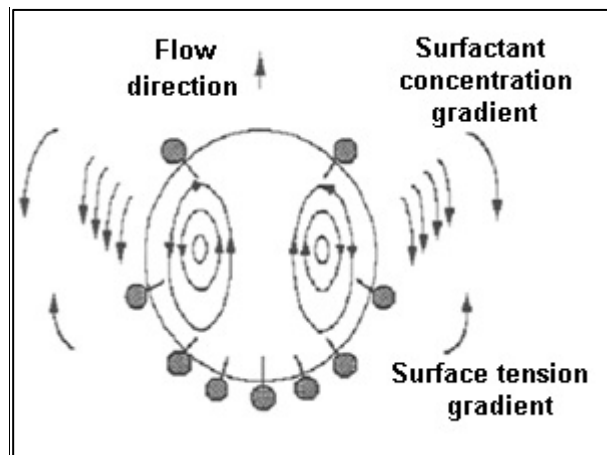


Figure 2.5 – Schematic of a rising bubble depicting internal and external flow patterns and a surface concentration gradient (Reprinted with permission from Elsevier. (Dukhin et al., 1998))

### 2.5.2 Bubble terminal velocity

A bubble reaches terminal velocity,  $U_T$ , when all forces acting on it (e.g., buoyancy, gravity, drag) are in equilibrium. Researchers note that in certain instances a bubble will not reach a

constant velocity but oscillates (Aybers and Tapucu, 1969a; Bachhuber and Sanford, 1974; Fan and Tsuchiya, 1990). In this case, the oscillations are either sufficiently small or an average velocity over a given distance is taken as the terminal velocity.

Detwiler and Blanchard (1978) showed that a certain amount of time (or rise distance) is required before the terminal condition is reached. These authors discuss how a 1 mm bubble may rise several meters before terminal velocity is attained even in relatively clean water. Larger bubbles were noted to take longer to reach terminal velocity. In contaminated water terminal velocity would be achieved over a shorter distance, possibly after 1 m of rise. Researchers (Aybers and Tapucu, 1969a,b; Detwiler and Blanchard; 1978) have related the time-dependent behaviour to the accumulation of surfactants (even in relatively clean systems) at the rear stagnation point on the bubble as it rises, a concept developed by Savic (1950) to help explain reduced rise velocity in surfactant solutions. Malysa et al. (2007) propose that shape and velocity variations relate to adsorption/desorption of solute as the bubble interfacial area oscillates showing that the forces acting on the bubble are not constant.

Zhang and Finch (1999) illustrated the effect of solution type on single bubble rise velocity (Figure 2.6). In pure water and concentrated solutions terminal velocity is achieved after a short distance with the terminal velocity being higher in the pure water system. For dilute solutions or tap water, bubbles quickly reach a maximum velocity after which velocity decreases with height (also noted by Aybers and Tapucu (1969a)), and the velocity may or may not reach terminal depending on distance travelled (height) and concentration. As illustrated, there appears to be little effect of solution type in the early stages of bubble rise (acceleration stage), it is only after maximum velocity is achieved that the effect of surfactants is seen (Acuña, 2007; Kracht and Finch, 2010). This being said, Krzan and Malysa (2002, 2007) noted higher bubble acceleration in the initial stage after release in water when compared to surfactant solutions.

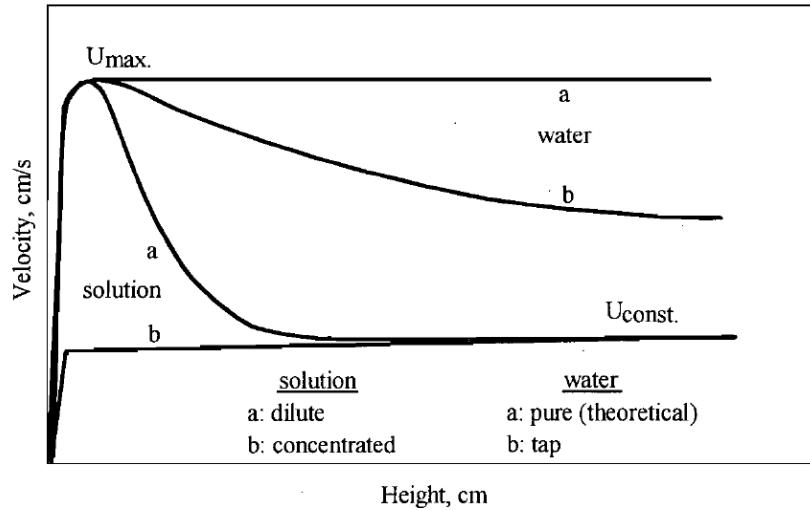


**Figure 2.6 – Typical single bubble velocity profiles (Reprinted with permission from Elsevier. (Zhang et al., 2001))**

Terminal velocity is a relatively straightforward concept but can be difficult to attain experimentally. As shown in the literature, certain researchers claim terminal velocity is achieved after 30 mm of rise (for a 1.45 mm bubble, Krzan et al. (2007)) while others note that terminal velocity is not necessarily attained even after up to 4 m of rise (Sam et al., 1996).

The method of bubble production (release) has also been shown to affect bubble shape, velocity and the time needed to achieve the terminal condition (Wu and Gharib, 2002; Tomiyama et al., 2002; Peters and Els, 2012). This will be discussed later.

Detwiler and Blanchard (1978) noted that typical laboratory setups (1 - 2 m of rise) do not allow sufficient time for terminal velocity to be reached. Many researchers seem to ignore the time-dependent behaviour when choosing a height at which to measure terminal velocity which could help explain certain discrepancies in the literature. It is clear that inconsistencies in terminal velocity measurements in the literature could be attributed to inadequate rise time which depends on bubble size, release mechanism and solution chemistry (presence of contaminants / surfactants).

### 2.5.3 Forces acting on a rising bubble

Equation (2.2) gives the force acting on a spherical bubble due to buoyancy ( $F_B$ ) and gravity ( $F_G$ ) which is a function of the density of the liquid and gas phases ( $\rho_L$  and  $\rho_g$ , respectively, with  $\Delta\rho = \rho_L - \rho_g$ ), gravitational acceleration ( $g$ ) and bubble volume ( $V_B$ ), which for a spherical bubble is:

$$F_{B-G} = \Delta\rho g V_B = \frac{4}{3} \Delta\rho g \pi d_b^3 \quad (2.2)$$

The drag force ( $F_D$ ) is given in Equation (2.3).

$$F_D = C_D A \frac{\rho_L U_T^2}{2} \quad (2.3)$$

where  $C_D$  is the dimensionless drag coefficient and  $A$  the reference area (projected area perpendicular to flow). The drag coefficient,  $C_D$ , is defined as follows:

$$C_D = \frac{4\Delta\rho g d_b}{3U_T^2 \rho_L} \quad (2.4)$$

Re-arranging Equation (2.4), bubble terminal velocity is obtained (Equation (2.5)).

$$U_T = \sqrt{\frac{4\Delta\rho g d_b}{3\rho_L C_D}} \quad (2.5)$$

### 2.5.4 Dimensionless numbers

The concept of dimensionless groups arises from dynamic similarity (Massey, 1983). Dynamic similarity implies that within two systems, the magnitude of forces acting at similar locations is in fixed ratios. Typically two or more dimensionless groups are needed to characterize behaviour of a system. As such it is useful to compare the relative forces acting on a bubble. Using dimensional analysis this is accomplished by taking ratios of the various forces which determine behaviour. As shown, buoyancy (Equation (2.2)) depends upon bubble diameter ( $d_b$ ), gravitational acceleration ( $g$ ), gas and liquid density ( $\rho_L, \rho_g$ ). As will be described, key variables which affect drag include viscosity ( $\mu$ ) and surface tension ( $\sigma$ ). Typically, the Morton number,  $Mo$ , or Eötvös number,  $Eo$  is taken as the independent variable (Equations (2.6) and (2.7)). The

Morton number characterizes the liquid phase as it depends only on the physical properties of the fluid. The Morton number for water is  $2.40 \times 10^{-11}$ , which is considered low. Examples of Morton numbers for various liquids are given in Table 2.8.

$$Mo = \frac{g\mu^4\Delta\rho}{\rho_L^2\sigma^3} \quad (2.6)$$

$$Eo = \frac{g\Delta\rho d_e^2}{\sigma} \quad (2.7)$$

**Table 2.8 – Example Morton numbers for various liquids**

Liquid	Morton Number*
Water (21°C)	$2.40 \times 10^{-11}$
(49°C)	$3.07 \times 10^{-12}$
Corn Syrup, 68%	$2.12 \times 10^{-3}$
Olive Oil	$7.16 \times 10^{-3}$
Syrup (18 Ns/m <sup>2</sup> )	$9.2 \times 10^6$

\*Jameson (1982)

Most commonly, dimensionless rise velocity is used as the dependent variable and a number of dimensionless velocity numbers are used depending on what is of interest. The dimensionless drag coefficient (Equation (2.4)) is a common choice, as are the Reynolds number ( $Re$ ) and Weber number ( $We$ ) (Equations (2.8) and (2.9), respectively).

$$Re = \frac{\rho_L d_e U_T}{\mu} \quad (2.8)$$

$$We = \frac{\rho_L U_T^2 d_e}{\sigma} \quad (2.9)$$

It should be noted that the analysis and correlations developed for bubble behaviour are based on experimental data which, as noted, have been found to be inconsistent largely due to the complexities in attaining terminal velocity. That being said, several authors have compiled large

databases from the literature and correlated against dimensionless groups to model bubble behaviour (Grace et al., 1976; Clift et al., 2005).

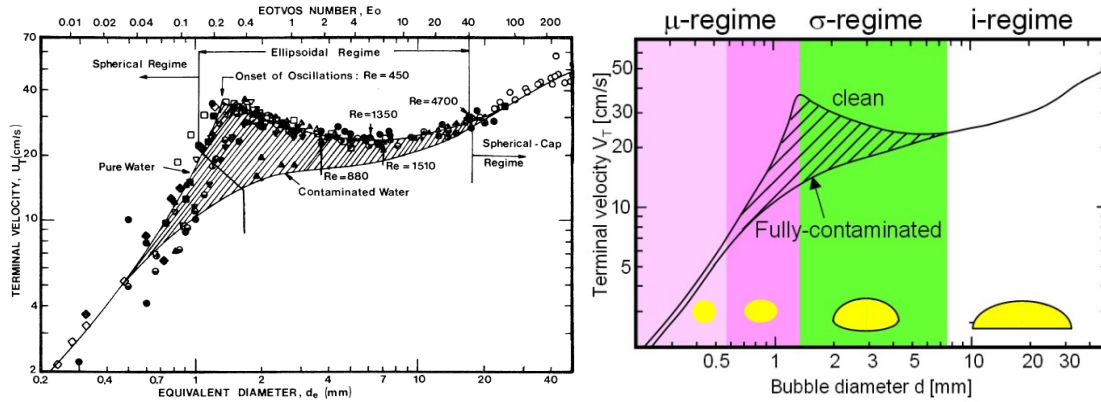
### 2.5.5 Single bubble regimes

Several researchers have categorized single bubbles based on their shape, dominant force regime and other characteristics (Grace et al., 1976; Mendelson, 1967; Clift et al., 2005; Tomiyama et al., 2002; Tomiyama and Hayashi, 2002).

Figure 2.7 (left) shows the relationship between bubble terminal velocity and bubble size (Eötvös number also shown) for a collection of data from the literature which was assembled by Clift et al. (2005). Three dominant shape regimes were identified: spherical for bubbles below 1 - 1.3 mm, ellipsoidal for bubbles between 1.3 mm and 18 mm, and spherical-cap for bubbles greater than 18 mm.

The upper curve in Figure 2.7 (left) shows terminal velocity in clean water while the lower curve indicates terminal velocity in contaminated water. It is interesting to note that in clean water (upper bound) bubble terminal velocity reaches a maximum (ca. 35 cm/s) at roughly 1.3 mm after which maximum terminal velocity decreases (Jameson, 1984) until ca. 6 mm when velocity again begins to rise. It is only when bubbles reach ca. 25 mm that terminal velocity again reaches 35 cm/s.

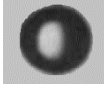
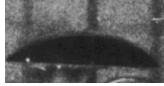
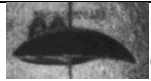
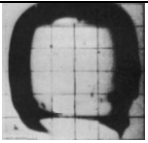
Tomiyama and Hayashi (2002) show a similar plot to Clift et al. (2005) but include the force dominant regimes (Figure 2.7 (right)). Bubble sizes below ca. 0.6 mm are spherical and lie in the viscous dominant regime ( $\mu$ -regime) and behave similarly independent of the presence of contaminants. Bubbles 0.6 mm - 1.3 mm are slightly ellipsoidal but bubbles in clean water tend to rise at higher velocities compared to contaminated water (Tomiyama, 2002). There is debate as to whether this regime is in the viscous or surface tension dominant regime. In the ellipsoidal region (shown here as ca. 1.3 - 7 mm), the effect of surfactants (surface tension dominant ( $\sigma$ -) regime) on bubble terminal velocity is pronounced. In the spherical-cap regime (shown here as > 7.5 mm) the inertial forces dominate (i-regime) and bubbles behave similarly with or without contaminants present.



**Figure 2.7 – Left: Terminal velocity of air bubbles in water at 20°C (Reprinted with permission from Dover Publishing, Inc. (Clift et al., 2005)), Right: bubble shapes and the force dominant regimes (modified from Tomiyama and Hayashi, 2002)**

The most recognized general graphical representation of bubble shape regimes is the plot of Reynolds number versus Eötvös number (Figure 2.8) (typically lines of constant Morton number are included). The position of the boundaries are somewhat arbitrary but the general trend is clear: bubbles are spherical at low Reynolds number (independent of  $E_o$ ) and low Eötvös number (independent of  $Re$ ), ellipsoidal at high Reynolds number and intermediate Eötvös number, and spherical- or ellipsoidal-cap at high  $Re$  and  $E_o$  (Clift et al., 2005). Bhaga and Weber (1981) extended the work of Grace (1976) and Grace et al. (1976) to include a range of ellipsoidal, spherical cap and skirted shapes as outlined in Table 2.9.

**Table 2.9 – Bubble shapes (abbreviations refer to Figure 2.8)**

<b>Bubble Shape</b>	<b>Abbreviation</b>	<b>Example Image</b>
Spherical	s	 (1)
Oblate ellipsoid	oe	 (2)
Oblate ellipsoidal (disk-like and wobbling)	oed	 (3)
Oblate ellipsoidal cap	oec	 (1)
Spherical cap with closed steady wake	scc	 (1)
Spherical cap with open, unsteady wake	sco	 (1)
Skirted with smooth, steady skirt	sks	 (1)
Skirted with wavy, unsteady skirt	skw	 (1)

<sup>1</sup> Modified from Bhaga and Weber, 1981

<sup>2</sup> Modified from Maldonado et al., 2013

<sup>3</sup> Modified from Raymond and Rosant, 2000

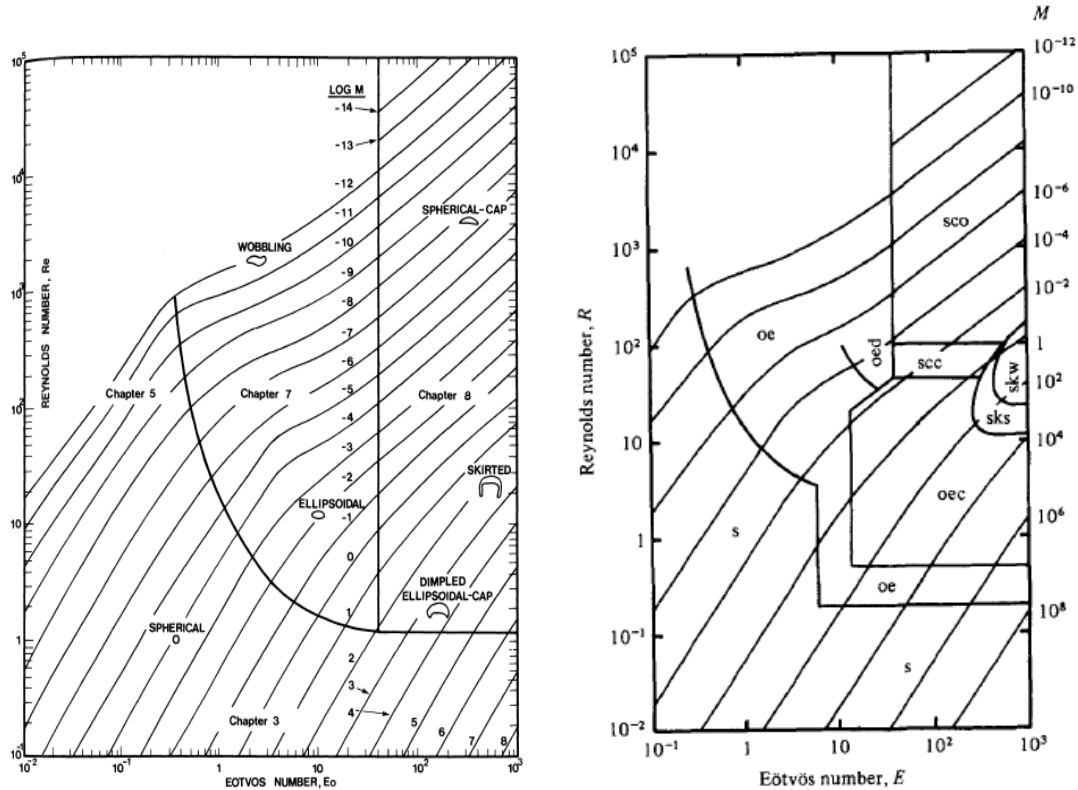


Figure 2.8 – Bubble shape regimes (Reprinted with permission of Dover Publications , Inc. (Clift et al., 2005) and Cambridge University Press (Bhaga and Weber, 1981))

### 2.5.6 Terminal velocity models

Numerous theoretical, empirical or semi-empirical models for terminal velocity of single bubbles rising in a quiescent liquid have been proposed. Most are limited to a specific bubble regime (e.g., a specific range of bubble size (or Reynolds number), or a force dominant regime).

Theoretical terminal velocity models have been shown to be accurate for fine (< 1mm) and large bubble sizes (> 18 mm) (Tomiyama et al., 2002). Small bubbles lie in the viscous dominant regime. Levich (1962) calculated the terminal velocity of a spherical bubble by potential flow theory (Equation (2.10)). The calculations were later extended by Moore (1963, 1965) for a deformed bubble. The Levich equation applies for  $Re \gg 1$  and Harper (1972) identified  $Re = 50$  as the lower applicable limit:

$$U_T = \frac{\Delta \rho g d_e^2}{36 \mu} \quad (2.10)$$

For large bubbles in the spherical-cap region inertial forces are dominant. Haberman and Morton (1954) solved the Davies and Taylor (1950) equation which predicts terminal velocity based on bubble size (Equation (2.11)).

$$U_T = 0.72\sqrt{gd_e} \quad (2.11)$$

Over the years, authors have noted the difficulties in estimating terminal velocity in the ellipsoidal region (Grace et al., 1976; Tomiyama et al., 2002). Most models only trace the pure water or fully contaminated cases (i.e., the upper and lower limits of terminal velocity). Difficulties arise from the presence of surface active contaminants which affect bubble shape and velocity. The degree of contamination was seen as an obstacle as each solute behaved in a particular manner. More recently authors have linked behaviour to bubble shape or possibly the method of formation/release.

Mendelson (1967) proposed a wave analogy to explain bubble behaviour in the ellipsoidal regime (the relationship also predicts the spherical cap regime). The author suggested that the bubble behaves like an interfacial disturbance similar to a surface wave propagating over deep water with the rate of propagation being governed by wave motion. The relationship (Equation (2.12)) correlated well with experimental data for the upper limit of the  $U_T$  curve.

$$U_T = \sqrt{\frac{2\sigma}{d_e\rho_L} + \frac{gd_e}{2}} \quad (2.12)$$

Clift et al. (2005) modified Mendelson's equation (2.12) and produced the empirical Equation (2.13) to fit experimental data from the literature for the upper bound of the terminal velocity curve in the ellipsoidal region.

$$U_T = \sqrt{\frac{2.14\sigma}{d_e\rho_L} + 0.505gd_e} \quad (2.13)$$

Tomiyama and co-workers noted the limited understanding of bubble behaviour in the surface tension dominant (ellipsoidal) regime and proposed a model for terminal velocity for ellipsoidal bubbles which is a function of bubble aspect ratio, bubble size and fluid properties (Equation (2.14)) (Tomiyama, 2002; Tomiyama et al., 2002). They showed the model fit well for bubbles of various shapes and sizes in water.

$$U_T = \frac{\sin^{-1} \sqrt{1-E^2} - E\sqrt{1-E^2}}{1-E^2} \sqrt{\frac{\Delta\rho g d_e}{2\rho_L} \frac{E^{2/3}}{1-E^2} + \frac{8\sigma}{\rho_L d_e} E^{4/3}}, E < 1 \quad (2.14)$$

Wellek et al. (1966) empirically correlated bubble (and droplet) mean aspect ratio in a fully contaminated system with the Eötvös number as shown in equation (2.15).

$$E = \frac{1}{1 + 0.163 Eo^{0.757}} \quad (2.15)$$

Figure 2.9 was constructed to present the various terminal velocity models for the water system. Dashed lines show the Tomiyama et al. (2002) model for aspect ratios ranging from 0.5 to 0.9. Tomiyama et al. (2002) combined equations (2.14) and (2.15) to trace the lower limit of the terminal velocity curve. The figure shows that as the bubble becomes more spherical (aspect ratio approaches unity) bubble terminal velocity decreases.

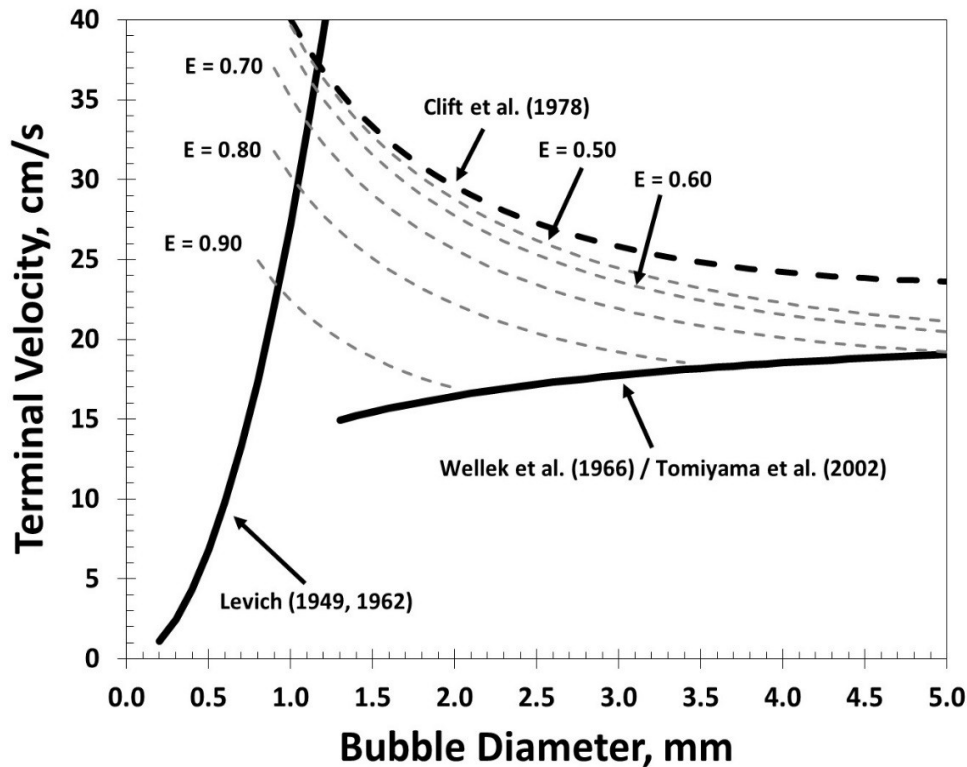
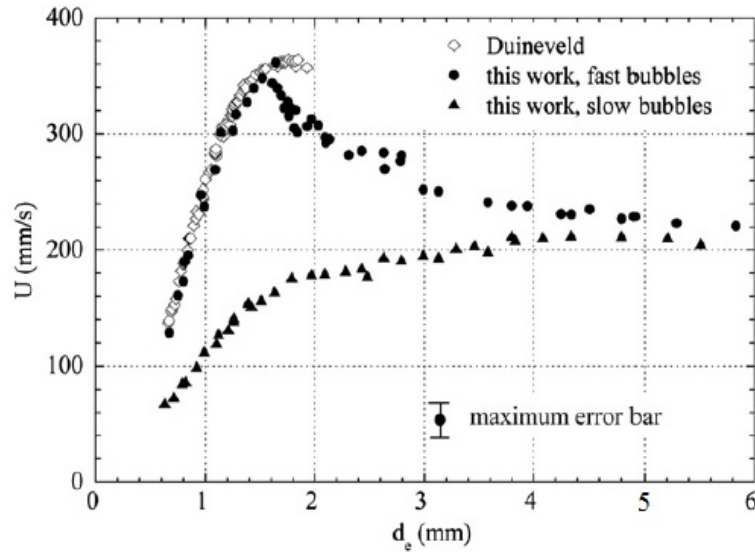


Figure 2.9 – Bubble terminal velocity models for water

### **2.5.7 Bubble shape, rise velocity and the effect of release condition**

Fuerstenau and Wayman (1958) studied the effect of frother on single rising bubbles ranging from 0.5 - 10 mm in diameter. The authors found frother created more spherical bubbles that rose at lower velocities. Recently, several researchers have found ellipsoidal bubble shape and velocity to be strongly interacting in various aqueous solutions (surfactants, polymers and inorganic salts) both close to and far from the point of bubble release (Bozzano and Dente, 2001; Tomiyama et al., 2002; Gomez et al., 2010; Kracht and Finch, 2010; Maldonado et al., 2013).

It has been demonstrated that the nature of bubble formation (release) affects bubble shape, velocity and motion (Tomiyama et al., 2002; Wu and Gharib, 2002; Javor et al., 2012; Peters and Els, 2012). Tomiyama et al. (2002) observed that bubbles released with small initial shape deformation resulted in more spherical bubbles (high aspect ratio) with low terminal velocities compared with bubbles with large initial shape deformation which resulted in oblate bubbles (low aspect ratio) with high terminal velocities. Tomiyama et al. (2002) noted that surfactant acted to damp initial shape deformation. Wu and Gharib (2002) reported that bubbles produced at a capillary of the same size (volume) rose at different velocities depending upon generation method (gentle push or pinch-off). More recently, Peters and Els (2012) investigated the effect of bubble release condition on bubble rise velocity in tap water. The results showed that velocity could be modified purely by changing the initial release condition. Bubbles in tap water either followed the upper or lower bound of the velocity – bubble size curve depending on the method of bubble release as shown in Figure 2.10 (results of Duineveld (1995) in ‘hyper-clean’ water are shown for reference). Peters and Els noted a relationship between bubble shape and velocity. Detwiler and Blanchard (1978) performed similar experiments on ‘new’ and ‘aged’ bubbles. Aged bubbles were held in place by a counter-current flow to allow adsorption of surface active species. Aged bubbles were found to rise at lower velocities when compared to newly created bubbles, the belief being that the longer formation time (prior to release) allowed contaminants to adsorb which lowered bubble rise velocity.



**Figure 2.10 – Rise velocities for fast and slow bubbles in tap water (Reprinted with permission from Elsevier. (Peters and Els, 2012))**

Kracht and Finch (2010) studied the relationship between ellipsoidal bubble shape and rise velocity in various frother and sodium chloride solutions close to the point of release at a capillary (first 400 ms of rise). They used high-speed photography (1000 fps) to capture single bubble rise velocity and aspect ratio (which they defined as the ratio of major to minor axis) for ca. 2.4 mm bubbles. Oscillations in shape and velocity were seen to be related (Figure 2.11A). The results suggest a relationship between bubble velocity and aspect ratio (Figure 2.11B, correlates data after the initial peak in velocity for various solutions). Sodium chloride was shown to have a similar effect (at high concentration) to frother in terms of its ability to modify bubble shape and velocity.

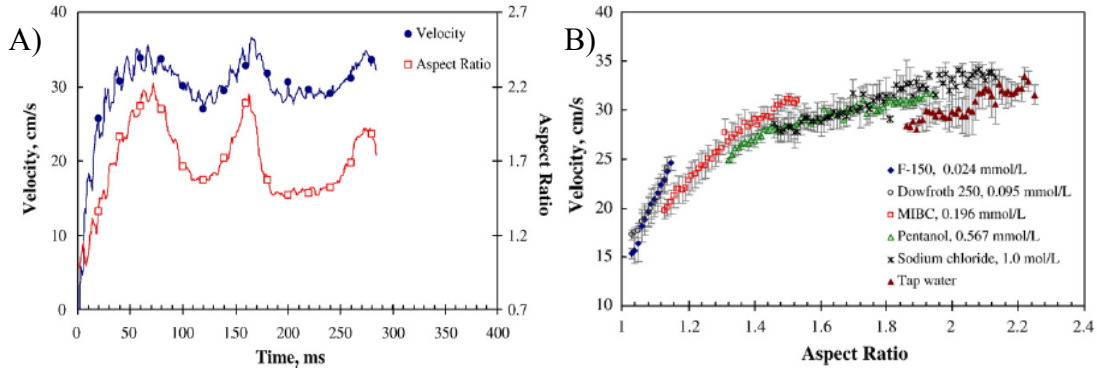


**Figure 2.11 – A) Velocity and aspect ratio as a function of time and B) velocity as a function of aspect ratio for various solution chemistries (Reprinted with permission from Elsevier. (Kracht and Finch, 2010))**

Gomez et al. (2010) reported a unique relationship between average bubble shape and velocity (Figure 2.12) for three bubble sizes (1.5 mm (capillary 1), 2.5 mm (capillary 2), and 3.8 mm (capillary 3)). The tests were performed in frother (Dowfroth 250) and polymer (polyacrylamide) solutions and measured shape and velocity ca. 1.3 m above the point of release. The results showed oscillations in shape and velocity with time which were damped in the presence of frother or polymer.

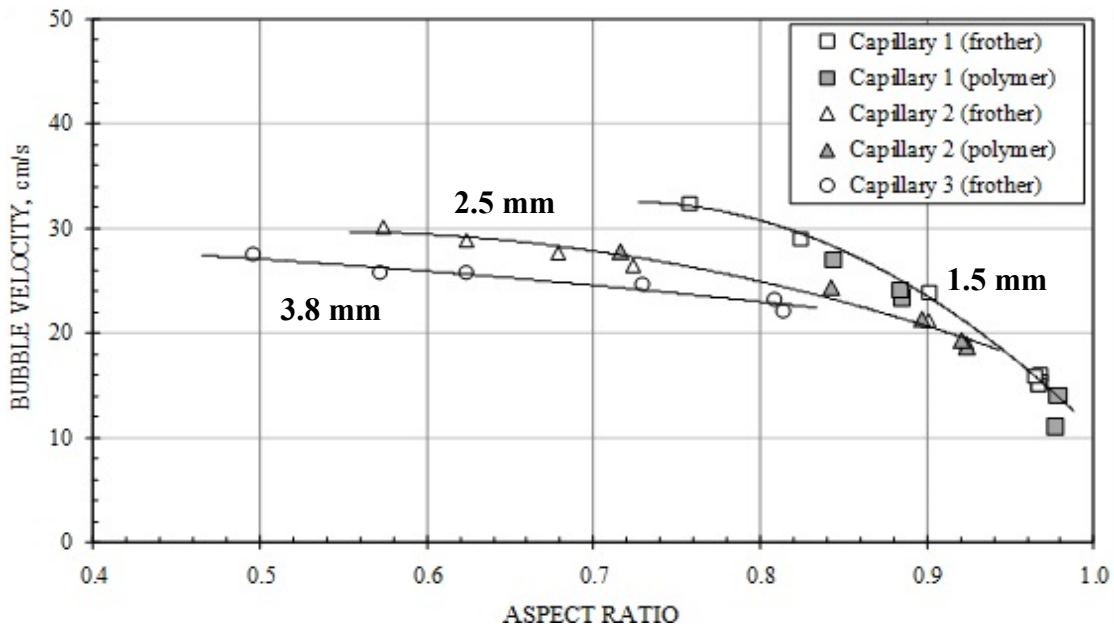


**Figure 2.12 – Bubble velocity as a function of aspect ratio for three bubble sizes (modified from Gomez et al., 2010)**

Maldonado et al. (2013) examined single bubbles of ca. 2.5 mm rising in presence of polymer (poly-acrylamide), frother (1-pentanol, MIBC, Dowfroth 250, F150) and inorganic salts (NaCl and Na<sub>2</sub>SO<sub>4</sub>). Rise velocity and aspect ratio were measured using high-speed photography ca. 1.2 m above the point of bubble release. Figure 2.13A shows the effect of MIBC concentration on average rise velocity and aspect ratio: the presence of solute created more spherical bubbles which rose at lower velocities. Figure 2.13B shows a unique relationship independent of solute type (or concentration).

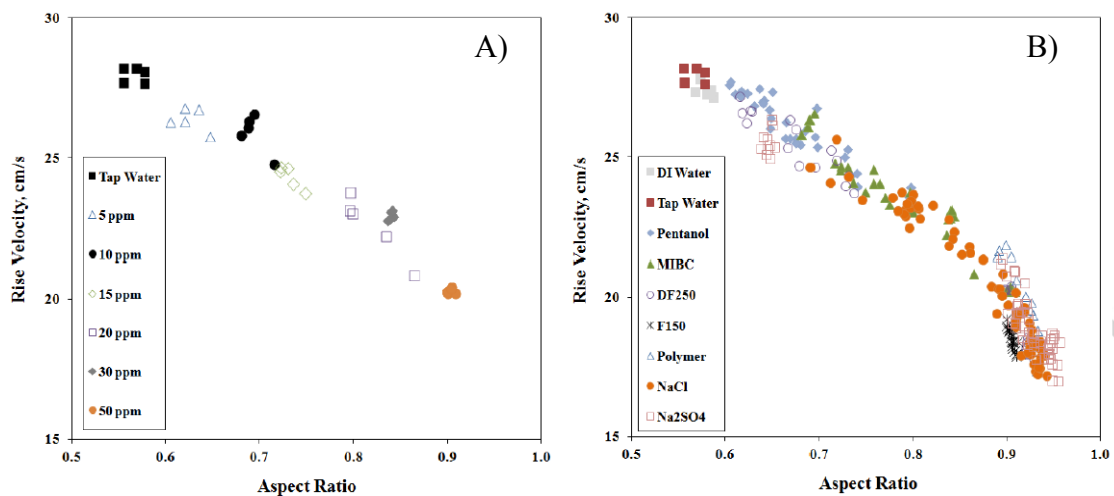


**Figure 2.13 – A) The effect of MIBC concentration on bubble rise velocity and aspect ratio (shape), and B) rise velocity as a function of aspect ratio for various solute types (for all concentrations tested) (Reprinted with permission from Elsevier. (Maldonado et al., 2013))**

There exists limited experimental data on bubble rise velocity in inorganic salt solutions. Much of the data comes from oceanography and typically focuses on bubble diameters below 1 mm in sea water or sodium chloride solutions (Detsch and Harris, 1989; Detsch, 1991; Kugou et al., 2003; Henry et al., 2008; Sato et al., 2010). Studies on low inorganic salt concentration showed little effect on rise velocity (Fuerstenau and Wayman, 1958; Okazaki, 1962).

Bozzano and Dente (2001, 2009) and van Wijngaarden and Veldhuis (2008) have attempted to explain the shape and velocity variations through energy balances which incorporate surface and kinetic energy.

## 2.6 Bubbles and sound

There are two general categories of acoustic measurements: active and passive. Active measurement entails generation of an acoustic wave (typically, low-powered ultrasound) and the measurement of the change in the wave transmitted through a process. Passive measurements involve monitoring acoustic emissions created by the process itself. The following review will focus on passive acoustic emission monitoring.

Acoustics have been used to monitor such processes as crushing and grinding circuits (Zeng and Forssberg, 2003), hydrocyclone operation (Hou et al., 1998), bubble formation (Minnaert, 1933; Leighton and Walton, 1987; Kracht and Finch, 2009b), effervescence (Cao et al., 1987), foaming / froth collapse / bubble bursting (Vanegas and Holtham, 2008), precipitation / gelation processes (Wentzell and Wade, 1989), acidification / neutralization (Betteridge et al., 1981) and electrolysis (Crowther et al., 1991). The non-intrusive nature, reliability / robustness, low cost and the ability for real-time continuous measurements make acoustics attractive in process monitoring and control (Boyd and Varley, 2001). The issue is relating the acoustic signal to actual process events and understanding the effect each process variable has on the acoustic signal which is often not a trivial problem.

The sound produced upon bubble detachment from an orifice was first studied by Minnaert (1933). He developed an energy balance based on a pulsating spherical bubble which gave a relationship between the sound frequency ( $\nu$ ) and equilibrium bubble diameter,  $d_b$ . The relationship is commonly termed the Minnaert frequency (Equation (2.16)):

$$\nu = \frac{1}{\pi d_b} \left( \frac{3\kappa p^o}{\rho_L} \right)^{1/2} \quad (2.16)$$

where  $\kappa$  is the ratio of specific heats of the gas phase,  $\rho_L$  the liquid density and  $p^o$  the hydrostatic pressure.

Figure 2.14 shows an example hydrophone output (voltage which is proportional to the sound pressure) revealing the sound emitted upon bubble formation at a nozzle (Leighton and Walton, 1987). The sound trace shows lightly damped harmonic oscillation which is typical of bubble

production. Deane and Czerski (2008) demonstrated that the sound was excited by the rapid decrease in volume accompanying the collapse of the bubble neck upon detachment.

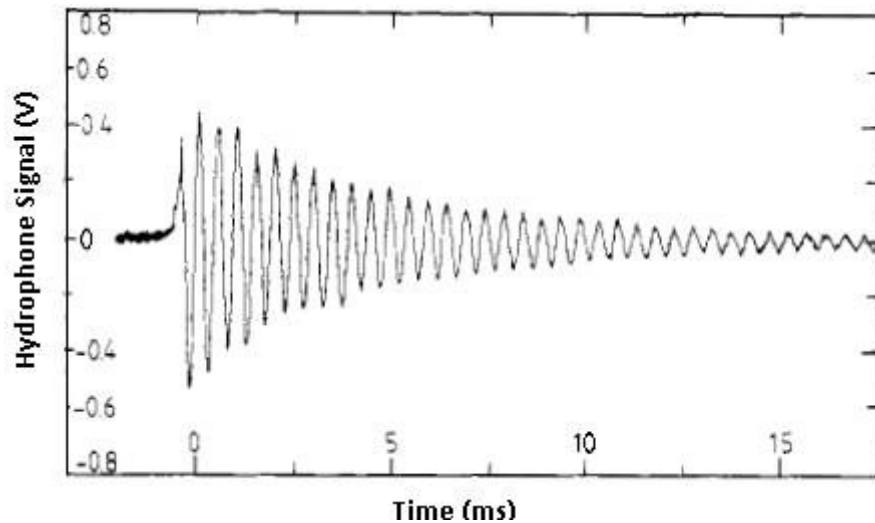


**Figure 2.14 – Example hydrophone output showing sound emitted upon bubble formation (modified from Leighton and Walton, 1987)**

Strasberg (1956) noted that when bubbles split or coalesce, a decaying sinusoidal pulse of sound is emitted, just as in bubble formation. Leighton et al. (1991) used high-speed photography to observe air bubbles in water formed at a 0.5 mm internal diameter nozzle. An individual bubble released from the orifice produced a single decaying sinusoidal acoustic signal. When bubble coalescence occurred in proximity to the nozzle a characteristic acoustic signal was produced: initial bubble detachment resulted in a decaying sinusoid with subsequent peaks in the acoustic signal related to each coalescence event (which created a larger bubble which emitted a lower frequency signal). Manasseh et al. (2008) studied the characteristic acoustic signals upon bubble coalescence and showed that the sound emitted upon coalescence agreed with the Minnaert frequency and suggested that the mechanism resulting in sound emission was the equalization of pressure in the coalescing bubbles. Czerski (2011) linked the pressure wave produced to the rapid increase in bubble volume upon coalescence.

As discussed earlier, bubbles produced at an orifice undergo various regime changes depending on gas flow rate. At low gas flow rates bubbles do not interact with one another. There is a

critical gas flow rate above which bubbles begin to interact, either bouncing or coalescing. Kracht and Finch (2009b) determined the transition flow rate between a non-coalescing and coalescing system using passive acoustic emission monitoring. The authors showed that the onset of coalescence could be detected by the characteristic sound wave produced when two bubbles coalesce. The findings showed that coalescence was delayed in frother and sodium chloride solutions (i.e., the transition flow rate between non-coalescence and coalescence occurred at a higher gas flow rate).

## References

- Acuña Perez, C.A., 2007. Measurement techniques to characterize bubble motion in swarms. Ph.D. Thesis, McGill University, Department of Mining and Materials Engineering.
- Acuña, C.A., and Finch, J.A., 2010. Tracking velocity of multiple bubbles in a swarm, *International Journal of Mineral Processing* 94, 147-158.
- Agrawal, S.K., and Wasan, D.T., 1979. The effect of interfacial viscosities on the motion of drops and bubbles, *The Chemical Engineering Journal* 18, 215-223.
- Alexander, S., Quinn, J., van der Spuy, J.E., and Finch, J.A., 2012. Correlation of graphite flotation and gas holdup in saline solutions, in Drelich, J. (Ed.), *Water in Mineral Processing: Proceedings of the First International Symposium*, SME, 41-50.
- Aston, J., Boskovic, S., Tindall, G., and Tsatouhas, G., 2013. Improving performance and efficiency of copper and copper-gold circuits with POLYFROTH W22 frother, presentation Flotation '13, Cape Town, Nov 18-21, 2013.
- Azgomi, F., Gomez, C.O., and Finch, J.A., 2007. Characterizing frothers using gas hold-up, *Canadian Metallurgical Quarterly* 46, 3, 237-242.
- Aybers N.M., and Tapucu, A., 1969a. The motion of gas bubbles rising through stagnant liquid. *Wärme- und Stoffübertragung* Bd. 2, S. 118-128.
- Aybers N.M., and Tapucu, A., 1969b. Studies on the drag and shape of gas bubbles rising through a stagnant liquid. *Wärme- und Stoffübertragung* Bd. 2, S. 171-177.

Bachhuber, C., and Sanford, C., 1974. The rise of small bubbles in water. *Journal of Applied Physics* 45, 2567-2569.

Bergman, T., and Mesler, R., 1981. Bubble nucleation studies. Part I: Formation of bubble nuclei in superheated water by bursting bubbles, *AIChE Journal* 27, 851-853.

Betteridge, D., Joshlin, M.T., and Lilley, T., 1981. Acoustic emissions from chemical reactions, *Analytical Chemistry* 53, 1064-1073.

Bhaga, D., and Weber, M.E., 1981. Bubbles in viscous liquids: shapes, wakes and velocities. *Journal of Fluid Mechanics* 105, 61-85.

Bikerman, J.J., 1938. The unit of foaminess, *Transactions of the Faraday Society* 34, 634.

Blin, P., and Dion-Ortega, A., June/July 2013. High and dry: With water in short supply, some are looking to the ocean for answers, *CIM Magazine*, 46-51.

Bonner, O.D., and Jumper, C.F., 1973. Effect of Ions on Water Structure, *Infrared Physics* 13, 233-242.

Boyd, J.W.R., and Varley, J., 2001. The use of passive measurement of acoustic emissions from chemical engineering processes, *Chemical Engineering Science* 56, 1749-1767.

Bozzano, G., and Dente, M., 2001. Shape and terminal velocity of single bubble motion: a novel approach, *Computers and Chemical Engineering* 25, 571-576.

Cain, F.W., and Lee, J.C., 1984. A technique for studying the drainage and rupture of unstable liquid films formed between two captive bubbles: Measurement on KCl Solutions, *Journal of Colloid and Interface Science* 106, 1, 70-85.

Cao, Z., Wang, B.-F., Wang, K.-M., Lin, H.-G., and Yu, R.-Q., 1998. Chemical acoustic emissions from gas evolution processes recorded by a piezoelectric transducer, *Sensors and Actuators B* 50, 27-37.

Cappuccitti, F., and Finch, J.A., 2007. Development of new frothers through hydrodynamic characterization, In: Folinsbee, J. (Ed.), *Proceedings 39th Annual Meeting of the Canadian Mineral Processors of CIM*, 399–412.

- Cappuccitti, F., and Nasset, J.E., 2009. Frother and collector effects on flotation cell hydrodynamics and their implication on circuit performance, *Advances in Mineral Processing Science and Technology - Conference of Metallurgists, Sudbury*, 169-182.
- Castro, S., 2012. Challenges in flotation of Cu-Mo sulfide ores in sea water. In: Drelich, J. (Ed.), *Water in Mineral Processing: Proceedings of the First International Symposium*. SME, Englewood, USA, 29-40.
- Cole, R., 2009. *KCGM News and Views, Issue 8, August 2009*. 1-4.
- Chen, F., Gomez, C.O., and Finch, J.A., 2001. Bubble size measurement in flotation machines, *Minerals Engineering* 14, 427-432.
- Cho, Y.S., and Laskowski, J.S., 2002a. Effect of flotation frothers on bubble size and foam stability, *International Journal Minerals Processing* 64, 69-80.
- Cho, Y.S., and Laskowski, J.S., 2002b. Bubble coalescence and its effect on bubble size and foam stability, *Canadian Journal of Chemical Engineering* 80, 299-305.
- Christenson, H.K., Bowen, R.E., Carlton, J.A., Denne, J.R.M., and Lu, Y., 2008. Electrolytes that show transition to bubble coalescence inhibition at high concentrations. *Journal of Physical Chemistry C* 112, 794-796.
- Clift, R., Grace, J.R., and Weber, M., 2005. *Bubble, Drops, and Particles*. Dover Publications, Inc., Mineola, New York.
- Comley, B.A., Harris, P.J., Bradshaw, D.J., and Harris, M.C., 2002. Frother characterization using dynamic surface tension measurements. *International Journal of Mineral Processing*, 64, 2, 81-100.
- Craig, V.S.J., Ninham, B.W., and Pashley, R.M., 1993. The effect of electrolytes on bubble coalescence in water, *Journal of Physical Chemistry* 97, 10192-10197.
- Craig, V.S.J., 2004. Bubble coalescence and specific-ion effects, *Current Opinion in Colloid and Interface Science* 9, 178-184.
- Craig, V.S.J., 2011. Do hydration forces play a role in thin film drainage and rupture observed in electrolyte solution? *Current Opinion in Colloid and Interface Science* 16, 597-600.

Crowther, T.G., Wade, A. P., Wentzell, P.D., and Gopal, R. 1991. Characterization of acoustic emission from an electrolysis cell, *Analytica Chimica Acta* 254, 223-234.

Crozier, R.D., and Klimpel, R.R., 1989. Frothers: Plant Practice, *Mineral Processing and Extractive Metallurgy Review* 5, 257-279.

Cytec Industries Inc., *Mining Chemicals Handbook*, Revised Edition, 2002.

Czarnecki, J., Malysa, K., and Pomianowski, A., 1982. Dynamic Frothability Index, *Journal of Colloid and Interface Science* 86, 570–572.

Czerski, H., 2011. A candidate mechanism for exciting sound during bubble coalescence. *The Journal of the Acoustical Society of America*, 129, 3, EL83-EL88.

Davies, J.T., 1957. A quantitative kinetic theory of emulsion type, In: *Physical Chemistry of the Emulsifying Agent, Gas/Liquid and Liquid/Liquid Interface*. Proceedings of the International Congress of Surface Activity, 426-438.

Davies, R.M., and Taylor, G., 1950. The mechanics of large bubbles rising through extended liquids and through liquids in tubes. *Proceedings of the Royal Society of London, Series A, Mathematical and Physical Sciences* 200, 1060, 375-390.

Deane, G.B., and Czerski, H., 2008. A mechanism stimulating sound production from air bubbles released from a nozzle, *Journal of the Acoustical Society of America* 123, 6, EL126-EL132.

Detsch, R.M., 1991. Small air bubbles in reagent grade water and seawater: Rise velocities of 20 to 1000- $\mu$ m diameter bubbles. *Journal of Geophysical Research* 96, C5, 8901-8906.

Detsch R., and Harris, I., 1989. Dissolution and rise velocity of small air bubbles in water and salt water, in *Proceedings of OCEANS'89*, 1, 286–291.

Detwiler, A., and Blanchard, D.C., 1978. Aging and Bursting bubbles in trace-contaminated water. *Chemical Engineering Science* 33, 9-13.

Drogaris, G., and Weiland, P., 1983. Coalescence of gas bubbles in aqueous solutions of n-alcohols and fatty acids, *Chemical Engineering Science* 38, 9, 1501-1506.

Duineveld, P.C., 1995. The rise velocity and shape of bubbles in pure water at high Reynolds number. *Journal of Fluid Mechanics* 292, 325-332.

Dukhin, S.S., Miller, R., and Loglio, G., 1998. Physico-chemical hydrodynamics of rising bubbles. In: Mubius, D., Miller, R. (Eds.), *Studies in interfacial Science, Drops and Bubbles in Interfacial Research*, Elsevier Science 6, 367-432.

Dunne, R., 2012. Water water everywhere and not a drop to drink, nor do I know its whereabouts. In: Drelich, J., *Water in Mineral Processing: Proceedings of the First International Symposium*, Englewood, USA, 1-16.

Fan, L.S., and Tsuchiya, K., 1990. Bubble wake dynamics in liquids and liquid-solid suspensions, Butterworth and Heinemann, 363.

Finch, J.A., and Dobby, G.S., 1990. *Column Flotation*, Permagnon Press, Toronto.

Finch, J.A., Gelinias, S., and Moyo, P., 2006. Frother-related research at McGill University, *Minerals Engineering* 19, 726-733.

Finch, J.A., Nasset, J.E., and Acuna, C., 2008. Role of frother in bubble production and behaviour in flotation, *Minerals Engineering* 21, 949–957.

Fouk, C.W., and Miller, J.N., 1931. Experimental evidence in support of the balanced-layer theory of liquid film formation, *Industrial and Engineering Chemistry* 23, 11, 1283-1288.

Frumkin, A., and Levich, V.G., 1947. On surfactants and interfacial motion. *Zh. Fiz. Khim.* 21, 1183.

Fuerstenau, D.W., and Wayman, C.H., 1958. Effect of chemical reagents on the motion of single air bubbles in water, *Mining Engineering, Transactions of AIME*, 694-699.

George, C., 1996. Mt. Keith Operation. In: Grimsey, E.J., and Neuss, I. (Eds.), *Nickel '96, Conference Series - Australasian Institute of Mining and Metallurgy*, 6, 19-23.

Gomez, C.O., and Finch, J.A., 2002. Gas dispersion measurements in flotation machines, *CIM Bulletin* 95, 1066, 73-78.

Gomez, C.O., and Finch, J.A., 2007. Gas dispersion measurements in flotation cells. *International Journal of Mineral Processing* 84, 1, 51-58.

Gomez, C.O., Maldonado, M., Araya, R., and Finch, J.A., 2010. Frother and viscosity effects on bubble shape and velocity. In: *Proceedings of the 49<sup>th</sup> Conference of Metallurgists (COM)*:

Rheology in Mineral Processing, The 8<sup>th</sup> UBC-McGill-U of A International Symposium on the Fundamentals of Mineral Processing, The Metallurgical Society of CIM, 57-74.

Gorain, B.K., Franzidis, J.P., and Manlapig, E.V., 1997. Studies on impeller type, impeller speed and air flow rate in an industrial flotation cell. Part 4: Effect of bubble surface area flux on flotation performance. *Minerals Engineering* 10, 4, 367-379.

Grace, J.R., 1973. Shapes and velocities of bubbles rising in infinite liquids. *Transactions of the Institute of Chemical Engineers* 51, 116-120.

Grace, J.R., Wairegi, T., and Nguyen, T.H., 1976. Shapes and velocities of single drops and bubbles moving freely through immiscible liquids. *Transactions of the Institute of Chemical Engineers* 54, 167-173.

Grau, R.A., Laskowski, J.S., and Heiskanen, K., 2005. Effect of frothers on bubble size, *International Journal of Mineral Processing* 76, 225-233.

Griffin, W.C., 1949. Classification of surface-active agents by HLB, *Journal of the Society of Cosmetic Chemists* 1, 311, 1949.

Griffin, W.C., 1954. Calculation of HLB values of non-ionic surfactants, *Journal of the Society of Cosmetic Chemists* 5, 259.

Haig-Smillie, L.D., 1974. Sea water flotation, In: *Proceedings of the Canadian Mineral Processors Conference*, 263-281.

Harper, J.F., 1972. The motion of bubbles and drops through liquids. In: Yih, C.-S. (Ed.), *Advances in Applied Mechanics*. Vol. 12, Academic Press Inc., New York, 59-124.

Harris, P.J., 1982. Frothing phenomenon and frothers, In: King, R.P. (Ed.), *Principles of Flotation*. Monograph Series No. 3. South African Institute of Mining and Metallurgy, 237-250.

Heiskanen, K., Javor, Z., Wierink, G., Omelka, B., and Schreithofer, N., 2012. Effect of frother mobility on the bubble behaviour in bubble rise velocity measurements at the initial stages of bubble formation, In: Young, C.A., and Luttrell, G.H. (Eds.), *Separation Technologies: For Minerals, Coal, and Earth Resources*, SME, Englewood, USA, 1-5.

Helsby, F.W., and Tuson, K.R., 1955. Behaviour of air bubbles in aqueous solutions, *Research* 8, 270.

Henry, C.L., Parkinson, L., Ralston, J.R., and Craig, V.S.J., 2008. A mobile gas – water interface in electrolyte solutions, *The Journal of Physical Chemistry Letters* C 112, 15094-15097.

Herman, J., and Mesler, R. 1987. Bubble entrainment from bursting bubbles. *Journal of Colloid and Interface Science* 117, 565-569.

Hernandez-Aguilar, J.R., Gomez, C.O., and Finch, J.A., 2002. A Technique for the direct measurement of bubble size distributions in industrial flotation cells; In: Nasset, J.E. (Ed.), *Proceedings of the 34<sup>th</sup> Annual Meeting of the Canadian Mineral Processors*, 389-402.

Hernandez-Aguilar, J.R., Cunningham, R., and Finch, J. A., 2006. A test of the Tate equation to predict bubble size at an orifice in the presence of frother. *International Journal of Mineral Processing* 79, 2, 89-97.

Hesketh, R.P., Etchells, A.W., and Russell, T.W.F., 1991. Bubble breakage in pipeline flow, *Chemical Engineering Science* 46, 1.

Hinze, J.O., 1955. Fundamentals of the hydrodynamic mechanism of splitting in dispersion processes. *AIChE Journal*, 1, 3, 289-295.

Hofmeier, U., Yaminsky, V.V., and Christensen, H.K., 1995. Observations of solute effects on bubble formation, *Journal of Colloid and Interface Science* 174, 199-210.

Hou, R., Hunt, A., and Williams, R.A., 1998, Acoustic monitoring of hydrocyclone performance, *Minerals Engineering* 11, 11, 1047-1059.

Hunter, T.N., Pugh, R.J., Franks, G.V., and Jameson, G.J., 2008. The role of particles in stabilizing foams and emulsions, *Advances in Colloid and Interface Science* 137, 57–81.

Jameson, G.J., *Physics and hydrodynamics of bubbles*. In: Ives, K.J. (Ed.), *The Scientific Basis of Flotation. Series E: Applied Sciences – No. 75*. Martinus Nijhoff Publishers. Boston. 53-78.

Javor. Z., Scheithofer, N., and Heiskanen, K., 2012. The effect of bubble release techniques on their behaviour at the initial stages of rise, *Minerals Engineering* 36-38, 254-261.

Johnson, B.D., and Gershet, R.M., 1991. Bubble formation at a cylindrical frit surface in a shear field, *Chemical Engineering Science* 46, 2753-2756.

Karamanev, G.G., 1994. Rise of gas bubbles in quiescent liquids. *AIChE* 38, 1843-1846.

Khristov, K., Malysa, K., and Exerowa, D., 1984. Steady-state foams: Influence of the type of liquid films, *Colloids and Surfaces* 11, 39-49.

Klimpel, R.R, and Isherwood, S., 1991. Some industrial implications of changing frother chemical structure, *International Journal of Mineral Processing* 33, 369-381.

Kracht, W., and Finch, J.A., 2009a. Bubble break-up and the role of frother and salt, *International Journal of Mineral Processing* 92, 153–161.

Kracht, W., and Finch, J.A., 2009b. Using sound to study bubble coalescence, *Journal of Colloid and Interface Science* 332, 237–245.

Kracht, W., and Finch, J.A., 2010. Effect of frother on initial bubble shape and velocity, *International Journal of Mineral Processing* 94, 115-120.

Krzan, M., and Malysa, K., 2002a. Profiles of local velocities of bubbles in n-butanol, n-hexanol and n-nonanol solutions. *Colloids and Surfaces A: Physicochemical and Engineering Aspects* 207, 279-291.

Krzan, M., and Malysa, K., 2002b. Influence of frother concentration on bubble dimensions and rising velocities. *Physicochemical Problems of Mineral Processing* 36, 65-76.

Krzan, M., Lunkenheimer, K., and Malysa, K., 2004. On the influence of the surfactant's polar group on the local and terminal velocities of bubbles. *Colloids and Surfaces A: Physicochemical Engineering Aspects* 250, 431-441.

Krzan, M., Zawala, J., and Malysa, K., 2007. Development of steady state adsorption distribution over interface of a bubble rising in solutions of *n*-alkanols (C<sub>5</sub>, C<sub>8</sub>) and *n*-alkyltrimethylammonium bromides (C<sub>8</sub>, C<sub>12</sub>, C<sub>16</sub>). *Colloids and Surfaces A: Physicochemical Engineering Aspects* 298, 42-51.

Kulkarni, A.A., and Joshi, J.B., 2005. Bubble formation and bubble rise velocity in gas-liquid systems: A review. *Industrial and Engineering Chemistry Research* 44, 5873-5931.

Kugou, N., Ishida, K., and Yoshida, A., 2003. Experimental study on motion of air bubbles in seawater (terminal velocity and drag coefficient of air bubble rising in seawater). *Transactions on the Built Environment* 68, 145-158.

Kupferberg, A. and G.J. Jameson, 1969. Bubble formation at a submerged orifice above a gas chamber of finite volume, *Transactions of the Institute of Chemical Engineers* 47, T241-T250.

Kyriakides, N.K., Kasrinakis, E.G., Nychas, S.G., and Goulas, A., 1997. Bubbling from nozzles submerged in water: Transitions between bubbling regimes, *The Canadian Journal of Chemical Engineering* 75, 684-691.

Laskowski, J.S., 2004. Testing flotation frothers, *Physicochemical Problems in Mineral Processing* 38, 13-34.

Laskowski, J.S., Cho, Y.S., and Ding, K., 2003a. Effect of frothers on bubble size and foam stability in potash ore flotation systems, *The Canadian Journal of Chemical Engineering* 81, 63-69.

Laskowski, J.S., Tlhone, T., Williams, P., and Ding, K., 2003b. Fundamental properties of the polyoxypropylene alkyl ether flotation frothers, *International Journal of Mineral Processing* 72, 289-299.

Lee, C.-H., Herickson, L.E., and Glasgow, L.A., 1987. Bubble break-up and coalescence in turbulent gas-liquid dispersion, *Chemical Engineering Communications* 59, 65-84.

Leighton, T. G., 1994. *The Acoustic Bubble*. Academic Press Inc., London.

Leighton, T.G., Fagan K.J., and Field, J.E., 1991. Acoustic and photographic studies of injected bubbles, *European Journal of Physics* 12, 77-85.

Leighton, T.G., and Walton, A.J., 1987. An experimental study of the sound emitted from gas bubbles in a liquid. *European Journal of Physics* 8, 2, 98-104.

Lekki, J., and Laskowski, J., 1975. A new concept of frothing in flotation systems and general classification of flotation frothers, In: *Proceedings of the 11<sup>th</sup> International Mineral Processing Congress*, Cagliari, 429-448.

Lessard, R.D., and Zieminski, S.A., 1971. Bubble coalescence and gas transfer in aqueous electrolytic solutions; *Industrial and Engineering Chemistry Fundamentals* 10, 260-289.

Levich, V. G., 1962. *Physicochemical Hydrodynamics*, Vol. 689. Englewood Cliffs, NJ, Prentice-Hall.

Lewis, D., and Davidson, J.F., 1982. Bubble splitting in shear flow. *Transactions of the Institution of Chemical Engineers* 60, 5, 283-291.

Maldonado, M., Quinn, J.J., Gomez, C.O., and Finch, J.A., 2013. An experimental study examining the relationship between bubble shape and rise velocity. *Chemical Engineering Science* 98, 7-11.

Malysa, K., 1992. Wet foams: Formation, properties and mechanism of stability, *Advances in Colloid and Interface Science* 40, 37-83.

Malysa, K., and Pawlikowska-Czubak, J., 1975. Frothability and surface elasticity of aqueous solutions of some frothers, *Bulletin de l'Academie Polonaise des Sciences* 5, 423-427.

Manasseh, R., Riboux, G., and Risso, F., 2008. Sound generation on bubble coalescence following detachment. *International Journal of Multiphase Flow*, 34, 10, 938-949.

Martinez-Bazan, C., Montanes, J.L., and Lasheras, J.C., 2000. Bubble size distribution resulting from the break-up of an air cavity injected into a turbulent water jet. *Physics of Fluids* 12, 145–148.

Marrucci, G., and Nicodemo, L., 1967. Coalescence of gas bubbles in aqueous solutions of inorganic electrolytes. *Chemical Engineering Science* 22, 1257-1265.

Melo, F., and Laskowski, J.S., 2006. Fundamental properties of flotation frothers and their effect on flotation, *Minerals Engineering* 19, 766-773.

Mendelson, H.D., 1967. The prediction of bubble terminal velocities from wave theory. *AIChE Journal* 13, 2, 250-253.

Minnaert, M., 1933. On musical air-bubbles and the sounds of running water, *Philosophical Magazine* 16, 235–248.

Miyahara, T., Iwata, M. and Takahashi, T., 1984. Bubble formation pattern with weeping at a submerged orifice, *Journal of Chemical Engineering of Japan* 17, 592-597.

Miyahara, T., Tanimoto, M., and Takahashi, T., 1982. Bubble formation from an orifice at high gas injection rates, *Kagaku Kogaku Ronbunshu* 8, 18-24.

- Miyhara, T., Tsuchiya, K., and Fan, L-S, 1991. Effect of turbulent wakes on bubble–bubble interaction in a gas–liquid–solids Fluidized bed, *Chemical Engineering Science* 46, 9, 2368–2373.
- Moyo, P., Gomez, C.O., and J.A. Finch, 2006. Characterization of frothers by water carrying rate, in *Interfacial Phenomena in Fine Particle Technology*, 6th UBC-McGill UA International Symposium on Fundamentals of Mineral Processing (Eds. Z. Xu and Q. Liu), COM 2006, Montreal, 133-146.
- Moyo, P., Gomez, C.O. and J.A. Finch, 2007. Characterization frothers using water carrying rate, *Canadian Metallurgical Quarterly* 46, 3, 215-220.
- Nesset, J.E., Finch, J.A., and Gomez, C.O., 2007. Operating variables affecting the bubble size in forced-air mechanical flotation machines, *Ninth Mill Operators' Conference*, Fremantle, WA, 55-66.
- Nesset, J.E., Hernandez-Aguilar, J.R., Acuna, C., Gomez, C.O., and Finch, J.A., 2006. Some gas dispersion characteristics of mechanical flotation machines. *Minerals Engineering* 19, 807-815.
- Nguyen, P.T., Hampton, M.A., Nguyen, A.V., and Birkett, G.R., 2012. The influence of gas velocity, salt type and concentration on transition concentration for bubble coalescence inhibition and gas holdup, *Chemical Engineering Research and Design* 90, 1, 33-39.
- Nguyen, A.V., and Schulze, H.J. (eds.), 2004. *Colloidal Science of Flotation*. Surfactant science series, vol. 118. Marcel Dekker. New York.
- Ohnishi, M., Azuma, H., and Straub, J., 1999. Study on secondary bubble creation induced by bubble coalescence, *Advances in Space Research* 24, 10, 1331-1336.
- Okazaki,S., 1962. The velocity of air bubble ascending in aqueous solution of surface active substance and inorganic electrolyte. *Kolloid-Zeitschrift und Zeitschrit für Polymere*, Band 185·Heft 2, 154-157.
- Oosterwegel, G.G., and de Groot, H.J., 1980. On the possibility to measure volumes of small gas bubbles and the bubble producing gas flow rates acoustically, *Review of Scientific Instrumentation* 51, 2, 201-205.

Peng, Y., and Seaman, D., 2011. The flotation of slime-fine fractions of Mt. Keith pentlandite ore in de-ionised and saline water, *Minerals Engineering* 24, 5, 479-481.

Peters, F., and Els, C., 2012. An experimental study on slow and fast bubbles in tap water. *Chemical Engineering Science* 82, 194-199.

Pomianowski, A., Malysa, K., and Para, G., 1973. Annual Report for the Institute of Nonferrous Metals, 6.

Prince, M.J., and Blanch, H.W., 1990. Bubble coalescence and break-up in air-sparged bubble columns, *AIChE Journal* 36, 1485-1499.

Pugh, R.J., 1996. Foaming, foam films, antifoaming and defoaming, *Advances in Colloid and Interface Science* 64, 67-142.

Pugh, R.J., 2007. The physics and chemistry of frothers, In: Fuerstenau, M.C., Jameson, G., and Yoon, R.-H. (Eds.), *Froth Flotation: A Century of Innovation*, SME, Littleton, Colorado, USA.

Pugh, R.J., Weissenborn, P., and Paulson, O. 1997. Flotation in inorganic electrolytes; the relationship between recovery of hydrophobic particles, surface tension, bubble coalescence and gas solubility. *International Journal of Mineral Processing* 51, 125-138.

Quinn, J.J., Kracht, W., Gomez, C.O., Gagnon, C., and Finch, J.A., 2007. Comparing the effects of salts and frother (MIBC) on gas dispersion and froth properties, *Minerals Engineering* 20, 1296-1302.

Quinn, J.J., Maldonado, M., Gomez, C.O., and Finch, J.A., 2013. An experimental study on bubble shape and rise velocity in frother, polymer and inorganic salt solutions, In: Proceedings of the 52<sup>nd</sup> Conference of Metallurgists: Water and Energy in Mineral Processing, The 9<sup>th</sup> UBC-McGill-U of A International Symposium on the Fundamentals of Mineral Processing, The Metallurgical Society of CIM, 1981-1992.

Quinn, J.J., Sovechles, J.M., Finch, J.A., and Waters, K.E., 2014. Critical coalescence concentrations of inorganic salt solutions. *Minerals Engineering* 58, 1-6.

Raymond, F., and Rosant, J.-M., 2000. A numerical and experimental study of the terminal velocity and shape of bubbles in viscous liquids. *Chemical Engineering Science* 55, 943-955.

Riggs, W.F., 1986. Frothers - An Operator's Guide. In: Chemical Reagents in the Mineral Processing Industry, 110-116.

Roberts, J.D., and Caserio, M.C., 1977, Basic Principles of Organic Chemistry, Second Edition, W.A. Benjamin Inc.

Sam, A., Gomez, C.O., and Finch, J.A., 1996. Axial Velocity Profiles of Single Bubbles in Water/Frother Solutions, International Journal of Mineral Processing 47, 177-196.

Sato, A., Aoki, M., and Watanabe, M., 2010. Single Rising Bubble Motion in Aqueous Solution of Electrolyte, Journal of Fluid Science and Technology, 5, 1, 14-25.

Savic, P., 1953. Circulation and distortion of liquid drops falling through viscous medium, Nat. Res. Council of Canada, Div. of Mech. Eng., Rep. No. NRC-MT-22, 36.

Schäfer, R., Merten, C., and Eigenberger, G., 2002. Bubble size distributions in a column reactor under industrial conditions, Experimental Thermal and Fluid Science 26, 595-604.

Sevik, M., and Park, S.H., 1973. The splitting of drops and bubbles by turbulent fluid flow. Journal of Fluids Engineering 95, 53-60.

Smolianski, A., Haario, H., and Luukka, P., 2008, Numerical study of dynamics of single bubbles and bubble swarms. Applied Mathematical Modelling 32, 641-659.

Stewart, C.W., 1995. Bubble interaction in low-viscosity liquids. International Journal of Multiphase Flow 21, 1037-1046.

Stokes, G.G., 1851. On the effect of the internal friction of fluid on the motion of pendulums. Trans. Cambridge Phi. Soc. 9, 8.

Sweet, C., van Hoogstraten, J., Harris, M., and Laskowski, J.S., 1997. The effect of frothers on bubble size and frothability of aqueous solutions, In: Finch, J.A., Rao, S.R., Holubec, I. (Eds.), Processing of Complex Ores, 2nd UBC-McGill Symposium on Fundamentals in Mineral Processing, The Metallurgical Society of CIM, 235-246.

Sweet, C., van Hoogstraten, J., Harris, M., and Laskowski, J.S., 1997. The effect of frothers on bubble size and frothability of aqueous solutions, In: Finch, J.A., Rao, S.R., Holubec, I. (Eds.), Processing of Complex Ores, 2nd UBC-McGill Symposium on Fundamentals in Mineral Processing, The Metallurgical Society of CIM, 235-246.

Talaia, M.A.R., 2007. Terminal velocity of a bubble rise in a liquid column, *World Academy of Science, Engineering and Technology* 28, 264-268.

Tan, S.N., Pugh, R.J., Fornasiero, D., Sedev, R., and Ralston, J., 2005. Foaming of Polypropylene Glycols and Glycol/MIBC Mixtures, *Minerals Engineering* 18, 179-188.

Tan, S.N., Pugh, R.J., Fornasiero, D., Sedev, R., and Ralston, J., 2006. The interfacial conformation of polypropylene glycols and their foam properties, *Minerals Engineering* 19, 703-712.

Tan, Y.H., Rafiei, A.A, Elmahdy, A., and Finch, J.A., 2013. Bubble size, gas holdup and bubble velocity profile of some alcohols and commercial frothers. *International Journal of Mineral Processing* 119, 1-5.

Tate, T., 1864. On the magnitude of a drop of liquid formed under different circumstances. *The London, Edinburgh, and Dublin Philosophical Magazine and Journal of Science*, 27, 181, 176-180.

Tomiyama, A., 2002. Single bubbles in stagnant liquids and in linear shear flows (Keynote Lecture). In: Prasser, H.-M. (Ed.), *Proceedings of Measurement Techniques for Steady and Transient Multiphase Flows*, Rossendorf, September 18 – 20.

Tomiyama, A., Celata, G.P., Hosokawa, S., and Yoshida, S., 2002. Terminal velocity of single bubbles in surface tension force dominant regime. *International Journal of Multiphase Flow* 28, 1497-1519.

Tomiyama, A., and Hayashi, K., 2011, Interface tracking and multi-fluid simulations of bubble flows in bubble columns. (Keynote Lecture) 8th International Conference on Computational Fluid Dynamics in the Oil & Gas, Metallurgical and Process Industries (CFD 2011), Trondheim, Norway.

Tsang, Y.H., Koh, Y.-H., and Koch, D.L., 2004. Bubble-size dependence of the critical electrolyte concentration for inhibition of coalescence, *Journal of Colloid and Interface Science* 275, 290-297.

Tse, K.L., Martin, T., McFarlane, C.M., and A.W. Nienow, 2003. Small bubble formation via a coalescence dependent break-up mechanism, *Chemical Engineering Science* 58, 275-286.

- Tucker, J.P., Deglon, D.A., Franzidis, J.P., Harris, M.C., and O'Connor, C.T., 1994. An Evaluation of Direct Method of Bubble Size Distribution Measurements in a Laboratory Batch Flotation Cell, *Minerals Engineering* 7, 667-680.
- Tuson, K.R., 1955. Single exposure photography of high speed event, *British Journal of Applied Physics* 6, 99-100.
- van Wijngaarden, L., and Veldhuis, C., 2008. On hydrodynamical properties of ellipsoidal bubbles. *Acta Mechanica* 201, 37-46.
- Vanegas, C., and Holtham, P., 2008. On-line froth acoustic emission measurements in industrial sites, *Minerals Engineering* 21, 883-888.
- Vera, M.A., Mathe, Z.T., Franzidis, J.-P., Harris, M.C., Manlapig, E.V., and O'Connor, C.T., 2002. The modelling of froth zone recovery in batch and continuously operated laboratory flotation cells, *International Journal of Mineral Processing* 64, 135-151.
- Wang, B., and Peng, Y., 2013. The behaviour of mineral matter in fine coal flotation using saline water. *Fuel* 109 309-315.
- Wentzell, P. D., and Wade, A. P., 1989. Chemical acoustic emission analysis in the frequency domain, *Analytical Chemistry* 61, 2638-2642.
- Wichterle, K., Sutná, K., and Večeř, M., 2009. Shape and rising velocity of bubbles. In: Markoš, J. (Ed.), *Proceedings: 36<sup>th</sup> International Conference of Slovak Society of Chemical Engineering*, 090-1 - 090-12.
- Wilkinson, P.M., Van Schayk, A., and Spronken, J.P., 1993. The influence of gas density and liquid properties on bubble breakup. *Chemical Engineering Science* 48, 7, 1213-1226.
- Wills, B.A., and Napier-Munn, T., 2006. *Wills' Mineral Processing Technology: An Introduction to the Practical Aspects of Ore Treatment and Mineral Recovery*. Butterworth-Heinemann, Burlington, MA, USA.
- Wu, M., and Gharib, M., 2002. Experimental studies on the shape and path of small air bubbles rising in clean water. *Physics of Fluids* 14, 7, L49-L52.

Yañez, A.B., Morales, P., Coddou, F., Elgueta, H., Ortiz, J.M., Perez, C., Cortes, G., Gomez, C.O., and Finch, J.A., 2009. Gas dispersion characterization of TANKCELL®-300 at Chuquicamata concentrator, Conference of Metallurgists, Sudbury, 313-324.

Yoon, R. H., and Sabey, J. B., 1989. Coal flotation in inorganic salt solutions, Surfactant Science Series: Interfacial Phenomena in Coal Technology 32, 87-114.

Zahradnik, J., Fialová, M., and Linek, V., 1999. The effect of surface additives on bubble coalescence in aqueous media, Chemical Engineering Science 54, 4757-4766.

Zeng, Y., and Forssberg, E., 1993. Monitoring Grinding parameters by signal measurements for an industrial ball mill, International Journal of Mineral Processing 40, 1-16.

Zhang, F.H., and Thoroddsen, S.T., 2008. Satellite generation during bubble coalescence, Physics of Fluids 20, 022104.

Zhang, L., and Shoji, M., 2001. Aperiodic bubble formation from a submerged orifice. Chemical Engineering Science 56, 5371-5381.

Zhang, W., Nasset, J.E., Rao, R., and Finch, J.A., 2012a. Concentration (CCC)95-hydrophile-lipophile balance (HLB) relationship. Minerals 2, 3, 208-227.

Zhang, W., Zhou, X., and Finch, J.A., 2012b. Determining independent control of dual-frother systems – gas holdup, bubble size and water overflow rate. Minerals Engineering 39, 106-116.

Zhang, Y., McLaughlin, J.B., and Finch, J.A., 2001. Bubble velocity profile and model of surfactant mass transfer to bubble surface. Chemical Engineering Science 56, 6605-6616.

Zieminski, S.A., Hume III, R.M., and Durham, R., 1976. Rates of oxygen transfer from air bubbles to aqueous NaCl solutions at various temperatures, Marine Chemistry 4, 333-346.

Zieminski, S.A., and Lessard, R.D., 1969. Effects of chemical additives on performance of an air-water contactor, I & EC Process Design and Development 8, 1, 69-75.

Zieminski, S.A., and Whittemore, R.C., 1971. Behavior of gas bubbles in aqueous electrolyte solutions; Chemical Engineering Science 26, 509-520.

# Chapter 3 – Origin of bi-modal bubble size distributions in the absence of frother

## 3.1 Introduction

Bubble formation in flotation machines results from an interplay of the gas dispersing device and solute properties. In the absence of coalescence-inhibiting agents bi-modal bubble size distributions (BSD) are often observed (Quinn et al., 2007; Finch et al., 2008; Cappuccitti and Nasset, 2009; Yañez et al., 2009; Acuña and Finch, 2010).

Figure 3.1 shows an example of a bi-modal BSD with supporting visual evidence observed in water in a laboratory flotation column with a porous sparger processing a Pb/Zn ore (Quinn et al., 2007). The water-only system produced a fine mode at ca. 0.5 mm and a coarse mode at ca. 5 mm (i.e., fine/coarse ratio ca. 1/10). The fine mode and the bi-modal distribution are eliminated in the presence of frother (10 ppm MIBC) replaced by a mono-modal distribution centered ca. 1.5 mm. Quinn et al. found  $> 0.2$  M NaCl likewise eliminated the bi-modal distribution.

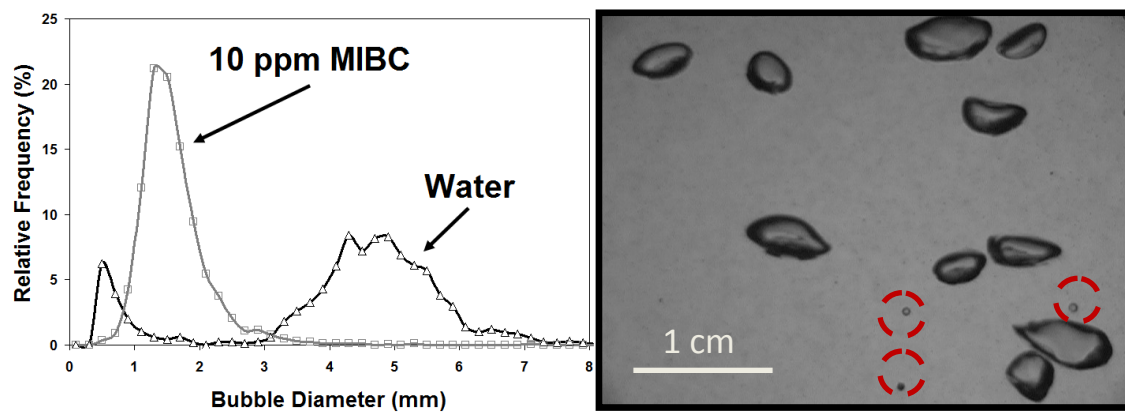


Figure 3.1 – Left: Bubble size distribution (number frequency) in water and 10 ppm MIBC solution, Right: Example image showing large irregular shaped bubbles and fine bubbles (identified by dashed circle) in the water-only system (modified from Quinn et al., 2007)

In another example, Finch et al. (2008) show bi-modal distribution in a mechanical cell in water only with a fine mode (ca. 0.5 mm) and coarse mode (ca. 5 mm), i.e., ca. 1/10 ratio similar to Figure 3.1. Sequential addition of frother was illustrated to progressively eliminate the bi-modal distribution eventually realizing a mono-modal distribution centered in that case at ca. 0.8 mm.

The origin of the bi-modal distribution in water-only and its elimination by adding frother, or salt, needs an explanation. One possible origin of the bi-modal distribution is the fact that the large bubbles expected without frother are unstable and prone to break-up (Leighton, 1991). Another possibility is that the bi-modal distribution originates from bubble-bubble interactions. Tse et al. (2003), trying to explain the origin of fine bubbles as the swarm rose in a bubble column, observed coalescing bubbles expelling a fine bubble. They argued that an annular wave is set up in the newly formed bubble which travels the length of the bubble resulting in extension and pinching-off of a daughter bubble. The mechanism was observed in experiments contacting two bubbles at facing capillaries. The process will be called ‘coalescence-induced bubble break-up’. Ohnishi et al. (1999) described a similar phenomenon.

Zhang and Thoroddsen (2008) studied coalescence-induced break-up. Experimentally, they launched one bubble into a second bubble held at a capillary and showed that for equal sized parent bubbles, the daughter bubble is roughly 1/10<sup>th</sup> the parent size. Using high-speed video imaging the authors identified the capillary waves which converged at the bubble apex and pinched off the daughter bubble.

Exploring the origin of bi-modal distributions in the absence of frother in flotation systems, Finch et al. (2008) found they could control bubble interactions and generate coalescence-induced break-up by manipulating gas rate at a capillary. In the example shown, addition of frother prevented coalescence and the related fine bubble formation. The intention was to pursue this experimental technique and determine the gas rate at which coalescence-induced break-up occurred as a function of frother addition, following the previous work that tracked the transition gas rate between non-coalescence and coalescence (Kracht and Finch, 2009). It became apparent, however, that the mechanism described by Tse et al. (2003) was only one possibility. The purpose of this paper is to identify other mechanisms that may promote small bubble formation and bi-modal distributions using high-speed imaging of bubble interactions at a capillary.

### 3.2 Experimental

The experimental set-up (Figure 3.2) comprised a 50 cm (l) x 20 cm (w) x 50 cm (h) acrylic tank holding 30 L Montreal tap water (average conductivity: 293  $\mu$ S/cm, major constituents: 30 mg/L Ca, 24 mg/L SO<sub>4</sub>, 23 mg/L Cl, 13 mg/L Na, 8 mg/L Mg (Remillard et al., 2009)) in which air bubbles were formed at a glass capillary tube with internal diameter of nominally 500  $\mu$ m ( $508 \pm 25.4 \mu$ m). The water was at room temperature, 20 - 22 °C. Air flow rate was regulated using a Sierra model 840DL1V1 (0 - 500 sccm) mass flow meter controller. Tests were operated at air flow rates ranging from 70 - 250 sccm.

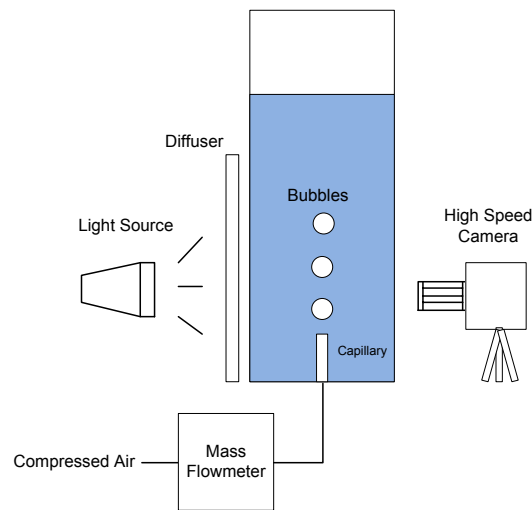


**Figure 3.2 – Experimental setup**

A Fastec Troubleshooter HR digital high-speed camera equipped with a 60 mm macro lens (Nikon, AFMicro Nikkor) was used to capture events close to the point of generation. Images (320 x 240 pixels) were collected at rates of 500-2000 frames per second.

Bubble size estimates were made for the coarse and fine bubbles shown in the example images. Large bubbles assumed an oblate ellipsoidal shape typically 10 - 20 mm above the point of generation. Images taken under these conditions were analyzed using ImageJ software. An ellipse was fitted to the bubble with major (a) and minor (b) semi-axis being calculated. An equivalent diameter ( $d_e$ ) was calculated based on Equation (3.1).

$$d_e = \sqrt[3]{(2a)^2 \times (2b)} \quad (3.1)$$

Due to the fine bubble sizes obtained and the image resolution, fine bubble sizes were estimated by manual inspection using ImageJ software.

### **3.3 Results**

Six mechanisms resulting in fine bubbles were observed, four related to coalescence and two to wake effects.

#### **3.3.1 Coalescence-induced**

##### **a) Bubble break-up**

Figure 3.3 shows a sequence of events at the 500  $\mu\text{m}$  capillary with air flow rate 70 sccm. The sequence shows coalescence (at 1.0 ms) and subsequent bubble detachment from the orifice (3.0 ms) to produce the capillary wave which travels up the bubble and leads to the expulsion of a fine bubble (12.5 - 13.0 ms). The equivalent spherical diameter of the large bubble is ca. 3.6 mm (equivalent spherical diameter), and the fine bubble is ca. 0.4 mm, i.e., ca. 1/9<sup>th</sup> the parent bubble size.

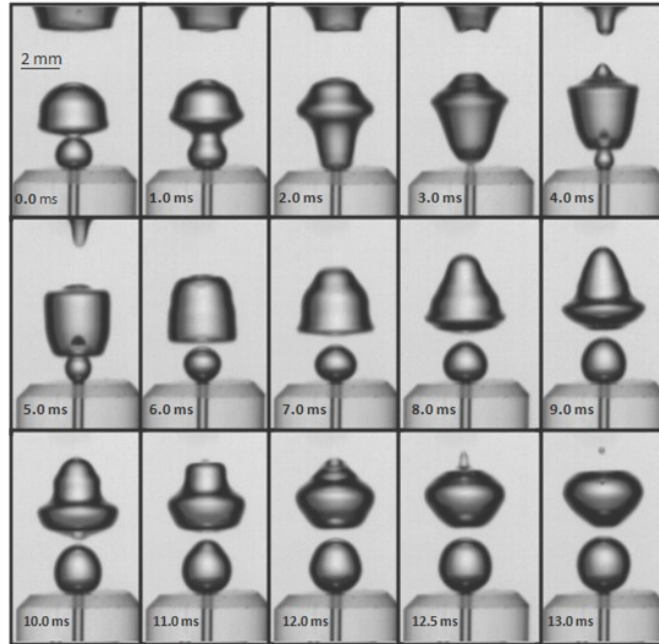


**Figure 3.3 – Coalescence-induced bubble break-up (note the reduced time interval - 0.5 ms - for final three frames). Bubble produced at 500  $\mu\text{m}$  capillary at 70 sccm.**

**b) Droplet formation, collision and bubble expulsion**

The image sequence in Figure 3.4 was taken under the same conditions as those in Figure 3.3. In this case, however, there is evidence of coalescence-induced droplet formation inside the newly created bubble. The droplet is formed as the trailing edge of the bubble recoils soon after detachment from the orifice (6 - 8 ms). The droplet travels the length of the bubble (6 - 12 ms) and impacts the forward bubble wall (14 ms) which in this example expels two small daughter bubbles (16 ms). The parent bubble is ca. 4.0 mm while the daughter bubbles ca. 0.4 and 0.2 mm (ca.  $1/10^{\text{th}}$  and  $1/20^{\text{th}}$  the parent bubble size).

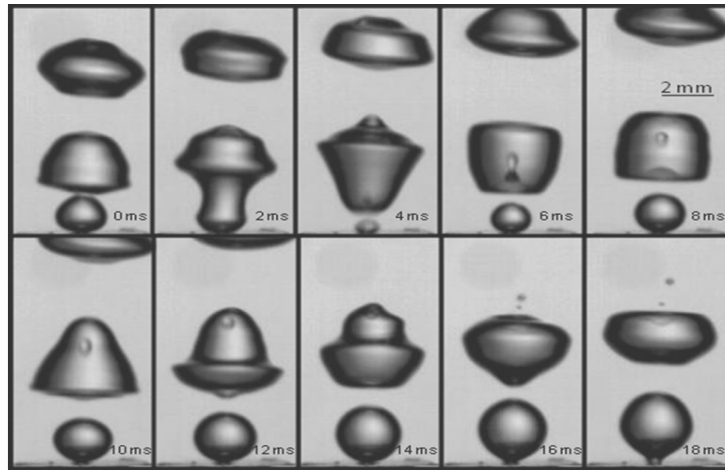


**Figure 3.4 – Coalescence-induced droplet formation (4 - 8 ms images) and subsequent bubble expulsion (16 and 18 ms images). Bubble produced at 500  $\mu\text{m}$  capillary at 70 sccm.**

**c) Jet formation, collision and bubble expulsion**

Increasing air flow rate to 250 sccm, instead of the droplet, the liquid enters the bubble as a jet (Figure 3.5, at 3 ms) which shoots through the opposite bubble wall, this time expelling 3 fine bubbles (3.5 - 4.5 ms). The parent bubble diameter is ca. 4.7 mm and the fine bubble diameters are ca. 0.2, 0.4 and 0.7 mm (ca.  $1/24^{\text{th}}$  -  $1/7^{\text{th}}$  the parent bubble size).

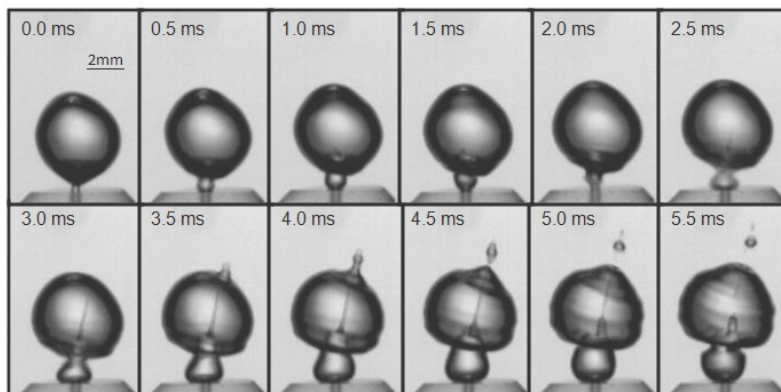


**Figure 3.5 – Coalescence-induced liquid jet formation and subsequent bubble expulsion. Bubble produced at a 500  $\mu\text{m}$  capillary with air flow rate 250 sccm.**

#### d) Jet disruption to droplet, collision and bubble expulsion

The liquid jet in Figure 3.5 can also disintegrate into droplets inside the bubble (Figure 3.6, 6 - 8 ms). In this case, the droplets impacted with the rearward bubble wall (11 and 12 ms) causing fine bubble formation (13 ms). The parent bubble is ca. 4.8 mm in diameter, while the fine bubbles are smaller than 0.2 mm in diameter (ca. 1/24<sup>th</sup> the parent bubble size).

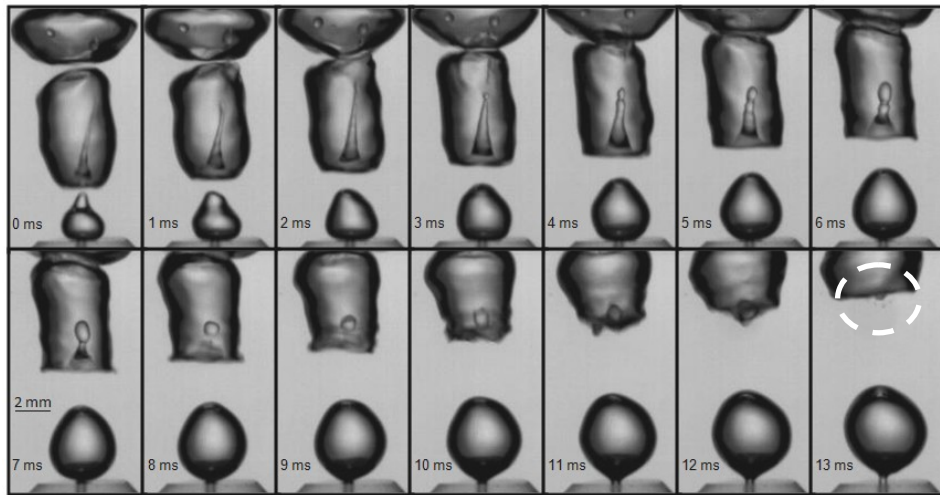


**Figure 3.6 – Disruption of liquid jet inside bubble leads to droplet which upon impact with the rear bubble wall expels fine bubbles (13 ms image - indicated with dashed circle). Bubbles produced at 500  $\mu\text{m}$  capillary at 250 sccm.**

### 3.3.2 Wake-related events

#### a) Elongation

Figure 3.7 shows bubble elongation induced by the low pressure region in the wake of the previous bubble. Elongation can sometimes be sufficient to form a lobe (7 - 8 ms) which pinches off to produce a bubble (10 ms). The elongation appears to be associated with liquid jet formation in the first bubble (evident from 2 ms onwards) as the subsequent bubble appears to be drawn (elongate) in the direction of the liquid jet. The elongated bubble had an equivalent spherical bubble diameter of ca. 4.6 mm which formed two bubbles upon break-up of ca. 2.6 (upper bubble) and 4.3 mm (lower bubble).

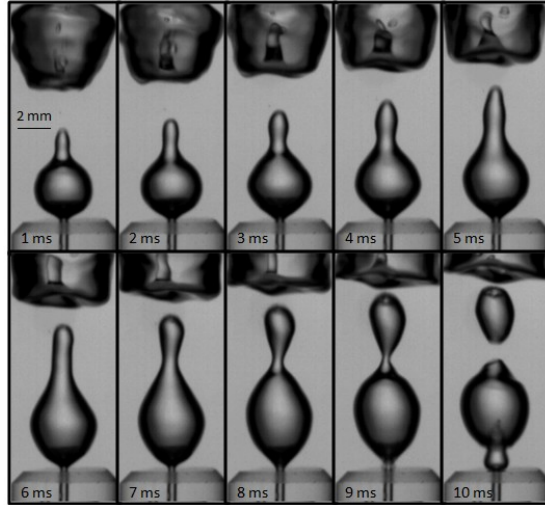


**Figure 3.7 – Wake-related force causes subsequent bubble deformation and break-up. Bubble produced at 500  $\mu\text{m}$  capillary at 250 sccm.**

**b) Premature detachment**

Figure 3.8 shows bubbles formed at the 500  $\mu\text{m}$  capillary with air flow rate of 100 sccm. Coalescence (not shown) and subsequent detachment (0.5 - 1.0 ms) is followed by the bubble base recoiling which seems to extract a bubble from the capillary before it can grow to normal release size. The initially released bubble diameter is roughly 4.5 mm while the fine bubble is about 0.4 mm (ca. 1/11<sup>th</sup> the parent bubble size).

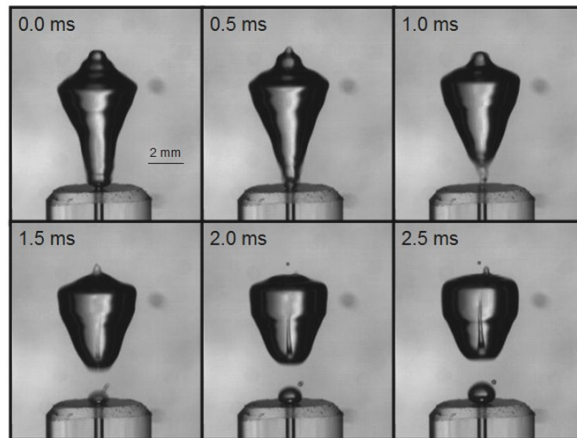


**Figure 3.8 – Fine bubble formed by premature detachment from the orifice due to the wake of a previous bubble. Bubble produced at 500  $\mu\text{m}$  capillary at 100 sccm.**

### 3.3.3 Summary of daughter to parent bubble size ratio

Table 3.1 summarizes the daughter/parent bubble size ratios for each mechanism identified compared to the fine/coarse ratio for flotation systems in the absence of coalescence inhibiting reagents taken from Figure 3.1.

**Table 3.1 – Summary of daughter to parent bubble sizes**

<b>Mechanism</b>	<b>Relative Size</b>
Flotation	1/10
1) Coalescence-induced	
a) Break-up	1/9
b) Droplet	1/20 – 1/10
c) Jet	1/24 – 1/7
d) Jet/droplet	1/24
2) Wake-induced	
a) Elongation	1/1.8 – 1/1.1
b) Premature	1/11

### 3.4 Discussion

The bi-modal distributions in water only imply a mechanism forming small bubbles, typically < 1 mm. The hypothesis was that the formation mechanism was related to bubble-bubble interactions. One way to induce interaction of bubbles is at a capillary by manipulating air rate, which was the model approach adopted. The study identified six mechanisms that caused small bubbles to form. The established mechanism, coalescence-induced bubble break-up, was observed (mechanism 1a). Evidence of the capillary wave that forms on coalescence to travel the bubble and pinch off a small bubble is illustrated in Figure 3.9a. A similar mechanism seems to be at play in formation of a liquid droplet inside the bubble (the start of mechanism 1b): the capillary wave appears to reverse into the bubble extending a finger of liquid which pinches off as a droplet (Figure 3.9b). The droplet subsequently collides with the leading edge of the bubble and expels a small bubble (Figure 3.9c).

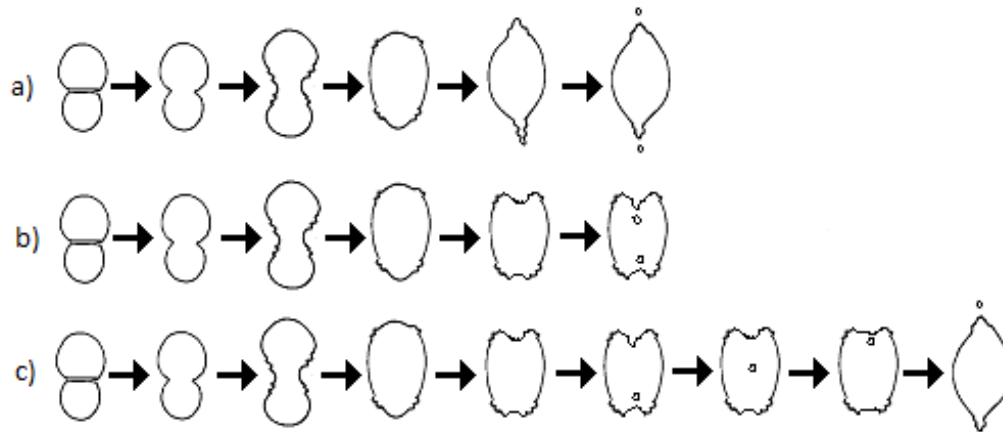


**Figure 3.9 – Schematics showing: a) coalescence-induced bubble break-up, b) coalescence-induced droplet formation and, c) coalescence-induced droplet formation and subsequent bubble break-up.**

Mechanism 1c sees conditions forming a liquid jet which shoots across the bubble to expel a small bubble. Liquid jets were noted by Leighton (1994) and Mitrovic (1997) who gave photographic evidence of an upward axial jet within a newly created bubble; the present work shows the jet can form on coalescence and give rise to small bubbles. The jet sometimes disintegrates into droplets which, in this case, impact the rear bubble wall and eject fine bubbles (mechanism 1d). Jetting and jet disruption phenomena are seen in bubbles bursting at a free surface (Boulton-Stone and Blake, 1993; Duchemin et al., 2002; Lee et al., 2011); the present work identifies the phenomena with coalescing bubbles.

In addition to coalescence-related mechanisms the study identified two apparently wake-related events. The low pressure region in the bubble wake tends to draw in a trailing bubble, extending it and sometimes causing a lobe to form which pinches off (mechanism 2a). Splitting of the trailing bubble is due to shear caused by the flow generated by the leading bubble (Tsuchiya et al., 1989). If present, liquid jet formation also seems to contribute to the wake forces as the trailing bubble appears to deform in the direction of the liquid jet. The second wake-related phenomenon (mechanism 2b) is reminiscent of events described by Hofmeier et al. (1995) in which small bubbles form between larger bubbles in a chain due to inertia from the preceding large bubble.

The purpose of the study was to identify mechanisms giving rise to small bubbles and thus bi-modal size distributions. One way to identify is to compare the observed ratio of daughter to parent bubble in the present experiments with the fine/coarse mode ratio for flotation systems in the absence of frother or salts (Table 3.1). We can apply our understanding that frothers and salts inhibit coalescence to suggest that only the coalescence-related mechanisms should be retained. Of those four, the comparison suggests that mechanism 1d is likely not a factor, the fine bubbles being too small.

We can now offer a possible explanation of Figure 3.1. Recognizing the coalescence suppressing effect of frothers has led to the hypothesis that flotation machines produce small bubbles and frothers preserve them (Gomez and Finch, 2002; Cho and Laskowski, 2002). Applying this to Figure 3.1 means the original bubbles were ca. 1.5 mm (i.e., the size observed in presence of frother) which in the absence of frother coalesced to form the ca. 5 mm bubbles, an act that also induced fine bubble production from mechanisms 1a-c resulting in the bi-modal distribution. There are difficulties with this interpretation, as discussed elsewhere (Finch et al., 2008), for instance coalescence to form a 5 mm bubble requires 37 1.5 mm bubbles. We will follow up this qualitative study by determining the transition air rate dividing coalescence without break-up from coalescence with break-up, i.e., transition to mechanisms 1a-c, and how this air rate depends on frother and salt concentration.

### **3.5 Conclusions**

Bi-modal bubble size distributions observed in the absence of coalescence inhibiting agents may result from bubble-bubble interactions. The work utilized high-speed photography to examine bubble interactions at a capillary. Conditions could be adjusted to observe coalescence-related and wake-related mechanisms giving fine bubbles and bi-modal distributions. Three coalescence-related mechanisms are argued to be at play in flotation systems where bi-modal bubble size distributions are reported.

### **References**

Boulton-Stone, J.M., and Blake, J.R., 1993. Gas bubble bursting at a free surface. *Journal of Fluid Mechanics* 254, 437-466.

Cappuccitti, F., and Nasset, J.E., 2009. Frother and collector effects on flotation cell hydrodynamics and their implication on circuit performance. In: *Advances in Mineral Processing Science and Technology – 48<sup>th</sup> Conference of Metallurgists*, 169-182.

Cho, Y.S., and Laskowski, J.S., 2002. Effect of flotation frothers on bubble size and foam stability. *International Journal of Mineral Processing* 64, 69-80.

Duchemin, L., Popinet, S., Josserand, C., and Zaleski, S., 2002. Jet formation in bubbles bursting at a free surface. *Physics of Fluids* 14, 9, 3000-3008.

Finch, J.A., Nasset, J.E. and Acuña, C., 2008. Role of frother on bubble production and behaviour in flotation. *Minerals Engineering* 21, 949–957.

Gomez, C.O., and Finch, J.A., 2002. Gas dispersion measurements in flotation machines. *CIM Bulletin* 95, 1066, 73-78.

Hofmeier, U., Yaminsky, V.V. and Christensen, H.K., 1995. Observations of solute effects on bubble formation. *Journal of Colloid and Interface Science* 174, 199-210.

Kracht, W., and Finch, J.A., 2009. Using sound to study bubble coalescence. *Journal of Colloid and Interface Science* 332, 237–245.

Lee, J.S., Weon, B.M., Park, S.J., Le, J.H., Fezaa, K., and Lee, W.-K., 2011. Size limits the formation of liquid jets during bubble bursting. *Nature Communications* 2, 367, 1-7.

Leighton, T. G., 1994. *The Acoustic Bubble*. Academic Press Inc., London.

Leighton, T.G., Fagan, K.J., and Field, J.E., 1991. Acoustic and photographic studies of injected bubbles. *European Journal of Physics* 12, 77-85.

Mitrovic, J., 1997. Formation of a liquid jet after detachment of a vapour bubble. *International Journal of Heat and Mass Transfer* 40, 18, 4309-4317.

Ohnishi, M., Azuma, H. and Straub, J., 1999. Study on secondary bubble creation induced by bubble coalescence. *Advances in Space Research* 24, 10, 1331-1336.

Quinn, J.J., Kracht, W., Gomez, C.O., Gagnon, C., and Finch, J.A., 2007. Comparing the effects of salts and frother (MIBC) on gas dispersion and froth properties. *Minerals Engineering* 20, 1296-1302.

Remillard, M., Joseph, M., and Laroche, L., 2009. Municipal drinking water produced by Atwater and Charles-J Des Bailleurs drinking water treatment plant: Annual Summary. Montreal: Division de l'expertise technique.

Tse, K.L., Martin, T., McFarlane, C.M. and A.W. Nienow, 2003. Small bubble formation via a coalescence dependent break-up mechanism. *Chemical Engineering Science* 58, 275-286.

Yañez, A.B., Morales, P., Coddou, F., Elgueta, H., Ortiz, J.M., Perez, C., Cortes, G., Gomez, C.O., and Finch, J.A., 2009. Gas dispersion characterization of TANKCELL®-300 at Chuquicamata concentrator. In: *Advances in Mineral Processing Science and Technology – 48<sup>th</sup> Conference of Metallurgists*, 313-324.

Zhang, F.H. and Thoroddsen, S.T., 2008. Satellite generation during bubble coalescence. *Physics of Fluids* 20, 022104.

# Chapter 4 – Effect of frother and inorganic salts on bubble regimes at a capillary

## 4.1 Introduction

### 4.1.1 Gas dispersion: Frothers and inorganic salts

Gas dispersion properties in mineral flotation systems result from an interplay of the gas dispersing device with frothers and sometimes high concentrations of salts. The initial mechanism involved in dispersing gas (air) in a flotation cell is the break-up of a continuous gas phase into discrete bubbles (formation process). Subsequent bubble coalescence or break-up are secondary events which occur and determine overall gas dispersion properties. There is extensive literature on the ability of frothers to inhibit bubble coalescence which helps explain decreased bubble size and increased frothing (Fouk and Miller, 1931; Zhou et al., 1993; Sweet et al., 1997; Cho and Laskowski, 2002, 2003; Finch et al., 2006; Finch et al., 2008). A combination of Gibbs elasticity and the Marangoni effect form the basis for understanding how frothers resist coalescence (Harris, 1982; Pugh, 1996).

Some flotation processes are in saline solutions (Alexander et al., 2012). In certain instances, the presence of inorganic salts can replace the function of frother (Quinn et al., 2007). Relatively high concentrations ( $>0.05$  M) of inorganic salts are required for coalescence inhibition (Lessard and Zieminski, 1971; Craig et al., 1993; Zahradnik et al., 1999) compared to a few parts per million ( $<1$  mM) of frother (Cho and Laskowski, 2002a,b). For coalescence inhibiting salts, researchers have shown correlations between solution ionic strength and gas dispersion properties, i.e., bubble size and gas holdup, with salts containing multi-valent ions showing a greater effect than mono-valent salts (Lessard and Zieminski, 1969; Zieminski and Whittemore, 1971; Quinn et al., 2007).

Contacting two bubbles to quantify the effect of surfactants or inorganic salts on bubble coalescence is a common experimental technique (Lessard and Zieminski, 1971; Kim and Lee, 1988; Craig, 1993; Hofmeier et al., 1995; Tse et al., 1998, 2003; Tsang et al., 2004; Christenson et al., 2008; Wang and Qu, 2012; Bournival et al., 2012). Indirect measurements of coalescence, such as bubble size and gas holdup, have been used to quantify the effect of solutes in bubble

swarms (Marrucci and Nicodemo, 1967; Zieminski and Whittemore, 1971; Cho and Laskowski, 2002a,b; Laskowski et al., 2003, Azgomi et al., 2007; Nasset et al. 2007; Quinn et al., 2007; Zhang et al., 2012). An action of frother promoting fine bubble production through break-up has been speculated (Grau and Laskowski, 2006; Finch et al., 2008) but there are few experimental studies into the role of solutes on bubble break-up (Tse et al., 2003; Kracht and Finch, 2009a; Chu and Finch, 2013).

One fine bubble generation mechanism is coalescence-induced break-up (Tse et al., 2003). By adapting the technique of Kracht and Finch (2009b), who manipulated gas rate to study interactions between bubbles generated at a capillary, both coalescence and coalescence-induced break-up is reported in this paper.

#### **4.1.2 Effect of gas rate on bubble formation at a capillary**

At sufficiently low gas rate bubble size is determined by orifice specifications (e.g., material and dimension) and solution surface tension, given by the Tate equation (Tate, 1864; Hernandez-Aguilar et al., 2002). At concentrations of industrial interest frothers and salts typically have little impact on surface tension and thus little impact on the size of a single bubble produced at a capillary as shown by several authors (Zhang and Shoji, 2001; Cho and Laskowski, 2002a; Hofmeier et al., 1995). The effect of frothers or salts is only seen once bubbles begin to interact, typically close to the point of bubble generation (Marrucci and Nicodemo, 1967). Bubble interaction at a capillary can be controlled using gas flow rate.

Marrucci and Nicodemo (1967) ascribed increased coalescence at increasing gas flow rate at an orifice to the increased number of bubbles increasing collision frequency coupled with convection forces resulting in more effective coalescence-producing impacts. As turbulence is further increased by increasing gas rate the system becomes chaotic with relatively large bubbles being formed (through coalescence) and fine bubbles formed due to break-up (Hofmeier et al., 1995). Prince (1990) noted a maximum in average bubble size as a function of gas rate due to the competing effects of coalescence and break-up.

Tse et al. (2003), trying to explain the ongoing production of fine bubbles as a bubble swarm rose in a column, observed coalescing bubbles expelling fine bubbles. Contacting two bubbles at

facing capillaries, the authors showed that an annular wave is set up in the newly formed bubble which travels the length of the bubble resulting in extension and pinching-off of a daughter bubble. The process was termed ‘coalescence-induced (or -mediated) bubble break-up’ (Ohnishi et al., 1999; Tse et al., 2003). Expulsion of fines bubbles has been noted with bubbles bursting at a free surface (Duchemin et al., 2002), and of fine droplets being expelled upon coalescence of oil droplets (Hansen and Brown, 1967). In the air-water system, Quinn and Finch (2012) described various mechanisms resulting in breakaway of fine bubbles (bubble break-up) at a capillary, including, coalescence-induced break-up, liquid jet formation inside the bubble that ruptures the bubble wall, and wake forces causing premature bubble detachment. Coalescence events appear to play an important role in bubble break-up. The question posed is does the presence of frother and salt enhance this break-up mechanism or suppress it?

The literature on the effect of solutes on bubble break-up is ambiguous. Otake et al. (1977) observing bubble coalescence and break-up in a bubble swarm stated that for liquids with otherwise comparable physical properties those with lower surface tension resulted in increased bubble break-up. Hofmeier et al. (1995) compared bubbles produced in water and in 1M NaCl solutions which increases surface tension and noted it ‘seemed evident that break-up played a role in fine bubble production’ in the salt solution.

#### **4.1.3 Motivation for the present study**

Kracht and Finch (2009b) utilized high-speed photography and an acoustic emission monitoring technique to determine the transition gas flow rate (in units of standard cubic centimeters per minute (scm)) at which the bubble regime changed from non-coalescing to coalescing at a 200  $\mu\text{m}$  capillary. An example ‘coalescence plots’ is shown in Figure 4.1 for 1-pentanol. Comparison of the plots for different frothers gave a ranking for frother ‘strength’ in terms of coalescence prevention, the stronger frother requiring a higher gas rate for onset of coalescence.

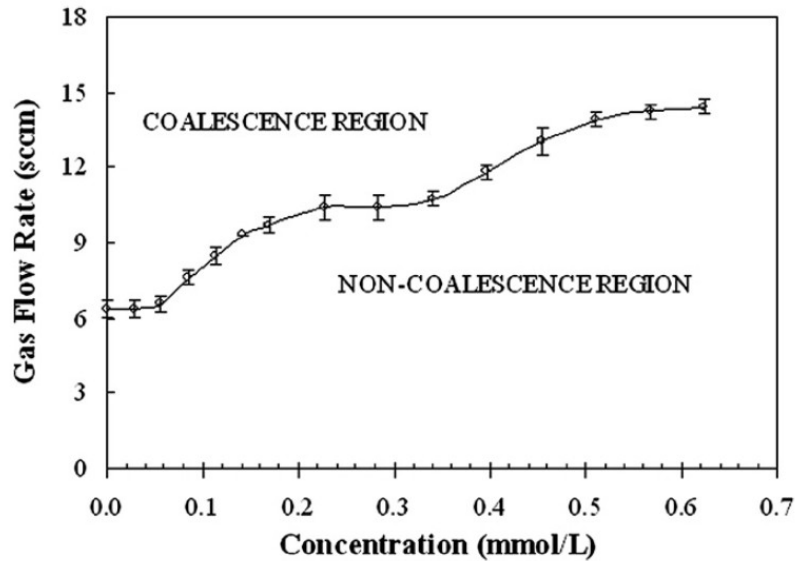


Figure 4.1 – Coalescence plot for 1-pentanol (Reprinted with permission from Elsevier. (Kracht and Finch (2009b))

Recently, Kracht and Rebolledo (2013) used the acoustic technique to test 1-alcohols, commercial frothers, and inorganic salts. The concept of a local critical coalescence concentration (*l*-CCC) curve was developed to compare the coalescence prevention strength of the solutes. Similar to the work of Kracht and Finch (2009b), the authors found that certain inorganic salts (NaCl, KCl, and CaCl<sub>2</sub>) showed a transition range of partial coalescence, i.e., not all bubble collisions resulted in coalescence.

Finch et al. (2008) found they could control coalescence-induced break-up by manipulating gas rate at a capillary. This introduces a second transition gas rate between coalescence and coalescence with break-up. Addition of frother prevented coalescence and the related coalescence-induced fine bubble formation. The current study extends that work to a variety of frothers and inorganic salts utilising high-speed photography to determine the transition air flow rates between bubble regimes at a 300 μm capillary. The first transition gas rate between non-coalescence (single bubble production) and coalescence, and the second between coalescence and coalescence with fine bubble production (bubble break-up) were determined.

## 4.2 Experimental

### 4.2.1 Setup

The experimental set-up (Figure 4.2) comprised a 50 liter (50 cm (length) x 20 cm (width) x 50 cm (height)) rectangular acrylic tank filled with distilled water (30 L) into which air bubbles were injected from a glass capillary with internal diameter nominally 300  $\mu\text{m}$  ( $305 \pm 10 \mu\text{m}$ ). All tests were at room temperature, 18 - 22°C. Air flow rate was regulated using an Omega model FMA-3704 (0 - 100 sccm) mass flow meter controller (accuracy  $\pm 1$  sccm).

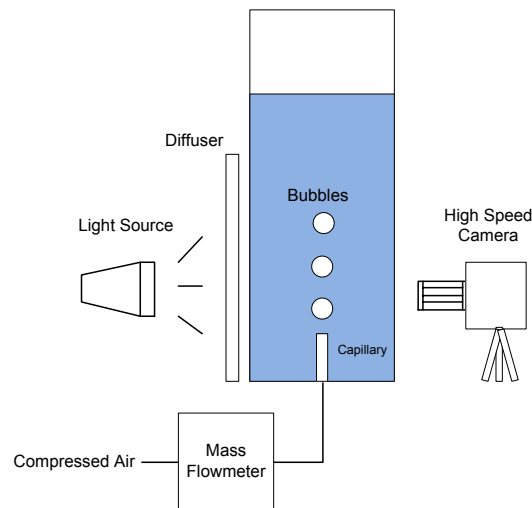


Figure 4.2 – Experimental set-up

### 4.2.2 Determining bubble regime transitions

A Fastec Troubleshooter HR digital high-speed camera equipped with a 60 mm macro lens (Nikon, AFMicro Nikkor) was used to capture images of events close to the point of bubble generation (up to ca. 40 mm above the capillary tip). Images (320 x 240 pixels) were captured at a rate of 2000 frames per second (fps). Air flow rate was increased at increments of 1 sccm. A minimum of 500 bubble formation events were captured for each gas flow rate tested. From the visual record the two transition air flow rates were determined: 1) non-coalescence to coalescence, and 2) coalescence to coalescence with fine bubble production (break-up). The chemicals used in the test work are summarized in Table 4.1. The three commercial frothers are

among the most common and the salts represent ions commonly encountered in mineral flotation systems (Alexander et al., 2012).

**Table 4.1 – Reagent specifications**

Chemical	Supplier	Grade
1-Pentanol	Sigma-Aldrich	ACS
1-Hexanol		≥ 98%
1-Heptanol		≥ 98%
1-Octanol		ACS
MIBC <sup>1</sup>	Sigma-Aldrich	GC
DF250C <sup>2</sup>	Dow Chemical	-
F150 <sup>3</sup>	Flottec	-
KCl	Fisher Scientific	ACS
NaCl		
Na <sub>2</sub> SO <sub>4</sub>		
CaCl <sub>2</sub> ·2H <sub>2</sub> O		
MgSO <sub>4</sub> ·7H <sub>2</sub> O		

<sup>1</sup> Methyl isobutyl carbinol (4-methyl-2-pentanol)

<sup>2</sup> Polypropylene methyl ether-type

<sup>3</sup> Polypropylene glycol-type

### 4.2.3 Bubble sizing and image analysis

To illustrate the regime transitions, bubble size distributions were determined in water and 100 ppm (0.98 mM) MIBC solution as a function of air flow rate (2 - 40 sccm). Focusing 10 mm above the orifice to record the stable size distribution, images were taken using a Canon EOS 60D camera (equipped with a Canon EF 100 mm 1:1.28 USM macro lens) at a rate of 1 fps. Typical image resolution was 170 pixels / mm. A minimum of 1000 bubbles were measured for each condition tested.

An automated image analysis procedure using ImageJ software was used to determine the bubble size distribution. The software fits an ellipse to the projected bubble area and tabulates the major,  $d_{maj}$ , and minor axis,  $d_{min}$ , of each bubble. The volume-equivalent spherical diameter ( $d_e$ ) was calculated using Equation (4.1) (assuming the bubble to be an oblate ellipsoid (Clift et al., 2005)):

$$d_e = \sqrt[3]{(d_{maj})^2 \times (d_{min})} \quad (4.1)$$

### 4.3 Results

Figure 4.3A shows an image sequence of a bubble formed in water at 5 sccm. The initial bubble is released (0 - 4 ms) and rises (4 - 20 ms). A second bubble begins to form (8 ms) at the capillary but does not interact with the initial bubble. This is an example of the non-coalescence bubble regime.

Figure 4.3B shows an image sequence of a bubble formed in water at 15 sccm. An initially released (not shown) bubble rises (0 - 1.0 ms) and the second bubble begins to form (0 - 1.0 ms) with the two bubbles subsequently coming into contact and coalescing (1 - 1.5 ms). These events may be repeated (multiple coalescence events). The large bubble formed through coalescence eventually outpaces the subsequent bubble forming at the capillary and rises freely. This is an example of the coalescence regime. Note the short time periods involved in coalescence events (less than 1 ms) and that the coalescing bubbles are of different size, the initial bubbles is much larger (ca. 2.5 mm) than the subsequent bubble (ca. 0.5 mm).

Figure 4.3C shows an image sequence of bubble formation in water at 25 sccm. Similar to the events shown in Figure 4.3B, an initial bubble forms and rises (not shown) and a second bubble forms (0 ms) and coalesces with the initial bubble (0 - 2 ms). Coalescence and bubble detachment (2 - 4 ms) results in the recoil of the bubble tail which leads to droplet formation inside the bubble (4 ms). The droplet rises to impact the upper wall of the bubble (8 - 10 ms) expelling a fine bubble (11 ms). This is an example of the coalescence with break-up regime. A marker of the regime is a bi-modal bubble size distribution, large bubbles produced through coalescence events and fine bubbles produced through break-up.

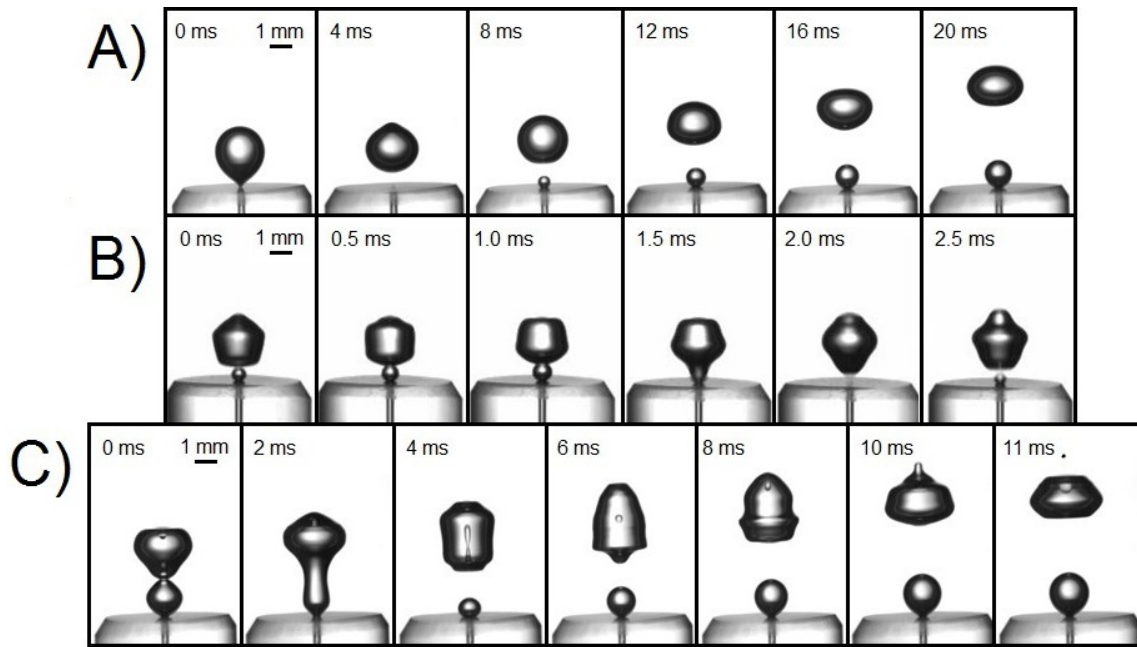


**Figure 4.3 – Example image sequence showing bubble formation, coalescence and/or fine bubble production at A) 5 sccm, B) 15 sccm, C) 25 sccm**

Figure 4.4 shows the bubble regime plot for MIBC. Literature data from Kracht and Finch (2009b) is shown as a reference. Disparity may result from the different capillary sizes used in each of the test work (200  $\mu\text{m}$  vs. 300  $\mu\text{m}$  used here). At low air flow rates (in the non-coalescence region) bubbles are released individually from the orifice. At intermediate air flow rates, bubble coalescence occurs. A small region of partial coalescence was observed. At higher air flow rates, coalescence led to fine bubble production. Transition flow rates increased with increasing concentration (i.e., both onset of coalescence and fine bubble production is delayed in the presence of MIBC). The 95% confidence interval (CI) was estimated using a pooled standard deviation. As the window of partial coalescence is small for frother (and only certain inorganic salts show a region of partial coalescence (Kracht and Rebolledo, 2013)), for comparison purposes only the transition to complete coalescence will be plotted for the frother and inorganic salt systems.

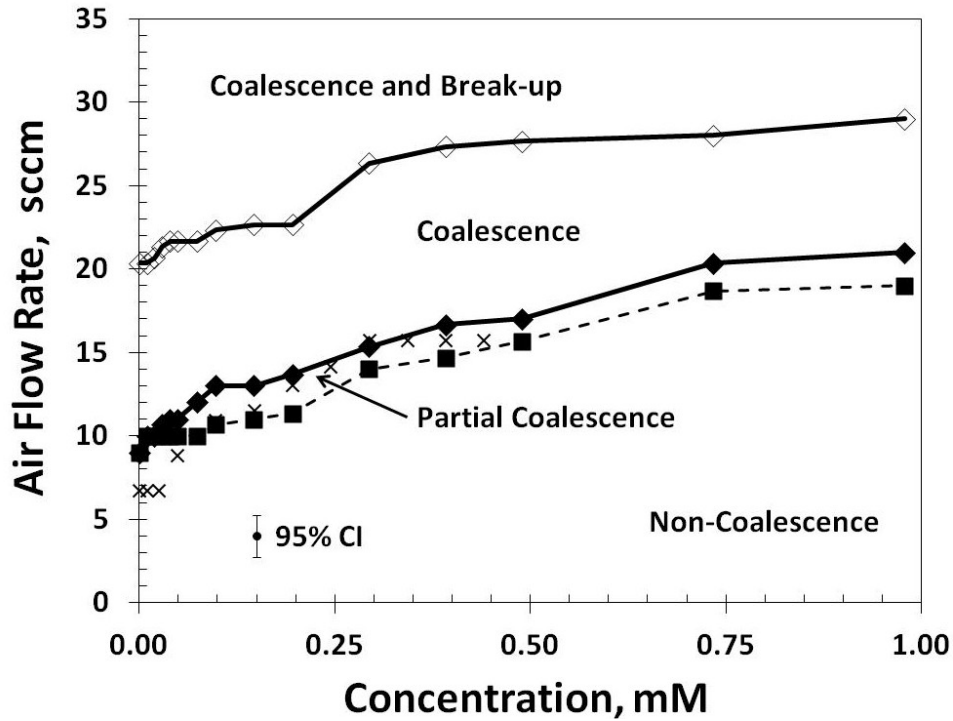


Figure 4.4 – Bubble regime plot for MIBC showing the three regimes and the two major transitions (i.e., ignoring partial coalescence) (Kracht and Finch (2009b) coalescence data shown as x's)

Figure 4.5 shows the bubble size distributions (BSD) in water and in 0.98 mM (100 ppm) MIBC at air flow rates of 5, 15, 20 and 40 sccm. The water results show a shift in the BSD to larger bubble sizes as air flow rate is increased from 5 sccm to 15 sccm as the bubble regime crosses the first transition. As shown in Figure 4.3B, coalescence occurs between a large bubble (ca. 2.5 mm) and a small bubble (ca. 0.5 mm) resulting in only a slight shift in bubble size upon coalescence (from a BSD centered at ca. 2.3 mm to ca. 2.5 mm). In 0.98 mM MIBC solution the 5 sccm and 15 sccm BSDs are almost identical as they both lie in the non-coalescence regime.

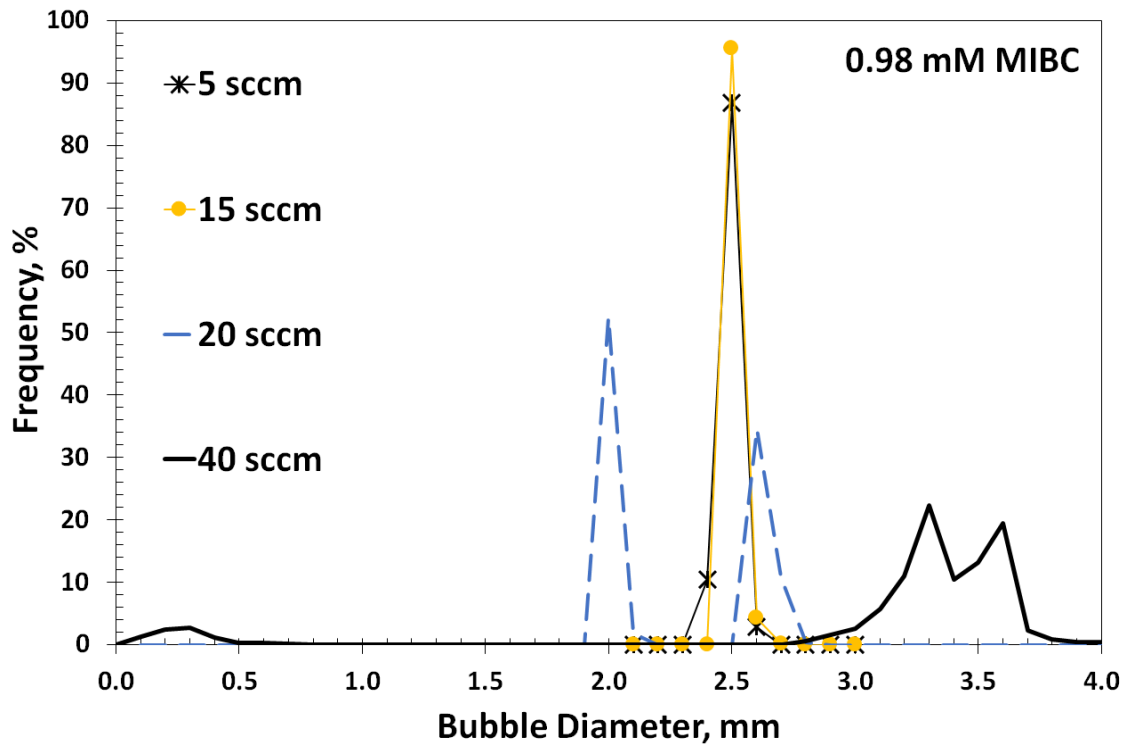
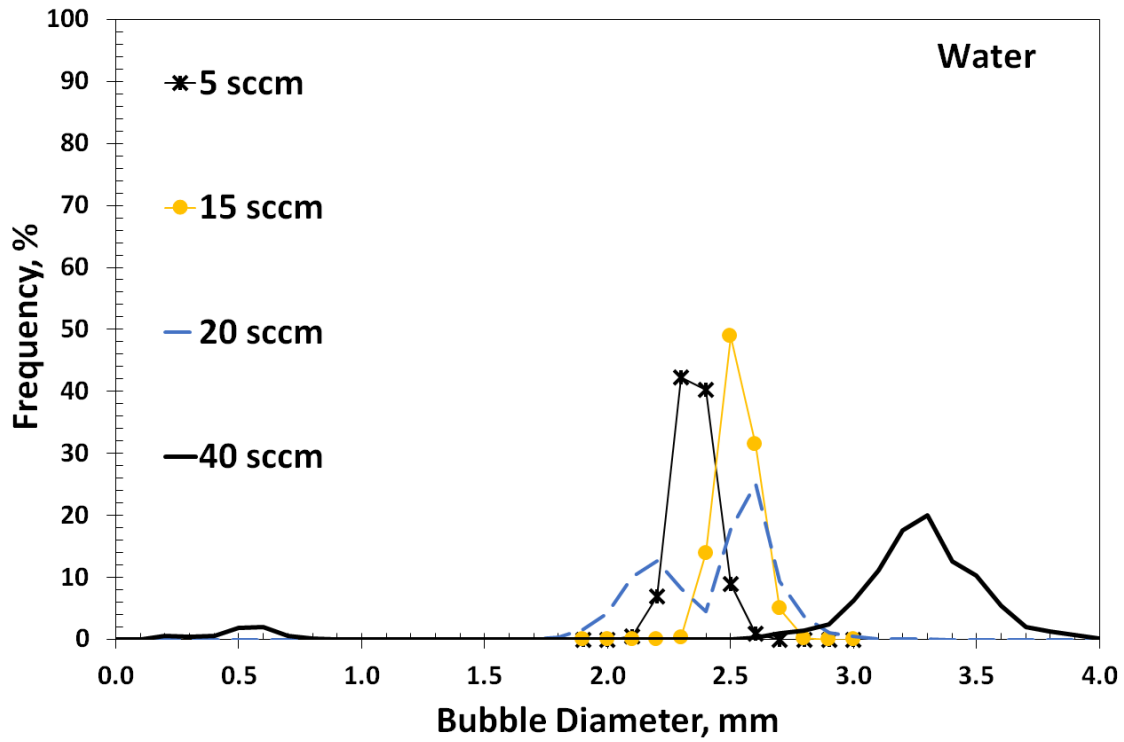
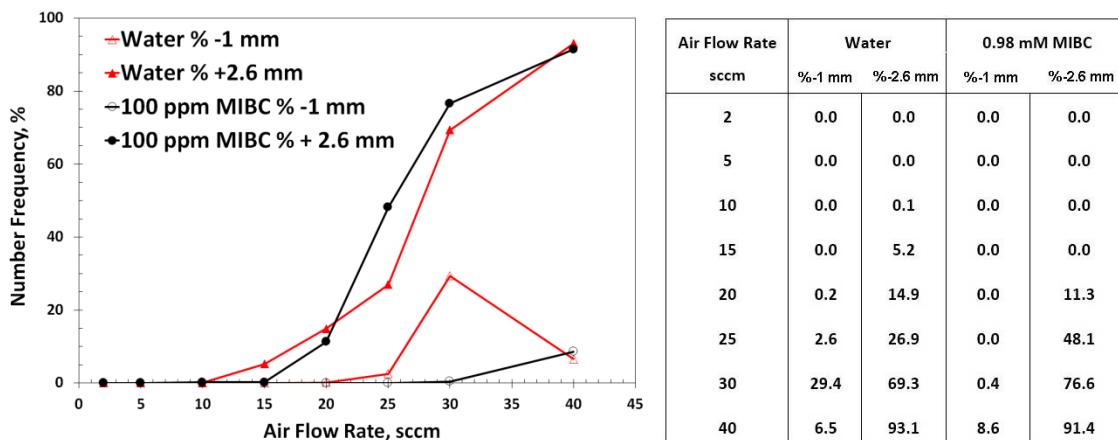


Figure 4.5 – Bubble size distributions in water and 0.98 mM MIBC solution at various air flow rates

At 20 sccm the BSD in water and 0.98 mM MIBC become bi-modal with slightly larger and finer bubbles sizes present when compared to bubbles produced in the non-coalescence region (i.e., 5 sccm in water and at 5 and 15 sccm in 0.98 mM MIBC). As seen in Figure 4.6, in water the beginning of a fine bubble fraction (< 1 mm) is seen at 20 sccm which corresponds to the coalescence with break-up regime. In 0.98 mM MIBC the onset of break-up is delayed to 30 sccm.

At low air flow rates (i.e., 2 and 5 sccm) bubble size does not exceed 2.6 mm. With increasing air flow rate bubbles greater than 2.6 mm are observed that indicates coalescence. Figure 4.6 shows the number frequency of bubbles greater than 2.6 mm in water and 0.98 mM MIBC solution. The production of bubbles greater than 2.6 mm begins at 10 sccm in water and 20 sccm with frother and coincides with the transition into the coalescence regime.

It should be noted that although the production of fine bubbles occurred at lower gas flow rates in water only (compared to frother or salt solutions) re-coalescence of the fine bubbles occurred. This did not occur with increased frother or salt concentration as all coalescence events are inhibited.



**Figure 4.6 – Number frequency of bubbles below 1 mm and greater than 2.6 mm in water and 0.98 mM MIBC**

Figure 4.7 shows the bubble regime plots for the commercial frothers: MIBC, DF250C and F150. For the non-coalescence to coalescence transition, MIBC is seen to be the weakest frother,

DF250C intermediate and F150 the strongest frother. The transition from coalescence to coalescence with fine bubble production follows the same ranking, although the frothers appear to behave similarly at low concentration.

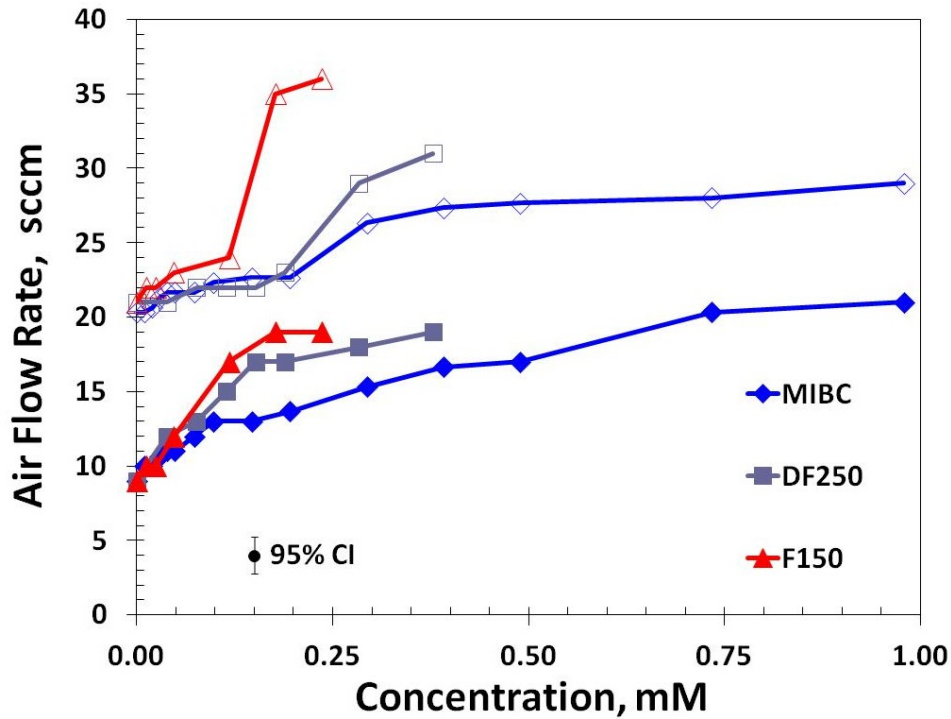


Figure 4.7 – Bubble regime plots for commercial frothers (closed markers identify the transition to coalescence and open markers identify the transition to fine bubble production)

Figure 4.8 shows the bubble regime plots for the 1-alcohols: pentanol, hexanol, heptanol, and octanol. For the non-coalescence to coalescence transition, 1-pentanol is the weakest frother with 1-hexanol, 1-heptanol and 1-octanol all behaving similarly, which corresponds to the findings of Kracht and Finch (2009b). At low concentrations ( $< 0.4$  mM) the transition to break-up behaves similarly to the transition to coalescence displaced to higher concentrations ( $> 0.4$  mM); the alcohols appear to show a distinct behaviour with strength increasing with hydrocarbon chain length ( $C_5$  to  $C_8$ ), i.e., 1-pentanol  $<$  1-hexanol  $<$  1-heptanol  $<$  1-octanol.

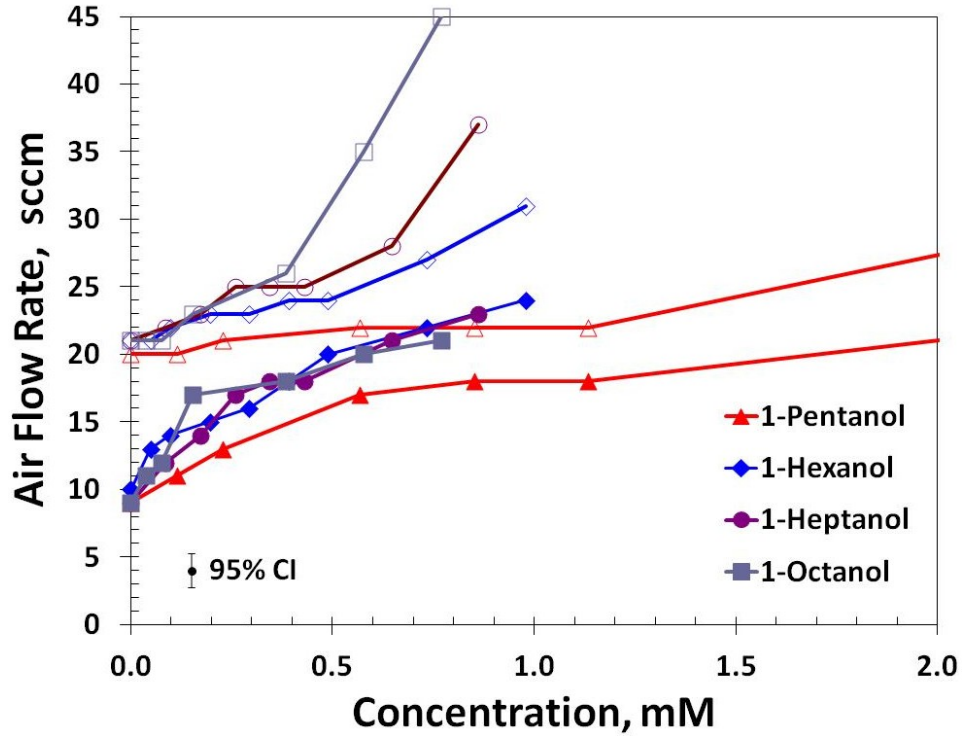


Figure 4.8 – Bubble regime plots for 1-alcohols (closed symbols represent lower transition, open symbols represent upper transition)

Figure 4.9 shows the bubble regime plots for the inorganic electrolytes: KCl, NaCl, Na<sub>2</sub>SO<sub>4</sub>, CaCl<sub>2</sub>, and MgSO<sub>4</sub>. Kracht and Rebolledo (2013) showed that certain inorganic salt solutions (e.g., NaCl, KCl, CaCl<sub>2</sub>) exhibit a relatively large region of partial coalescence. As such only the transition to complete coalescence is shown (i.e., the lower transition curve). For the transition to complete coalescence, KCl and NaCl are seen as weak while Na<sub>2</sub>SO<sub>4</sub>, CaCl<sub>2</sub> and MgSO<sub>4</sub> have a stronger effect. For the transition from coalescence to coalescence with break-up, salt strength appears to follow a similar order, although MgSO<sub>4</sub> now overlaps with Na<sub>2</sub>SO<sub>4</sub>.

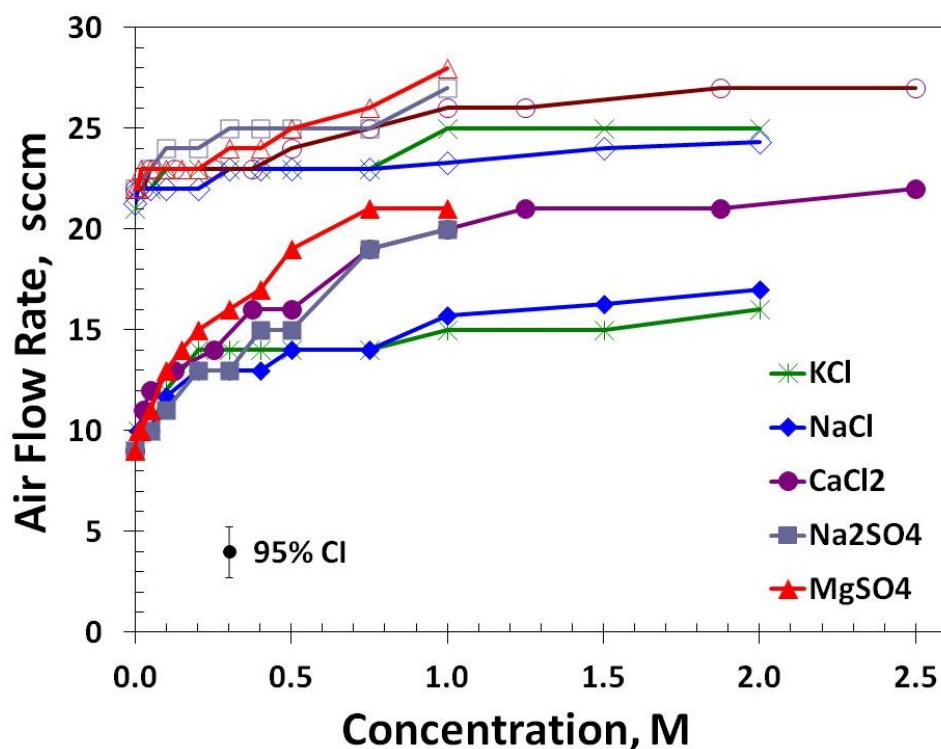


Figure 4.9 – Bubble regime plots for inorganic salts

#### 4.4 Discussion

The present work demonstrates the ability of frothers and inorganic salts to inhibit bubble coalescence, shown as an increase in the transition air flow rate between non-coalescence and coalescence. Several techniques have been proposed for frother / salt strength characterization: bubble coalescence (Zieminski and Whittemore, 1971; Drogaris and Weiland, 1983; Kracht and Finch, 2009b; Kracht and Rebolledo, 2013), bubble size (Sweet et al., 1997, Cho and Laskowski, 2002a,b; Zhang et al., 2013), gas retention (dynamic foamability index) (Pomianowski et al., 1973; Malysa and Pawlikowska-Czubak, 1975; Sweet et al. 1997), gas holdup (Azgomi et al., 2007; Quinn et al., 2007), and water carrying rate (Finch et al., 2006; Moyo, 2007). Based on coalescence prevention our data agree with the rankings in the literature, for example that of the commercial frothers tested rank MIBC < DF250 < F150. In general, the trends for the non-coalescence to coalescence transition and coalescence to break-up transition followed the same order although the transition to break-up appears to show more sensitivity in certain cases (Figures 4.7 and 4.8). The 1-hexanol, 1-heptanol and 1-octanol behaved similarly in terms of

coalescence behaviour, as shown previously by Kracht and Finch (2009b) but showed distinct strengths in terms of break-up, strength increasing with hydrocarbon chain length. For inorganic salts, the 1-1 (cation-anion valence) salts were weakest, all salts containing multi-valent ions inhibited coalescence and break-up at lower molar concentrations. The results follow the literature; salts containing multi-valent ions have a stronger effect (Marrucci and Nicodemo, 1967; Lessard and Zieminski, 1971; Craig et al., 1993; Quinn et al., 2007). Some authors have shown a dependence on ionic strength (Lessard and Zieminski, 1971; Quinn et al., 2007). Figure 4.10 shows the bubble regime plot for inorganic salts as a function of ionic strength. There is spread in the data but the curves do tend to collapse into one.

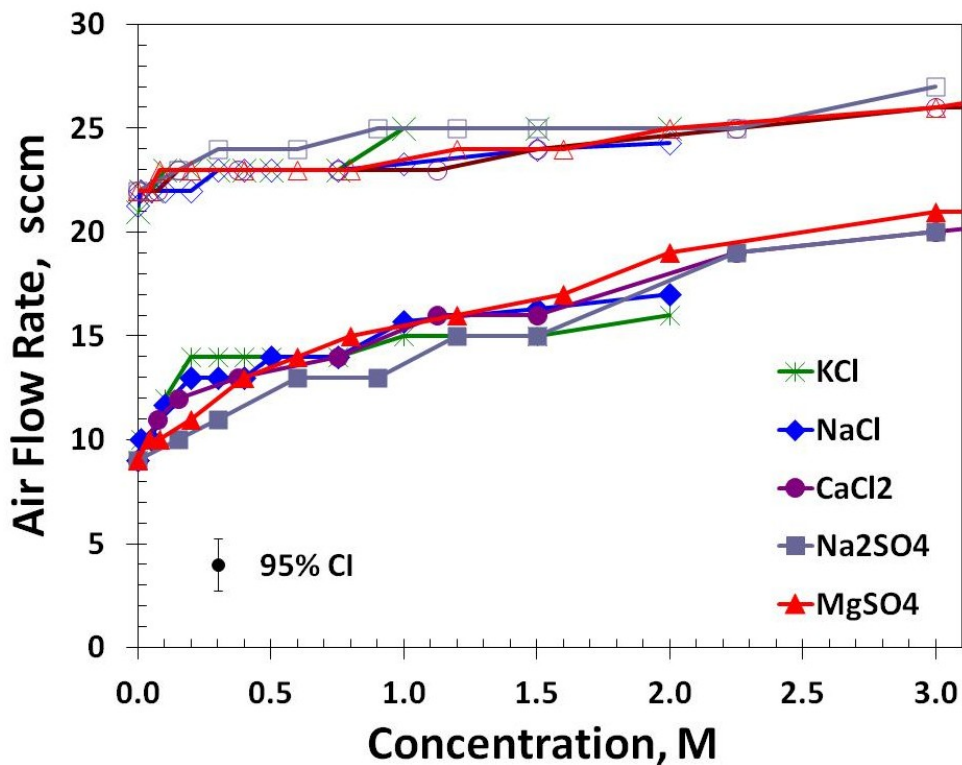


Figure 4.10 – Bubble regime transitions for inorganic salts as a function of ionic strength

Based on the visual evidence, all fine bubble production mechanisms at a capillary proposed by Quinn and Finch (2012) seem to be at play both in the absence and presence of frother or inorganic salt. As gas rate is increased in the fine bubble production region, liquid jet formation

and subsequent fine bubble formation seems to be the dominant fine bubble production mechanism.

Liquid droplet formation was identified by Quinn and Finch (2012) as one mechanism that could result in fine bubble production. In the present results there was visual evidence of droplet formation at high frother concentration but these droplets tended to bounce inside the bubble as it rose and not pierce the wall. This may have been a result of lower droplet velocities compared to the prior work or interfacial properties which resisted deformation. The ability of frothers or inorganic salts to delay the onset of break-up may be related to their ability to inhibit bubble coalescence. As shown by several authors, break-up can be brought on by coalescence events (Tse et al., 2003; Quinn and Finch, 2012), thus delaying the onset of coalescence may delay the onset of coalescence-induced break-up. Other explanations may include: convective wake forces reach a critical value (Marrucci and Nicodemo, 1967) or a critical bubble size (and associated surface instabilities) is reached which allows for break-up (Hinze, 1955).

The presence of frother or salt has been shown to modify the shape of a rising bubble (Krzan and Malysa, 2002a,b; Maldonado et al., 2013) and dampen shape oscillations (Tomiyama et al., 2002). Figure 4.11 shows example images of bubbles in water and 0.98 mM MIBC solution produced at 5 sccm (both in the non-coalescence regime). The bubble produced in frother solution is more spherical than the bubble produced in water. The link between shape deformation and break-up was discussed by Hinze (1955). Tse et al. (2003) noted that increased flexibility of the interface and significant shape distortion, especially in the water system, promoted bubble break-up. Coalescence events appear to be a major contributor to shape instabilities and induce break-up. Bubble shape is related to the bubble interfacial properties which dictate whether a bubble is susceptible to break-up.

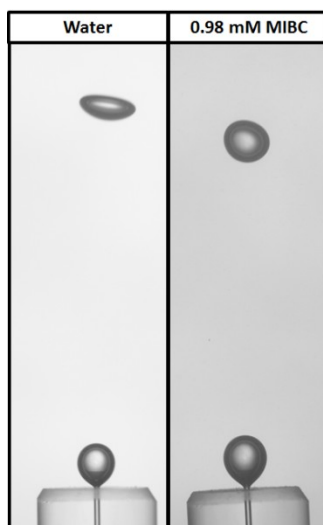


Figure 4.11 – Example images of bubbles formed in water and in 0.98 mM MIBC

## 4.5 Conclusions

High-speed photography (HSP) was used to determine transitions between bubble regimes at a 300  $\mu\text{m}$  capillary in solutions of commercial flotation frothers (MIBC, F150, and DF250C), 1-alcohols ( $\text{C}_5\text{--}\text{C}_8$ ), and inorganic salts ( $\text{KCl}$ ,  $\text{NaCl}$ ,  $\text{Na}_2\text{SO}_4$ ,  $\text{CaCl}_2$  and  $\text{MgSO}_4$ ). Three regimes were identified: non-coalescence (single bubble production), bubble coalescence, and coalescence with fine bubble production with defined transition air rate as a function of solute concentration. In certain instances a transition region of partial coalescence is seen. The addition of surfactants and inorganic salts inhibited bubble coalescence and delayed the onset of fine bubble production. The result support that coalescence events play a role in the break-up process. The tests allow for frother strength characterization in terms of retarding bubble coalescence and break-up.

## References

Alexander, S., Quinn, J., van der Spuy, J.E., and Finch, J.A., 2012. Correlation of graphite flotation and gas holdup in saline solutions. In: Drelich, J. (Ed.), *Water in Mineral Processing: Proceedings of the First International Symposium*, SME, 41-50.

- Azgomi, F., Gomez, C.O., and Finch, J.A., 2007. Characterizing frothers using gas hold-up. *Canadian Metallurgical Quarterly* 46, 3, 237-242.
- Bournival, G., Pugh, R. J., and Ata, S., 2012. Examination of NaCl and MIBC as bubble coalescence inhibitor in relation to froth flotation. *Minerals Engineering* 25, 1, 47-53.
- Cain, F.W., and Lee, J.C., 1984. A technique for studying the drainage and rupture of unstable liquid films formed between two captive bubbles: Measurement on KCl solutions. *Journal of Colloid and Interface Science* 106, 1, 70-85.
- Cho, Y.S., and Laskowski, J.S., 2002a. Effect of flotation frothers on bubble size and foam stability. *International Journal of Mineral Processing* 64, 69-80.
- Cho, Y.S., and Laskowski, J.S., 2002b. Bubble coalescence and its effect on bubble size and foam stability. *Canadian Journal of Chemical Engineering* 80, 299-305.
- Christenson, H.K., Bowen, R.E., Carlton, J.A., Denne, J.R.M., and Lu, Y., 2008. Electrolytes that show transition to bubble coalescence inhibition at high concentrations. *Journal of Physical Chemistry C* 112, 794-796.
- Chu, P., and Finch, J.A., 2013. Frother and breakup in small bubble formation. In: *Proceedings of the 52<sup>nd</sup> Conference of Metallurgists (hosted by Materials Science & Technology (MS&T) 2013): Water and Energy in Mineral Processing, The 9<sup>th</sup> UBC-McGill-U of A International Symposium on the Fundamentals of Mineral Processing, The Metallurgical Society of CIM, 2034-2043.*
- Clift, R., Grace, J.R., and Weber, M., 2005. *Bubble, Drops, and Particles*. Dover Publications Inc., Mineola, New York. 169-202.
- Craig, V.S.J., Ninham, B.W., and Pashley, R.M., 1993. The effect of electrolytes on bubble coalescence in water. *Journal of Physical Chemistry* 97, 10192-10197.
- Drogaris, G., and Weiland, P., 1983. Coalescence of gas bubbles in aqueous solutions of n-alcohols and fatty acids. *Chemical Engineering Science* 38, 9, 1501-1506.
- Finch, J.A., Gelinas, S., and Moyo, P., 2006. Frother-related research at McGill University. *Minerals Engineering* 19, 726-733.

Finch, J.A., Nasset, J.E., and Acuna, C., 2008. Role of frother in bubble production and behaviour in flotation. *Minerals Engineering* 21, 949–957.

Fouk, C.W., and Miller, J.N., 1931. Experimental evidence in support of the balanced-layer theory of liquid film formation. *Industrial and Engineering Chemistry* 23, 11, 1283-1288.

George, C., 1996. Mt. Keith Operation. In: Grimsey, E.J., and Neuss, I. (Eds.), *Nickel '96, Conference Series- Australasian Institute of Mining and Metallurgy*, 6, 19-23.

Haig-Smillie, L.D., 1974. Sea Water Flotation. *Proceedings Canadian Mineral Processors Conference*, 263-281.

Harris, P.J., 1982. Frothing phenomenon and frothers. In: King, R.P. (Ed.), *Principles of Flotation. Monograph Series No. 3. S. African IMM*, 237-250.

Hernandez-Aguilar, J.R., Cunningham, R., and Finch, J.A., 2006. A test of the Tate equation to predict bubble size at an orifice in the presence of frother. *International Journal of Mineral Processing*, 79, 2, 89-97.

Hinze, J.O., 1955. Fundamentals of the hydrodynamic mechanism of splitting in dispersion processes. *AIChE Journal*, 1, 3, 289-295.

Hofmeier, U., Yaminsky, V.V. and Christensen, H.K., 1995. Observations of solute effects on bubble formation. *Journal of Colloid and Interface Science* 174, 199-210.

Kim, J. W., and Lee, W. K., 1988. Coalescence behavior of two bubbles growing side-by-side. *Journal of Colloid and Interface Science* 123, 1, 303-305.

Kracht, W., and Finch, J.A., 2009a. Bubble break-up and the role of frother and salt, *International Journal of Mineral Processing* 92, 153–161.

Kracht, W., and Finch, J.A. 2009b, Using sound to study bubble coalescence. *Journal of Colloid and Interface Science* 332, 237–245.

Kracht, W., and Rebolledo, H., 2013, Study of the local critical coalescence concentration (*I*-CCC) of alcohols and salts at bubble formation in two-phase systems. *Minerals Engineering* 50-51, 77-82.

- Krzan, M., and Malysa, K., 2002a. Profiles of local velocities of bubbles in n-butanol, n-hexanol and n-nonanol solutions. *Colloids and Surfaces A: Physicochemical and Engineering Aspects* 207, 279-291.
- Krzan, M., and Malysa, K., 2002b. Influence of frother concentration on bubble dimensions and rising velocities. *Physicochemical Problems of Mineral Processing* 36, 65-76.
- Kyriakides, N.K., Kasrinakis, E.G., Nychas, S.G., and Goulas, A., Bubbling from nozzles submerged in water: Transitions between bubbling regimes. *The Canadian Journal of Chemical Engineering* 75, 684-691, 1997.
- Laskowski, J.S., Cho, Y.S., and Ding, K., 2003. Effect of frothers on bubble size and foam stability in potash ore flotation systems. *The Canadian Journal of Chemical Engineering* 81, 63-69.
- Lessard, R.D., and Zieminski, S.A., 1971. Bubble coalescence and gas transfer in aqueous electrolytic solutions. *Industrial and Engineering Chemistry Fundamentals* 10, 260-289.
- Maldonado, M., Quinn, J.J., Gomez, C.O., and Finch, J.A., 2013. An experimental study examining the relationship between bubble shape and rise velocity. *Chemical Engineering Science* 98, 7-11.
- Malysa, K., and Pawlikowska-Czubak, J., 1975. Frothability and surface elasticity of aqueous solutions of some frothers, *Bulletin de l'Academie Polonaise des Sciences* 5, 423-427.
- Marrucci, G., and Nicodemo, L., 1967. Coalescence of gas bubbles in aqueous solutions of inorganic electrolytes. *Chemical Engineering Science* 22, 1257-1265.
- Moyo, P., Gomez, C.O., and Finch, J.A., 2007. Characterization frothers using water carrying rate. *Canadian Metallurgical Quarterly* 46, 3, 215-220.
- Nesset, J.E., Finch, J.A., and Gomez, C.O., 2007. Operating variables affecting bubble size in forced-air mechanical flotation machines. In: *Proceedings of the 9<sup>th</sup> Mill Operators' Conference*, Fremantle, Australia, 55-65.
- Otake, T., Tone, S., Nakao, K., and Mitsuhashi, Y., 1977. Coalescence and breakup of bubbles in liquids. *Chemical Engineering Science* 32, 4, 377-383.

Pomianowski, A., Malysa, K., and Para, G., 1973, Annual Report for the Institute of Nonferrous Metals, 6.

Pugh, R.J., 1996. Foaming, foam films, antifoaming and defoaming. *Advances in Colloid and Interface Science* 64, 67-142.

Prince, M.J., and Blanch, H.W. 1990. Bubble coalescence and break-up in air-sparged bubble columns. *AIChE Journal* 36, 10, 1485-1499.

Quinn, J.J., and Finch, J.A., 2012. On the origin of bi-modal bubble size distributions in the absence of frother. *Minerals Engineering* 36-38, 237-241.

Quinn, J.J., Kracht, W., Gomez, C.O., Gagnon, C., and Finch, J.A., 2007. Comparing the effects of salts and frother (MIBC) on gas dispersion and froth properties. *Minerals Engineering* 20, 1296-1302.

Sweet, C., van Hoogstraten, J., Harris, M., and Laskowski, J.S., 1997. The effect of frothers on bubble size and frothability of aqueous solutions. In: Finch, J.A., Rao, S.R., Holubec, I. (Eds.), *Processing of Complex Ores*, 2nd UBC-McGill Symposium Series on Fundamental in Mineral Processing, The Metallurgical Society of CIM, 235–246.

Tate, T., 1864. On the magnitude of a drop of liquid formed under different circumstances. *The London, Edinburgh, and Dublin Philosophical Magazine and Journal of Science* 27, 181, 176-180.

Tomiyama, A., Celata, G.P., Hosokawa, S., and Yoshida, S., 2002. Terminal velocity of single bubbles in surface tension force dominant regime. *International Journal of Multiphase Flow* 28, 1497-1519.

Tsang, Y.H., Koh, Y-H, and Koch, D.L., 2004. Bubble-size dependence of the critical electrolyte concentration for inhibition of coalescence. *Journal of Colloid and Interface Science* 275, 290-297.

Tse, K., Martin, T., McFarlane, C.M., and Nienow, A.W., 1998. Visualization of bubble coalescence in a coalescence cell, a stirred tank and a bubble column. *Chemical Engineering Science* 53, 23, 4031-4036.

- Tse, K.L., Martin, T., McFarlane, C.M., and A.W. Nienow, 2003. Small bubble formation via a coalescence dependent break-up mechanism. *Chemical Engineering Science* 58, 275-286.
- Wang, L., and Qu, X., 2012. Impact of interface approach velocity on bubble coalescence. *Minerals Engineering* 26, 50-56.
- Zahradnik, J., Fialová, M., and Linek, V., 1999. The effect of surface additives on bubble coalescence in aqueous media. *Chemical Engineering Science* 54, 4757-4766.
- Zhang, L., and Shoji, M., 2001. Aperiodic bubble formation from a submerged orifice. *Chemical Engineering Science* 56, 5371-5381.
- Zhang, W., Nasset, J.E., Rao, R., and Finch, J.A., 2012. Characterizing frothers through critical coalescence concentration (CCC)95-hydrophile-lipophile balance (HLB) relationship. *Minerals* 2, 208-227.
- Zhou, Z.A., Egiebor, N.O., and Plitt, L.R., 1993. Frother effects on bubble size estimation in a flotation column. *Minerals Engineering* 6, 1, 55-67.
- Zieminski, S.A., and Whittemore, R.C., 1971. Behavior of gas bubbles in aqueous electrolyte solutions. *Chemical Engineering Science* 26, 509-520.

# Chapter 5 – Passive acoustic emission monitoring to detect bubble coalescence in presence of solid particles

## 5.1 Introduction

Optical techniques are typically used to investigate the action of solutes in retarding bubble coalescence in air/water systems (Hofmeier et al., 1995; Zahradnik et al., 1999; Cho and Laskowski, 2002a,b; Tse et al., 2003). To be closer to flotation conditions solid particles should be present. Slurries render systems opaque that means direct visual techniques cannot be used. This introduces the idea of acoustic monitoring.

Passive acoustic emission monitoring (PAEM) has been used on a variety of unit operations and processes in the minerals industry: crushing and grinding (Zeng and Forssberg, 2003), hydrocycloning (Hou et al., 1998), bubble formation (Kracht and Finch, 2009), flotation machines (Spencer et al., 2012), and frothing (Vanegas and Holtham, 2008). The reliability, non-intrusive nature, low cost and the capability of real-time continuous measurement make acoustics an attractive tool for monitoring and control (Boyd and Varley, 2001; Vanegas and Holtham, 2010).

In his classic book ‘The Flotation Process’, T.A. Rickard (1916) noted “the noise made by the bursting bubble suggests the fact that it is a receptacle of energy.” The first systematic study of sound production upon bubble formation was undertaken by Minnaert (1933) and was entitled “On musical air-bubbles and the sounds of running water”. He introduced an energy balance which related the sound frequency produced (commonly termed the Minnaert frequency),  $\nu$ , and equilibrium bubble diameter,  $d_b$ :

$$\nu = \frac{1}{\pi d_b} \left[ \frac{3\kappa p^\circ}{\rho_L} \right] \quad (5.1)$$

where  $\kappa$  is the ratio of specific heats of the gas phase,  $\rho_L$  the liquid density and  $p^\circ$  the hydrostatic pressure. A range of bubble sizes and gas types were fit by the equation.

Strasberg (1956) noted that when bubbles split or coalesce, a decaying sinusoidal pulse of sound is emitted, just as in bubble formation. Deane and Czernski (2008) demonstrated that sound was

excited by the rapid decrease in volume accompanying the collapse of the bubble neck upon detachment. Manasseh (1998) studied initial bubble deformation upon release from a nozzle using high-speed photography to understand the physical mechanisms generating sound. After bubble release (bubble neck breaking) a liquid jet was shown to enter the bubble corresponding to increased pressure within the bubble.

Leighton et al. (1991) used high-speed photography to observe air bubble behaviour in water at a 0.5 mm internal diameter nozzle. An individual bubble released from the orifice produced a single decaying sinusoidal acoustic signal. At higher gas rates ( $0.1 - 5 \text{ ml s}^{-1}$ ) coalescence occurred in proximity to the nozzle resulting in a characteristic acoustic signal: initial bubble detachment resulted in a decaying sinusoid with subsequent peaks in the acoustic signal relating to each coalescence event (which created a larger bubble which emitted a lower frequency signal). The authors noted that bubble shape oscillations could promote coalescence.

Using a stroboscope and digital video camera Hofmeier et al. (1995) observed bubble formation at a capillary and frit in various solutions (including sodium chloride). Similar to Leighton et al. (1991), Hofmeier et al. noted bubble regimes which were flow rate dependent: 1) At low gas flow rates bubbles were released individually and anti-coalescence agents (some surfactants and inorganic salts) had little effect on bubble generation; and 2) At intermediate gas rate bubbles interacted close to the orifice with the initial bubble either bouncing off or coalescing with the subsequently bubble(s). In pure liquids, bubbles were more likely to coalesce and create larger bubbles. In systems containing certain surfactants or inorganic salts, bubbles were more likely to bounce.

The presence of frothers or certain inorganic salts have been shown to inhibit bubble coalescence (Lessard and Zieminski, 1971; Zahradnik et al., 1999; Finch et al., 2008). The mechanism in the case of surfactants has been attributed to surface tension gradients stabilizing thin liquid surface films against drainage through the Gibbs elasticity and the Marangoni effects (Dukhin et al., 1998; Finch et al., 2008). Inorganic salts (at relatively high concentrations) may act in a similar manner as surface tension gradients can be generated (Quinn et al., 2013).

The effect of solid particles on bubble coalescence has attracted attention but mainly related to properties of the froth phase (Pugh, 1996; Ata et al., 2004; Pugh, 2005; Ata, 2012). While potentially of some relevance to bubble formation the role of solids in the froth phase, is likely

different to that in the pulp phase (Ata, 2012). Hydrophobic particles have been shown to stabilize or de-stabilize the froth depending on concentration, size and shape (Dippenaar, 1982; Garrett, 1993; Pugh, 1996; Ata, 2012). Pugh (2007) noted that increasing contact angle (increasing hydrophobicity) initially tended to increase froth stability (decrease bubble coalescence) but highly hydrophobic particles could destabilize the froth by promoting coalescence probably due to bubble bridging by the hydrophobic particle. With hydrophilic particles any bridging could have the opposite effect and cause liquid retention in the film thus delaying coalescence (Ip et al., 1999; Pugh, 2007; Ata, 2008).

Several techniques have been used to quantify the effect of solutes on bubble coalescence with no solid particles present. The contacting of bubble pairs at adjacent capillaries has been widely used (Lessard and Zieminski, 1971; Zahradnik et al., 1999; Christenson et al., 2008). Contacting mineralized bubbles (bubbles covered by hydrophobic particles) showed increased resistance to coalescence (Ata, 2008; Gallegos-Acevedo et al., 2010). An indirect measure of bubble coalescence is determination of the critical coalescence concentration (Cho and Laskowski, 2002a,b; Zhang et al., 2012). Again these data are largely derived on air/water systems but the close comparison with bubble size data from flotation systems suggests little effect of solid particles (Nesset et al., 2006). The presence of solid particles may adsorb some frothers (Kulkarni et al., 1977; Kuan and Finch, 2010) and cause bubbles to coalesce but this is an indirect effect of solids.

Kracht and Finch (2009) utilized high-speed photography and acoustic emission monitoring to determine the transition gas flow rate at which the bubble regime changed from non-coalescing to coalescing (termed coalescence plots) at a 200  $\mu\text{m}$  capillary. The characteristic acoustic signal upon coalescence (as described by Leighton et al. (1991)) was used to determine the onset of coalescence as air flow rate was increased. Example coalescence plots are given in Figure 5.1 for MIBC and sodium chloride which show the transition gas flow rate between non-coalescence and coalescence. For NaCl the presence of a partial coalescence region is seen (i.e., not all bubble-bubble interactions resulted in coalescence). Comparison of the plots gave a ranking of frother 'strength' in terms of coalescence prevention, the stronger frother requiring a higher transition gas rate for the onset of coalescence.

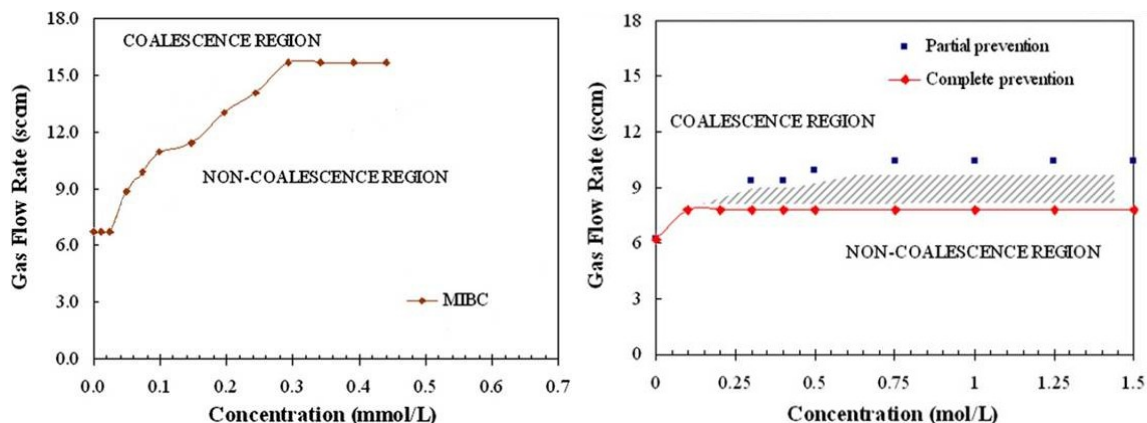


Figure 5.1 – Coalescence plots for MIBC and sodium chloride (modified from Kracht and Finch, 2009)

Recently, Kracht and Rebolledo (2013) used the acoustic technique to test 1-alcohols, commercial frothers, and inorganic salts. The concept of a local critical coalescence concentration (*l*-CCC) curve was developed to compare the coalescence prevention strength of the solutes. Similar to the work of Kracht and Finch (2010) (for NaCl), the authors found that certain inorganic salts (NaCl, KCl, and CaCl<sub>2</sub>) showed a region of partial coalescence.

The present paper extends the work of Kracht and Finch (2009) to determine the effect of hydrophobic and hydrophilic solid particles on the transition between bubble regimes at a capillary using passive acoustic emission monitoring.

## 5.2 Experimental

The experimental set-up (Figure 3.2) comprised a 50 L (50 cm (L) x 20 cm (W) x 50 cm (H)) acrylic tank filled with distilled water (30 L) into which air bubbles were launched from a glass capillary with internal diameter  $305 \pm 10 \mu\text{m}$ . All tests were at 18 - 22°C. Air flow rate was controlled using an Omega model FMA-3704 (0 - 100 standard cubic centimeters per minute (sccm)) mass flow meter controller (accuracy of  $\pm 1\%$  full scale).

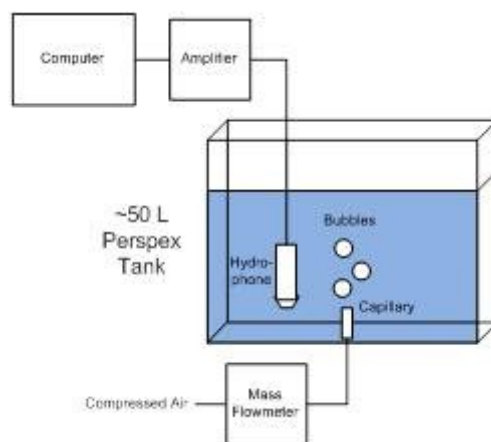


**Figure 5.2 – Experimental set-up**

Acoustic emissions were measured using a hydrophone (Lab-40 hydrophone from LAB-core System) with a frequency range 5 to 85000 Hz. Acoustic emissions were recorded using Audacity audio editing software.

Tests were in water (Montreal tap) with silica (as a model hydrophilic solid) or talc (hydrophobic) at 1% and 10% w/w. The effect of MIBC (4-methyl-2-pentanol) frother (0 - 0.98 mM (0 - 100 ppm (mg/l)) and sodium chloride (0 - 2 M) concentration was tested. Reagent specifications are given in Table 5.1. Relatively fine particle sizes were used in the test work (-44  $\mu\text{m}$  silica and -10  $\mu\text{m}$  talc) to minimize the impact of particle settling. An overhead stirrer (RW20 Digital IKA stirrer) equipped with a 3-bladed radial-flow impeller was used to disperse/suspend the solids prior to measurement. Each test was performed three times with the average transition flow rate shown.

**Table 5.1 – Reagent specifications**

Reagents	Supplier	Specifications
Silica	Unimin	-44 $\mu\text{m}$ powder >99% Silica
Talc	Sigma-Aldrich	-10 $\mu\text{m}$ powder >99% Talc
MIBC	Sigma-Aldrich	GC
NaCl	Fisher	ACS

### 5.3 Results

Figure 5.3 shows example acoustic recordings in 0.01M NaCl (no solids present) at air flow rates of 8, 9, and 10 sccm. The 8 sccm case shows the characteristic acoustic signal associated with single bubble production, namely a decaying sinusoid indicating a non-coalescing system. Increasing air flow rate to 9 sccm resulted in a mixed signal indicating the production of single bubbles and coalesced bubbles identified as the partial coalescence regime. At 10 sccm, all bubbles produced coalesced and show the resulting characteristic acoustic signal, namely an initial decaying sinusoidal signal associated with the initial bubble formation followed by a second decaying sinusoid of greater magnitude and lower frequency indicative of the larger bubble produced through coalescence.

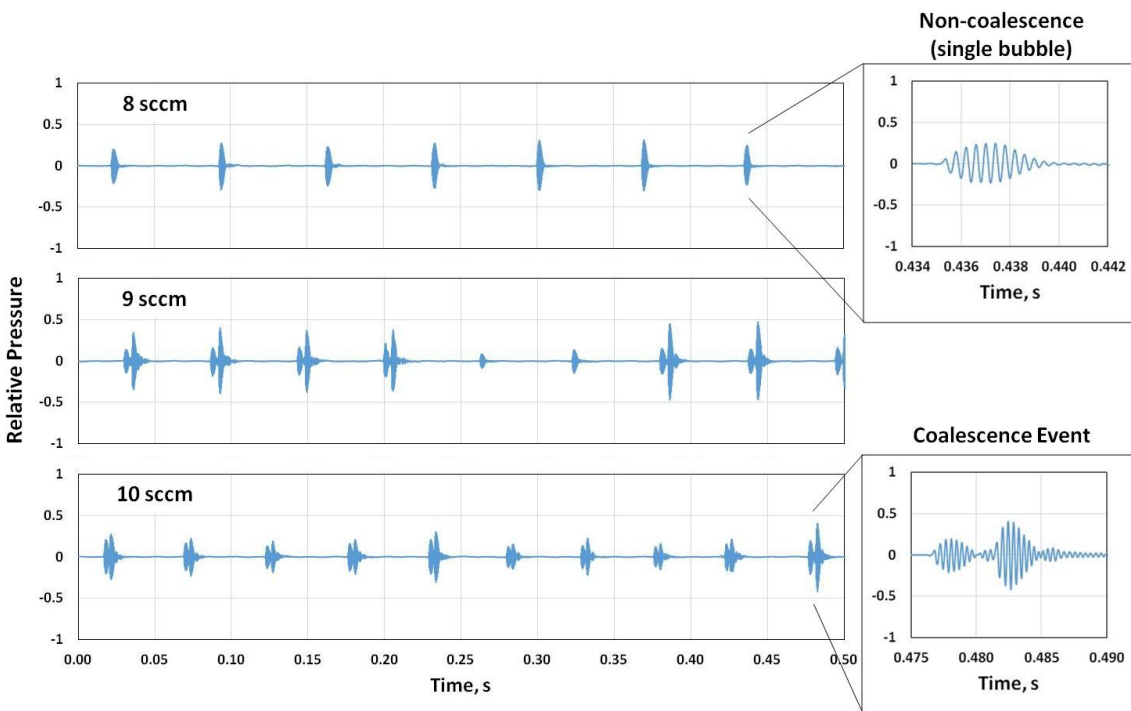


Figure 5.3 – Example acoustic signals in 0.01 M NaCl at air flow rates of 8 sccm (non-coalescence), 9 sccm (partial coalescence), and 10 sccm (complete coalescence)

Figure 5.4 shows the results with increasing MIBC concentration (no solids present). The partial coalescence curve indicates the onset of coalescence (i.e., no coalescence is seen below this flow

rate). The complete coalescence curve indicates that all bubbles produced above this flow rate coalesced. Literature values from Kracht and Finch (2009) are shown for reference. Unlike the work of Kracht and Finch who found no partial coalescence in the presence of frother the present study reveals a small region of partial coalescence in the MIBC system. At MIBC concentrations below ca. 0.1 mM (10 ppm), the Kracht and Finch (2009) data show a lower transition flow rate while at higher concentrations the literature transition data fall in the partial coalescence region.

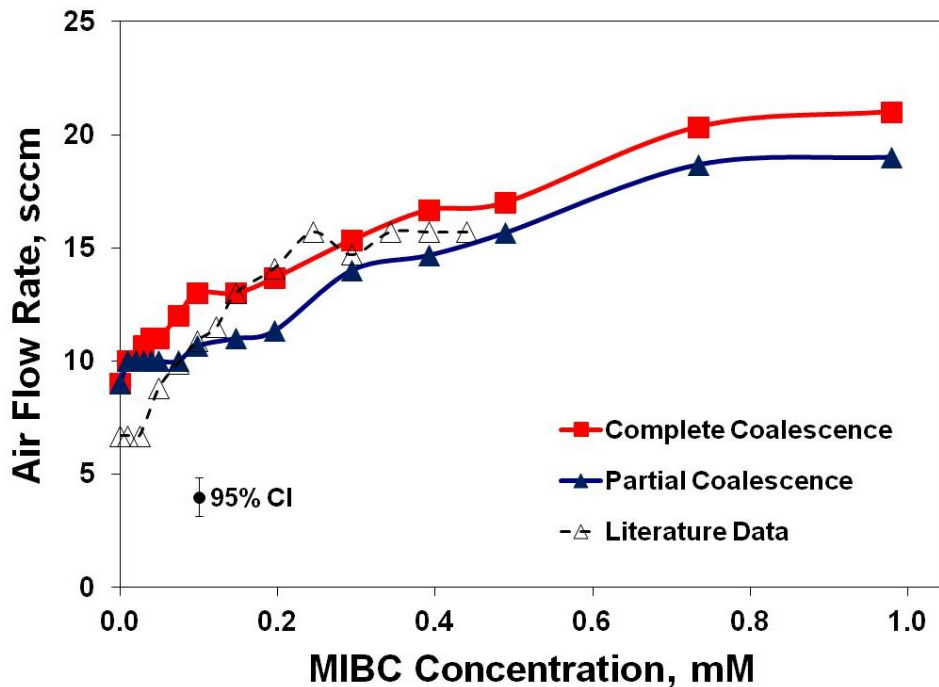


Figure 5.4 – Coalescence plot (transition flow rate vs. concentration) for MIBC (Kracht and Finch (2009) data shown as closed triangles)

Figure 5.5 shows the results for increasing sodium chloride concentration. The transition flow rates are higher than the results of Kracht and Finch (2009) but both results show a relatively large region of partial coalescence. The difference may be due to the different capillary size used in the studies.

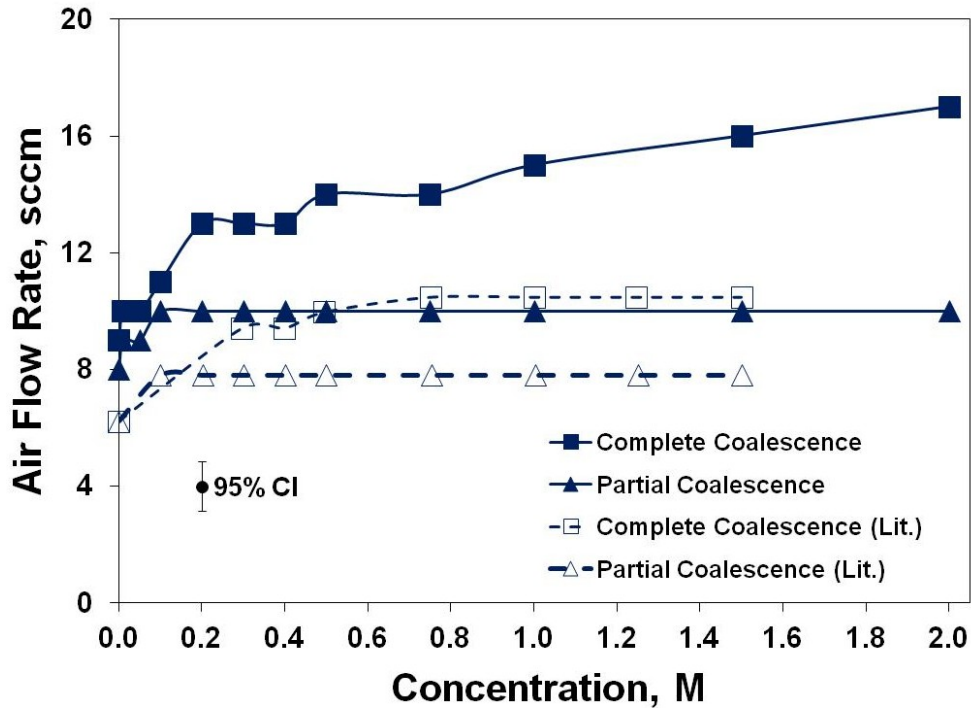


Figure 5.5 – Coalescence plot for NaCl (literature data (Lit.) from Kracht and Finch (2009) shown)

Figure 5.6 and Figure 5.7, respectively, show the coalescence plots in the presence of talc and silica for MIBC from 0 - 0.98 mM (1 - 100 ppm). With both solids, there was little impact on the transition to full coalescence inhibition (upper curve of the pair). For talc at both concentrations there was a slight upward shift in the partial coalescence curve which indicates the presence of talc gave additional coalescence inhibition. The results for 1% silica were similar to talc as was the result for 1% silica with regards to the complete coalescence curve but the higher silica concentration (10% w/w) shifted the partial coalescence curve downwards above ca. 0.2 mM (20 ppm) which indicates coalescence is enhanced.

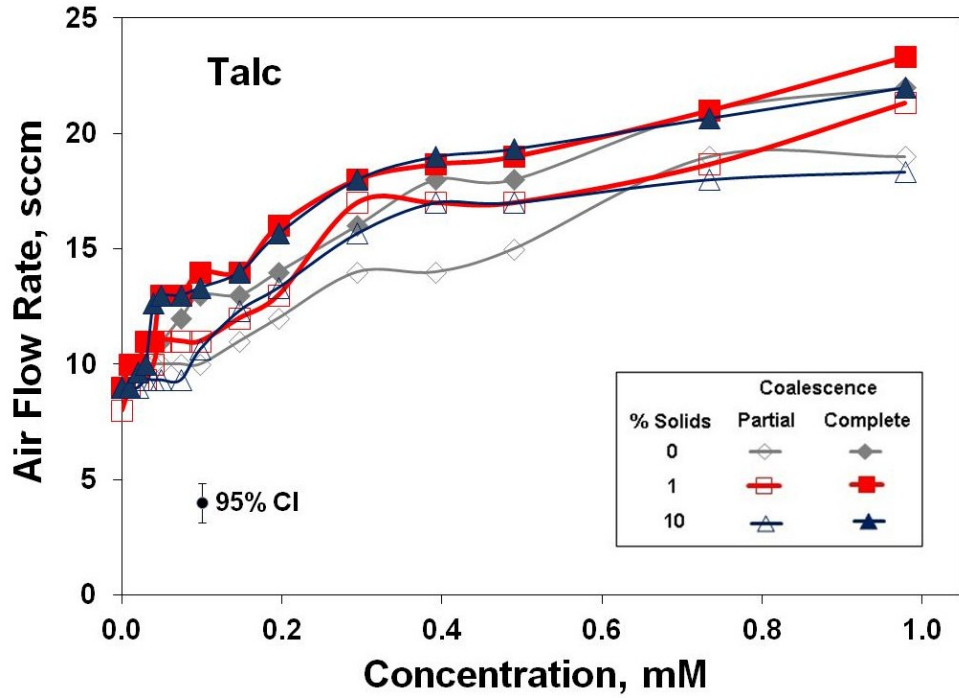


Figure 5.6 – Coalescence plots for 0%, 1% and 10% w/w talc in MIBC solution

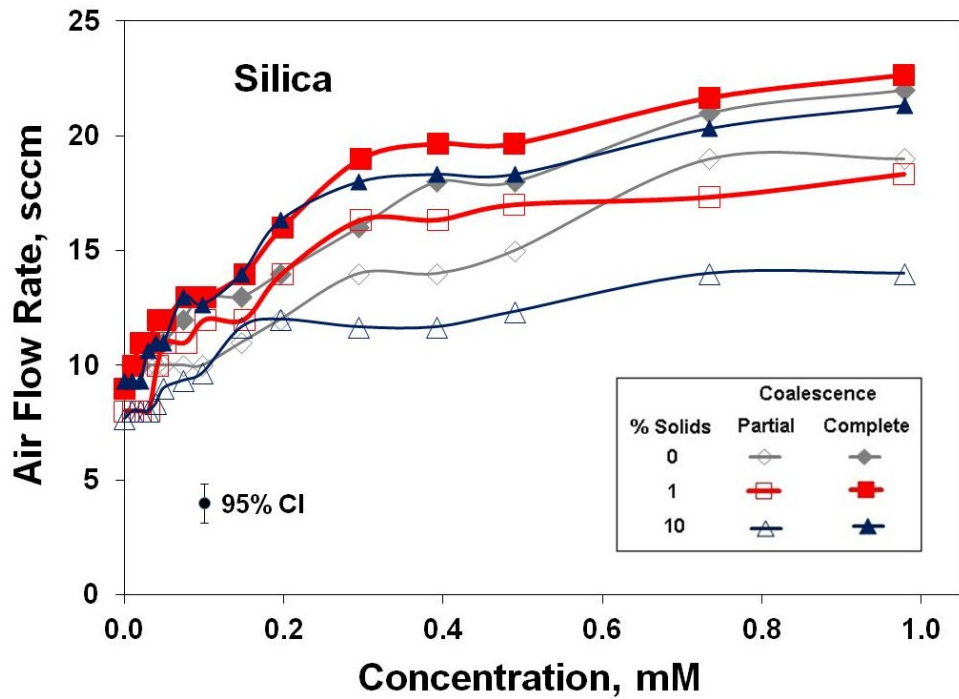


Figure 5.7 – Coalescence plots for 0%, 1% and 10% w/w silica in MIBC solution

Figure 5.8 and Figure 5.9 show the results for talc and silica, respectively, in sodium chloride solution ranging from 0 to 2 M. For both talc and silica there was little change in the transition to complete coalescence inhibition (upper curve of the pair). Both solids showed a slight upward shift in the partial coalescence curve indicating coalescence inhibition. The effect of increasing solids concentration from 1% to 10% showed little effect in either system.

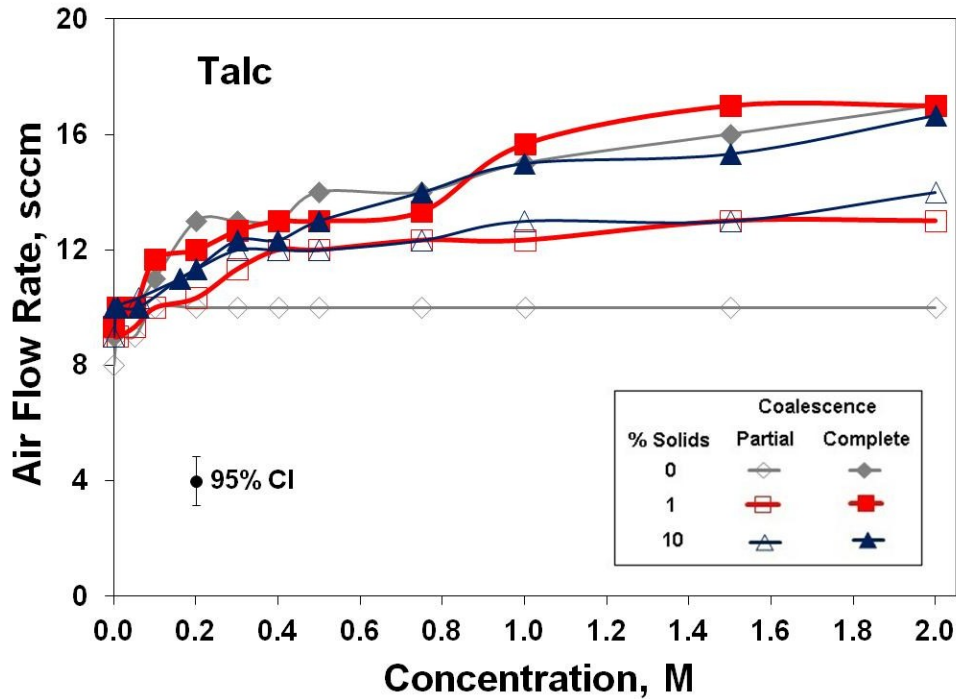


Figure 5.8 – Coalescence plots for 0%, 1%, and 10% w/w talc in sodium chloride solution

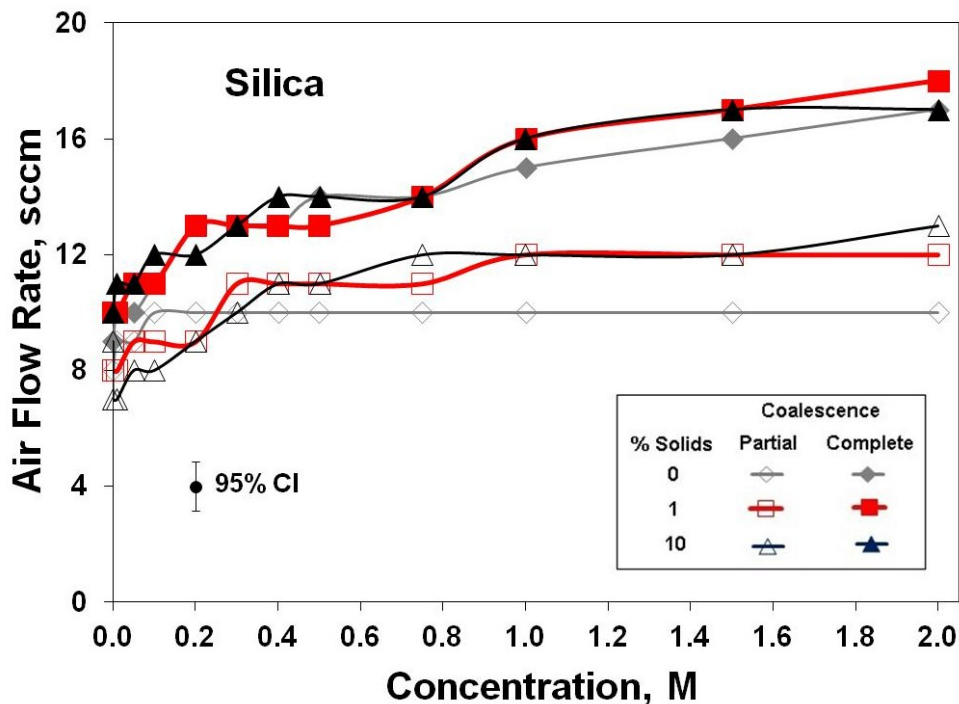


Figure 5.9 – Coalescence plots for 0%, 1%, and 10% w/w silica in sodium chloride solution

## 5.4 Discussion

The use of passive acoustic emission monitoring allowed direct examination of bubble-bubble interactions at a capillary in the presence of solids which produce opaque systems where the use of visual techniques is limited. This extends the work of Kracht and co-workers (Kracht and Finch, 2009; Kracht and Rebolledo, 2013) who used a similar capillary-based acoustic setup to study coalescence in air-water systems. In the same air-water systems tested by Kracht and co-workers the present results were similar except we noted a partial coalescence region for MIBC (Figure 5.5) as well as for NaCl. The partial coalescence region proved important in identifying an effect of solids.

With both MIBC and NaCl the transition to complete coalescence (the upper curve of the pair) was hardly influenced by the presence of talc or silica. This suggests no impact on coalescence. The lower coalescence curve indicating transition to partial coalescence did reveal an effect of solids. For all cases except 10% silica with greater than ca. 0.2 mM (20 ppm) MIBC the partial coalescence curve was shifted upward which indicates both hydrophobic talc and hydrophilic

silica inhibited coalescence. Based on the theories emerging from froth studies this could mean inhibition by particle coated bubbles in the case of talc, and water retention in the case of silica. The 10% silica / MIBC case gave the opposite effect: the partial coalescence curve was shifted downwards indicating coalescence was enhanced. This is difficult to reconcile with theory as silica is unlikely to bridge to promote coalescence the way bridging is understood to function. It is doubtful that theories from studies of froth are applicable to bubble production as noted by Ata (2012). Researchers have noted increased bubble size in flotation systems at increasing solids concentration in the presence of frother (O'Connor et al., 1990; Tucker et al., 1994). The effect may be related to slurry viscosity which could allow bubbles to linger in proximity to the gas dispersing device which could promote bubble coalescence.

Depending on the significance of partial coalescence, overall the observations do not suggest a major impact of solid particles on bubble production in flotation machines. The particles selected represent the range in wettability encountered in flotation systems but arguably other particle sizes or much higher solids concentration may have more effect. High solids concentrations, for example, could have an influence through increased slurry viscosity (Grau and Laskowski, 2006). Coupled with the observation that industrial bubble size data fall in the range predicted by the bubble size model developed in the air-water system (Finch et al., 2008; Nasset, 2011), this supports that particles have limited impact on the bubble production process. This is perhaps as well since a significant impact might necessitate bubble size control to offset particle effects which may vary through a circuit as composition (ratio of hydrophobic to hydrophilic particles) and size varied, an unwanted additional level of complexity. We are left with bubble size being dominated by the interplay of the air dispersion mechanism and solution composition.

## **5.5 Conclusions**

Passive acoustic emission monitoring was used to detect air bubble formation and coalescence at a 300  $\mu\text{m}$  capillary in slurry containing talc or silica particles. The effect of frother (MIBC) or inorganic salt (NaCl) was to inhibit bubble coalescence, as indicated by increasing transition flow rates between the non-coalescence, partial coalescence and complete coalescence bubble regimes. The presence of silica with MIBC created a wider range of partial coalescence when compared to talc. The effect of both solids was to slightly inhibit bubble coalescence except for

the case of 10% silica which appeared to promote coalescence at high frother concentration. Talc and silica behaved similarly in the presence of sodium chloride with slight additional coalescence inhibition detected. Overall, neither solid had a large effect supporting that particles do not have much impact on bubble formation in flotation machines.

## References

Ata, S., Ahmed, N., and Jameson, G.J., 2004. The effect of hydrophobicity on the drainage of gangue minerals in flotation froths. *Minerals Engineering* 17, 7, 897-901.

Ata, S., 2008. Coalescence of bubbles covered by particles. *Langmuir* 24, 12, 6085-6091.

Ata, S., 2012. Phenomena in the froth phase of flotation - A review. *International Journal of Mineral Processing* 102, 1-12.

Betteridge, D., Joshlin, M.T., and Lilley, T., 1981. Acoustic emissions from chemical reactions. *Analytical Chemistry* 53, 1064-1073.

Boyd, J.W.R., and Varley, J., 2001. The use of passive measurement of acoustic emissions from chemical engineering processes. *Chemical Engineering Science* 56, 1749-1767.

Cao, Z., Wang, B.-F., Wang, K.-M., Lin, H.-G., and Yu, R.-Q., 1998. Chemical acoustic emissions from gas evolution processes recorded by a piezoelectric transducer. *Sensors and Actuators B* 50, 27-37.

Cho, Y.S., and Laskowski, J.S., 2002a. Effect of flotation frothers on bubble size and foam stability. *International Journal of Mineral Processing* 64, 2, 69-80.

Cho, Y.S., and Laskowski, J.S., 2002b. Bubble coalescence and its effect on dynamic foam stability. *The Canadian Journal of Chemical Engineering* 80, 2, 299-305.

Christenson, H.K., Bowen, R.E., Carlton, J.A., Denne, J.R.M., and Lu, Y., 2008. Electrolytes that show a transition to bubble coalescence inhibition at high concentrations. *Journal of Physical Chemistry C* 112, 794-796.

Craig, V.S.J., Ninham, B.W., and Pashley, R.M., 1993. The effect of electrolytes on bubble coalescence in water. *Journal of Physical Chemistry* 97, 10192-10197.

Crowther, T.G., Wade, A.P., Wentzell, P.D., and Gopal, R., 1991. Characterization of acoustic emission from an electrolysis cell. *Analytica Chimica Acta* 254, 223-234.

Dippenaar, A., 1982. The destabilization of froth by solids. I. The mechanism of film rupture. *International Journal of Mineral Processing* 9, 1, 1-14.

Dukhin, S.S., Miller, R., Loglio, G., 1998. Physico-chemical hydrodynamics of rising bubbles. In: Möbius, D., Miller, R. (Eds.), *Studies in Interfacial Science, Drops and Bubbles in Interfacial Research*, Elsevier Science 6, 367-432.

Finch, J.A., Nasset, J.E., and Acuña, C., 2008. Role of frother on bubble production and behaviour in flotation. *Minerals Engineering* 21, 12, 949-957.

Gallegos-Acevedo, P.M., Espinoza-Cuadra, J., Pérez-Garibay, R., and Pecina-Treviño, 2010. Bubble Coalescence: Hydrophobic particles effect. *Journal of Mining Science* 46, 3, 333-337.

Garrett, P.R., 1993. Defoaming. *Surfactant Science Series*, volume 45, Marcel Dekker, New York.

Hofmeier, U., Yaminsky, V.V., and Christensen, H.K., 1995. Observations of solute effects on bubble formation. *Journal of Colloid and Interface Science* 174, 199-210.

Hou, R., Hunt, A., and Williams, R.A., 1998. Acoustic monitoring of hydrocyclone performance. *Minerals Engineering* 11, 11, 1047-1059.

Ip, S.W., Wang, Y., and Toguri, J.M., 1999. Aluminum foam stabilization by solid particles. *Canadian Metallurgical Quarterly* 38, 1, 81-92.

Kracht, W., and Finch, J.A., 2009. Using sound to study bubble coalescence. *Journal of Colloid and Interface Science* 332, 237-245.

Kulkarni, R.D., Goddard, E.D., and Kanner, B., 1977. Mechanism of antifoaming: Role of filler particle. *Industrial & Engineering Chemistry Fundamentals* 16, 4, 472-474.

Kuan, S.H., and Finch, J.A., 2010. Impact of talc on pulp and froth properties in F150 and 1-pentanol frother systems. *Minerals Engineering* 23, 11, 1003-1009.

Kyriakides, N.K., Kasrinakis, E.G., Nychas, S.G., and Goulas, A., 1997. Bubbling from nozzles submerged in water: Transitions between bubbling regimes, *The Canadian Journal of Chemical Engineering* 75, 684-691.

Leighton, T.G., Fagan K.J., and Field, J.E., 1991. Acoustic and photographic studies of injected bubbles. *European Journal of Physics* 12, 77-85.

Minnaert, M., 1933. On musical air-bubbles and the sounds of running water. *Philosophical Magazine* 16, 235-248.

Nesset, J.E., 2011. Modeling the Sauter mean bubble diameter in mechanical, forced-air flotation machines. Ph.D. Thesis, McGill University, Department of Mining and Materials Engineering.

Pugh, R.J., 2007. The physics and chemistry of frothers. In: Fuerstenau, M. C., Jameson, G. J., and Yoon, R. H. (Eds.). *Froth Flotation: A Century of Innovation*, SME, Littleton, USA, 259-281.

Quinn, J.J., and Finch, J.A., 2012. On bi-modal bubble size distributions in the absence of frother. *Minerals Engineering* 36-38, 237-241.

Quinn, J.J., Kracht, W., Gomez, C.O., Gagnon, C., and Finch, J.A., 2007. Comparing the effects of salts and frother (MIBC) on gas dispersion and froth properties. *Minerals Engineering* 20, 1296-1302.

Quinn, J.J., Maldonado, M., Gomez, C.O., and Finch, J.A., 2013. An experimental study on bubble shape and rise velocity in frother, polymer and inorganic salt solutions, In: *Proceedings of the 52<sup>nd</sup> Conference of Metallurgists (hosted by Materials Science & Technology (MS&T) 2013): Water and Energy in Mineral Processing, The 9<sup>th</sup> UBC - McGill - U of A International Symposium on the Fundamentals of Mineral Processing, 1981-1992.*

Spencer, S.J., Bruniges, R., Sharp, V., Catanzano, V., Roberts, G., Bruckard, W.J., and Davey, K., 2010. Acoustic emission monitoring of froth flotation. In: *Proceedings of the XXV International Mineral Processing Congress. AUSIMM, Melbourne, 3489-3500.*

Tse, K.L., Martin, T., McFarlane, C.M., and Nienow, A.W., 2003. Small bubble formation via a coalescence dependent break-up mechanism. *Chemical Engineering Science* 58, 2, 275-286.

Vanegas, C., and Holtham, P., 2010. Possibility for flotation acoustics monitoring - a review. In: *Proceedings of the XXV International Mineral Processing Congress. AUSIMM, Melbourne, 2457-2470.*

Vanegas, C., and Holtham, P., 2008. On-line froth acoustic emission measurements in industrial sites. *Minerals Engineering* 21, 883–888.

Wentzell, P.D., and Wade, A.P., 1989. Chemical acoustic emission analysis in the frequency domain. *Analytical Chemistry* 61, 2638-2642.

Zahradnik, J., Fialová, M., and Linek, V., 1999. The effect of surface additives on bubble coalescence in aqueous media. *Chemical Engineering Science* 54, 4757-4766.

Zeng, Y., and Forssberg, E., 1993. Monitoring grinding parameters by signal measurements for an industrial ball mill. *International Journal of Mineral Processing* 40, 1-16.

Zhang, W., Nasset, J.E., Rao, R., and Finch, J.A., 2012. Characterizing frothers through critical coalescence concentration (CCC) 95-hydrophile-lipophile balance (HLB) relationship. *Minerals* 2, 3, 208-227.

# **Chapter 6 – Experimental study on the shape - velocity relationship of an ellipsoidal bubble in inorganic salt solutions**

## **6.1 Introduction**

Froth flotation and gas dispersion in saline solutions has garnered increased attention in recent years (Craig, 2011; Alexander et al., 2012; Castro, 2012; Wang and Peng, 2013). The scarcity of fresh water especially in remote mining locales has forced several plants to recycle process water (which typically concentrates contaminants) or to use saline bore or sea water. The presence of certain soluble inorganic ions has been shown to decrease bubble size and increase gas holdup in flotation systems (Laskowski et al., 2003; Nessel et al., 2006). Quinn et al. (2007) showed that inorganic solutions with ionic strength ca. 0.4 gave similar gas holdup to 8 - 10 ppm MIBC frother in water. One flotation concentrator, Xstrata's Raglan operation in northern Quebec, operates without frother due to the high salt content of the process water which provides adequate bubble size reduction and frothing characteristics. Several authors have investigated the effect of saline process water on flotation performance (Yoon and Sabey, 1989; Pugh et al., 1997; Castro, 2012).

Frother is typically added to flotation circuits with one function being the reduction of bubble rise velocity (Klimpel and Isherwood, 1991). The ability of surfactants (frothers) to lower single bubble rise velocity is well documented (Fuerstenau and Wayman, 1958; Sam et al., 1996; Bozzano and Dente, 2001; Krzan and Malysa, 2002a, 2002b; Finch et al., 2008). The stagnant cap model describes how surfactant molecules on the bubble surface are swept to the rear of a rising bubble creating surface tension gradients which increase drag and thus retard bubble rise (Savic, 1953; Dukhin et al., 1998). A similar mechanism seems to control bubble shape, surface tension gradients resisting deformation (Dukhin et al., 1998; Finch et al., 2008). In comparison, the mechanism(s) by which inorganic salts act to modify shape and velocity of rising bubbles is not clear although surface tension gradients may be at play as most inorganic salts slightly increase surface tension.

Much of the literature concerning bubble dispersions in inorganic salt solutions discusses their ability to inhibit bubble coalescence (Lessard and Zieminski, 1971; Craig et al., 1993; Craig, 2011). All inorganic salts tested here retard coalescence and encompass a range of coalescence inhibiting strength, ranking as follows:  $\text{NaClO}_4 < \text{KCl} < \text{NaCl} < \text{Na}_2\text{SO}_4 < \text{CaCl}_2$  (Lessard and Zieminski, 1971; Zieminski and Whittemore, 1971; Craig et al., 1993; Zahradnik et al., 1999; Christenson et al., 2008).

Much of the data on bubble rise velocity in inorganic salt solutions comes from oceanography and typically focuses on bubble diameters below 1 mm in sea water or sodium chloride solutions (Detsch and Harris, 1989; Detsch, 1991; Henry et al., 2008). Bubble sizes below roughly 1 mm diameter are spherical and show little effect of contaminants on shape or velocity (Clift et al., 2005). The present work uses bubbles ca. 2.3 mm sphere-volume equivalent diameter which lie in the ellipsoidal shape regime where surface tension forces are dominant (Bhaga and Weber, 1981; Clift et al., 2005). This size was chosen as bubble shape and velocity are sensitive to the presence of contaminants (Clift et al., 2005). The bubble size is within the range encountered in flotation systems (Nesset et al., 2006). Tomiyama et al. (2002) noted that bubble behaviour in the ellipsoidal regime was not well understood and that no theoretical models for terminal velocity existed.

Researchers have found that bubble shape and velocity strongly interact in surfactant, polymer and inorganic salt solutions both close to and far from bubble generation (Bozzano and Dente, 2001; Tomiyama et al., 2002; Kracht and Finch, 2010). Gomez et al. (2010) reported a unique relationship between bubble shape and velocity for a given bubble volume independent of surfactant (frother) type or polymer. Maldonado et al. (2013) tested bubbles in polymer, frother and two inorganic salt solutions and also showed a unique dependence between bubble shape and velocity independent of solute type. The researchers found that for ca. 2.5 mm bubbles in water, aspect ratio was ca. 0.57 and rise velocity was ca. 28 cm/s while in concentrated solutions (frother, polymer or salt), aspect ratio increased to ca. 0.95 and rise velocity decreased to ca. 17 cm/s.

It has been demonstrated that the nature of bubble formation (release) affects bubble shape, velocity and motion (Wu and Gharib, 2002; Tomiyama et al., 2002; Peters and Els, 2012). Tomiyama et al. (2002) observed that bubbles released with small initial shape deformation

resulted in more spherical bubbles (high aspect ratio) with low terminal velocities compared to bubbles with large initial shape deformation which resulted in oblate bubbles (low aspect ratio) with high terminal velocities. Tomiyama et al. (2002) noted the presence of surfactant acted to damp initial shape deformation.

The present work aims to build upon the work of Gomez et al. (2010) and Maldonado et al. (2013) and test the bubble shape - rise velocity relationship in a series of inorganic salt solutions ( $\text{NaClO}_4$ ,  $\text{KCl}$ ,  $\text{NaCl}$ ,  $\text{Na}_2\text{SO}_4$ ,  $\text{CaCl}_2$ ). The results are compared to MIBC, a typical flotation frother. The inorganic salts tested were chosen based on ions which are typically present in flotation concentrator process water (Alexander et al., 2012) and to encompass a range of bubble coalescence inhibiting behaviour. For the bubble size used (ca. 2.3 mm) the Reynolds numbers range from ca. 280 - 670 and Eötvös numbers range from ca. 0.65 - 0.85, showing bubbles to be in the ellipsoidal shape regime (Bhaga and Weber, 1981; Clift et al., 2005).

## 6.2 Experimental

### 6.2.1 Setup and image collection

The experimental setup is shown in Figure 6.1. Individual air bubbles were created at a glass capillary tube ( $406 \pm 25 \mu\text{m}$  inner diameter) in the various test solutions (Table 6.1). All inorganic salts were supplied by Fisher Scientific and were ACS grade. The MIBC sample was supplied by Sigma Aldrich and was GC grade. Bubble generation frequency was controlled at 5 seconds using a high-precision pressure regulator (Fairchild, model M4100A, 0-5 psi). The aim was to form bubbles under constant release conditions to restrict effects of release on initial shape. Bubble formation time was  $71 \text{ ms} \pm 2 \text{ ms}$  (95% confidence interval, CI). The pressure regulator was connected to the capillary via coiled tubing with inner diameter  $200 \mu\text{m}$ . After detachment, the bubble rose through a 1 m vertical clear PVC pipe ( $0.025 \text{ m}$  diameter) to a rectangular viewing chamber (height  $0.60 \text{ m}$ , width  $0.22 \text{ m}$ , depth  $0.14 \text{ m}$ ). Liquid level was maintained at  $1.35 \text{ m}$  above the capillary. The viewing chamber was back-lit using an arrangement of light emitting diodes (Phlox, model LLUB-QIR-24V) covering an area of  $0.10 \times 0.10 \text{ m}$ . Images were collected of bubbles rising between a height of ca.  $1.15 \text{ m}$  to  $1.20 \text{ m}$  above the capillary.

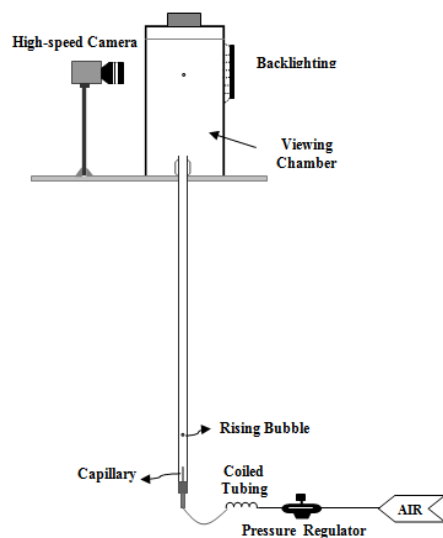


**Figure 6.1 – Experimental setup**

**Table 6.1 – Reagents and concentration range**

<b>Inorganic Salt</b>	<b>Concentration, M</b>
NaClO <sub>4</sub> ·H <sub>2</sub> O	0.01 - 2.0
KCl	0.0125 - 1.0
NaCl	0.01 - 1.0
Na <sub>2</sub> SO <sub>4</sub> (anhydrous)	0.01 - 1.0
CaCl <sub>2</sub> ·2H <sub>2</sub> O	0.005 - 1.0
<b>Frother</b>	<b>Concentration, ppm (mg/l)</b>
MIBC (4-methyl-2-pentanol)	1 – 100

A Fastec Imaging (model no. HiSpec5 8G Mono) high-speed camera equipped with a Nikon - AF Micro Nikkor 60 mm 1:2.8 D lens was used to capture images at 1000 frames per second (fps). Typical images were 800 × 1710 pixels. The magnification was chosen to ensure horizontal bubble diameters comprised a minimum of 80 pixels with a typical image resolution 35 pixels/mm. The viewing area was ca. 0.023 m (horizontal) x 0.049 m (vertical). Image sequences of ten bubbles were collected and analyzed for each condition. Image sequences consisted of ca. 180-300 images depending on the bubble rise velocity.

## 6.2.2 Image analysis

Image sequences were analyzed off-line using ImageJ software and a macro which automatically calculated and tabulated: 1) bubble size, 2) bubble aspect ratio, and 3) bubble velocity. These parameters were tracked at intervals of 1 ms.

### 1) Bubble size

The sphere-volume equivalent diameter ( $d_e$ ) was calculated using the major ( $a$ ) and minor ( $b$ ) semi-axes of an ellipse fitted to the projected bubble area (Equation (6.1)), assuming the bubble to be an oblate spheroid (i.e., symmetric about the minor axis):

$$d_e = \sqrt[3]{(2a)^2 \times (2b)} \quad (6.1)$$

Figure 6.2 depicts the ellipse fitting procedure and semi-axes determination.

### 2) Aspect ratio

Aspect ratio ( $E$ ) was used to characterize bubble shape (Equation (6.2)). Values of  $E$  less than 1.0 denote the bubble is an oblate spheroid (Clift et al., 2005).

$$E = \frac{b}{a} \quad (6.2)$$

### 3) Bubble rise velocity

Bubble rise velocity was calculated from the vertical displacement of the center of the fitted ellipse over two consecutive frames.

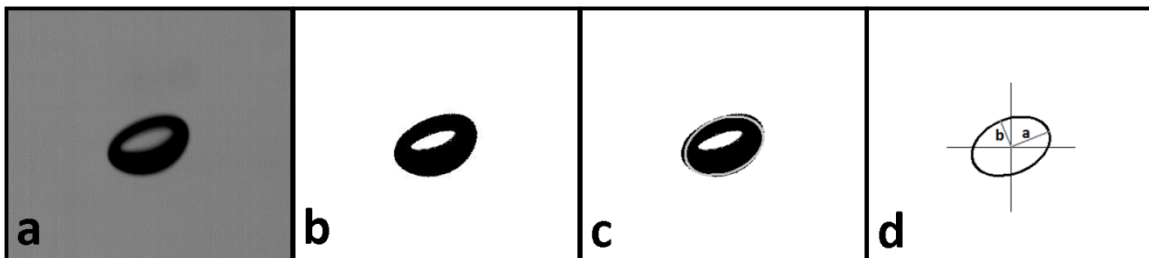


Figure 6.2 – Image analysis procedure: a) original bubble image, b) image after applying threshold, c) ellipse fitting, and d) determination of major (a) and minor (b) semi-axes

### 6.3 Results

Constancy of bubble size in order to compare solutes is a necessary pre-condition. A total of 490 image sequences of rising bubbles were analyzed and an average bubble size was determined from each sequence. The average bubble size for all image sequences was 2.29 mm. Figure 6.2 shows the average bubble size ( $d_e$ ), 95% CI, image resolution and standard error for the chemistries tested. Comparing the 95% CI it is concluded that there is no significant difference in bubble size between the solutes.

**Table 6.2 – Bubble size population data for each chemistry tested**

<b>Chemistry</b>		<b>Water</b>	<b>NaClO<sub>4</sub></b>	<b>KCl</b>	<b>NaCl</b>	<b>Na<sub>2</sub>SO<sub>4</sub></b>	<b>CaCl<sub>2</sub></b>	<b>MIBC</b>
<b>Bubble Sequences</b>		10	90	90	70	70	90	70
<b>Avg D<sub>e</sub></b>	mm	2.26	2.27	2.26	2.36	2.33	2.30	2.26
<b>95% CI (±)</b>	mm	0.01	0.10	0.07	0.05	0.14	0.13	0.09
<b>Image Resolution</b>	mm	0.03	0.03	0.03	0.03	0.03	0.03	0.03
<b>Standard Error</b>		0.006	0.005	0.004	0.003	0.008	0.007	0.005

Figure 6.3 shows superimposed example images of three rising bubbles in water, 0.02M NaCl, and 1.0M NaCl taken at 20 ms intervals. Average aspect ratio over the image sequence was 0.524 (water), 0.795 (0.02 M NaCl), and 0.940 (1.0 M NaCl). The decreasing inter-bubble distance illustrates the decrease in rise velocity with increasing salt concentration. Average bubble rise velocity for each image sequence was 27.1 cm/s (water), 23.0 cm/s (0.02 M NaCl), and 17.5 cm/s (1.0 M NaCl), i.e., the velocity decreases as aspect ratio increases.

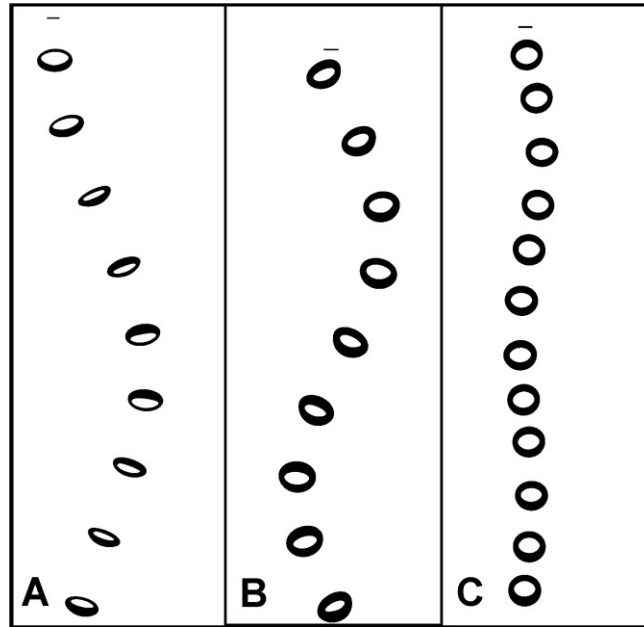


**Figure 6.3 – Image sequences (at 20 ms time intervals) of a rising bubble in: A) water, B) 0.02 M NaCl, and C) 1 M NaCl solutions (1 mm reference bar is shown above the uppermost bubble in each sequence)**

Figure 6.4 shows an example of oscillations over time in the vertical and horizontal diameters (with  $2a$  being the horizontal diameter ( $d_h$ ) and  $2b$  the vertical diameter ( $d_v$ ) of the ellipse) and the calculated equivalent diameter for the 0.02 M NaCl case in Figure 6.3. The vertical and horizontal diameters oscillated between ca. 2.36 and 2.41 mm, and 2.18 and 2.36 mm, respectively. The calculated equivalent diameter ranged from 2.32 to 2.37 mm, i.e., within the 95% CI (Table 6.2).

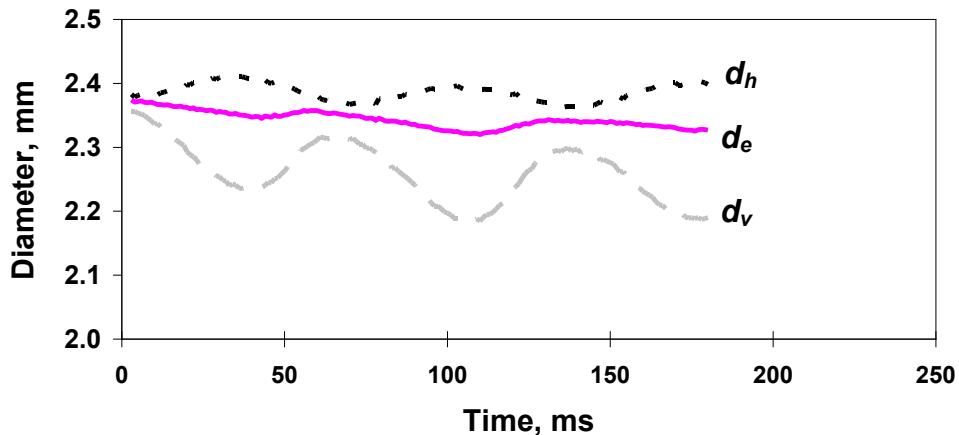


Figure 6.4 – Example of oscillations in the length of the major and minor axis and the calculated volume equivalent diameter as a function of time in 0.02 M NaCl

Figure 6.5 shows bubble aspect ratio and rise velocity at 1 ms time intervals for the example image sequences shown in Figure 6.3. It is evident that the variation in aspect ratio follows the inverse in rise velocity: as aspect ratio increases (bubble becomes more spherical) velocity decreases and vice versa. The effect of sodium chloride concentration is to change the magnitude of each but not this inverse relationship. All the salts and the MIBC showed a similar ability to increase bubble aspect ratio and decrease rise velocity with increasing concentration.

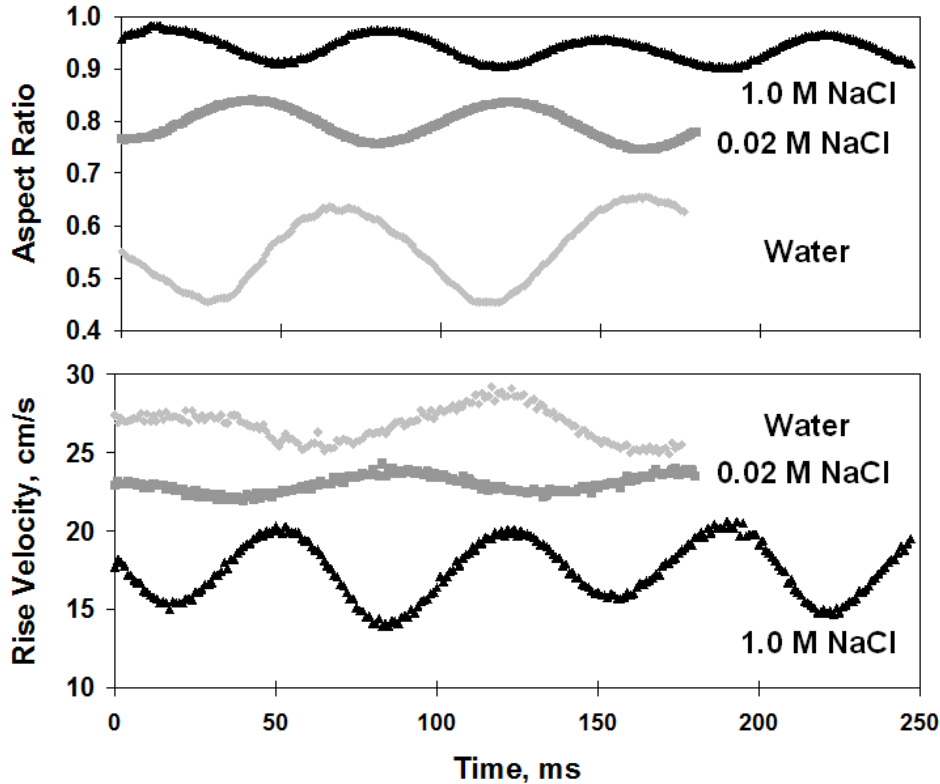


Figure 6.5 – Examples of bubble aspect ratio (upper) and rise velocity (lower) as a function of time in water, 0.02 M NaCl and 1.0 M NaCl

Figure 6.6 shows the average (of the ten bubbles tested for each condition) bubble rise velocity and aspect ratio as a function of concentration for two salts, potassium chloride and sodium perchlorate. For potassium chloride, average rise velocity decreased from ca. 28 to 17 cm/s while average aspect ratio increased from ca. 0.55 to 0.93; and for sodium perchlorate rise velocity decreased from ca. 28 to 19 cm/s and aspect ratio increased from ca. 0.55 to 0.90 over the same concentration range. Error bars (95% CI) show the uncertainty for both rise velocity and aspect ratio becomes larger at low salt concentration. The remaining salts generally fell in between these two (and are not shown for clarity). Table 6.3 lists aspect ratio and rise velocity for each salt tested at concentrations 0.05 M and 0.5 M. In terms of increasing aspect ratio (for both concentrations), the salts order as follows:  $\text{NaClO}_4 < \text{CaCl}_2 < \text{NaCl} < \text{KCl} < \text{Na}_2\text{SO}_4$ . The rise velocity does not show a clear order and as such the authors conclude no clear trend in salt ‘strength’ with regard to control of velocity or shape based on the present data.

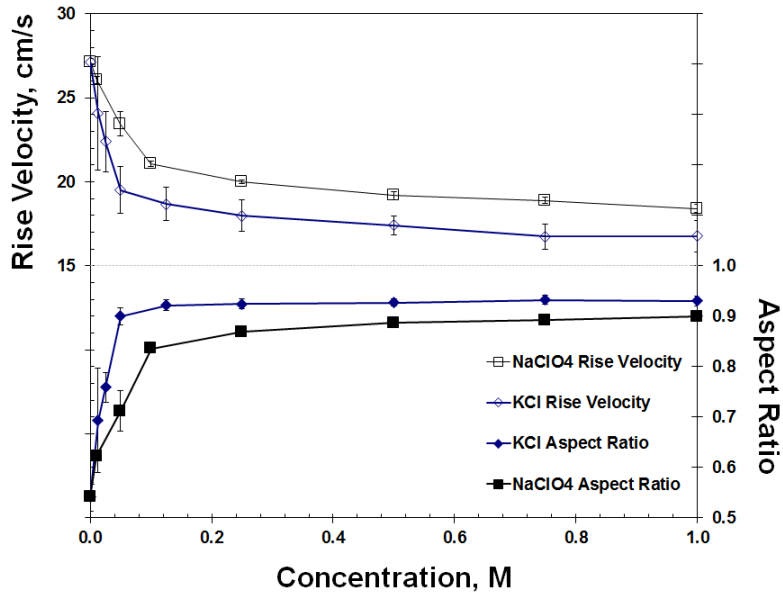


Figure 6.6 – Examples of the effect of salt ( $\text{NaClO}_4$  and  $\text{KCl}$ ) concentration on bubble rise velocity and aspect ratio

Table 6.3 – Bubble aspect ratio (E) and rise velocity (Vel.) at 0.05 M and 0.5 M

Salt Type	0.05 M		0.5 M	
	E	Vel., cm/s	E	Vel., cm/s
$\text{NaClO}_4$	0.71	23.4	0.89	19.2
$\text{KCl}$	0.90	19.5	0.93	17.4
$\text{NaCl}$	0.81	22.9	0.92	18.3
$\text{Na}_2\text{SO}_4$	0.92	20.2	0.95	18.3
$\text{CaCl}_2$	0.79	22.6	0.91	19.1

Figure 6.7 shows average bubble rise velocity as a function of average aspect ratio for the calcium chloride system. As concentration increased, aspect ratio increased (bubble became more spherical) and rise velocity decreased. Whilst for a given calcium chloride concentration there is a range of aspect ratios and velocities all the data seem to describe a single shape (aspect ratio) - velocity trend: that is, the effect of concentration was to change location on the trend but not the trend itself.

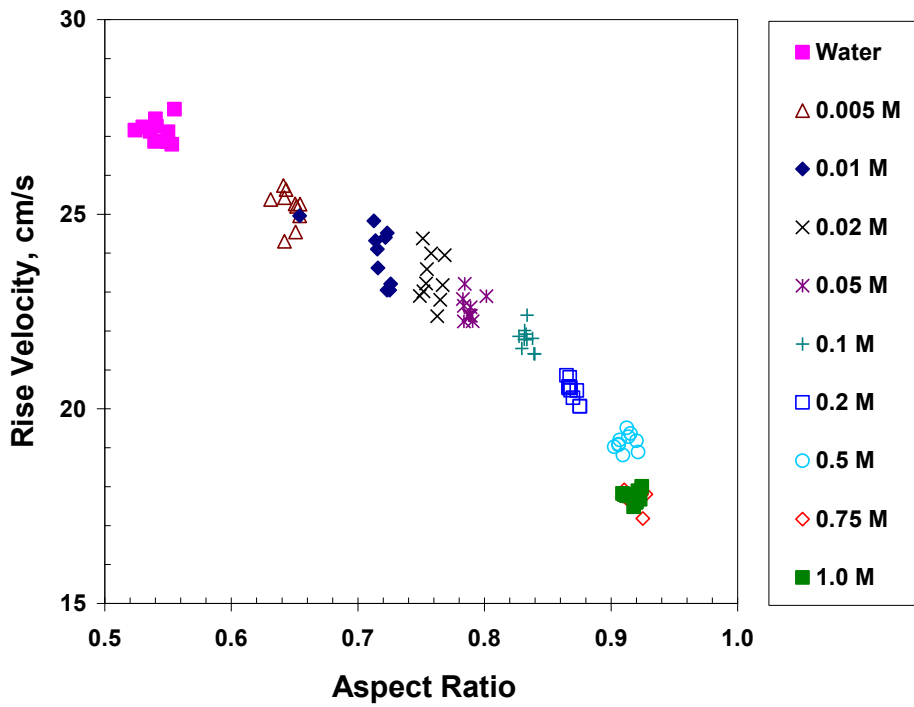


Figure 6.7 – Average bubble rise velocity and aspect ratio for various concentrations of calcium chloride

Figure 6.8 shows average bubble velocity as a function of average aspect ratio in the presence of MIBC. The result is similar to that for the calcium chloride; increased concentration resulted in increased aspect ratio and decreased rise velocity, which followed a single trend.

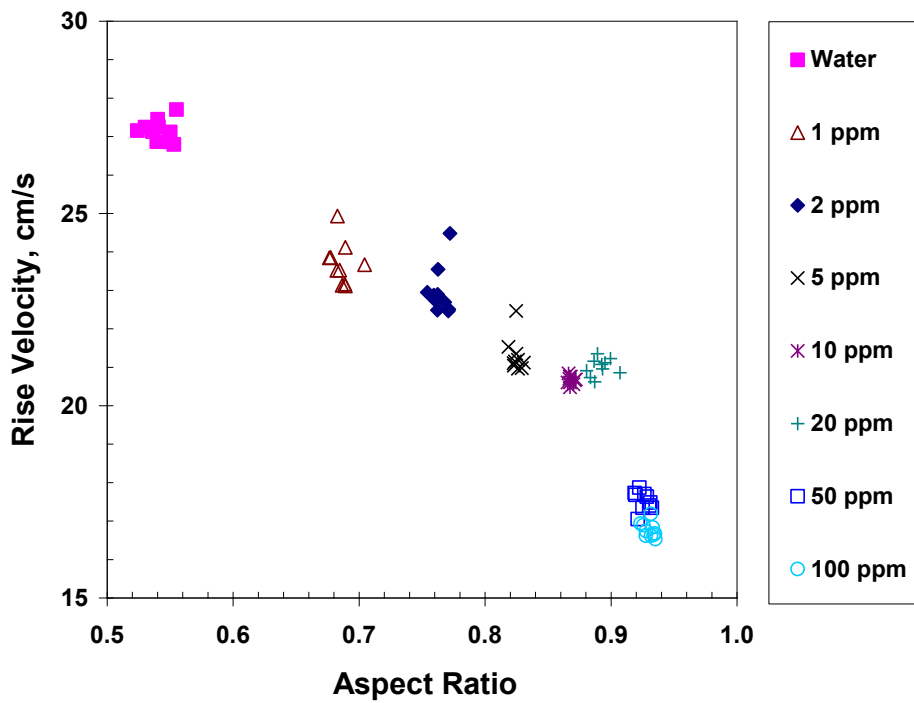


Figure 6.8 – Average bubble rise velocity and aspect ratio for various MIBC solutions

Figure 6.9 summarizes all the bubble rise velocity and aspect ratio data. The results include all concentrations of each solute type tested (i.e., all data points in Figure 6.7 and Figure 6.8 are present in Figure 6.9 for the KCl and MIBC data, respectively). The data appear to describe a single trend independent of solute type. The result implies that there is a unique relationship between shape and velocity for a given bubble volume.

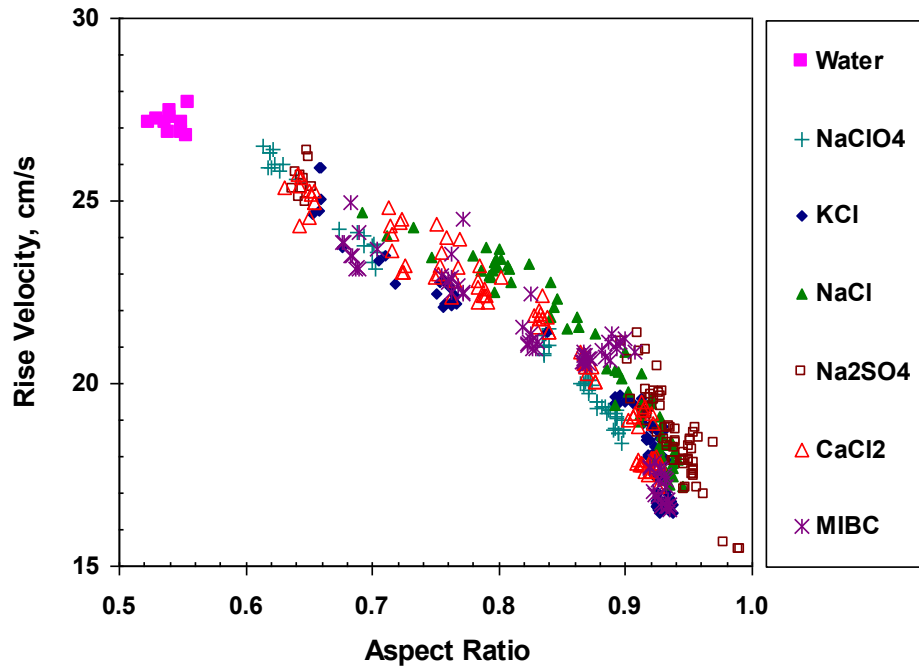


Figure 6.9 – Average bubble rise velocity and aspect ratio for all conditions tested

## 6.4 Discussion

As noted by several researchers, the dynamic behaviour of a rising bubble is reflected by changes in shape and velocity (Wu and Gharib, 2002; Tomiyama et al., 2002; Krzan and Malysa, 2002a, 2002b; Krzan et al., 2004, 2007). Some (Wu and Gharib, 2002; Tomiyama et al., 2002; Peters and Els, 2012) have shown a relationship between shape and velocity in water by altering the bubble shape at release. The present results suggest that the relationship is general regardless of how bubble shape or velocity is manipulated. This may mean that shape and velocity are controlled by the same mechanism. Part of the argument could be that since it takes energy to oppose deformation for the bubble to become more spherical this energy is taken from the kinetic energy of the rising bubble, hence the intimate connection between shape and velocity independent of solute type. van Wijngaarden and Veldhuis (2008) discuss the transformation of kinetic energy into surface energy as an ellipsoidal bubble oscillates.

A feature of the aspect ratio - rise velocity relationship in Figure 6.9 is the increase in slope as aspect ratio increases. This means that a small change in aspect ratio at high values ( $E > 0.85$ ) results in relatively large changes in velocity. This effect is evident in Figure 6.5, where

oscillations in aspect ratio between 0.90 and 0.98 for the 1.0 M NaCl case resulted in velocity oscillations between 14 and 21 cm/s while in water the relatively large oscillations in aspect ratio (between 0.45 and 0.65) resulted in relatively minor velocity oscillations (between 25 and 29 cm/s). Tomiyama et al. (2002) state that the presence of solute damps shape oscillations while Smolianski et al. (2008) note that the magnitude of oscillations in rise velocity are larger for bubbles which are more resistant to deformation: both of these effects are seen here.

Surface tension gradients help explain both bubble coalescence inhibition and reduced single bubble rise velocity with solute present. Several authors have characterized coalescence-inhibiting salt strength which correlates well with ionic strength (Zieminski and Whittemore, 1971; Lessard and Zieminski, 1971; Craig et al., 1993). In contrast, from our data there appears to be no clear trend in strength based on a salt's ability to modify bubble shape and rise velocity.

Gas dispersion parameters (e.g. bubble size and gas holdup) play a key role in determining flotation kinetics (Gorain et al., 1997). In the case of inorganic salts, coalescence inhibition helps explain reduced bubble size (Zieminski and Whittemore, 1971; Craig et al., 1993) and, because small bubbles rise slower than large bubbles (at least for bubbles < ca. 3 mm (Clift et al., 2005)), also helps explain increased gas holdup (Quinn et al., 2007). In addition, the present work indicates that rise velocity for a given bubble size (at least > 1 mm) is reduced in inorganic salt solutions, which also contributes to increased gas holdup. Alexander et al. (2012) showed that flotation recovery of graphite in salt solutions correlated with gas holdup independent of salt type.

The correlation noted between graphite recovery and gas holdup reflects the particle collection process which depends on bubble surface area and rise velocity. Collection would seem favored by high surface area which can increase the number of particles transported, and by low rise velocity, i.e., high bubble retention time, which increases the number of collision events. Given that surface area increases as a spheroid becomes more oblate (i.e., for a given bubble volume a sphere is the geometry with the least interfacial surface area), Figure 6.10 explores the relationship between specific bubble surface area ( $\text{mm}^2/\text{mm}^3$  or  $\text{mm}^{-1}$ ) and bubble rise velocity derived from the present data. The figure poses an interesting question: which is preferable, an increased bubble surface area or reduced bubble rise velocity as both cannot be achieved

simultaneously? This discrimination could be a good exercise for a fundamental bubble-particle capture model to examine.

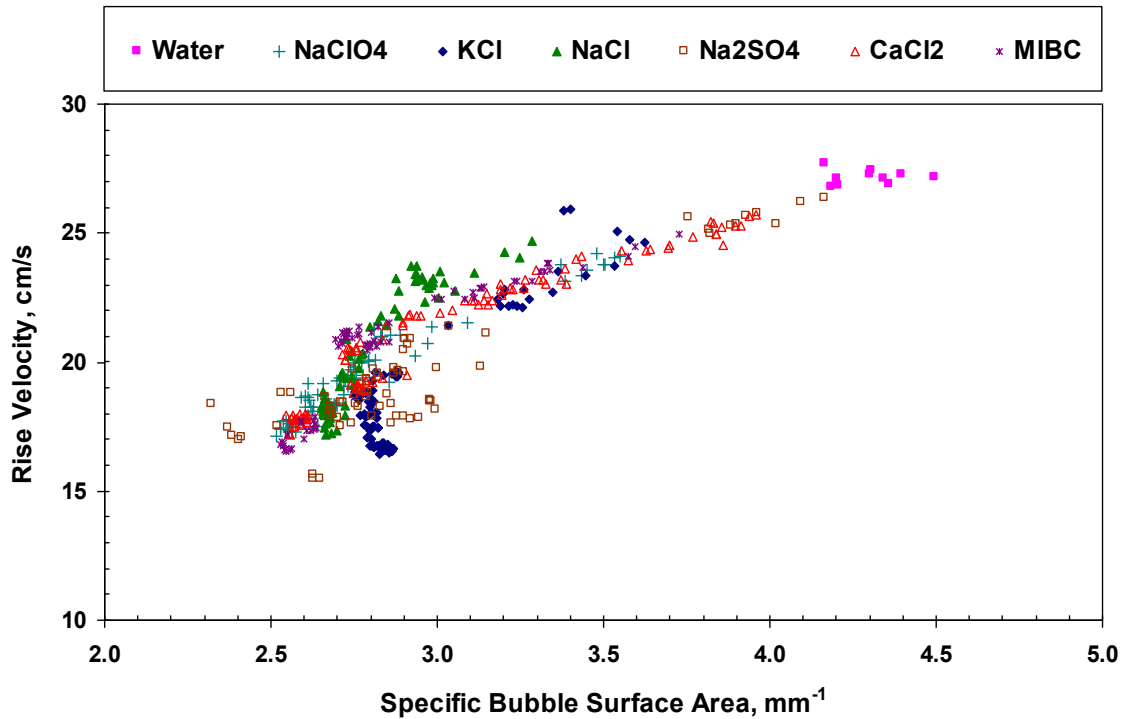


Figure 6.10 – Rise velocity and specific bubble surface area for all conditions tested

## 6.5 Conclusions

Ellipsoidal bubbles of 2.3 mm equivalent diameter were produced at a capillary in water containing a series of inorganic salts and MIBC frother. The shape and velocity were measured over a distance of 1.15 to 1.20 m above the launch point. The shape and velocity oscillated in a linked fashion with increasing concentration creating more spherical bubbles with reduced rise velocity. There appears to be a unique bubble shape - rise velocity relationship independent of solute type.

## References

- Alexander, S., Quinn, J., van der Spuy, J.E., and Finch, J.A., 2012. Correlation of graphite flotation and gas holdup in saline solutions. In: Drelich, J. (Ed.), *Water in Mineral Processing: Proceedings of the First International Symposium*, SME, Englewood, 41-50.
- Bhaga, D., and Weber, M.E., 1981. Bubbles in viscous liquids: shapes, wakes and velocities. *Journal of Fluid Mechanics* 105, 61-85.
- Bozzano, G., and Dente, M., 2001. Shape and terminal velocity of single bubble motion: a novel approach. *Computers and Chemical Engineering* 25, 571-576.
- Castro, S., 2012. Challenges in flotation of Cu-Mo sulphide ores in sea water. In: Drelich, J. (Ed.), *Water in Mineral Processing: Proceedings of the First International Symposium*, SME, Englewood, 29-40.
- Christenson, H.K., Bowen, R.E., Carlton, J.A., Denne, J.R.M., and Lu, Y., 2008. Electrolytes that show transition to bubble coalescence inhibition at high concentrations. *The Journal of Physical Chemistry C* 112, 794-796.
- Clift, R., Grace, J.R., and Weber, M., 2005. *Bubble, Drops, and Particles*. Dover Publications Inc., Mineola, New York. 169-202.
- Craig, V.S.J., Ninham, B.W., and Pashley, R.M. 1993. The effect of electrolytes on bubble coalescence in water. *The Journal of Physical Chemistry* 97, 10192-10197.
- Craig, V.S.J., 2011. Do hydration forces play a role in thin film drainage and rupture observed in electrolyte solution? *Current Opinion in Colloid and Interface Science* 16, 597-600.
- Detsch, R.M., 1991. Small air bubbles in reagent grade water and seawater: rise velocities of 20- to 1000- $\mu\text{m}$  diameter bubbles. *Journal of Geophysical Research* 96, C5, 8901-8906.
- Detsch R., and Harris, I., 1989. Dissolution and rise velocity of small air bubbles in water and salt water. In: *Proceedings of OCEANS'89*, 1, 286-291.
- Dukhin, S.S., Miller, R., and Loglio, G., 1998. Physico-chemical hydrodynamics of rising bubbles. In: Mobius, D., Miller, R. (Eds.), *Studies in interfacial Science, Drops and Bubbles in Interfacial Research*, vol. 6. Elsevier Science, 367-432.

Finch, J.A., Nasset, J.E., and Acuna, C., 2008. Role of frother on bubble production and behaviour in flotation. *Minerals Engineering* 21, 949-957.

Fuerstenau, D.W., and Wayman, C.H., 1958. Effect of chemical reagents on the motion of single air bubbles in water. *Mining Engineering, Transactions of AIME*, 694-699.

Gomez, C.O., Maldonado, M., Araya, R., and Finch, J.A., 2010. Frother and viscosity effects on bubble shape and velocity. In: Pawlik, M. (Ed.), *Proceedings of the 49<sup>th</sup> Conference of Metallurgists: Rheology in Mineral Processing, The 8<sup>th</sup> UBC - McGill - U of A International Symposium on the Fundamentals of Mineral Processing*, 57-74.

Gorain, B.K., Franzidis, J.P., and Manlapig, E.V., 1997. Studies on impeller type, impeller speed and air flow rate in an industrial flotation cell. Part 4: Effect of bubble surface area flux on flotation performance. *Minerals Engineering* 10, 4, 367-379.

Henry, C.L., Parkinson, L., Ralston, J.R., and Craig, V.S.J., 2008. A mobile gas – water interface in electrolyte solutions. *The Journal of Physical Chemistry Letters* C 112, 15094-15097.

Kracht, W., and Finch, J.A., 2010. Effect of frother on initial bubble shape and velocity. *International Journal of Mineral Processing* 94, 115-120.

Krzan, M., and Malysa, K., 2002a. Profiles of local velocities of bubbles in n-butanol, n-hexanol and n-nonanol solutions. *Colloids and Surfaces A: Physicochemical and Engineering Aspects* 207, 279-291.

Krzan, M., and Malysa, K., 2002b. Influence of frother concentration on bubble dimensions and rising velocities. *Physicochemical Problems of Mineral Processing* 36, 65-76.

Krzan, M., Lunkenheimer, K., and Malysa, K., 2004. On the influence of the surfactant's polar group on the local and terminal velocities of bubbles. *Colloids and Surfaces A: Physicochemical Engineering Aspects* 250, 431-441.

Krzan, M., Zawala, J., and Malysa, K., 2007. Development of steady state adsorption distribution over interface of a bubble rising in solutions of *n*-alkanols (C<sub>5</sub>, C<sub>8</sub>) and *n*-alkyltrimethylammonium bromides (C<sub>8</sub>, C<sub>12</sub>, C<sub>16</sub>). *Colloids and Surfaces A: Physicochemical Engineering Aspects* 298, 42-51.

Laskowski, J.S., Cho, Y.S., and Ding, K., 2003. Effect of frothers on bubble size and foam stability in potash ore flotation systems. *The Canadian Journal of Chemical Engineering* 81, 63-69.

Lessard, R.R., and Zieminski, S.A., 1971. Bubble coalescence and gas transfer in aqueous electrolyte solutions. *Industrial and Engineering Chemistry Fundamentals* 10, 2, 260-269.

Maldonado, M., Quinn, J.J., Gomez, C.O., and Finch, J.A., 2013. An experimental study examining the relationship between bubble shape and rise velocity. *Chemical Engineering Science* 98, 7-11.

Nesset, J.E., Hernandez-Aguilar, J.R., Acuna, C., Gomez, C.O., and Finch, J.A., 2006. Some gas dispersion characteristics of mechanical flotation machines, *Minerals Engineering* 19, 807-815.

Peters, F., and Els, C., 2012. An experimental study on slow and fast bubbles in tap water. *Chemical Engineering Science* 82, 194-199.

Pugh, R.J., Weissenborn, P., and Paulson, O., 1997. Flotation in inorganic electrolytes; the relationship between recovery of hydrophobic particles, surface tension, bubble coalescence and gas solubility. *International Journal of Mineral Processing* 51, 125-138.

Quinn, J.J., Kracht, W., Gomez, C.O., Gagnon, C., and Finch, J.A., 2007. Comparing the effects of salts and frother (MIBC) on gas dispersion and froth properties. *Minerals Engineering* 20, 1296-1302.

Sam, A., Gomez, C.O., and Finch, J.A., 1996. Axial velocity profiles of single bubbles in water/frother solutions. *International Journal of Mineral Processing* 47, 177-196.

Savic, P., 1953. Circulation and distortion of liquid drops falling through viscous medium. *Natural Resources Council of Canada, Div. Mech. Eng., Rep. No. NRC-MT-22*, 36.

Smolianski, A., Haario, H., and Luukka, P., 2008. Numerical study of dynamics of single bubbles and bubble swarms. *Applied Mathematical Modelling* 32, 641-659.

Tomiya, A., Celata, G.P., Hosokawa, S., and Yoshida, S., 2002. Terminal velocity of single bubbles in surface tension force dominant regime. *International Journal of Multiphase Flow* 28, 1497-1519.

Wang, B., and Peng, Y., 2013. The behaviour of mineral matter in fine coal flotation using saline water. *Fuel* 109, 309-315.

van Wijngaarden, L., and Veldhuis, C., 2008. On hydrodynamical properties of ellipsoidal bubbles. *Acta Mechanica* 201, 37-46.

Wu, M., and Gharib, M., 2002. Experimental studies on the shape and path of small air bubbles rising in clean water. *Physics of Fluids* 14, 7, L49-L52.

Yoon, R.H., and Sabey, J.B. 1989. Coal flotation in inorganic salt solutions. *Surfactant Science Series: Interfacial Phenomena in Coal Technology* 32, 87-114.

Zahradnik, J., Fialová, M., and Linek, V., 1999. The effect of surface additives on bubble coalescence in aqueous media. *Chemical Engineering Science* 54, 4757-4766.

Zieminski, S.A., and Whittemore, R.C., 1971. Behavior of gas bubbles in aqueous electrolyte solutions. *Chemical Engineering Science* 26, 509-520.

## Chapter 7 – Unifying discussion

The effect of frother in the pulp phase of a flotation cell is to inhibit bubble coalescence and reduce bubble rise velocity (Klimpel and Isherwood, 1991). Inorganic salts have been shown to have a similar capability (Detsch, 1991; Craig et al., 1993; Quinn et al., 2007). Much of the literature focuses on the role of bubble coalescence on the production of fine bubbles (Keitel and Onken, 1982; Cho and Laskowski, 2002a,b). Researchers have hinted that the presence of frother may also affect bubble break-up (Otake et al., 1977; Finch et al., 2008; Chu and Finch, 2013).

The topics covered in the thesis include: a review of bubble break-up mechanisms at a capillary, the effect of frother and inorganic salt on bubble coalescence and break-up, the use of acoustics to detect bubble coalescence in the presence of solid particles, and the relationship between ellipsoidal bubble shape and rise velocity.

As a unifying discussion we offer some speculation on the role solute plays in determining bubble coalescence and break-up, and link to the effect on bubble shape and rise velocity. It would seem that a common mechanism(s) is determining the behaviour.

Bubble coalescence inhibition in the presence of frother has been explained by the presence of surface tension gradients at the bubble surface. As bubbles approach one another an intervening liquid film is formed. We can expect that the air-water interfaces in this region become deficient in frother being swept away by the liquid being expelled from the film by the forces bringing the bubbles together. As frother molecules diffuse to the interface region of low concentration liquid is transported back into the film and counteracts the liquid drainage. Although inorganic salts typically increase surface tension (unlike frothers) a similar surface tension gradient-driven mechanism can be argued.

Similarly in the case of an ellipsoidal rising bubble, the commonly considered mechanism for reduction in rise velocity results from the flow of liquid over the bubble surface that sweeps adsorbed surfactant from the upstream side to the rear of the bubble. The re-distribution of surfactant results in a concentration gradient with concentration increasing towards the bubble rear which is associated with a surface tension gradient in the opposite direction, (i.e., surface tension increases towards the bubble front). The surface tension gradient induces a force that increases drag (Duhkin et al., 1998).

Single rising bubbles tend to become more spherical upon the addition of surfactant. The change in bubble shape can also be related to the surface tension gradient, the associated force opposing deformation due to the dynamic pressure across the rising bubble (Hinze, 1955; Dukhin et al., 1998; Finch et al., 2008). The combination of opposition to deformation and increased drag results in the observation that as bubbles become spherical they slow down.

Bubble shape can also be invoked in discussing bubble coalescence and break-up. Leighton et al. (1991) noted that shape oscillations upon bubble release from an orifice could result in bubble coalescence. Ohnishi et al. (1999) and Tse et al. (2003) observed a coalescence-induced bubble break-up mechanism. Coalescence was shown to impart shape oscillations which could lead to break-up. Solutes have been shown to damp shape oscillations (Tomiyama et al., 2002; Smolianski et al. 2008). Hinze (1955) noted the possibility of determining a critical bubble size with associated surface instabilities (shape deformation) which allowed for break-up. Similar explanations include a critical convective wake force above which bubbles are prone to break-up (Marrucci and Nicodemo, 1967). Tse et al. (2003) noted that increased flexibility of the interface and significant shape distortion, especially in the water only, promoted bubble break-up. The tendency of solutes to make a bubble spherical and reduce shape distortions reflects the action of solute at the interface which appears to inhibit bubble break-up.

An alternate explanation for the phenomena (coalescence and break-up inhibition, reduced rise velocity and shape change in surfactant systems) may lie in the hydrogen bonds (H-bonds) that form between the hydrophilic group(s) of the surfactant ( $\text{OH}^-$  in the case of frothers) and water molecules. We can envisage that the H-bonding creates a network of water molecules around the bubble that resists bubble deformation and induces a surface viscosity higher than the bulk value that slows bubble rise (Nguyen and Schulze, 2002) or inhibits coalescence (by slowing film drainage).

In the case of inorganic salts the surface tension gradient argument could apply but since salts tend to increase surface tension rather than decrease it as do surfactants the solute concentration would have to be in the opposite sense to that for surfactant. For example, for a bubble rising in a solution of inorganic salt to generate a surface tension gradient towards the front of the bubble requires that the surface salt concentration increase towards the bubble front. Perhaps the action of the liquid passing over the bubble is to transport the free water molecules to the rear rather

than the large hydrated ions which remain in the bulk solution. The H-bonding argument may also be tenable in the case of salts as the hydration sheaths which would impose a certain order (network) on the water molecules around the bubbles.

The role of solids in the thesis was only examined with respect to coalescence and their impact related to bubble formation appears limited. There may be a situation where hydrophobic particles of sufficient small size (nano-particles) may start to act as surfactants and retard coalescence (Ng et al., 2013). Certainly hydrophobic particles can be expected to slow bubble rise upon attachment. The presence of hydrophilic particles may also slow bubble rise due to the potential impact on slurry viscosity. Given the demonstrated connection between velocity and shape, would a bubble slowed by a particle load adjust its shape to conform with the relationship observed in the absence of particles?

## References

Cho, Y.S., and Laskowski, J.S., 2002a. Effect of flotation frothers on bubble size and foam stability. *International Journal of Mineral Processing*, 64, 2, 69-80.

Cho, Y.S., and Laskowski, J.S., 2002b. Bubble coalescence and its effect on dynamic foam stability. *The Canadian Journal of Chemical Engineering* 80, 2, 299-305.

Chu, P., and Finch, J.A., 2013. Frother and breakup in small bubble formation. In: *Proceedings of the 52<sup>nd</sup> Conference of Metallurgists (hosted by Materials Science & Technology (MS&T) 2013): Water and Energy in Mineral Processing, The 9<sup>th</sup> UBC-McGill-U of A International Symposium on the Fundamentals of Mineral Processing, The Metallurgical Society of CIM*, 2034-2043.

Craig, V.S., Ninham, B.W., and Pashley, R.M., 1993. The effect of electrolytes on bubble coalescence in water. *The Journal of Physical Chemistry* 97, 39, 10192-10197.

Detsch, R.M., 1991. Small air bubbles in reagent grade water and seawater: Rise velocities of 20 to 1000- $\mu\text{m}$  diameter bubbles. *Journal of Geophysical Research* 96, C5, 8901-8906.

- Dukhin, S.S., Miller, R., Loglio, G., 1998. Physico-chemical hydrodynamics of rising bubbles. In: Möbius, D., Miller, R. (Eds.), *Studies in Interfacial Science, Drops and Bubbles in Interfacial Research*, Elsevier Science, 6, 367-432.
- Finch, J.A., Nasset, J.E., and Acuña, C., 2008. Role of frother on bubble production and behaviour in flotation. *Minerals Engineering* 21, 12, 949-957.
- Keitel, G., and Onken, U., 1982. Inhibition of bubble coalescence by solutes in air/water dispersions. *Chemical Engineering Science*, 37, 11, 1635-1638.
- Ng, K.Y., Law, E., Lim, M., and Ata, S., 2013. Influence of particle on the formation of bubbles from a submerged capillary. In: *Proceedings Flotation'13*, Cape Town.
- Nguyen, A.V., and Schulze, H.J. (Eds.), 2004. *Colloidal Science of Flotation*. Surfactant science series, vol. 118. Marcel Dekker. New York.
- Otake, T., Tone, S., Nakao, K., and Mitsuhashi, Y., 1977. Coalescence and breakup of bubbles in liquids. *Chemical Engineering Science* 32, 4, 377-383.
- Quinn, J.J., Kracht, W., Gomez, C.O., Gagnon, C., and Finch, J.A., 2007. Comparing the effect of salts and frother (MIBC) on gas dispersion and froth properties. *Minerals Engineering* 20, 14, 1296-1302.
- Smolianski, A., Haario, H., and Luukka, P., 2008. Numerical study of dynamics of single bubbles and bubble swarms. *Applied Mathematical Modelling* 32, 641-659.

# Chapter 8 – Conclusions, contributions, and future work

## 8.1 Conclusions

The thesis addressed bubble coalescence and break-up in water and frother or inorganic salt solutions at a capillary, the use of acoustics to detect bubble coalescence in the presence of hydrophobic and hydrophilic solid particles, and the relationship between ellipsoidal bubble shape and rise velocity. The following conclusions can be drawn from the individual studies:

- Conditions at a capillary could be adjusted to observe coalescence-related and wake-related mechanisms giving fine bubbles and bi-modal distributions.
- Bi-modal bubble size distributions observed in the absence of coalescence inhibiting agents may result from bubble-bubble interactions.
- Three coalescence-related mechanisms are argued to be at play in flotation systems where bi-modal bubble size distributions are reported.
- The addition of surfactant or inorganic salts inhibited bubble coalescence and delayed the onset of fine bubble production (break-up) at a capillary.
- Three bubble regimes were identified: non-coalescence (single bubble production), bubble coalescence, and coalescence with fine bubble production with defined transition air rates as a function of solute concentration.
- In certain instances, a region of partial coalescence was observed in frother and inorganic salt solutions.
- Frother and inorganic salt strength was characterized in terms of bubble coalescence inhibiting and bubble break-up inhibiting strength. Commercial frothers ranked: MIBC < DF250 < F150. Inorganic salts containing multi-valent ions were stronger than mono-valent salts.
- Passive acoustic emission monitoring was used to detect air bubble coalescence at a capillary in an opaque slurry system containing talc or silica particles.

- The effect of frother (MIBC) or inorganic salt (NaCl) in the slurry was to inhibit bubble coalescence.
- The presence of silica particles with MIBC created a wider range of partial coalescence when compared to talc.
- The effect of both solids (talc and silica) was to slightly inhibit bubble coalescence except for the case of 10% w/w silica which appeared to promote coalescence at high frother concentration.
- Neither solid (talc or silica) had a large effect on coalescence supporting that particles do not have much impact on bubble formation in flotation systems.
- For ellipsoidal bubbles of ca. 2.3 mm equivalent diameter in inorganic salt solutions, bubble shape and velocity were seen to oscillate.
- Bubble shape and velocity oscillated in a linked fashion with increasing concentration creating more spherical bubbles with reduced rise velocity.
- There appears to be a unique bubble shape - rise velocity relationship independent of solute type.

## **8.2 Contributions to original knowledge**

- Mechanisms resulting in bubble break-up at a capillary in water were determined.
- Experiments quantified the effect of frothers and inorganic salts on bubble coalescence and break-up at a capillary
- Frothers and inorganic salts delayed the onset of bubble coalescence and break-up.
- The results appear to indicate that the action of solute in delaying coalescence also results in delayed coalescence-induced break-up.
- Acoustics were used to detect bubble coalescence in a three-phase (opaque) system where visual techniques cannot be used.

- The role of hydrophobic talc and hydrophilic silica on coalescence was investigated. The presence of talc created a fairly narrow range of incomplete coalescence. The presence of silica created a wider range of incomplete coalescence. Silica appeared to have a slight ability to promote bubble coalescence at 10% w/w.
- The shape and rise velocity of single bubbles was measured in various inorganic salt solutions.
- For a single rising bubble, the presence of inorganic salt and frother resulted in more spherical bubbles that rose at lower velocities.
- There appears to be a unique relationship between ellipsoidal bubble shape and velocity (for a given bubble volume) independent for solute type or concentration.

### **8.3 Suggestions for future work**

- Explore the effect of solute on coalescence and break-up in a swarm (produced in a flotation column or a mechanical cell)
- Explore the use of passive acoustic emission monitoring in a flotation cell to infer information regarding the bubble size distribution
- The use of two high-speed cameras at right angles to further understand the link between bubble shape, rise velocity and motion (spiral vs. zig-zag). A setup that enables accurate reconstruction of the bubble shape, volume, motion and velocity as a function of bubble size, height of rise, solution chemistry and the method of formation could prove useful in fully understanding the behaviour of a single rising bubble.
- The shape-velocity data should be tested against theoretical and empirical models that link ellipsoidal bubble shape and rise velocity.
- Linking the behaviour of a single rising bubble to the behaviour of a swarm could improve modeling gas dispersion properties in flotation systems.

## References

- Acuña Perez, C.A., 2007. Measurement techniques to characterize bubble motion in swarms. Ph.D. Thesis, McGill University, Department of Mining and Materials Engineering.
- Acuña, C.A., and Finch, J.A., 2010. Tracking velocity of multiple bubbles in a swarm. *International Journal of Mineral Processing* 94, 147-158.
- Agrawal, S.K., and Wasan, D.T., 1979. The effect of interfacial viscosities on the motion of drops and bubbles. *The Chemical Engineering Journal* 18, 215-223.
- Alexander, S., Quinn, J., van der Spuy, J.E., and Finch, J.A., 2012. Correlation of graphite flotation and gas holdup in saline solutions. In: Drelich, J. (Ed.), *Water in Mineral Processing: Proceedings of the First International Symposium*, SME, Englewood, 41-50.
- Ata, S., Ahmed, N., and Jameson, G.J., 2004. The effect of hydrophobicity on the drainage of gangue minerals in flotation froths. *Minerals Engineering* 17, 7, 897-901.
- Ata, S., 2008. Coalescence of bubbles covered by particles. *Langmuir* 24, 12, 6085-6091.
- Ata, S., 2012. Phenomena in the froth phase of flotation - A review. *International Journal of Mineral Processing* 102, 1-12.
- Aybers N.M., and Tapucu, A., 1969a. The motion of gas bubbles rising through stagnant liquid. *Wärme- und Stoffübertragung Bd. 2*, S. 118-128.
- Aybers N.M., and Tapucu, A., 1969b. Studies on the drag and shape of gas bubbles rising through a stagnant liquid. *Wärme- und Stoffübertragung Bd. 2*, S. 171-177.
- Azgomi, F., Gomez, C.O., and Finch, J.A., 2007. Characterizing frothers using gas hold-up. *Canadian Metallurgical Quarterly* 46, 3, 237-242.
- Bachhuber, C., and Sanford, C., 1974. The rise of small bubbles in water. *Journal of Applied Physics* 45, 2567-2569.
- Bean, J.J., May 1971. Tale of tails. *Mining World*, 59.
- Bergman, T., and Mesler, R., 1981. Bubble nucleation studies. Part I: Formation of bubble nuclei in superheated water by bursting bubbles. *AIChE Journal* 27, 851-853.

Betteridge, D., Joshlin, M.T., and Lilley, T. 1981. Acoustic emissions from chemical reactions. *Analytical Chemistry* 53, 1064-1073.

Bhaga, D., and Weber, M.E., 1981. Bubbles in viscous liquids: shapes, wakes and velocities. *Journal of Fluid Mechanics* 105, 61-85.

Bikerman, J. J., 1938. The unit of foaminess. *Transactions of the Faraday Society* 34, 634.

Blin, P., and Dion-Ortega, A., June/July 2013. High and dry: With water in short supply, some are looking to the ocean for answers. *CIM Magazine*, 46-51.

Bonner, O.D., and Jumper, C.F., 1973. Effect of ions on water structure. *Infrared Physics* 13, 233-242.

Boulton-Stone, J.M., and Blake, J.R., 1993. Gas bubble bursting at a free surface. *Journal of Fluid Mechanics* 254, 437-466.

Bournival, G., Pugh, R.J., and Ata, S., 2012. Examination of NaCl and MIBC as bubble coalescence inhibitor in relation to froth flotation. *Minerals Engineering* 25, 1, 47-53.

Boyd, J.W.R., and Varley, J., 2001. The use of passive measurement of acoustic emissions from chemical engineering processes. *Chemical Engineering Science* 56, 1749-1767.

Bozzano, G., and Dente, M., 2001. Shape and terminal velocity of single bubble motion: a novel approach. *Computers and Chemical Engineering* 25, 571-576.

Cain, F.W., and Lee, J.C., 1984. A technique for studying the drainage and rupture of unstable liquid films formed between two captive bubbles: Measurement on KCl Solutions. *Journal of Colloid and Interface Science* 106, 1, 70-85.

Cao, Z., Wang, B.-F., Wang, K.-M., Lin, H.-G., and Yu, R.-Q., 1998. Chemical acoustic emissions from gas evolution processes recorded by a piezoelectric transducer. *Sensors and Actuators B* 50, 27-37.

Cappuccitti, F., and Finch, J.A., 2007. Development of new frothers through hydrodynamic characterization. In: Folinsbee, J. (Ed.), *Proceedings 39th Annual Meeting of the Canadian Mineral Processors of CIM*, 399–412.

- Cappuccitti, F., and Nasset, J.E., 2009. Frother and collector effects on flotation cell hydrodynamics and their implication on circuit performance. In: *Advances in Mineral Processing Science and Technology – 48<sup>th</sup> Conference of Metallurgists*, Sudbury, 169-182.
- Castro, S., 2012. Challenges in flotation of Cu-Mo sulfide ores in sea water. In: Drelich, J. (Ed.), *Water in Mineral Processing: Proceedings of the First International Symposium*. SME, Englewood, 29-40.
- Chen, F., Gomez, C.O., and Finch, J.A., 2001. Bubble size measurement in flotation machines. *Minerals Engineering* 14, 427-432.
- Cho, Y.S., and Laskowski, J.S., 2002a. Effect of flotation frothers on bubble size and foam stability. *International Journal Minerals Processing* 64, 69-80.
- Cho, Y.S., and Laskowski, J.S., 2002b. Bubble coalescence and its effect on bubble size and foam stability. *Canadian Journal of Chemical Engineering* 80, 299-305.
- Christenson, H.K., Bowen, R.E., Carlton, J.A., Denne, J.R.M., and Lu, Y., 2008. Electrolytes that show transition to bubble coalescence inhibition at high concentrations. *Journal of Physical Chemistry C* 112, 794-796.
- Chu, P., and Finch, J.A., 2013. Frother and breakup in small bubble formation. In: *Proceedings of the 52<sup>nd</sup> Conference of Metallurgists (hosted by Materials Science & Technology (MS&T) 2013): Water and Energy in Mineral Processing, The 9<sup>th</sup> UBC-McGill-U of A International Symposium on the Fundamentals of Mineral Processing, The Metallurgical Society of CIM*, 2034-2043.
- Clift, R., Grace, J.R., and Weber, M., 2005. *Bubble, Drops, and Particles*. Dover Publications, Inc., Mineola, New York.
- Cole, R., 2009. *KCGM News and Views*, Issue 8, August 2009. 1-4.
- Comley, B.A., Harris, P.J., Bradshaw, D.J., and Harris, M.C., 2002. Frother characterization using dynamic surface tension measurements. *International Journal of Mineral Processing*, 64, 2, 81-100.
- Craig, V.S.J., Ninham, B.W., and Pashley, R.M., 1993. The effect of electrolytes on bubble coalescence in water. *Journal of Physical Chemistry* 97, 10192-10197.

Craig, V.S.J., 2004. Bubble coalescence and specific-ion effects. *Current Opinion in Colloid and Interface Science* 9, 178-184.

Craig, V.S.J., 2011. Do hydration forces play a role in thin film drainage and rupture observed in electrolyte solution? *Current Opinion in Colloid and Interface Science* 16, 597-600.

Crowther, T. G., Wade, A. P., Wentzell, P. D., and Gopal, R. 1991. Characterization of acoustic emission from an electrolysis cell. *Analytica Chimica Acta* 254, 223-234.

Crozier, R.D., and Klimpel, R.R., 1989. Frothers: plant practice. *Mineral Processing and Extractive Metallurgy Review*, 5, 1-4, 257-279.

Cytec Industries Inc., *Mining Chemicals Handbook*, Revised Edition, 2002.

Czarnecki, J., Malysa, K., and Pomianowski, A., 1982. Dynamic Frothability Index. *Journal of Colloid and Interface Science* 86, 570–572.

Czerski, H., 2011. A candidate mechanism for exciting sound during bubble coalescence. *The Journal of the Acoustical Society of America*, 129, 3, EL83-EL88.

Davies, J.T., 1957. A quantitative kinetic theory of emulsion type. In: *Physical Chemistry of the Emulsifying Agent, Gas/Liquid and Liquid/Liquid Interface*. Proceedings of the International Congress of Surface Activity, 426-438.

Davies, R.M., and Taylor, G., 1950. The mechanics of large bubbles rising through extended liquids and through liquids in tubes. *Proceedings of the Royal Society of London, Series A, Mathematical and Physical Sciences* 200, 1060, 375-390.

Deane, G.B., and Czerski, H., 2008. A mechanism stimulating sound production from air bubbles released from a nozzle. *Journal of the Acoustical Society of America* 123, 6, EL126-EL132.

Detsch, R.M., 1991. Small air bubbles in reagent grade water and seawater: Rise velocities of 20 to 1000- $\mu\text{m}$  diameter bubbles. *Journal of Geophysical Research* 96, C5, 8901-8906.

Detsch R., and Harris, I., 1989. Dissolution and rise velocity of small air bubbles in water and salt water. In: *Proceedings of OCEANS'89*, 1, 286–291.

Detwiler, A., and Blanchard, D.C., 1978. Aging and Bursting bubbles in trace-contaminated water. *Chemical Engineering Science* 33, 9-13.

Dippenaar, A., 1982. The destabilization of froth by solids. I. The mechanism of film rupture. *International Journal of Mineral Processing* 9, 1, 1-14.

Drogaris, G., and Weiland, P., 1983. Coalescence of gas bubbles in aqueous solutions of n-alcohols and fatty acids. *Chemical Engineering Science* 38, 9, 1501-1506.

Duchemin, L., Popinet, S., Josserand, C., and Zaleski, S., 2002. Jet formation in bubbles bursting at a free surface. *Physics of Fluids* 14, 9, 3000-3008.

Duineveld, P.C., 1995. The rise velocity and shape of bubbles in pure water at high Reynolds number. *Journal of Fluid Mechanics* 292, 325-332.

Dukhin, S.S., Miller, R., and Loglio, G., 1998. Physico-chemical hydrodynamics of rising bubbles. In: Möbius, D., Miller, R. (Eds.), *Studies in interfacial Science, Drops and Bubbles in Interfacial Research*, Elsevier Science 6, 367-432.

Dunne, R., 2012. Water water everywhere and not a drop to drink, nor do I know its whereabouts. In: Drelich, J., *Water in Mineral Processing: Proceedings of the First International Symposium*, Englewood, USA, 1-16.

Elmore, F.E., 1898. British Patent 21,948.

Fan, L.S., and Tsuchiya, K., 1990. Bubble wake dynamics in liquids and liquid-solid suspensions, Butterworth and Heinemann, 363.

Finch, J.A., and Dobby, G.S., 1990. *Column Flotation*, Permagnon Press, Toronto.

Finch, J.A., Gelinas, S., and Moyo, P., 2006. Frother-related research at McGill University. *Minerals Engineering* 19, 726-733.

Finch, J.A., Nasset, J.E., and Acuña, C., 2008. Role of frother in bubble production and behaviour in flotation. *Minerals Engineering* 21, 949–957.

Fouk, C.W., and Miller, J.N., 1931. Experimental evidence in support of the balanced-layer theory of liquid film formation. *Industrial and Engineering Chemistry* 23, 11, 1283-1288.

Frumkin, A., and Levich, V. G., 1947. On surfactants and interfacial motion. *Zh. Fiz. Khim.* 21, 1183.

Fuerstenau, D.W., 1999. The froth flotation century. In: Parekh, B. K., and Miller, J. D. (Eds.). *Advances in Flotation Technology*. SME, 3-21.

Fuerstenau, D.W., 2007. A century of developments in the chemistry of flotation processing. In: Fuerstenau, M.C., Jameson, G.J., and Yoon, R.H. (Eds.), *Froth flotation: A Century of Innovation*. SME, 3-64.

Fuerstenau, D.W., and Wayman, C.H., 1958. Effect of chemical reagents on the motion of single air bubbles in water. *Mining Engineering, Transactions of AIME*, 694-699.

Gallegos-Acevedo, P.M., Espinoza-Cuadra, J., Pérez-Garibay, R., and Pecina-Treviño, 2010. Bubble Coalescence: Hydrophobic particles effect. *Journal of Mining Science* 46, 3, 333-337.

Garrett, P.R., 1993. Defoaming. *Surfactant Science Series*, volume 45, Marcel Dekker, New York.

Gaudin, A.M., 1934. Flotation's future beset with difficult problems. *Engineering and Mining Journal* 135, 1, 29.

Gebrueder Bessel, 1877. Verfahren zur Reinigung von Graphit (process for the purification of graphite). German patent 42, Class 22.

Gelinas, S., and Finch, J.A., 2005. Colorimetric determination of common industrial frothers. *Minerals Engineering* 18, 2, 263-266.

Gélinas, S., and Finch, J.A., 2007. Frother analysis: Some plant experience. *Minerals Engineering* 20, 14, 1303-1308.

George, C., 1996. Mt. Keith Operation. In: Grimsey, E.J., and Neuss, I. (Eds.), *Nickel '96, Conference Series - Australasian Institute of Mining and Metallurgy*, 6, 19-23.

Gomez, C.O., and Finch, J.A., 2002. Gas dispersion measurements in flotation machines. *CIM Bulletin* 95, 1066, 73-78.

Gomez, C.O., and Finch, J.A., 2007. Gas dispersion measurements in flotation cells. *International Journal of Mineral Processing* 84, 1-4, 51-58.

Gomez, C.O., Maldonado, M., Araya, R., and Finch, J.A., 2010. Frother and viscosity effects on bubble shape and velocity. In: Pawlik, M. (Ed.), *Proceedings of the 49<sup>th</sup> Conference of*

Metallurgists (COM): Rheology in Mineral Processing, The 8<sup>th</sup> UBC - McGill - U of A International Symposium on the Fundamentals of Mineral Processing, 57-74.

Gorain, B.K., Franzidis, J.P., and Manlapig, E.V., 1997. Studies on impeller type, impeller speed and air flow rate in an industrial flotation cell. Part 4: Effect of bubble surface area flux on flotation performance. *Minerals Engineering* 10, 4, 367-379.

Grace, J.R., 1973. Shapes and velocities of bubbles rising in infinite liquids. *Transactions of the Institute of Chemical Engineers* 51, 116-120.

Grace, J.R., Wairegi, T., and Nguyen, T.H., 1976. Shapes and velocities of single drops and bubbles moving freely through immiscible liquids. *Transactions of the Institute of Chemical Engineers* 54, 167-173.

Grau, R.A., Laskowski, J.S., and Heiskanen, K., 2005. Effect of frothers on bubble size. *International Journal of Mineral Processing* 76, 225-233.

Griffin, W.C., 1949. Classification of surface-active agents by HLB. *Journal of the Society of Cosmetic Chemists* 1, 311, 1949.

Griffin, W.C., 1954. Calculation of HLB values of non-ionic surfactants. *Journal of the Society of Cosmetic Chemists* 5, 259.

Haig-Smillie, L. D., 1974. Sea water flotation. In: *Proceedings of the Canadian Mineral Processors Conference*, 263-281.

Haynes, W., 1860. British Patent 488.

Harper, J.F., 1972. The motion of bubbles and drops through liquids. In: Yih, C.-S. (Ed.), *Advances in Applied Mechanics*. Vol. 12, Academic Press Inc., New York, 59-124.

Harris, P.J., 1982. Frothing phenomenon and frothers. In: King, R.P. (Ed.), *Principles of Flotation*. Monograph Series No. 3. South African Institute of Mining and Metallurgy, 237–250.

Heiskanen, K., Javor, Z., Wierink, G., Omelka, B., and Schreithofer, N., 2012. Effect of frother mobility on the bubble behaviour in bubble rise velocity measurements at the initial stages of bubble formation. In: Young, C.A., and Luttrell, G.H. (Eds.), *Separation Technologies: For Minerals, Coal, and Earth Resources*, SME, Englewood, USA, 1-5.

Helsby, F.W., and Tuson, K.R., 1955. Behaviour of air bubbles in aqueous solutions. *Research* 8, 270.

Henry, C.L., Parkinson, L., Ralston, J.R., and Craig, V.S.J., 2008. A mobile gas – water interface in electrolyte solutions. *The Journal of Physical Chemistry Letters* C 112, 15094-15097.

Herman, J., and Mesler, R. 1987. Bubble entrainment from bursting bubbles. *Journal of Colloid and Interface Science* 117, 565-569.

Hernandez-Aguilar, J.R., Gomez, C.O., and Finch, J.A., 2002. A technique for the direct measurement of bubble size distributions in industrial flotation cells. In: Nasset, J.E. (Ed.), *Proceedings of the 34<sup>th</sup> Annual Meeting of the Canadian Mineral Processors*, 389-402.

Hernandez-Aguilar, J.R., Cunningham, R., and Finch, J.A., 2006. A test of the Tate equation to predict bubble size at an orifice in the presence of frother. *International Journal of Mineral Processing* 79, 2, 89-97.

Hesketh, R. P., Etchells, A.W., and Russell, T.W.F. 1991. Bubble breakage in pipeline flow. *Chemical Engineering Science* 46, 1.

Hinze, J. O., 1955. Fundamentals of the hydrodynamic mechanism of splitting in dispersion processes. *AIChE Journal*, 1, 3, 289-295.

Hofmeier, U., Yaminsky, V.V., and Christensen, H.K., 1995. Observations of solute effects on bubble formation. *Journal of Colloid and Interface Science* 174, 199-210.

Hou, R., Hunt, A., and Williams, R.A., 1998, Acoustic monitoring of hydrocyclone performance. *Minerals Engineering* 11, 11, 1047-1059.

Hunter, T.N., Pugh, R.J., Franks, G.V., and Jameson, G.J., 2008. The role of particles in stabilizing foams and emulsions. *Advances in Colloid and Interface Science* 137, 57–81.

Ip, S.W., Wang, Y., and Toguri, J.M., 1999. Aluminum foam stabilization by solid particles. *Canadian Metallurgical Quarterly* 38, 1, 81-92.

Jameson, G.J., 1984. Physics and hydrodynamics of bubbles. In: Ives, K.J. (Ed.), *The Scientific Basis of Flotation. Series E: Applied Sciences – No. 75*. Martinus Nijhoff Publishers. Boston. 53-78.

Javor, Z., Scheithofer, N., and Heiskanen, K., 2012. The effect of bubble release techniques on their behaviour at the initial stages of rise. *Minerals Engineering* 36-38, 254-261.

Johnson, B.D., and Gershet, R.M., 1991. Bubble formation at a cylindrical frit surface in a shear field. *Chemical Engineering Science* 46, 2753-2756.

Karamanev, G.G., 1994. Rise of gas bubbles in quiescent liquids. *AIChE* 38, 1843-1846.

Khrstov, K., Malysa, K., and Exerowa, D., 1984. Steady-state foams: Influence of the type of liquid films. *Colloids and Surfaces* 11, 39-49.

Kim, J.W., and Lee, W.K., 1988. Coalescence behavior of two bubbles growing side-by-side. *Journal of Colloid and Interface Science* 123, 1, 303-305.

Klimpel, R.R., and Isherwood, S., 1991. Some industrial implications of changing frother chemical structure. *International Journal of Mineral Processing* 33, 369-381.

Kracht, W., and Finch, J.A., 2009. Bubble break-up and the role of frother and salt. *International Journal of Mineral Processing* 92, 153-161.

Kracht, W., and Finch, J.A., 2009. Using sound to study bubble coalescence. *Journal of Colloid and Interface Science* 332, 237-245.

Kracht, W., and Finch, J.A., 2010. Effect of frother on initial bubble shape and velocity. *International Journal of Mineral Processing* 94, 115-120.

Kracht, W., and Rebolledo, H., 2013. Study of the local critical coalescence concentration (*l*-CCC) of alcohols and salts at bubble formation in two-phase systems. *Minerals Engineering* 50-51, 77-82.

Krzan, M., and Malysa, K., 2002a. Profiles of local velocities of bubbles in n-butanol, n-hexanol and n-nonanol solutions. *Colloids and Surfaces A: Physicochemical and Engineering Aspects* 207, 279-291.

Krzan, M., and Malysa, K., 2002b. Influence of frother concentration on bubble dimensions and rising velocities. *Physicochemical Problems of Mineral Processing* 36, 65-76.

Krzan, M., Lunkenheimer, K., and Malysa, K., 2004. On the influence of the surfactant's polar group on the local and terminal velocities of bubbles. *Colloids and Surfaces A: Physicochemical Engineering Aspects* 250, 431-441.

Krzan, M., Zawala, J., and Malysa, K., 2007. Development of steady state adsorption distribution over interface of a bubble rising in solutions of *n*-alkanols (C<sub>5</sub>, C<sub>8</sub>) and *n*-alkyltrimethylammonium bromides (C<sub>8</sub>, C<sub>12</sub>, C<sub>16</sub>). *Colloids and Surfaces A: Physicochemical Engineering Aspects* 298, 42-51.

Kuan, S.H., and Finch, J.A., 2010. Impact of talc on pulp and froth properties in F150 and 1-pentanol frother systems. *Minerals Engineering* 23, 11, 1003-1009.

Kulkarni, R.D., Goddard, E.D., and Kanner, B., 1977. Mechanism of antifoaming: Role of filler particle. *Industrial & Engineering Chemistry Fundamentals* 16, 4, 472-474.

Kulkarni, A.A., and Joshi, J.B., 2005. Bubble formation and bubble rise velocity in gas-liquid systems: A review. *Industrial and Engineering Chemistry Research* 44, 5873-5931.

Kugou, N., Ishida, K., and Yoshida, A., 2003. Experimental study on motion of air bubbles in seawater (terminal velocity and drag coefficient of air bubble rising in seawater). *Transactions on the Built Environment* 68, 145-158.

Kupferberg, A. and G.J. Jameson, 1969. Bubble formation at a submerged orifice above a gas chamber of finite volume. *Transactions of the Institute of Chemical Engineers* 47, T241-T250.

Kyriakides, N.K., Kasrinakis, E.G., Nychas, S.G., and Goulas, A., 1997. Bubbling from nozzles submerged in water: Transitions between bubbling regimes. *The Canadian Journal of Chemical Engineering* 75, 684-691.

Laskowski, J.S., 2004. Testing flotation frothers. *Physicochemical Problems in Mineral Processing* 38, 13-34.

Laskowski, J.S., Cho, Y.S., and Ding, K., 2003a. Effect of frothers on bubble size and foam stability in potash ore flotation systems. *The Canadian Journal of Chemical Engineering* 81, 63-69.

Laskowski, J.S., Tlhone, T., Williams, P., and Ding, K., 2003b. Fundamental properties of the polyoxypropylene alkyl ether flotation frothers. *International Journal of Mineral Processing* 72, 289-299.

Lee, C.-H., Herickson, L. E., and Glasgow, L. A., 1987. Bubble break-up and coalescence in turbulent gas-liquid dispersion. *Chemical Engineering Communications* 59, 65-84.

- Lee, J.S., Weon, B.M., Park, S.J., Le, J.H., Fezaa, K., and Lee, W.-K., 2011. Size limits the formation of liquid jets during bubble bursting. *Nature Communications* 2, 367, 1-7.
- Leighton, T.G., 1994. *The Acoustic Bubble*, Academic Press Inc., London.
- Leighton, T.G., Fagan K.J., and Field, J.E., 1991. Acoustic and photographic studies of injected bubbles. *European Journal of Physics* 12, 77-85.
- Leighton, T.G., and Walton, A.J., 1987. An experimental study of the sound emitted from gas bubbles in a liquid. *European Journal of Physics* 8, 2, 98-104.
- Lekki, J., and Laskowski, J., 1975. A new concept of frothing in flotation systems and general classification of flotation frothers. In: *Proceedings of the 11<sup>th</sup> International Mineral Processing Congress*, Cagliari, 429-448.
- Lessard, R.D., and Zieminski, S.A., 1971. Bubble coalescence and gas transfer in aqueous electrolytic solutions. *Industrial and Engineering Chemistry Fundamentals* 10, 260-289.
- Levich, V.G., and Spalding, D.B., 1962. *Physicochemical Hydrodynamics*, Vol. 689, Englewood Cliffs, NJ, Prentice-Hall.
- Lewis, D., and Davidson, J.F., 1982. Bubble splitting in shear flow. *Transactions of the Institution of Chemical Engineers* 60, 5, 283-291.
- Lynch, A.J., Watt, J.S., Finch, J.A., and Harbort, G.E., 2007. History of flotation technology. In: Fuerstenau, M.C., Jameson, G.J., and Yoon, R.H. (Eds.), *Froth Flotation: A Century of Innovation*. SME, 65-92.
- Maldonado, M., Quinn, J.J., Gomez, C.O., and Finch, J.A., 2013. An experimental study examining the relationship between bubble shape and rise velocity. *Chemical Engineering Science* 98, 7-11.
- Malysa, K., 1992. Wet foams: Formation, properties and mechanism of stability. *Advances in Colloid and Interface Science* 40, 37-83.
- Malysa, K., and Pawlikowska-Czubak, J., 1975. Frothability and surface elasticity of aqueous solutions of some frothers. *Bulletin de l'Academie Polonaise des Sciences* 5, 423-427.
- Manasseh, R., Riboux, G., and Risso, F., 2008. Sound generation on bubble coalescence following detachment. *International Journal of Multiphase Flow* 34, 10, 938-949.

- Martinez-Bazan, C., Montanes, J.L., and Lasheras, J.C., 2000. Bubble size distribution resulting from the break-up of an air cavity injected into a turbulent water jet. *Physics of Fluids* 12, 145–148.
- Marrucci, G., and Nicodemo, L., 1967. Coalescence of gas bubbles in aqueous solutions of inorganic electrolytes. *Chemical Engineering Science* 22, 1257-1265.
- Melo, F., and Laskowski, J.S., 2006. Fundamental properties of flotation frothers and their effect on flotation. *Minerals Engineering* 19, 766-773.
- Mendelson, H.D., 1967. The prediction of bubble terminal velocities from wave theory. *A.I.Ch.E Journal* 13, 2, 250-253.
- Minnaert, M., 1933. On musical air-bubbles and the sounds of running water. *Philosophical Magazine* 16, 235–248.
- Mitrovic, J., 1997. Formation of a liquid jet after detachment of a vapour bubble. *International Journal of Heat and Mass Transfer* 40, 18, 4309-4317.
- Miyahara, T., Iwata, M., and Takahashi, T., 1984. Bubble formation pattern with weeping at a submerged orifice. *Journal of Chemical Engineering of Japan* 17, 592-597.
- Miyahara, T., Tanimoto, M., and Takahashi, T., 1982. Bubble formation from an orifice at high gas injection rates. *Kagaku Kogaku Ronbunshu* 8, 18-24.
- Miyahara, T., Tsuchiya, K., and Fan, L-S, 1991. Effect of turbulent wakes on bubble–bubble interaction in a gas–liquid–solids fluidized bed. *Chemical Engineering Science* 46, 9, 2368–2373.
- Moyo, P., Gomez, C.O., and Finch, J.A., 2006. Characterization of frothers by water carrying rate. In: Xu, Z., and Liu, Q. (Eds.), *Interfacial Phenomena in Fine Particle Technology*, 6th UBC-McGill UA International Symposium on Fundamentals of Mineral Processing, COM 2006, Montreal, 133-146.
- Moyo, P., Gomez, C.O., and Finch, J.A., 2007. Characterization frothers using water carrying rate. *Canadian Metallurgical Quarterly* 46, 3, 215-220.

- Nesset, J.E., 2008. 100 years of blowing bubbles for profit (with an emphasis on the bubbles). Canadian Institute of Mining, Metallurgy and Petroleum, Distinguished Lecturer Presentation 2008-2009.
- Nesset, J.E., 2011. Modeling the Sauter mean bubble diameter in mechanical, forced-air flotation machines. Ph.D. Thesis, McGill University, Department of Mining and Materials Engineering.
- Nesset, J.E., Finch, J.A., and Gomez, C.O., 2007. Operating variables affecting the bubble size in forced-air mechanical flotation machines. In: Proceedings of the 9<sup>th</sup> Mill Operators' Conference, Fremantle, WA, 55-66.
- Nesset, J.E., Hernandez-Aguilar, J.R., Acuna, C., Gomez, C.O., and Finch, J.A., 2006. Some gas dispersion characteristics of mechanical flotation machines. *Minerals Engineering* 19, 807-815.
- Ng, K.Y., Law, E., Lim, M., and Ata, S., 2013. Influence of particle on the formation of bubbles from a submerged capillary. In: Proceedings Flotation'13, Cape Town.
- Nguyen, P.T., Hampton, M.A., Nguyen, A.V., and Birkett, G.R., 2012. The influence of gas velocity, salt type and concentration on transition concentration for bubble coalescence inhibition and gas holdup. *Chemical Engineering Research and Design* 90, 1, 33-39.
- Nguyen, A.V., and Schulze, H.J. (eds.), 2004. *Colloidal Science of Flotation*, Surfactant science series, vol. 118. Marcel Dekker. New York.
- Ohnishi, M., Azuma, H., and Straub, J., 1999. Study on secondary bubble creation induced by bubble coalescence. *Advances in Space Research* 24, 10, 1331-1336.
- Okazaki, S., 1962. The velocity of air bubble ascending in aqueous solution of surface active substance and inorganic electrolyte. *Kolloid-Zeitschrift und Zeitschrift für Polymere*, Band 185·Heft 2, 154-157.
- Oosterwegel, G.G., and de Groot, H.J., 1980. On the possibility to measure volumes of small gas bubbles and the bubble producing gas flow rates acoustically. *Review of Scientific Instrumentation* 51, 2, 201-205.
- Otake, T., Tone, S., Nakao, K., and Mitsuhashi, Y., 1977. Coalescence and breakup of bubbles in liquids. *Chemical Engineering Science* 32, 4, 377-383.

Peng, Y., and Seaman, D., 2011. The flotation of slime-fine fractions of Mt. Keith pentlandite ore in de-ionised and saline water. *Minerals Engineering* 24, 5, 479-481.

Perkins, C.L., and Sayre, R.E., 1921. Flotation of Minerals, United States Patent Office, serial number 284,981. Publication number US1364308 A.

Peters, F., and Els, C., 2012. An experimental study on slow and fast bubbles in tap water. *Chemical Engineering Science* 82, 194-199.

Pomianowski, A., Malysa, K., and Para, G., 1973. Annual Report for the Institute of Nonferrous Metals, 6.

Prince, M.J., and Blanch, H.W., 1990. Bubble coalescence and break-up in air-sparged bubble columns. *AIChE Journal* 36, 1485-1499.

Pugh, R.J., 1996. Foaming, foam films, antifoaming and defoaming. *Advances in Colloid and Interface Science* 64, 67-142.

Pugh, R.J., 2007. The physics and chemistry of frothers. In: Fuerstenau, M.C., Jameson, G., and Yoon, R.-H. (Eds.), *Froth Flotation: A Century of Innovation*, SME, Littleton, USA, 259-281.

Pugh, R.J., Weissenborn, P., and Paulson, O., 1997. Flotation in inorganic electrolytes; the relationship between recovery of hydrophobic particles, surface tension, bubble coalescence and gas solubility. *International Journal of Mineral Processing* 51, 125-138.

Quinn, J.J., and Finch, J.A., 2012. On the origin of bi-modal bubble size distributions in the absence of frother. *Minerals Engineering* 36, 237-241.

Quinn, J.J., Kracht, W., Gomez, C.O., Gagnon, C., and Finch, J.A., 2007. Comparing the effects of salts and frother (MIBC) on gas dispersion and froth properties. *Minerals Engineering* 20, 1296-1302.

Quinn, J.J., Maldonado, M., Gomez, C.O., and Finch, J.A., 2013. An experimental study on bubble shape and rise velocity in frother, polymer and inorganic salt solutions, In: *Proceedings of the 52<sup>nd</sup> Conference of Metallurgists (hosted by Materials Science & Technology (MS&T) 2013): Water and Energy in Mineral Processing, The 9<sup>th</sup> UBC - McGill - U of A International Symposium on the Fundamentals of Mineral Processing, The Metallurgical Society of CIM, 1981-1992.*

Quinn, J.J., Sovechles, J.M., Finch, J.A., and Waters, K.E., 2014. Critical coalescence concentrations of inorganic salt solutions. *Minerals Engineering* 58, 1-6.

Raymond, F., and Rosant, J.-M., 2000. A numerical and experimental study of the terminal velocity and shape of bubbles in viscous liquids. *Chemical Engineering Science* 55, 943-955.

Remillard, M., Joseph, M., and Laroche, L., 2009. Municipal drinking water produced by Atwater and Charles-J Des Bailleurs drinking water treatment plant: Annual Summary. Montreal: Division de l'expertise technique.

Rickard, T.A. (Ed.), 1916. *The Flotation Process*, Mining and Scientific Press, Dewey Publishing Company, San Francisco.

Riggs, W.F., 1986. Frothers - An Operator's Guide. In: *Chemical Reagents in the Mineral Processing Industry*, SME, 110-116.

Roberts, J.D., and Caserio, M.C., 1977, *Basic Principles of Organic Chemistry*, Second Edition, W.A. Benjamin Inc.

Sam, A., Gomez, C.O., and Finch, J.A. 1996. Axial velocity profiles of single bubbles in water/frother solutions. *International Journal of Mineral Processing* 47, 177-196.

Sato, A., Aoki, M., and Watanabe, M., 2010. Single rising bubble motion in aqueous solution of electrolyte. *Journal of Fluid Science and Technology* 5, 1, 14-25.

Savic, P., 1953. Circulation and distortion of liquid drops falling through viscous medium. Natural Resource Council of Canada, Div. of Mech. Eng., Rep. No. NRC-MT-22, 36.

Sevik, M., and Park, S.H., 1973. The splitting of drops and bubbles by turbulent fluid flow. *Journal of Fluids Engineering* 95, 53-60.

Schäfer, R., Merten, C., and Eigenberger, G., 2002. Bubble size distributions in a column reactor under industrial conditions. *Experimental Thermal and Fluid Science* 26, 595-604.

Smolianski, A., Haario, H., and Luukka, P., 2008. Numerical study of dynamics of single bubbles and bubble swarms. *Applied Mathematical Modelling* 32, 641-659.

Spencer, S.J., Bruniges, R., Roberts, G., Sharp, V., Catanzano, A., Bruckard, W. J., Davey, K.J., and Zhang, W., 2012. An acoustic technique for measurement of bubble solids mass loading: (b)

Monitoring of Jameson cell flotation performance by passive acoustic emissions. *Minerals Engineering* 36, 21-30.

Spencer, S.J., Bruniges, R., Sharp, V., Catanzano, V., Roberts, G., Bruckard, W.J., and Davey, K., 2010. Acoustic emission monitoring of froth flotation. In: *Proceedings of the XXV International Mineral Processing Congress*. AUSIMM, Melbourne, 3489-3500.

Stewart, C.W., 1995. Bubble interaction in low-viscosity liquids. *International Journal of Multiphase Flow* 21, 1037-1046.

Stokes, G.G., 1851. On the effect of the internal friction of fluid on the motion of pendulums. *Transactions of the Cambridge Philosophical Society* 9, 8.

Sweet, C., van Hoogstraten, J., Harris, M., and Laskowski, J.S., 1997. The effect of frothers on bubble size and frothability of aqueous solutions. In: Finch, J.A., Rao, S.R., Holubec, I. (Eds.), *Processing of Complex Ores, 2nd UBC-McGill Symposium on Fundamentals in Mineral Processing*, The Metallurgical Society of CIM, 235–246.

Talaia, M.A.R., 2007. Terminal velocity of a bubble rise in a liquid column. *World Academy of Science, Engineering and Technology* 28, 264-268.

Tan, S.N., Pugh, R.J., Fornasiero, D., Sedev, R., and Ralston, J., 2005. Foaming of polypropylene glycols and glycol/MIBC mixtures. *Minerals Engineering* 18, 179-188.

Tan, S.N., Pugh, R.J., Fornasiero, D., Sedev, R., and Ralston, J., 2006. The interfacial conformation of polypropylene glycols and their foam properties. *Minerals Engineering* 19, 703-712.

Tan, Y.H., Rafiei, A.A, Elmahdy, A., and Finch, J.A., 2013. Bubble size, gas holdup and bubble velocity profile of some alcohols and commercial frothers. *International Journal of Mineral Processing* 119, 1-5.

Tate, T., 1864. On the magnitude of a drop of liquid formed under different circumstances. *The London, Edinburgh, and Dublin Philosophical Magazine and Journal of Science*, 27, 181, 176-180.

- Tomiyama, A., 2002. Single bubbles in stagnant liquids and in linear shear flows (Keynote Lecture). In: Prasser, H.-M. (Ed.), Proceedings of Measurement Techniques for Steady and Transient Multiphase Flows, Rossendorf, September 18 – 20.
- Tomiyama, A., Celata, G.P., Hosokawa, S., and Yoshida, S., 2002. Terminal velocity of single bubbles in surface tension force dominant regime. *International Journal of Multiphase Flow* 28, 1497-1519.
- Tomiyama, A., and Hayashi, K., 2011, Interface tracking and multi-fluid simulations of bubble flows in bubble columns. The 8th International Conference on Computational Fluid Dynamics in the Oil & Gas (Keynote Lecture), Metallurgical and Process Industries (CFD 2011), Trondheim, Norway.
- Tsang, Y.H., Koh, Y.-H., and Koch, D.L., 2004. Bubble-size dependence of the critical electrolyte concentration for inhibition of coalescence. *Journal of Colloid and Interface Science* 275, 290-297.
- Tse, K., Martin, T., McFarlane, C.M., and Nienow, A.W., 1998. Visualization of bubble coalescence in a coalescence cell, a stirred tank and a bubble column, *Chemical Engineering Science* 53, 23, 4031-4036.
- Tse, K.L., Martin, T., McFarlane, C.M., and Nienow, A.W., 2003. Small bubble formation via a coalescence dependent break-up mechanism. *Chemical Engineering Science* 58, 275-286.
- Tucker, J.P., Deglon, D.A., Franzidis, J.P., Harris, M.C., and O'Connor, C.T., 1994. An evaluation of direct method of bubble size distribution measurements in a laboratory batch flotation cell. *Minerals Engineering* 7, 667-680.
- Tuson, K.R., 1955. Single exposure photography of high speed event. *British Journal of Applied Physics* 6, 99-100.
- van Wijngaarden, L., and Veldhuis, C., 2008. On hydrodynamical properties of ellipsoidal bubbles. *Acta Mechanica* 201, 37-46.
- Vanegas, C., and Holtham, P., 2008. On-line froth acoustic emission measurements in industrial sites. *Minerals Engineering* 21, 883–888.

- Vanegas, C., and Holtham, P., 2010. Possibility for flotation acoustics monitoring - a review. In: Proceedings of the XXV International Mineral Processing Congress. AUSIMM, Melbourne, 2457-2470.
- Vera, M.A., Mathe, Z.T., Franzidis, J.-P., Harris, M.C., Manlapig, E.V., and O'Connor, C.T., 2002. The modelling of froth zone recovery in batch and continuously operated laboratory flotation cells. *International Journal of Mineral Processing* 64, 135-151.
- Wang, B., and Peng, Y., 2013. The behaviour of mineral matter in fine coal flotation using saline water. *Fuel* 109 309-315.
- Wang, L., and Qu, X., 2012. Impact of interface approach velocity on bubble coalescence, *Minerals Engineering* 26, 50-56.
- Wentzell, P.D., and Wade, A. P., 1989. Chemical acoustic emission analysis in the frequency domain. *Analytical Chemistry* 61, 2638-2642.
- Wichterle, K., Sutná, K., and Večeř, M., 2009. Shape and rising velocity of bubbles. In: Markoš, J. (Ed.), Proceedings: 36<sup>th</sup> International Conference of Slovak Society of Chemical Engineering, 090-1 - 090-12.
- Wilkinson, P.M., Van Schayk, A., and Spronken, J.P., 1993. The influence of gas density and liquid properties on bubble breakup. *Chemical Engineering Science*, 48, 7, 1213-1226.
- Wills, B.A., and Napier-Munn, T. (Eds.), 2006. *Wills' Mineral Processing Technology: An Introduction to the Practical Aspects of Ore Treatment and Mineral Recovery*. Butterworth-Heinemann, Burlington, USA.
- Wu, M., and Gharib, M., 2002. Experimental studies on the shape and path of small air bubbles rising in clean water. *Physics of Fluids* 14, 7, L49-L52.
- Yañez, A.B., Morales, P., Coddou, F., Elgueta, H., Ortiz, J.M., Perez, C., Cortes, G., Gomez, C.O., and Finch, J.A., 2009. Gas dispersion characterization of TANKCELL®-300 at Chuquicamata concentrator. *Conference of Metallurgists, Sudbury*, 313-324.
- Yoon, R.-H., and Sabey, J.B., 1989. Coal flotation in inorganic salt solutions. *Surfactant Science Series: Interfacial Phenomena in Coal Technology* 32, 87-114.

Zahradnik, J., Fialová, M., and Linek, V., 1999. The effect of surface additives on bubble coalescence in aqueous media. *Chemical Engineering Science* 54, 4757-4766.

Zeng, Y., and Forssberg, E., 1993. Monitoring Grinding parameters by signal measurements for an industrial ball mill. *International Journal of Mineral Processing* 40, 1-16.

Zhang, F.H., and Thoroddsen, S.T., 2008. Satellite generation during bubble coalescence. *Physics of Fluids* 20, 022104.

Zhang, L., and Shoji, M., 2001. Aperiodic bubble formation from a submerged orifice. *Chemical Engineering Science* 56, 5371-5381.

Zhang, W., Nasset, J.E., Rao, R., and Finch, J.A., 2012a. Concentration (CCC)95-hydrophile-lipophile balance (HLB) relationship. *Minerals* 2, 3, 208-227.

Zhang, W., Zhou, X., and Finch, J.A., 2012b. Determining independent control of dual-frother systems – gas holdup, bubble size and water overflow rate. *Minerals Engineering* 39, 106-116.

Zhang, W., Nasset, J. E., Rao, R., and Finch, J. A., 2012. Characterizing frothers through critical coalescence concentration (CCC) 95-hydrophile-lipophile balance (HLB) relationship. *Minerals* 2, 3, 208-227.

Zhang, Y., McLaughlin, J.B., and Finch, J.A., 2001. Bubble velocity profile and model of surfactant mass transfer to bubble surface. *Chemical Engineering Science* 56, 6605-6616.

Zhou, Z.A., Egiebor, N.O., and Plitt, L.R., 1993. Frother effects on bubble size estimation in a flotation column, *Minerals Engineering* 6, 1, 55-67.

Zieminski, S.A., Hume III, R.M., and Durham, R., 1976. Rates of oxygen transfer from air bubbles to aqueous NaCl solutions at various temperatures. *Marine Chemistry* 4, 333-346.

Zieminski, S.A., and Lessard, R.D., 1969. Effects of chemical additives on performance of an air-water contactor. *I & EC Process Design and Development* 8, 1, 69-75.

Zieminski, S.A., and Whittemore, R.C., 1971. Behavior of gas bubbles in aqueous electrolyte solutions. *Chemical Engineering Science* 26, 509-520.

# Appendices

## Appendix 1 – Bubble coalescence and break-up data

Table A1.1 – Bubble coalescence and break-up data for MIBC solutions

[MIBC]		Complete Coalescence Transition					Break-up Transition				
		1	2	3	Avg.	95% CI	1	2	3	Avg.	95% CI
mM	ppm	sccm									
0.000	0	9	9	9	9.0	0.0	19	21	21	20.3	0.0
0.010	1	10	10	10	10.0	0.0	19	21	21	20.3	0.0
0.020	2	10	10	10	10.0	0.0	20	21	21	20.7	0.0
0.029	3	11	11	10	10.7	1.4	21	21	22	21.3	1.4
0.039	4	11	11	11	11.0	0.0	21	22	22	21.7	0.0
0.049	5	11	11	11	11.0	0.0	21	22	22	21.7	0.0
0.073	7.5	12	12	12	12.0	0.0	21	22	22	21.7	0.0
0.098	10	13	13	13	13.0	0.0	22	22	23	22.3	0.0
0.147	15	13	13	13	13.0	0.0	23	22	23	22.7	0.0
0.196	20	14	14	13	13.7	1.4	23	22	23	22.7	1.4
0.294	30	16	15	15	15.3	1.4	27	25	27	26.3	1.4
0.391	40	18	17	15	16.7	3.8	27	26	29	27.3	3.8
0.489	50	18	17	16	17.0	2.5	28	26	29	27.7	2.5
0.734	75	21	21	19	20.3	2.9	28	27	29	28.0	2.9
0.978	100	22	21	20	21.0	2.5	29	28	30	29.0	2.5

Table A1.2 – Bubble coalescence and break-up data for DF250 solutions

[DF250]		Complete Coalescence Transition	Break-up Transition
mM	ppm	sccm	
0.000	0	9	21
0.038	10	12	21
0.076	20	13	22
0.114	30	15	22
0.152	40	17	22
0.189	50	17	23
0.283	75	18	29
0.378	100	19	31

**Table A1.3 – Bubble coalescence and break-up data for F150 solutions**

[F150]		Complete Coalescence Transition	Break-up Transition
mM	ppm	sccm	
0.000	0	9	21
0.012	5	10	22
0.024	10	10	22
0.048	20	12	23
0.118	50	17	24
0.177	75	19	35
0.236	100	19	36

**Table A1.4 – Bubble coalescence and break-up data for 1-Pentanol solutions**

[1-Pentanol]		Complete Coalescence Transition	Break-up Transition
mM	ppm	sccm	
0.000	0	9	20
0.115	10	11	20
0.229	20	13	21
0.568	50	17	22
0.851	75	18	22
1.134	100	18	22
2.269	200	22	29

**Table A1.5 – Bubble coalescence and break-up data for 1-Hexanol solutions**

[1-Hexanol]		Complete Coalescence Transition	Break-up Transition
mM	ppm	sccm	
0.000	0	10	21
0.049	5	13	21
0.098	10	14	22
0.196	20	15	23
0.294	30	16	23
0.391	40	18	24
0.489	50	20	24
0.734	75	22	27
0.978	100	24	31

**Table A1.6 – Bubble coalescence and break-up data for 1-Heptanol solutions**

[1-Heptanol]		Complete Coalescence Transition	Break-up Transition
mM	ppm	sccm	
0.000	0	9	21
0.086	10	12	22
0.172	20	14	23
0.259	30	17	25
0.345	40	18	25
0.430	50	18	25
0.646	75	21	28
0.861	100	23	37

**Table A1.7 – Bubble coalescence and break-up data for 1-Octanol solutions**

[1-Octanol]		Complete Coalescence Transition	Break-up Transition
mM	ppm	sccm	
0.000	0	9	21
0.038	5	11	21
0.076	10	12	21
0.154	20	17	23
0.385	50	18	26
0.578	75	20	35
0.770	100	21	45

**Table A1.8 – Bubble coalescence and break-up data for NaCl solutions**

Water [NaCl]	Complete Coalescence Transition					Break-up Transition				
	1	2	3	Avg.	±95%CI	1	2	3	Avg.	±95%CI
<b>M</b>	<b>sccm</b>									
0.00	9	9	9	9.0	0.0	21	21	22	21.3	1.4
0.01	10	10	10	10.0	0.0	22	22	22	22.0	0.0
0.05	10	10	10	10.0	0.0	22	22	22	22.0	0.0
0.10	11	12	12	11.7	1.4	22	22	22	22.0	0.0
0.20	13	13	13	13.0	0.0	22	22	22	22.0	0.0
0.30	13	13	13	13.0	0.0	23	23	23	23.0	0.0
0.40	13	13	13	13.0	0.0	23	23	23	23.0	0.0
0.50	14	14	14	14.0	0.0	23	23	23	23.0	0.0
0.75	14	14	14	14.0	0.0	23	23	23	23.0	0.0
1.00	15	16	16	15.7	1.4	24	23	23	23.3	1.4
1.50	16	16	17	16.3	1.4	24	24	24	24.0	0.0
2.00	17	17	17	17.0	0.0	25	24	24	24.3	1.4

**Table A1.9 – Bubble coalescence and break-up data for KCl solutions**

<b>[KCl]</b>	<b>Complete Coalescence Transition</b>	<b>Break-up Transition</b>
<b>M</b>	<b>sccm</b>	
0.00	9	21
0.01	10	22
0.02	10	22
0.05	12	23
0.10	14	23
0.20	14	23
0.38	14	23
0.50	14	23
0.75	14	23
1.00	15	25
1.50	15	25
2.00	16	25

**Table A1.10 – Bubble coalescence and break-up data for CaCl<sub>2</sub> solutions**

<b>[CaCl<sub>2</sub>]</b>	<b>Complete Coalescence Transition</b>	<b>Break-up Transition</b>
<b>M</b>	<b>sccm</b>	
0.00	9	22
0.01	11	22
0.02	12	23
0.05	13	23
0.10	14	23
0.15	16	23
0.20	16	24
0.30	19	25
0.40	20	25
0.50	21	26
0.75	21	27
1.00	22	27

**Table A1.11 – Bubble coalescence and break-up data – Na<sub>2</sub>SO<sub>4</sub>**

<b>[Na<sub>2</sub>SO<sub>4</sub>]</b>	<b>Complete Coalescence Transition</b>	<b>Break-up Transition</b>
<b>M</b>	<b>sccm</b>	
0.00	9	22
0.05	10	23
0.10	11	24
0.20	13	24
0.30	13	25
0.40	15	25
0.50	15	25
0.75	19	25
1.00	20	27

**Table A1.12 – Bubble coalescence and break-up data – MgSO<sub>4</sub>**

<b>[MgSO<sub>4</sub>]</b>	<b>Complete Coalescence Transition</b>	<b>Break-up Transition</b>
<b>M</b>	<b>sccm</b>	
0.00	9	22
0.01	10	22
0.02	10	23
0.05	11	23
0.10	13	23
0.15	14	23
0.20	15	23
0.30	16	24
0.40	17	24
0.50	19	25
0.75	21	26
1.00	21	28

## Appendix 2 – Acoustics coalescence data

Table A2.1 – Bubble coalescence data for MIBC solutions (no solids)

Water [MIBC]		Partial Coalescence Transition					Complete Coalescence Transition				
		1	2	3	Avg.	±95% CI	1	2	3	Avg.	±95% CI
mM	ppm	sccm									
0.000	0	9	9	9	9.0	0.0	9	9	9	9.0	0.0
0.010	1	10	10	10	10.0	0.0	10	10	10	10.0	0.0
0.020	2	10	10	10	10.0	0.0	10	10	10	10.0	0.0
0.029	3	10	10	10	10.0	0.0	11	11	10	10.0	0.0
0.039	4	10	10	10	10.0	0.0	11	11	11	10.0	0.0
0.049	5	10	10	10	10.0	0.0	11	11	11	10.0	0.0
0.073	7.5	10	10	10	10.0	0.0	12	12	12	10.0	0.0
0.098	10	10	11	11	10.7	1.4	13	13	13	10.7	1.4
0.147	15	11	11	11	11.0	0.0	13	13	13	11.0	0.0
0.196	20	12	11	11	11.3	1.4	14	14	13	11.3	1.4
0.294	30	14	14	14	14.0	0.0	16	15	15	14.0	0.0
0.391	40	14	15	15	14.7	1.4	18	17	15	14.7	1.4
0.489	50	15	16	16	15.7	1.4	18	17	16	15.7	1.4
0.734	75	19	19	18	18.7	1.4	21	21	19	18.7	1.4
0.978	100	19	19	19	19.0	0.0	22	21	20	19.0	0.0

Table A2.2 – Bubble coalescence data for NaCl solutions (no solids)

Water [NaCl]		Partial Coalescence Transition					Complete Coalescence Transition				
		1	2	3	Avg.	±95% CI	1	2	3	Avg.	±95% CI
M		sccm									
0.00		8	9	9	8.7	1.4	9	10	10	9.7	1.4
0.01		9	9	9	9.0	0.0	10	10	10	10.0	0.0
0.05		9	9	10	9.3	1.4	10	10	10	10.0	0.0
0.10		10	10	10	10.0	0.0	11	12	12	11.7	1.4
0.20		10	10	10	10.0	0.0	13	13	13	13.0	0.0
0.30		10	10	10	10.0	0.0	13	13	13	13.0	0.0
0.40		10	10	10	10.0	0.0	13	13	13	13.0	0.0
0.50		10	10	10	10.0	0.0	14	14	14	14.0	0.0
0.75		10	10	10	10.0	0.0	14	14	14	14.0	0.0
1.00		10	10	10	10.0	0.0	15	16	16	15.7	1.4
1.50		10	10	10	10.0	0.0	16	16	17	16.3	1.4
2.00		10	10	10	10.0	0.0	17	17	17	17.0	0.0

**Table A2.3 – Bubble coalescence data – 1% Silica + MIBC**

1% Silica [MIBC]		Partial Coalescence Transition					Complete Coalescence Transition				
		1	2	3	Avg.	±95% CI	1	2	3	Avg.	±95% CI
mM	ppm	sccm									
0.000	0	8	8	8	8.0	0.0	9	9	9	9.0	0.0
0.010	1	8	8	8	8.0	0.0	10	10	10	10.0	0.0
0.020	2	8	8	8	8.0	0.0	11	11	11	11.0	0.0
0.029	3	8	8	8	8.0	0.0	11	11	11	11.0	0.0
0.039	4	10	10	10	10.0	0.0	12	12	12	12.0	0.0
0.049	5	11	11	11	11.0	0.0	12	12	12	12.0	0.0
0.073	7.5	11	11	11	11.0	0.0	13	13	13	13.0	0.0
0.098	10	12	12	12	12.0	0.0	13	13	13	13.0	0.0
0.147	15	12	12	12	12.0	0.0	14	14	14	14.0	0.0
0.196	20	14	14	14	14.0	0.0	16	16	16	16.0	0.0
0.294	30	16	17	16	16.3	1.4	19	19	19	19.0	0.0
0.391	40	16	17	16	16.3	1.4	19	20	20	19.7	1.4
0.489	50	17	17	17	17.0	0.0	19	20	20	19.7	1.4
0.734	75	17	17	18	17.3	1.4	22	22	21	21.7	1.4
0.978	100	18	18	19	18.3	1.4	23	23	22	22.7	1.4

**Table A2.4 – Bubble coalescence data – 10% Silica + MIBC**

10% Silica [MIBC]		Partial Coalescence Transition					Complete Coalescence Transition				
		1	2	3	Avg.	±95% CI	1	2	3	Avg.	±95% CI
mM	ppm	sccm									
0.000	0	7	8	7	7.3	1.4	9	9	9	9.0	0.0
0.010	1	8	7	8	7.7	1.4	9	9	9	9.0	0.0
0.020	2	8	8	8	8.0	0.0	9	9	9	9.0	0.0
0.029	3	8	8	8	8.0	0.0	10	11	11	10.7	1.4
0.039	4	8	8	9	8.3	1.4	11	11	11	11.0	0.0
0.049	5	9	9	9	9.0	0.0	11	11	11	11.0	0.0
0.073	7.5	10	9	9	9.3	1.4	13	13	13	13.0	0.0
0.098	10	10	10	10	10.0	0.0	12	13	13	12.7	1.4
0.147	15	11	12	12	11.7	1.4	14	14	14	14.0	0.0
0.196	20	12	12	13	12.3	1.4	17	16	16	16.3	1.4
0.294	30	12	12	12	12.0	0.0	18	19	19	18.7	1.4
0.391	40	12	12	12	12.0	0.0	19	19	19	19.0	0.0
0.489	50	13	13	13	13.0	0.0	19	19	19	19.0	0.0
0.734	75	14	14	15	14.3	1.4	20	21	21	20.7	1.4
0.978	100	15	15	15	15.0	0.0	22	22	22	22.0	0.0

**Table A2.5 – Bubble coalescence data – 1% Talc + MIBC**

1% Talc [MIBC]		Partial Coalescence Transition					Complete Coalescence Transition				
		1	2	3	Avg.	±95% CI	1	2	3	Avg.	±95% CI
mM	ppm	sccm									
0.000	0	8	8	8	8.0	0.0	9	9	9	9.0	0.0
0.010	1	9	9	9	9.0	0.0	10	10	10	10.0	0.0
0.020	2	9	10	9	9.3	1.4	10	10	10	10.0	0.0
0.029	3	9	10	9	9.3	1.4	11	11	11	11.0	0.0
0.039	4	10	10	10	10.0	0.0	11	11	11	11.0	0.0
0.049	5	11	11	11	11.0	0.0	13	13	13	13.0	0.0
0.073	7.5	11	11	11	11.0	0.0	13	13	13	13.0	0.0
0.098	10	11	11	11	11.0	0.0	14	14	14	14.0	0.0
0.147	15	12	12	12	12.0	0.0	14	14	14	14.0	0.0
0.196	20	13	13	13	13.0	0.0	16	16	16	16.0	0.0
0.294	30	17	17	17	17.0	0.0	18	18	18	18.0	0.0
0.391	40	17	17	17	17.0	0.0	19	18	19	18.7	1.4
0.489	50	17	17	17	17.0	0.0	19	19	19	19.0	0.0
0.734	75	19	19	18	18.7	1.4	21	21	21	21.0	0.0
0.978	100	21	21	22	21.3	1.4	23	23	24	23.3	1.4

**Table A2.6 – Bubble coalescence data – 10% Talc + MIBC**

10% Talc [MIBC]		Partial Coalescence Transition					Complete Coalescence Transition				
		1	2	3	Avg.	±95% CI	1	2	3	Avg.	±95% CI
mM	ppm	sccm									
0.000	0	9	9	9	9.0	0.0	9	9	9	9.0	0.0
0.010	1	9	9	9	9.0	0.0	9	9	9	9.0	0.0
0.020	2	9	9	9	9.0	0.0	10	9	10	9.7	1.4
0.029	3	10	9	9	9.3	1.4	10	10	10	10.0	0.0
0.039	4	10	9	9	9.3	1.4	13	12	13	12.0	1.4
0.049	5	10	9	9	9.3	1.4	13	13	13	13.0	0.0
0.073	7.5	10	9	9	9.3	1.4	13	13	13	13.0	0.0
0.098	10	11	10	11	10.7	1.4	13	13	14	13.3	1.4
0.147	15	12	12	13	12.3	1.4	14	14	14	14.0	0.0
0.196	20	13	13	14	13.3	1.4	15	15	17	15.7	2.9
0.294	30	16	16	15	15.7	1.4	18	18	18	18.0	0.0
0.391	40	17	17	17	17.0	0.0	19	19	19	19.0	0.0
0.489	50	17	17	17	17.0	0.0	19	19	20	19.3	1.4
0.734	75	18	18	18	18.0	0.0	20	21	21	20.7	1.4
0.978	100	18	19	18	18.3	1.4	22	22	22	22.0	0.0

**Table A2.7 – Bubble coalescence data – 1% Silica + NaCl**

1% Silica [NaCl]	Partial Coalescence Transition					Complete Coalescence Transition				
	1	2	3	Avg.	±95%CI	1	2	3	Avg.	±95%CI
<b>M</b>	<b>sccm</b>									
0.00	8	9	9	8.7	1.4	10	10	10	10.0	0.0
0.01	8	8	9	8.3	1.4	10	10	10	10.0	0.0
0.05	9	9	9	9.0	0.0	11	11	11	11.0	0.0
0.10	9	9	9	9.0	0.0	11	11	11	11.0	0.0
0.20	9	10	10	9.7	1.4	13	13	12	12.7	1.4
0.30	11	11	11	11.0	0.0	13	13	13	13.0	0.0
0.40	11	11	11	11.0	0.0	13	13	13	13.0	0.0
0.50	11	12	12	11.7	1.4	13	13	14	13.3	1.4
0.75	11	12	12	11.7	1.4	14	14	15	14.3	1.4
1.00	12	12	12	12.0	0.0	16	17	18	17.0	2.5
1.50	12	13	12	12.3	1.4	17	18	19	18.0	2.5
2.00	12	13	12	12.3	1.4	18	18	19	18.3	1.4

**Table A2.8 – Bubble coalescence data – 10% Silica + NaCl**

10% Silica [NaCl]	Partial Coalescence Transition					Complete Coalescence Transition				
	1	2	3	Avg.	±95%CI	1	2	3	Avg.	±95%CI
<b>M</b>	<b>sccm</b>									
0.00	7	7	7	7.0	0.0	10	10	10	10.0	0.0
0.01	7	7	7	7.0	0.0	11	11	10	10.7	1.4
0.05	8	8	8	8.0	0.0	11	11	11	11.0	0.0
0.10	8	8	8	8.0	0.0	12	12	12	12.0	0.0
0.20	9	9	9	9.0	0.0	12	12	12	12.0	0.0
0.30	10	10	11	10.3	1.4	13	13	14	13.3	1.4
0.40	11	11	11	11.0	0.0	14	14	14	14.0	0.0
0.50	11	11	11	11.0	0.0	14	14	14	14.0	0.0
0.75	12	12	12	12.0	0.0	14	14	15	14.3	1.4
1.00	12	12	12	12.0	0.0	16	16	16	16.0	0.0
1.50	12	12	12	12.0	0.0	17	17	17	17.0	0.0
2.00	13	13	12	12.7	1.4	17	17	18	17.3	1.4

**Table A2.9 – Bubble coalescence data – 1% Talc + NaCl**

1% Talc [NaCl]	Partial Coalescence Transition					Complete Coalescence Transition				
	1	2	3	Avg.	±95%CI	1	2	3	Avg.	±95%CI
<b>M</b>	<b>sccm</b>									
0.00	9	9	9	9.0	0.0	10	9	9	9.3	1.4
0.01	9	9	9	9.0	0.0	10	10	10	10.0	0.0
0.05	9	9	10	9.3	1.4	10	10	10	10.0	0.0
0.10	10	10	10	10.0	0.0	12	11	12	11.7	1.4
0.20	10	10	11	10.3	1.4	12	12	12	12.0	0.0
0.30	11	11	12	11.3	1.4	13	12	13	12.7	1.4
0.40	12	12	12	12.0	0.0	13	13	13	13.0	0.0
0.50	12	12	12	12.0	0.0	13	13	13	13.0	0.0
0.75	12	12	13	12.3	1.4	13	13	14	13.3	1.4
1.00	12	12	13	12.3	1.4	16	15	16	15.7	1.4
1.50	13	13	13	13.0	0.0	17	17	17	17.0	0.0
2.00	13	13	13	13.0	0.0	17	17	17	17.0	0.0

**Table A2.10 – Bubble coalescence data – 10% Talc + NaCl**

10% Talc [NaCl]	Partial Coalescence Transition					Complete Coalescence Transition				
	1	2	3	Avg.	±95%CI	1	2	3	Avg.	±95%CI
<b>M</b>	<b>sccm</b>									
0.00	9	9	9	9.0	0.0	10	10	10	10.0	0.0
0.01	10	10	10	10.0	0.0	10	10	10	10.0	0.0
0.06	10	10	11	10.3	1.4	10	10	10	10.0	0.0
0.16	11	11	11	11.0	0.0	11	11	11	11.0	0.0
0.20	11	11	12	11.3	1.4	11	11	12	11.3	1.4
0.30	12	12	12	12.0	0.0	12	12	13	12.3	1.4
0.40	12	12	12	12.0	0.0	12	12	13	12.3	1.4
0.50	12	12	12	12.0	0.0	13	13	13	13.0	0.0
0.75	12	12	13	12.3	1.4	14	14	14	14.0	0.0
1.00	13	13	13	13.0	0.0	15	15	15	15.0	0.0
1.50	13	13	13	13.0	0.0	15	16	15	15.3	1.4
2.00	14	14	14	14.0	0.0	17	17	16	16.7	1.4

## Appendix 3 – Bubble shape and rise velocity data

Table A3.1 – Bubble shape and rise velocity tests tap water data

Tap Water	Test	Bubble Diameter	Average Aspect Ratio	Average Rise Velocity	Specific Bubble Surface Area
M	#	mm		cm/s	mm <sup>-1</sup>
0.00	1	2.25	0.530	27.2	4.40
0.00	2	2.22	0.524	27.2	4.49
0.00	3	2.26	0.541	27.3	4.30
0.00	4	2.27	0.553	26.8	4.18
0.00	5	2.28	0.550	26.9	4.21
0.00	6	2.23	0.539	26.9	4.36
0.00	7	2.25	0.536	27.1	4.34
0.00	8	2.26	0.540	27.4	4.31
0.00	9	2.28	0.550	27.1	4.20
0.00	10	2.28	0.555	27.7	4.16

Table A3.2 – Bubble shape and rise velocity data tests – NaClO<sub>4</sub> data

[NaClO <sub>4</sub> ]	Test	Bubble Diameter	Average Aspect Ratio	Average Rise Velocity	Specific Bubble Surface Area
M	#	mm		cm/s	mm <sup>-1</sup>
0.010	1	2.46	0.640	25.6	4.16
0.010	2	2.44	0.614	26.5	4.24
0.010	3	2.45	0.630	26.0	4.20
0.010	4	2.40	0.627	25.8	4.03
0.010	5	2.39	0.618	25.9	4.06
0.010	6	2.41	0.618	26.3	4.13
0.010	7	2.43	0.622	26.0	4.15
0.010	8	2.46	0.622	26.4	4.27
0.010	9	2.46	0.619	26.3	4.29
0.010	10	2.42	0.621	25.9	4.14
0.050	1	2.34	0.868	20.7	2.97
0.050	2	2.29	0.699	23.8	3.37
0.050	3	2.30	0.702	23.1	3.38
0.050	4	2.34	0.693	24.0	3.53
0.050	5	2.34	0.701	23.8	3.50
0.050	6	2.34	0.689	24.1	3.55
0.050	7	2.29	0.673	24.2	3.48
0.050	8	2.33	0.694	23.8	3.50
0.050	9	2.32	0.700	23.3	3.43
0.050	10	2.33	0.703	23.6	3.45
0.100	1	2.24	0.835	21.3	2.81
0.100	2	2.25	0.836	21.0	2.84
0.100	3	2.25	0.835	21.0	2.83
0.100	4	2.25	0.835	21.0	2.83
0.100	5	2.28	0.839	21.1	2.89
0.100	6	2.24	0.836	20.8	2.81
0.100	7	2.24	0.836	20.8	2.81

[NaClO <sub>4</sub> ]	Test	Bubble Diameter	Average Aspect Ratio	Average Rise Velocity	Specific Bubble Surface Area
M	#	mm		cm/s	mm <sup>-1</sup>
0.100	8	2.31	0.836	21.4	2.98
0.100	9	2.36	0.839	21.5	3.09
0.100	10	2.26	0.835	21.0	2.86
0.250	1	2.25	0.864	20.0	2.75
0.250	2	2.25	0.871	19.8	2.75
0.250	3	2.32	0.870	20.3	2.93
0.250	4	2.27	0.868	20.0	2.79
0.250	5	2.28	0.872	20.1	2.81
0.250	6	2.25	0.867	20.0	2.77
0.250	7	2.25	0.867	20.0	2.77
0.250	8	2.25	0.871	19.7	2.74
0.250	9	2.27	0.871	20.1	2.79
0.250	10	2.26	0.873	20.0	2.77
0.500	1	2.26	0.881	19.4	2.76
0.500	2	2.26	0.893	19.0	2.73
0.500	3	2.25	0.884	19.4	2.71
0.500	4	2.25	0.897	18.4	2.69
0.500	5	2.26	0.878	19.3	2.75
0.500	6	2.25	0.877	19.5	2.73
0.500	7	2.27	0.897	19.0	2.75
0.500	8	2.25	0.893	19.3	2.71
0.500	9	2.27	0.877	19.5	2.78
0.500	10	2.26	0.888	19.3	2.72
0.750	1	2.21	0.885	19.2	2.61
0.750	2	2.22	0.890	18.7	2.64
0.750	3	2.21	0.895	18.6	2.59
0.750	4	2.22	0.899	18.7	2.60
0.750	5	2.23	0.892	19.2	2.66
0.750	6	2.21	0.894	18.7	2.61
0.750	7	2.23	0.892	18.8	2.66
0.750	8	2.26	0.898	18.7	2.72
0.750	9	2.24	0.887	19.3	2.70
0.750	10	2.26	0.893	19.1	2.72
1.000	1	2.26	0.901	18.3	2.70
1.000	2	2.22	0.899	18.3	2.60
1.000	3	2.22	0.897	18.5	2.62
1.000	4	2.22	0.895	18.3	2.62
1.000	5	2.24	0.894	18.6	2.66
1.000	6	2.26	0.905	18.3	2.70
1.000	7	2.31	0.891	19.2	2.86
1.000	8	2.26	0.904	18.4	2.70
1.000	9	2.23	0.903	18.1	2.62
1.000	10	2.23	0.901	18.2	2.63
1.500	1	2.20	0.910	17.7	2.55
1.500	2	2.23	0.908	17.9	2.61
1.500	3	2.21	0.910	17.7	2.58
1.500	4	2.22	0.912	17.7	2.59
1.500	5	2.20	0.912	17.7	2.54
1.500	6	2.21	0.912	17.6	2.55
1.500	7	2.20	0.907	17.7	2.55
1.500	8	2.21	0.914	17.5	2.56

[NaClO <sub>4</sub> ]	Test	Bubble Diameter	Average Aspect Ratio	Average Rise Velocity	Specific Bubble Surface Area
M	#	mm		cm/s	mm <sup>-1</sup>
1.500	9	2.22	0.912	17.7	2.59
1.500	10	2.21	0.914	17.5	2.56
2.000	1	2.19	0.916	17.1	2.52
2.000	2	2.19	0.907	17.4	2.53
2.000	3	2.20	0.912	17.3	2.55
2.000	4	2.19	0.910	17.4	2.53
2.000	5	2.20	0.910	17.4	2.55
2.000	6	2.22	0.917	17.3	2.58
2.000	7	2.21	0.913	17.3	2.56
2.000	8	2.21	0.912	17.3	2.56
2.000	9	2.24	0.910	17.5	2.64
2.000	10	2.21	0.913	17.5	2.57

Table A3.3 – Bubble shape and rise velocity tests – KCl data

[KCl]	Test	Bubble Diameter	Average Aspect Ratio	Average Rise Velocity	Specific Bubble Surface Area
M	#	mm		cm/s	mm <sup>-1</sup>
0.0125	1	2.24	0.838	21.4	3.03
0.0125	2	2.25	0.705	23.4	3.45
0.0125	3	2.42	0.660	25.9	3.38
0.0125	4	2.28	0.717	22.7	3.35
0.0125	5	2.29	0.710	23.5	3.36
0.0125	6	2.27	0.653	24.7	3.63
0.0125	7	2.27	0.676	23.7	3.53
0.0125	8	2.31	0.659	25.0	3.54
0.0125	9	2.29	0.658	24.7	3.58
0.0125	10	2.41	0.659	25.9	3.40
0.025	1	2.25	0.751	22.5	3.28
0.025	2	2.28	0.761	22.6	3.20
0.025	3	2.29	0.756	22.8	3.20
0.025	4	2.26	0.763	22.2	3.23
0.025	5	2.26	0.753	22.8	3.26
0.025	6	2.28	0.766	22.4	3.18
0.025	7	2.28	0.767	22.2	3.19
0.025	8	2.25	0.756	22.1	3.25
0.025	9	2.27	0.762	22.1	3.22
0.025	10	2.26	0.757	22.2	3.24
0.050	1	2.25	0.896	19.7	2.88
0.050	2	2.25	0.895	19.5	2.88
0.050	3	2.25	0.892	19.6	2.88
0.050	4	2.27	0.913	19.6	2.81
0.050	5	2.27	0.915	19.3	2.80
0.050	6	2.26	0.905	19.5	2.84
0.050	7	2.26	0.892	19.5	2.88
0.050	8	2.29	0.902	19.6	2.82
0.050	9	2.25	0.891	19.4	2.88
0.050	10	2.25	0.899	19.5	2.86

[KCl]	Test	Bubble Diameter	Average Aspect Ratio	Average Rise Velocity	Specific Bubble Surface Area
M	#	mm		cm/s	mm <sup>-1</sup>
0.125	1	2.27	0.919	18.5	2.79
0.125	2	2.28	0.921	18.8	2.79
0.125	3	2.29	0.929	18.8	2.75
0.125	4	2.27	0.917	18.5	2.81
0.125	5	2.28	0.920	18.9	2.79
0.125	6	2.28	0.927	18.5	2.77
0.125	7	2.29	0.930	18.7	2.75
0.125	8	2.28	0.924	18.7	2.77
0.125	9	2.27	0.917	18.6	2.80
0.125	10	2.27	0.914	18.9	2.81
0.250	1	2.26	0.921	18.1	2.80
0.250	2	2.27	0.923	18.3	2.80
0.250	3	2.25	0.920	17.8	2.82
0.250	4	2.26	0.918	18.1	2.82
0.250	5	2.27	0.930	18.0	2.78
0.250	6	2.27	0.928	17.9	2.78
0.250	7	2.27	0.928	17.9	2.79
0.250	8	2.27	0.931	17.9	2.77
0.250	9	2.27	0.924	17.9	2.79
0.250	10	2.26	0.918	18.0	2.81
0.500	1	2.25	0.925	17.5	2.81
0.500	2	2.25	0.927	17.4	2.80
0.500	3	2.26	0.926	17.0	2.80
0.500	4	2.25	0.929	17.5	2.81
0.500	5	2.24	0.924	17.5	2.82
0.500	6	2.25	0.930	17.4	2.80
0.500	7	2.26	0.929	17.5	2.79
0.500	8	2.26	0.932	17.6	2.78
0.500	9	2.24	0.923	17.5	2.82
0.500	10	2.25	0.925	17.5	2.81
0.750	1	2.24	0.936	16.7	2.80
0.750	2	2.22	0.924	16.8	2.85
0.750	3	2.23	0.936	16.7	2.82
0.750	4	2.21	0.927	16.6	2.85
0.750	5	2.23	0.928	16.7	2.83
0.750	6	2.23	0.935	16.8	2.82
0.750	7	2.22	0.934	16.8	2.83
0.750	8	2.21	0.935	16.9	2.84
0.750	9	2.22	0.933	16.7	2.83
0.750	10	2.24	0.934	16.7	2.81
1.000	1	2.23	0.926	16.9	2.83
1.000	2	2.24	0.934	16.7	2.81
1.000	3	2.24	0.925	16.7	2.83
1.000	4	2.23	0.938	16.7	2.81
1.000	5	2.24	0.934	16.8	2.81
1.000	6	2.23	0.926	16.6	2.84
1.000	7	2.25	0.931	16.8	2.80
1.000	8	2.26	0.933	17.1	2.79
1.000	9	2.24	0.934	16.8	2.80
1.000	10	2.24	0.924	16.8	2.82
2.000	1	2.21	0.926	16.5	2.86

[KCl]	Test	Bubble Diameter	Average Aspect Ratio	Average Rise Velocity	Specific Bubble Surface Area
M	#	mm		cm/s	mm <sup>-1</sup>
2.000	2	2.21	0.924	16.6	2.87
2.000	3	2.22	0.935	16.5	2.83
2.000	4	2.21	0.924	16.6	2.87
2.000	5	2.22	0.934	16.7	2.83
2.000	6	2.21	0.929	16.6	2.85
2.000	7	2.22	0.937	16.4	2.83
2.000	8	2.21	0.927	16.5	2.85
2.000	9	2.21	0.927	16.5	2.86
2.000	10	2.21	0.932	16.6	2.84

Table A3.4 – Bubble shape and rise velocity tests - NaCl data

[NaCl]	Test #	Bubble Diameter	Average Aspect Ratio	Average Rise Velocity	Specific Bubble Surface Area
M		mm		cm/s	mm <sup>-1</sup>
0.010	1	2.35	0.733	24.3	3.20
0.010	2	2.32	0.912	18.9	2.76
0.010	3	2.33	0.926	19.1	2.71
0.010	4	2.37	0.900	20.9	2.73
0.010	5	2.34	0.920	19.5	2.71
0.010	6	2.28	0.846	22.3	2.96
0.010	7	2.37	0.712	24.1	3.25
0.010	8	2.40	0.691	24.7	3.28
0.010	9	2.38	0.808	23.1	2.93
0.010	10	2.38	0.747	23.4	3.11
0.020	1	2.34	0.945	17.2	2.67
0.020	2	2.40	0.801	23.7	2.92
0.020	3	2.41	0.790	23.7	2.94
0.020	4	2.36	0.785	23.1	3.02
0.020	5	2.36	0.795	23.1	2.99
0.020	6	2.37	0.792	23.0	2.98
0.020	7	2.40	0.798	23.2	2.94
0.020	8	2.38	0.799	23.2	2.95
0.020	9	2.40	0.797	23.4	2.94
0.020	10	2.35	0.797	22.5	3.00
0.050	1	2.34	0.807	23.2	2.99
0.050	2	2.38	0.886	20.4	2.75
0.050	3	2.39	0.824	23.3	2.88
0.050	4	2.39	0.802	23.4	2.93
0.050	5	2.39	0.796	23.3	2.95
0.050	6	2.38	0.793	22.9	2.98
0.050	7	2.28	0.810	22.8	3.05
0.050	8	2.39	0.792	23.0	2.97
0.050	9	2.39	0.786	23.1	2.98
0.050	10	2.38	0.780	23.5	3.01
0.100	1	2.35	0.876	21.4	2.80
0.100	2	2.35	0.862	21.8	2.83
0.100	3	2.36	0.864	21.6	2.82

[NaCl]	Test #	Bubble Diameter	Average Aspect Ratio	Average Rise Velocity	Specific Bubble Surface Area
M		mm		cm/s	mm <sup>-1</sup>
0.100	4	2.35	0.843	22.1	2.87
0.100	5	2.35	0.841	21.8	2.88
0.100	6	2.33	0.932	17.4	2.70
0.100	7	2.35	0.854	21.5	2.85
0.100	8	2.35	0.913	19.4	2.72
0.100	9	2.35	0.840	22.8	2.88
0.100	10	2.34	0.935	17.2	2.68
0.200	1	2.32	0.926	18.3	2.72
0.200	2	2.33	0.912	20.3	2.74
0.200	3	2.34	0.921	19.6	2.71
0.200	4	2.33	0.902	19.8	2.77
0.200	5	2.33	0.912	19.1	2.75
0.200	6	2.33	0.920	17.9	2.72
0.200	7	2.34	0.892	20.4	2.78
0.200	8	2.34	0.895	20.3	2.77
0.200	9	2.34	0.897	20.1	2.76
0.200	10	2.34	0.912	19.4	2.73
0.500	1	2.37	0.928	18.6	2.66
0.500	2	2.38	0.928	18.8	2.66
0.500	3	2.38	0.927	18.2	2.65
0.500	4	2.36	0.892	19.4	2.75
0.500	5	2.37	0.933	18.3	2.65
0.500	6	2.37	0.932	18.3	2.66
0.500	7	2.36	0.925	18.0	2.68
0.500	8	2.38	0.928	18.0	2.66
0.500	9	2.36	0.925	18.1	2.68
0.500	10	2.36	0.931	17.6	2.66
1.000	1	2.35	0.940	18.1	2.66
1.000	2	2.36	0.936	18.4	2.67
1.000	3	2.35	0.937	18.4	2.67
1.000	4	2.34	0.934	18.3	2.68
1.000	5	2.35	0.937	17.5	2.66
1.000	6	2.34	0.939	18.1	2.67
1.000	7	2.34	0.937	17.8	2.68
1.000	8	2.35	0.941	17.9	2.66
1.000	9	2.34	0.937	17.7	2.68
1.000	10	2.36	0.936	17.5	2.66

Table A3.5 – Bubble shape and rise velocity tests – Na<sub>2</sub>SO<sub>4</sub> data

[Na <sub>2</sub> SO <sub>4</sub> ]	Test	Bubble Diameter	Average Aspect Ratio	Average Rise Velocity	Specific Bubble Surface Area
M	#	mm		cm/s	mm <sup>-1</sup>
0.010	1	2.40	0.640	25.8	3.96
0.010	2	2.35	0.647	25.6	3.76
0.010	3	2.37	0.637	25.3	3.90
0.010	4	2.37	0.647	25.0	3.82
0.010	5	2.36	0.643	25.1	3.82

[Na <sub>2</sub> SO <sub>4</sub> ]	Test	Bubble Diameter	Average Aspect Ratio	Average Rise Velocity	Specific Bubble Surface Area
M	#	mm		cm/s	mm <sup>-1</sup>
0.010	6	2.44	0.653	25.4	4.02
0.010	7	2.47	0.649	26.4	4.16
0.010	8	2.45	0.650	26.2	4.09
0.010	9	2.39	0.644	25.7	3.93
0.010	10	2.38	0.645	25.3	3.89
0.050	1	2.37	0.954	17.6	2.86
0.050	2	2.40	0.910	21.4	3.04
0.050	3	2.35	0.911	20.9	2.91
0.050	4	2.36	0.928	19.6	2.89
0.050	5	2.35	0.902	20.7	2.91
0.050	6	2.36	0.916	20.9	2.92
0.050	7	2.36	0.926	20.4	2.90
0.050	8	2.33	0.904	19.6	2.87
0.050	9	2.43	0.897	21.1	3.15
0.050	10	2.36	0.919	19.6	2.90
0.100	1	2.45	0.916	19.8	3.13
0.100	2	2.37	0.939	17.9	2.88
0.100	3	2.34	0.933	18.3	2.83
0.100	4	2.40	0.951	17.9	2.95
0.100	5	2.31	0.940	18.4	2.75
0.100	6	2.40	0.923	19.8	3.00
0.100	7	2.23	0.936	18.8	2.56
0.100	8	2.35	0.929	19.8	2.87
0.100	9	2.33	0.929	19.4	2.82
0.100	10	2.18	0.963	17.0	2.40
0.200	1	2.32	0.932	18.8	2.79
0.200	2	2.33	0.923	19.5	2.82
0.200	3	2.32	0.934	18.8	2.78
0.200	4	2.33	0.927	19.7	2.81
0.200	5	2.30	0.917	19.0	2.77
0.200	6	2.29	0.920	19.7	2.75
0.200	7	2.30	0.917	19.1	2.77
0.200	8	2.31	0.919	19.3	2.79
0.200	9	2.32	0.926	18.6	2.79
0.200	10	2.31	0.914	19.2	2.80
0.500	1	2.30	0.940	18.4	2.71
0.500	2	2.31	0.951	18.4	2.72
0.500	3	2.36	0.940	18.7	2.85
0.500	4	2.29	0.950	18.3	2.68
0.500	5	2.29	0.954	18.6	2.66
0.500	6	2.29	0.947	17.9	2.69
0.500	7	2.29	0.946	18.1	2.68
0.500	8	2.29	0.951	17.9	2.68
0.500	9	2.35	0.934	18.4	2.86
0.500	10	2.32	0.938	18.2	2.77
0.750	1	2.16	0.954	17.4	2.37
0.750	2	2.33	0.937	17.9	2.81
0.750	3	2.31	0.952	17.5	2.71
0.750	4	2.32	0.954	17.6	2.75
0.750	5	2.30	0.989	15.5	2.63
0.750	6	2.29	0.977	15.6	2.63

[Na <sub>2</sub> SO <sub>4</sub> ]	Test	Bubble Diameter	Average Aspect Ratio	Average Rise Velocity	Specific Bubble Surface Area
M	#	mm		cm/s	mm <sup>-1</sup>
0.750	7	2.31	0.991	15.5	2.65
0.750	8	2.30	0.955	17.8	2.70
0.750	9	2.17	0.947	17.1	2.41
0.750	10	2.17	0.957	17.1	2.38
1.000	1	2.15	0.970	18.4	2.32
1.000	2	2.23	0.956	18.8	2.53
1.000	3	2.42	0.952	18.5	2.98
1.000	4	2.42	0.959	18.5	2.98
1.000	5	2.43	0.953	18.2	3.00
1.000	6	2.39	0.947	17.8	2.92
1.000	7	2.40	0.930	18.5	2.98
1.000	8	2.23	0.954	17.5	2.52
1.000	9	2.24	0.948	17.1	2.56
1.000	10	2.38	0.945	17.9	2.90

Table A3.6 – Bubble shape and rise velocity tests – CaCl<sub>2</sub> data

[CaCl <sub>2</sub> ]	Test #	Bubble Diameter	Average Aspect Ratio	Average Rise Velocity	Specific Bubble Surface Area
M		mm		cm/s	mm <sup>-1</sup>
0.005	1	2.34	0.631	25.4	3.83
0.005	2	2.38	0.652	25.2	3.86
0.005	3	2.40	0.654	25.3	3.91
0.005	4	2.36	0.642	25.4	3.82
0.005	5	2.27	0.642	24.3	3.55
0.005	6	2.40	0.641	25.7	3.96
0.005	7	2.39	0.650	25.3	3.89
0.005	8	2.38	0.654	25.0	3.84
0.005	9	2.40	0.643	25.6	3.94
0.005	10	2.33	0.651	24.5	3.70
0.010	1	2.40	0.714	24.3	3.63
0.010	2	2.43	0.722	24.4	3.69
0.010	3	2.31	0.725	23.0	3.33
0.010	4	2.34	0.715	24.1	3.43
0.010	5	2.49	0.723	24.5	3.86
0.010	6	2.32	0.716	23.6	3.38
0.010	7	2.44	0.713	24.8	3.77
0.010	8	2.33	0.723	23.0	3.39
0.010	9	2.38	0.654	25.0	3.84
0.010	10	2.33	0.726	23.2	3.37
0.020	1	2.30	0.749	22.9	3.22
0.020	2	2.38	0.758	24.0	3.42
0.020	3	2.45	0.769	23.9	3.58
0.020	4	2.28	0.763	22.4	3.11
0.020	5	2.45	0.751	24.4	3.64
0.020	6	2.31	0.765	22.8	3.19
0.020	7	2.32	0.754	23.2	3.26
0.020	8	2.36	0.767	23.2	3.31

[CaCl <sub>2</sub> ]	Test #	Bubble Diameter	Average Aspect Ratio	Average Rise Velocity	Specific Bubble Surface Area
M		mm		cm/s	mm <sup>-1</sup>
0.020	9	2.34	0.755	23.6	3.30
0.020	10	2.30	0.752	23.0	3.19
0.050	1	2.30	0.789	22.4	3.08
0.050	2	2.31	0.784	22.2	3.12
0.050	3	2.30	0.788	22.4	3.10
0.050	4	2.34	0.789	22.6	3.19
0.050	5	2.33	0.791	22.2	3.15
0.050	6	2.34	0.783	22.8	3.23
0.050	7	2.32	0.784	22.6	3.15
0.050	8	2.38	0.802	22.9	3.26
0.050	9	2.38	0.784	23.2	3.32
0.050	10	2.32	0.788	22.4	3.14
0.100	1	2.28	0.838	21.8	2.91
0.100	2	2.29	0.831	21.8	2.94
0.100	3	2.33	0.832	22.0	3.05
0.100	4	2.38	0.834	22.4	3.16
0.100	5	2.32	0.833	21.9	3.01
0.100	6	2.28	0.827	21.9	2.92
0.100	7	2.28	0.840	21.4	2.90
0.100	8	2.29	0.834	21.8	2.95
0.100	9	2.27	0.830	21.6	2.90
0.100	10	2.26	0.839	21.4	2.85
0.200	1	2.26	0.867	20.8	2.77
0.200	2	2.24	0.868	20.5	2.74
0.200	3	2.28	0.865	20.9	2.83
0.200	4	2.25	0.868	20.5	2.76
0.200	5	2.24	0.867	20.6	2.73
0.200	6	2.24	0.870	20.3	2.72
0.200	7	2.26	0.873	20.5	2.76
0.200	8	2.25	0.875	20.1	2.72
0.200	9	2.25	0.875	20.1	2.72
0.200	10	2.24	0.867	20.5	2.74
0.500	1	2.28	0.906	19.1	2.74
0.500	2	2.29	0.909	18.8	2.75
0.500	3	2.30	0.920	19.2	2.76
0.500	4	2.28	0.903	19.0	2.76
0.500	5	2.31	0.921	18.9	2.78
0.500	6	2.31	0.907	19.2	2.80
0.500	7	2.35	0.913	19.5	2.91
0.500	8	2.30	0.914	19.3	2.79
0.500	9	2.33	0.915	19.4	2.83
0.500	10	2.29	0.906	19.1	2.76
0.750	1	2.21	0.920	17.9	2.55
0.750	2	2.22	0.924	17.8	2.57
0.750	3	2.24	0.921	18.0	2.61
0.750	4	2.21	0.912	17.8	2.56
0.750	5	2.22	0.916	17.6	2.59
0.750	6	2.22	0.925	17.2	2.56
0.750	7	2.21	0.911	17.9	2.57
0.750	8	2.24	0.923	18.0	2.60
0.750	9	2.23	0.928	17.8	2.59

[CaCl <sub>2</sub> ]	Test #	Bubble Diameter	Average Aspect Ratio	Average Rise Velocity	Specific Bubble Surface Area
M		mm		cm/s	mm <sup>-1</sup>
0.750	10	2.23	0.924	17.8	2.58
1.000	1	2.23	0.924	18.0	2.59
1.000	2	2.21	0.911	17.8	2.58
1.000	3	2.21	0.912	17.8	2.57
1.000	4	2.22	0.918	17.5	2.57
1.000	5	2.22	0.920	17.6	2.57
1.000	6	2.24	0.923	17.7	2.61
1.000	7	2.23	0.914	17.8	2.61
1.000	8	2.23	0.920	17.6	2.59
1.000	9	2.24	0.921	17.9	2.61
1.000	10	2.22	0.909	17.8	2.60

Table A3.6 – Bubble shape and rise velocity tests – MIBC data

[MIBC]	Test	Bubble Diameter	Average Aspect Ratio	Average Rise Velocity	Specific Bubble Surface Area
ppm (mg/l)	#	mm		cm/s	mm <sup>-1</sup>
1	1	2.23	0.689	23.2	3.24
1	2	2.25	0.682	23.5	3.31
1	3	2.25	0.689	23.1	3.28
1	4	2.25	0.676	23.8	3.34
1	5	2.23	0.687	23.1	3.23
1	6	2.32	0.704	23.7	3.44
1	7	2.35	0.689	24.1	3.57
1	8	2.39	0.683	24.9	3.73
1	9	2.26	0.685	23.5	3.32
1	10	2.25	0.677	23.9	3.33
2	1	2.29	0.762	22.9	3.13
2	2	2.28	0.759	22.9	3.13
2	3	2.46	0.772	24.5	3.59
2	4	2.25	0.771	22.5	3.01
2	5	2.36	0.763	23.5	3.34
2	6	2.29	0.771	22.5	3.11
2	7	2.28	0.768	22.7	3.11
2	8	2.24	0.762	22.5	2.99
2	9	2.25	0.760	22.8	3.05
2	10	2.28	0.754	22.9	3.14
5	1	2.34	0.825	22.5	3.08
5	2	2.24	0.819	21.5	2.86
5	3	2.20	0.831	21.1	2.73
5	4	2.24	0.825	21.4	2.82
5	5	2.21	0.823	21.1	2.76
5	6	2.20	0.826	21.2	2.73
5	7	2.23	0.824	21.1	2.80
5	8	2.21	0.823	21.0	2.76
5	9	2.20	0.829	21.0	2.73
5	10	2.20	0.826	21.0	2.72

[MIBC]	Test	Bubble Diameter	Average Aspect Ratio	Average Rise Velocity	Specific Bubble Surface Area
ppm (mg/l)	#	mm		cm/s	mm <sup>-1</sup>
10	1	2.27	0.871	20.7	2.78
10	2	2.27	0.872	20.7	2.79
10	3	2.27	0.867	20.7	2.80
10	4	2.27	0.866	20.8	2.81
10	5	2.28	0.867	20.8	2.83
10	6	2.27	0.867	20.6	2.80
10	7	2.29	0.868	20.8	2.86
10	8	2.27	0.870	20.6	2.80
10	9	2.27	0.866	20.6	2.82
10	10	2.26	0.868	20.5	2.79
20	1	2.25	0.887	21.2	2.71
20	2	2.27	0.907	20.9	2.71
20	3	2.26	0.895	21.1	2.72
20	4	2.25	0.884	20.7	2.72
20	5	2.24	0.881	20.9	2.69
20	6	2.25	0.887	20.6	2.70
20	7	2.27	0.900	21.2	2.73
20	8	2.26	0.893	21.1	2.73
20	9	2.27	0.889	21.4	2.76
20	10	2.27	0.893	21.0	2.75
50	1	2.26	0.931	17.5	2.64
50	2	2.25	0.929	17.6	2.63
50	3	2.25	0.923	17.9	2.63
50	4	2.25	0.933	17.3	2.61
50	5	2.23	0.920	17.7	2.59
50	6	2.23	0.921	17.1	2.60
50	7	2.24	0.925	17.3	2.62
50	8	2.25	0.927	17.7	2.63
50	9	2.23	0.919	17.7	2.59
50	10	2.25	0.930	17.4	2.63
100	1	2.22	0.935	16.7	2.55
100	2	2.22	0.932	17.2	2.55
100	3	2.21	0.928	16.7	2.54
100	4	2.22	0.935	16.5	2.54
100	5	2.21	0.933	16.8	2.53
100	6	2.21	0.926	16.9	2.54
100	7	2.21	0.928	16.6	2.54
100	8	2.23	0.934	16.6	2.56
100	9	2.21	0.923	16.9	2.53
100	10	2.22	0.932	16.6	2.56